PARP1 expression in breast cancer and effects of its inhibition in preclinical models

Memòria presentada per

Jetzabel Garcia Parra

per optar al Grau de Doctor

TESIS DOCTORAL UPF / 2012

UNIVERSITAT POMPEU FABRA

Hospital del Mar

Parc de Salut MAR Barcelona

A la meva família

ACKNOLEDGEMENTS

Per fi ha arribat el moment dels agraïments de la tesis... per fi un moment per aturar-me i adonar-me que estic molt a prop de tancar una gran etapa de la meva vida (no volia ser tan transcendental, però s'ha sortit així!). El temps ha passat volant. Han estat ben bé cinc intensos anys plens d'aprenentatge i experiències compartits amb molts de vosaltres a qui ara us voldria dedicar un immens GRÀCIES!(I per si de cas m'oblido d'algú, gràcies també!)

En primer lloc voldria agrair als meus directors de tesis el Dr. Joan Albanell i la Dra. Ana Rovira. Gràcies per haver-me donat l'oportunitat de realitzar la tesis en aquest grup. Tot plegat ha esta una valuosa experiència, des dels inicis, instal·lant-nos i posant a rodar un laboratori al PRBB, fins a veure com el potencial "translacional" del grup (que és el que em va agradar des del principi) s'ha anat transformant en una realitat. Gràcies per tota la formació rebuda, els consells, la supervisió i correccions perquè aquesta feina sortís el millor possible. I en especial a l'Ana, per la paciència, que a vegades sóc una mica tossuda, i pels moments més relaxats mostrant la part més divertida. Per altra banda, també voldria agrair-li al Fredi per les seves grans aportacions en l'anàlisi d'imatges, les primeres nocions amb l'ImageJ i per pràcticament ser el meu tercer director en els últims moments d'escriptura. A les oncòlogues, a l'Edurne i la Clara per la seva motivació i per aportar el punt de vista més clínic i aplicat, per ajudar a no perdre la perspectiva del "per què" investiguem el que investiguem; a la Montse A. sobretot per aportar el punt didàctic a les presentacions d'immunos, sempre s'aprèn alguna cosa; i a la Bea, sempre vital i sempre aportant les "novetats genòmiques" als lab meetings. Per altra banda també agrair a en Josep Lloreta haver acceptat ser el tutor d'aquesta tesis.

Per suposat agrair als qui més he compartit tots aquests anys, no només hores de feina, que han estat moooltes, sinó també soparets, intensos partits (i pre i post- partits!) de volley blots (i dirty cells! no oblidem els inicis!), la currada de vídeo per la Iru... i molts altres bons moments que formen part d'aquests anys. A l'Alba pel seu esperit alegre i motivat i per ser amb qui he pogut compartir més moments de "ciència"; a l'Isra pel seu bon rotllo i el seu bon caràcter (i ajudar-me sempre a agafar les coses dels prestatges més alts! ☺ Ah, i per l'ajuda amb els últims in vivos!); a l'Oriol per seu tarannà tranquil i bona gent i ajudar-me tant i tant amb els ratolinets, estàs fet un professional; a la Iru per les llargues xerreres compartides al lab i perquè quan no estàs agobiadilla ets una tia superdivertida! A les Sílvies, la Geraeerd per ser tan maca i diposada a ajudar i a la Menéndez, per la seva paciència amb les mostres de ratolins i

la vitalitat currant. Voldria agrair també a la Cristina Oliva els inicis ensenyant-me els primers protocols, a les oncòlogues Cristina Suàrez i Laura Lema per l'alegria de les dues i per la paciència a totes les preguntes mèdiques que els fèiem. No voldria oblidar-me dels estudiants que van passar, l'Ana, l'Isart i especialment la Sandra per aprendre tan ràpid i compartir un temps breu de la recerca de PARP.

Més enllà de del lab 271.03, no voldria deixar-me moltes altres persones quedaran a la memòria d'aquests anys de predoc. Al Xavi, per les converses entretingudes compartides sobretot a l'hora de dinar i per lo motivadíssim amb el volley i a la Rita, també pels molts dinars i xerreres compartides (et vull veure cantant un dia!). Als dos sols de noies que tenim al servei de microarrays, Lara i Eulàlia, sou molt maques, no canvieu mai, i gràcies també per lo bé que expliqueu! Als veïns de (sub-)passadís de laboratori, Carme, Ciscu, Clara, Ester... per ajudar sempre que vaig necessitar algo; a Rocío, Vera, Laia... per ser tan bones noies; al Jose Yélamos, per ser sempre tan amable a mi i per la seva gran ajuda amb PARP i per suposat també a la resta del seu grup, Coral, Jordi i Laura, que també m'han ajudat molt. També m'agradaria mencionar molts d'aquells amb qui he compartit llargues converses a les infinites hores passades a cultius, fent-se si més no, més entretingudes... al Sergi, l'Aina (i les ròtules!), el Guy (i el misteri de les maxis), la Laura murciana, l'Ana Belèn (fins a altes hores!), l'altra Aina (i el petit Jan), la Maeba (i al seva vitalitat), la Guida i el portunhol... I al fons del passadís, voldria també agrair a molta altra gent amb qui m'hagués agradat poder compartir i conèixer molt més, però això d'estar a un sub-passadís sempre ens ha aïllat una miqueta eh... A la Neus, per ser un súper-sol de noia i per poder compartir experiències d'aquests 9 mesos tan especials que estem vivint; a la Jelena, per ser un altre súper-sol de noia i ajudar-me amb els meus primers shRNAs, i evidement també la súpervital Rosa ajudant-me també, i molt, amb els virus; la Teresa, per ser tan maca i alegre;al Raúl per ajudar i resoldre dubtes sempre que vaig necessitar; la Sílvia per la seva simpatia i ajuda amb les seqüenciacions; a en Josep Baulida per les seves aportacions amb PARP;la secre Lorena per ser tan maja; i a moltes altres persones que m'inspireu molt bona energia, l'Estel, l'Alba, la Núria, l'Alícia, la Jordina, l'Erika, la Mari... sempre s'agraeix un bon ambient encara que sigui en una conversa de passadís o a la cambra fosca! A l'estabulari no puc oblidar-me de la Marisol i la seva alegria. Al repartidor Carlos, merengón però bona gent, i a la Eli, també molt bona persona amb mi.I també a Marta Calsina per lo simpàtica i per lo motivada a les visites d'estudiants

I més enllà del laboratori, agrair a aquells amb qui més pinya vaig fer durant els anys de uni descobrint la biologia humana, i que és en part el m'ha portat fins a on sóc ara... Emma, Niko, Adri, Anna, Guillem, Paula, Nano, Marta, Jesús, Míriam,

Beñat, Urko, Ixa...; durant les inoblidables pràctiques a la Lídia i l'Anna; i especialment a la Tània i al Ferran, gràcies per ser com sou. Com no agrair a les "noies encants", per escoltar les meves explicacions rares de ciència i fer-me desconnectar, i per suposat a DonaDanZa, aire fresc més enllà de la feina, a Vani, Tere, Mara i Sílvia, especialment Tere pel seu recolzament en l'sprint final d'escriptura (i maquetació!).I també els dinarets amb els biòlegs marins de l'ICM, sou penya molt maca!

Per suposat, agrair de tot cor a la meva família, per haver-me donat tots aquests anys d'educació que m'han portat fins a l'entrega d'aquesta tesis doctoral. Gràcies pel recolzament, tot i no entendre gaire cosa sobre el que investigava en aquest edifici tan modern... veure'ls orgullosos sempre ha estat una motivació per seguir endavant, i també agrair a la meva família de Chile, que tot i estar lluny es fan estimar.

I finalment, Claudio, no tinc paraules per agrair-te tota la teva ajuda i amor incondicionals. Sé que sense tu al meu costat potser res de tot això hagués estat possible. Gràcies per fer-me sentir tan a prop teu en tot moment, per la paciència, per animar-me quan ho he necessitat i per compartir el dia a dia amb l'alegria i la vitalitat que transmets. Gràcies amor! Ets un tresor. I gràcies al nostre estimadíssim i desitjadíssim pirihuin per ser l'altre gran motivació d'aquest treball final (gràcies per aguantar-me tantes hores asseguda i una mica estressadilla...). Gràcies fillet!!

ABSTRACT

Breast cancer is the most frequently diagnosed cancer in women worldwide and the main cause of cancer death in females. Improved treatments, prevention programs and earlier detection of the disease are reducing the rate of death from breast cancer. However, there is still a high percentage of mortality by this disease. The identification of novel targets that can predict the response to specific treatments is a key goal for personalizing breast cancer therapy and to improve survival. Few years ago, PARP inhibitors appeared as a promising therapy, particularly for patients with BRCA mutations. However, there was a clear need to conduct further preclinical and translational work to help to develop a rational development of PARP inhibition in breast cancer.

In this work we described PARP1 expression in breast tumour samples and characterized the effects of its inhibition in preclinical models. From these studies we found that nuclear PARP1 protein overexpression was associated with malignant transformation and poor prognosis in breast cancer. PARP1 overexpression was more common in triple negative breast cancer, but was also detectable in small subsets of estrogen receptor positive and HER2 positive breast cancers. In preclinical models, PARP1 appeared to play distinct roles in different molecular subtypes of breast cancer. Moreover, we described that PARP inhibitors had antitumour effects in various cancer subtypes, and a novel PARP inhibitor (olaparib) with the anti-HER2 antibody trastuzumab had greater antitumor effect than each agent given alone.

RESUM

El càncer de mama és el càncer que es diagnostica amb més freqüència en dones arreu del món. La millora dels tractaments, programes de prevenció i la detecció precoç de la malaltia estan reduint la taxa de mort deguda a aquest càncer. Tot i això, segueix havent un alt percentatge de mortalitat per aquesta malaltia. La identificació de noves dianes que puguin predir la resposta a tractaments específics és un objectiu clau per personalitzar les teràpies contra el càncer de mama i millorar-ne la supervivència. Fa pocs anys, els inhibidors de PARP van aparèixer com una teràpia prometedora, particularment per pacients amb mutacions de BRCA. Tot i això, hi ha una clara necessitat de dur a terme més estudis preclínics i translacionals per ajudar al foment d'un desenvolupament racional de la inhibició de PARP en càncer de mama.

En aquest treball vam descriure l'expressió de PARP1 en mostres de tumors mamaris i vam caracteritzar els efectes de la seva inhibició a models preclínics. D'aquests estudis vam trobar que la sobreexpressió nuclear de la proteïna PARP1 fou associada amb transformació maligna i a mal pronòstic en càncer de mama. La sobreexpressió de PARP1 fou més freqüent al càncer de mama triple negatiu, però també es va detectar en un petit subgrup de càncers de mama receptors d'estrogen positius, i HER2 positius. En models preclínics, PARP1 va semblar exercir rols diferents als diferents subtipus de càncer de mama. Per altra banda, vam descriure que els inhibidors de PARP tenen efectes antitumorals en diversos subtipus de càncer, i que un nou inhibidor de PARP (olaparib) combinat amb l'anticòs anti-HER2, trastuzumab, van exhibir majors efectes antitumorals que cadascun per separat.

PREFACE

The work presented in this PhD thesis has been conducted in the Molecular Therapeutics and Biomarkers in Cancer group of the Institut de Recerca Hospital del Mar (IMIM), at the Parc de Recerca Biomèdica de Barcelona (PRBB). The group is led by Dr. Joan Albanell, Head of the Medical Oncology Service at the Hospital del Mar, and the Research Programme in Cancer at IMIM.

The main goal of the group is to contribute to improving of cancer treatment through preclinical research with *in vitro*, *in vivo* and *ex vivo* models, predictive and pharmacodynamic biomarker studies in human samples and clinical trials. For this objective the group is structured along three linked multidisciplinary areas: the Preclinical laboratory, led by Dr. Ana Rovira, senior biologist; the Biomarker research area, led by Dr. Federico Rojo, pathologist; and the Clinical Research area, coordinated by Dr. Ignasi Tusquets and Dr. Sònia Servitja, oncologists. For the work showed in this PhD thesis we have also counted on the valuable collaboration of Dr. Ana Lluch, from Hospital Clínic de València, and Dr. José Yélamos, from IMIM.

Along the years as predoctoral student in this group I had the opportunity to learn a wide range of laboratory techniques and analyze and interpret data through participation in various research projects. From April 2007 until 2009 I began studying the PI3K pathway and the effects of its inhibition with a dual mTOR/PI3K inhibitor in breast cancer, as well as collaborations in other projects. Since late 2009 I have been working in the field of PARP1 protein focused in breast cancer.

PARP inhibition emerged few years ago as a promising novel strategy for the treatment of BRCA mutant tumours. However, the clinical development of PARP inhibitors in many instances was faster than the generation of a sufficient body of knowledge on the role of PARP in human tumours.

To address some translational aspects of PARP in breast cancer, the core of this PhD thesis has consisted in the study of PARP1 expression in breast tumour samples and in the characterization of the effects of its inhibition by different technical approaches in cancer cells. As a result of this work also a novel therapeutic strategy has been proposed.

INDEX

ABBREVIATIONS

3-AB	3-aminobenzamide
aCGH	Comparative Genomic Hybridization array
ADP	Adenosine Diphosphate
ADPRTs,ARTs	ADP-ribosyl transferases
AIF	Apoptotic Inducing Factor
AMD	Automodification Domain
AP	Apurinic or Apyrimidinic site
AP-1	Activator Protein 1
ARH3	ADP-ribosylhydrolase 3
ATM	Ataxia Telangiactasia Mutated
ATR	Ataxia Telangiectasia and Rad3-related
AUC	Area Under the Curve
BCCL	Breast Cancer Cell Lines
BER	Base Excision Repair
BRCA1/2	BReast CAncer susceptibility genes 1/2
BRCC	BRCA1 and BRCA2 Containing Complex
BRCT	BRCA1 C Terminus domain
CD	Catalytic Domain
CDDP	Cisplatin
Cdk1	Cyclin-dependent kinase 1
CHEK2	Cell cycle Checkpoint Kinase 2
CMF	Cyclophosphamide, Methotrexate and Fluorouracil
COSMIC	Catalogue of Somatic Mutations in Cancer
CPDs	Cyclobutane Pyrimidine Dimers
CR	Complete Response
CXCL1	Chemokine (C-X-C motif) Ligand 1
DBD	DNA Binding Domain
DCIS	Ductal Carcinoma In Situ
DDR	DNA Damage Response
DFS	Disease Free Survival
DNA-PK	DNA-dependent Protein Kinase
DSB	Double Strand Breaks

EC	Cytoplasmic Extracts
EGF	Epidermal Growth Factor
EGFR	Epithelial Growth Factor Receptor
EN	Nuclear Extract
ER	Estrogen Receptor
ERK1/2	Extracellular signal-Regulated Kinases
FANCA	Fanconi Anemia, Complementation group A
FFPE	Formalin-Fixed Paraffin-Embedded
FISH	Fluorescent In Situ Hybridization
GI	Genomic instability
H2AX	Histone H2A member X
HER2	Human Epidermal Growth Factor Receptor 2
HIF1/2α	Hypoxia Inducible Factor 1/2α
HR	Homologous Recombination
HzR	Hazard Ratio
ICAM-1	intercellular adhesion molecule 1
IDC	Infiltrating Ductal Carcinoma
IHC	Immunohistochemistry
IL-12	Interleukin-12
iNOS	inducible Nitric Oxide Synthase
IPA	Ingenuity Pathway Analysis software
IR	Ionising Radiation
KO	Knockout
LOH	Loss of Heterozigozity
MAPK	Mitogen Activated Protein Kinase
MEF	Mouse Embryonic Fibroblasts
MIP-1α	Macrophage Inflammatory Protein-1 α
miR	microRNA
MMR	MisMatch Repair
MTD	Maximum Tolerated Dose
MVD	Microvessel density
NAD⁺	Nicotinamide adenine dinucleotide
NCBI	National Center of Biotechnology Database
NER	Nucleotide Excision Repair

NFkappaB	Nuclear Factor Kappa Light polypeptide gene
enhancer in B-cells	
NHEJ	Non-Homologous End Joining
NLS	Nuclear Localization Signal
OH	Hydroxyl Radicals
ORR	Overal Response Rate
OS	Overall Survival
pADPr	Poly(ADP-ribose)
PARG	Poly(ADP-ribose)glycohydrolase
PARP	Poly(ADP-Ribose)polymerase
PFS	Progression Free Survival
PI3K	Phosphatidylinositol 3-Kinase
PgR	Progesterone Receptor
PR	Partial Response
PTEN	Phosphatase and Tensin homolog
qRT-PCR	quantitative Reverse Transcription real-time PCR
RECIST	Response Evaluation Criteria In Solid Tumours
RIN	RNA Integrity Number
ROC	Receiver-Operator Curve
ROS	Reactive Oxygen Species
SNP	Single Nucleotide Polymorphism
SSB	Single Strand Break
TK	Tyrosine Kinase
TMA	Tissue Microarray
TN	Triple Negative
TNBC	Triple Negative Breast Cancer
TNF-α	Tumour Necrosis Factor α
TNM	Tumour Node Metastasis
Top2A	Topoisomerase 2α
Topo I/II	Topoisomerase I/II
TP53	Tumour Protein p53
UV	Ultraviolet Light
VEGF	Vascular Epidermal Growth Factor
WB	Western Blot

XPA/B/C/D/F   Xeroderma pigmentosum complementation group
A/B/C/D

XRCC1   X-ray repair cross-complementing protein 1

INTRODUCTION

I.1. BREAST CANCER

I.1.1. Magnitude of breast cancer disease

Cancer is the leading cause of death in economically developed countries and the second cause of death in developing countries[1]. At present, the global burden of cancer is increasing due to the aging, the growth of the world's population and acquisition of cancer-associated lifestyles, particularly smoking, in economically developing countries[2].

Breast cancer is the most frequently diagnosed cancer in women worldwide and the main cause of cancer death in females, accounting in 2008 for 23% of the total cases and 14% of the cancer deaths[3]. Specifically in Spain, according to statistics from Globocan 2008, breast cancer accounted for 6008 deaths and 22027 of new cases[4]. Fortunately the rate of death from breast cancer is declining due to improved treatments, prevention programs and the earlier detection of the disease[5].

However, there is an urgent need to develop novel therapeutics to improve the outcome of many women that still die from this disease.
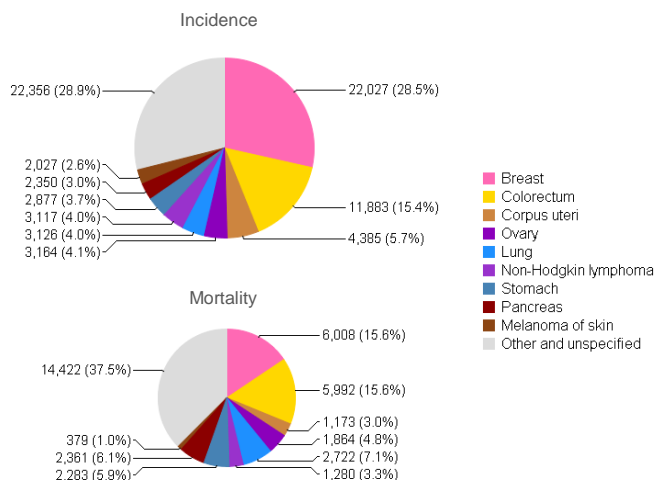
Figure I.1. Estimated cancer incidence and mortality in women in 2008 in Spain. Cancer incidence and mortality data for all ages. Adapted from[4].

I.1.2. Hereditary and spontaneous breast cancer

Breast cancer, like other forms of cancer, is considered to be the result of both, environmental and hereditary factors that lead to essential alterations in cell physiology, including self-sufficiency in growth signals, insensitivity to growth inhibitory signals, evasion of apoptosis, limitless replicative potential, sustained angiogenesis and tissue invasion and metastasis[6]. In a common core, these alterations affect systems that preserve the normal cell proliferation and lead to the malignant transformation of cells.

Breast cancer is a very heterogeneous disease at both histological and molecular level. Based on etiological parameters, breast cancer is classified in two main groups: Hereditary and sporadic breast cancer. It is

important to discuss hereditary breast cancer since it is a key focus in the development of PARP inhibitors.

Hereditary breast cancers represent 5-10% of all breast cancers, while the rest, much more common, are sporadic cancers. In sporadic breast cancer, risk factors are often hormonal in nature and are the accumulation of many genetic alterations in mammary epithelial cells that leads to the malignant transformation of breast.

Hereditary breast cancer occurs in women that carry identified germline mutations in specific predisposing genes which confers an inherited susceptibility to breast cancer. The main high penetrance genes described for hereditary breast cancer are: BReast CAncer susceptibility gene 1 (*BRCA1*) and BReast CAncer susceptibility gene 2 (*BRCA2*). These genes codify for key proteins that plays an important role in an essential DNA repair mechanism, the Homologous Recombination (HR) repair pathway (More detailed in Section 2.3 "DNA Repair Mechanisms"). Other genes that can be mutated in other forms of hereditary breast cancer are: *TP53*, coding for a key regulator of cell cycle and genome stability; the cell cycle checkpoint kinase gene (*CHEK2*), accounting for about 5% of the hereditary cases; and *PTEN*, coding for a protein also involved in cell cycle and proliferation, which are responsible for up to 1% of this class of breast cancer[7].

Focusing in BRCA, germ-line BRCA mutations can be inherited from either parent, whereas the somatic, or acquired, mutations in BRCA genes occur infrequently. Women with germ-line heterozygous mutations in *BRCA1* or *BRCA2* have an estimated 60-85% of lifetime risk of developing breast (and/or ovarian) cancer, among others[8]. Consistent

with this, BRCA-familial tumors usually carry higher frequency of *TP53* mutations[9], amplification of *c-MYC*, which codifies for a transcription factor with an important role in DNA replication, and/or elevated expression EGFR, an epithelial growth factor receptor important for proliferation, which could explain this increased risk of cancer[10]. Inherited mutations of *BRCA1* gene accounts for 40-45% of hereditary cancers[11], whereas *BRCA2* for a 35-40%[12].

Despite BRCA1 and BRCA2 have no significant sequence similarity, both proteins are implicated in similar processes of DNA repair. BRCA1 appears to play an initial role in signalling DNA damage and cell cycle checkpoint, whereas BRCA2 has a more direct involvement in DNA repair itself.

<u>*BRCA1*</u> gene is located in the chromosome 17q21 and encodes for a nuclear phosphoprotein of 220kDa with two recognized protein motifs important for its functions, a RING domain near the N-terminus and two tandem BRCT domains at C-terminus. Through the RING domain (a cystein-rich sequence) can heterodimerize with BARD1, an important RING-finger family member with transcriptional regulatory capacity. This domain also binds other proteins such as c-MYC or cyclin D1, involved in the regulation for cell cycle progression. The BRCA1 C-terminus (BRCT) domains are involved in transcription activation and protein binding (such as histone deacetylases). Through these domains also mediates the binding with complexes of proteins involved in the repair of DNA Double Strand Breaks (DSB) (reviewed in[13]).

Upon DNA damage, BRCA1 is rapidly phosphorylated by kinases involved in the process of DNA repair including Ataxia Telangiactasia

Mutated (ATM), Ataxia Telangiectasia and Rad3-related (ATR) and CHEK2, which activate signal transduction[14] and initiate the processing of DSB by the HR pathway.

BRCA2 gene is located in the chromosome 13q12 and encodes for a nuclear phosphoprotein of 384kDa which does not exhibit many well-defined domains as BRCA1. The central domain which contains BRC repeats binds with the recombinase RAD51. The nuclear localization signal promotes the shuttling of BRCA2/RAD51 from the cytoplasm to the nucleus where bind other components forming the BRCC complex responsible of further processing of DSBs (reviewed in [13]).

When high risk heterozygous mutations in BRCA1 and BRCA2 genes are combined with the loss of the functional copy (the wild-type allele) can give rise to truncated or non-functional BRCA proteins. The loss of the wild type allele is called Loss of Heterozigozity (LOH). Cells with lack of BRCA1 or BRCA2 wild-type protein expression need to repair DSBs by more error-prone repair mechanisms. This leads to increased errors in DNA repair and genomic instability which might induce alterations in essential cell-cycle checkpoints and/or proliferation signals, underlying the characteristic cancer predisposition caused by this deficiency (reviewed in [15]).

I.1.3. Predictive biomarkers

All breast cancers are routinely assessed for the expression of three predictive markers which will help to predict the response to a specific therapeutic treatment: Hormone receptors, including Estrogen Receptor

(ER) and Progesterone Receptor (PgR); and Human Epidermal Growth Factor Receptor 2 (HER2 receptor).

Hormone receptors

Estrogen Receptor (ER) is a nuclear hormone receptor activated by the hormone 17β-estradiol (estrogen) that regulates gene expression. In the normal resting breast about 15-25% of epithelial cells are ER-positive, although the percentage varies throughout the menstrual cycle. In non-tumoral conditions, the ER-positive cells are largely non-dividing whereas the ER-negative cells proliferate in response to oestrogen-stimulation. In fact, it is suggested that ER-positive cells promote the proliferation of the surrounding ER-negative cells through secretion of paracrine factors. In contrast, in breast tumours the ER-positive cells exhibit great oestrogen-dependent proliferation[16,17].

Progesterone Receptor (PgR) is also a nuclear hormone receptor that mediates the effects of progesterone hormone in the development of the mammary gland, specifically critical for lobuloalveolar development[18]. Like the ER, PgR is present about a 15-30% of luminal epithelial cells[16]. PR is an oestrogen-regulated gene and its synthesis in normal, and cancer, cells requires oestrogen and ER. Thus, it is not surprising to observe that ER-positive/PgR-positive tumours are more common than ER-positive/PgR-negative.

For this reason, the expression of these receptors reflects the hormonal status of the tumour and predicts the sensitivity to endocrine treatment based on the dependence of this type of tumour to steroid hormones as their main growth stimulus.

About two third of breast cancers are ER-positive, more than half of these also express PgR, and about 50% of the ER-positive respond to endocrine therapy[19]. The expression of hormone receptors is assessed by immunohistochemistry and defines the tumour as ER and PgR positive (>1% of tumour cells with positive nuclear-staining), or negative (<1% tumour cells with positive nuclear-staining)[20].

HER2 Receptor

HER2/ErbB-2 gene codifies for a transmembrane tyrosine kinase growth factor receptor that belongs to HER family of receptors (Further discussed in section "I.1.5.2.2. HER2-targeted therapies").

Amplification and overexpression of HER2 occurs in about 15-25% of breast cancers and is associated with aggressive disease course, poor disease free survival and shorter overall survival[21]. The status of HER2 predicts response to anti-HER2 therapy[22].

The HER2 status is assessed with two methods. By immunohistochemistry is defined the protein expression status ranging from 0 (negative), to 3+ (intense and uniform membrane staining in >30% of tumour cells). And by Fluorescent In Situ Hybridization (FISH) is assessed the *HER2* gene amplification. As stated by the guidelines of the American Society of Clinical Oncology/College of American Pathologists for HER2 testing: "a positive HER2 result is IHC staining of 3+ and FISH of more than six *HER2* gene copies per nucleus or a FISH ratio (HER2 gene signals to chromosome17 signals) of more than 2.2"[23].

I.1.4. Molecular subtypes

Classically breast cancers have been classified according the parameters described above and the expression of hormone receptors and HER2, which frequently help predicting prognosis and determining the most appropriate treatment. However, this classification has demonstrated to be limited being unable to define subgroups with similar prognostic and therapeutic features.

In the 2000' microarray technology allowed Perou et al.[24] to classify for the first time breast cancer in subgroups based on the gene expression profiling, introducing a new concept: the "molecular subypes". These molecular subtypes were confirmed in subsequent studies and were found to be associated with different clinical outcomes[25,26]. Furthermore, these subtypes not only associate with different prognosis but also exhibit different histological and physiopathological features and different response to treatments (Correspondence between molecular subtypes and clinicopathological features is summarized in the figure I.2.). To date, the five main subtypes defined by its gene expression profile are:

- <u>Normal breast-like</u> expresses genes characteristic of adipose and non-epithelial cell types which resembles to normal breast, which might be an artifact.

Luminal subtypes, which in general are ER+, express cytokeratin 8 and 18 and represents about 70% of breast cancers, are divided in:

- <u>Luminal A</u> is mostly ER and PgR positive and HER2 negative expression. Luminal-A subtype have better prognosis and sensitivity to endocrine therapy than Luminal-B.

- <u>Luminal-B</u> tends to be of higher grade, more aggressive, positive for HER2 and high density of Ki-67 expression. Luminal-B has worse prognosis than Luminal-A.

- <u>ERBB2 overexpressing</u> tends to be high grade tumours that together with the basal-like subtype have the worst overall and metastases free survival. This subtype exhibits overexpression of HER2 together with overexpression of other genes in the same amplicon such as *GRB7* and *Topo2A*. The majority are ER negative and respond to anti-HER2 treatment.

- <u>Basal-like</u> is the most aggressive subtype. Most of them exhibit negative expression of ER, PgR and HER2, for this reason in the clinical setting are also called triple-negative (TN), although not all the basal-like are TN. This subtype expresses high levels of genes characteristic of the basal (myoepithelial) cells of the mammary tissue such as cytokeratines5/6, EGFR, c-Kit. Besides, these tumours exhibit high index of genomic instability. Although there is no established therapeutic target for this subgroup, it is very sensitive to chemotherapy, but have high tendency to relapse and metastasize[27]. Another feature that differentiates basal-like tumours from luminal-like is the association with BRCA-1 pathway dysfunction. The similarities between basal-like subtype and BRCA1-associated breast cancers are further described in the point of "BRCAness phenotype" in the section "I.4.3.2.1. Synthetic lethality. Table I.1". Due to the lack of therapeutic target in this subtype and the similarity found with BRCA1-mutated cancers many efforts have been focused to novel targets. PARP inhibitors, which are the focus in this thesis, have been also studied clinically in triple-negative breast cancers.

Pathological Variables	Basal-like (%)	Luminal A (%)	Luminal B (%)	HER2-like (%)
HER2-positive (IHC)	10	12	20	100
ER-positive (IHC)	12	96	97	46
Grade III	84	19	53	74
Tumor size >2 cm	75	53	69	74
Node-positive	40	52	65	66
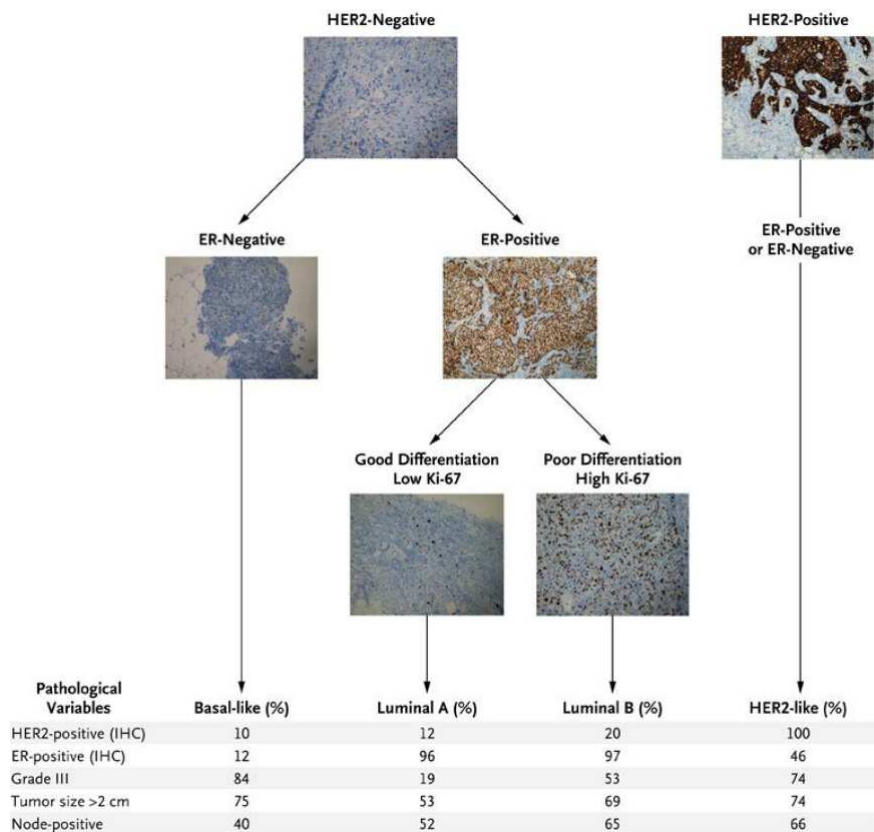
Figure I.2. Correspondence between Molecular subtypes and Clinicopathological Features of Breast Cancer. Adapted from[28].

I.1.5. Systemic treatments

I.1.5.1. Chemotherapy

Chemotherapy is a cancer treatment that uses cytotoxic drugs that affects cell proliferation to destroy or stop the growth of fast replicating cells, a general characteristic of tumoral cells, but also a characteristic of some high proliferative normal cells, which causes side effects such as alopecia or myelosuppression. Depending on the moment of administration

chemotherapy can be classified as: Neoadjuvant chemotherapy, administered before surgery to reduce the size of the tumour; adjuvant chemotherapy, administered after surgery to reduce the risk of recurrence; and palliative chemotherapy, administered to control the cancer after spreading. The most common chemotherapeutic drugs used in breast cancer are doxorubicin, epirubicin, docetaxel, paclitaxel, 5-fluorouracil and cyclophosphamide.

I.1.5.2. Targeted therapies

Targeted therapy is a cancer treatment that specifically targets essential markers of cancer cells responsible of the growth and survival of the tumour. The rational use of targeted therapies is frequently more effective and less toxic for normal cells than other treatments.

I.1.5.2.1. Hormone therapy

Hormone therapy acts blocking the effects of oestrogen on ER-positive breast cancer, which are dependent on oestrogen to grow. Current hormone treatments include anti-estrogen agents, aromatase inhibitors, and others. Antiestrogens compete with estrogens for the binding to ER in ER-positive cells, thus reducing its proliferation. The most successful antiestrogen drug is tamoxifen that exhibits about a 50% reduction in recurrence and >20% reduction in deaths[29]. Aromatase inhibitors block the aromatase enzyme, responsible of turning androgen into oestrogen, hence reducing the levels of estrogens.

I.1.5.2.2. HER2 targeted therapy

HER2 is a transmembrane tyrosine kinase (TK) receptor that belongs to the Epidermal Growth Factor (EGF) or HER receptor family which consist of EGFR/ErbB1 (HER1), ErbB2 (HER2), ErbB3 (HER3) and ErbB4 (HER4). All of them, except HER3, contain a cytoplasmic TK domain, and all, except HER2, bind specific ligands (members of the EGF family of growth factors) through the extracellular domain. After ligand binding, these receptors homo- or heterodimerize, being HER2 the preferential binding partner, and phosphorylates many residues from their intracellular domain that result in the recruitment of many signaling molecules and the activation of many signaling pathways. HER2 signaling triggers several cellular processes such as proliferation, survival, motility as well as resistance to apoptosis. The two of the main activated pathways are the phosphatidylinositol 3-kinase (PI3K)/Akt and RAS/Raf/Mitogen Activated Protein Kinase (MAPK) pathways. (Reviewed in[30]).

Therefore, HER2 is an ideal target for HER2+ breast cancer treatment for several reasons:

- HER2 levels correlate strongly with pathogenesis and prognosis of breast cancer.
- HER2 levels in overexpressing human cancers are much higher than in normal tissues, potentially diminishing the toxicity of HER2-targeting drugs.
- HER2 is present in a high proportion of malignant cells in HER2+ tumours, suggesting an optimal targeting of most of the cancer cells in a patient.

- HER2 overexpression is frequently found in both primary and metastatic sites, suggesting that anti-HER2 therapy might be effective at all disease sites.

Trastuzumab was the first HER2-targeted therapy approved for the treatment of HER2-overexpressing breast cancers. It is a humanized monoclonal antibody against the extracellular region of HER2[31]. As a single agent has obtained overall response rates (including complete and partial response) ranging from 15% to 30%, whereas when combined with standard chemotherapy in metastatic disease higher response rates ranging from 50% to 80% were obtained[32]. Since we addressed in this thesis the combination of a PARP inhibitor with trastuzumab, a further exploration of what is known on its mechanisms of action is provided below.

Several of the effects observed in experimental *in vitro* and *in vivo* models are[33]:

- Diminished receptor signalling: Disruption of downstream signalling, weak effect on receptor dimerization, internalization and degradation.
- G1 phase of cell cycle arrest: Accumulation of p27[kip1], a cyclin-depent kinase inhibitor.
- Induction of Apoptosis: Inhibition of Akt activity and other indirect mechanisms.
- Inhibition of angiogenesis: Reduction of tumour vasculature and expression of pro-angiogenic factors.
- Activation of immune-mediated responses.
- Inhibition of HER2 extracellular domain cleavage.

- Inhibition of DNA repair: Promoting DNA strand breaks and apoptosis

Another anti-HER2 drug approved for clinical use is lapatinib. Lapatinib is a small-molecule dual EGFR/HER2 tyrosine kinase inhibitor that prevents TK phosphorylation and subsequent downstream signalling[34]. Another antibody-based targeted therapy used in breast cancer is Bevacizumab, against the Vascular Epidermal Growth Factor (VEGF). However, there are no known predictive factors to select patients that benefit the most from this antibody

Apart from these, nowadays several targeted therapies are in clinical trials studying their efficacy in breast cancer, such as novel anti-HER2 drugs, inhibitors of PI3K/Akt/mTOR pathway, ERK1/2 pathway and PARP, the latter extensively covered throughout this thesis. Since PARP is key enzymatic system involved in DNA repair, this topic is reviewed in the following section.

I.2. DNA DAMAGE AND REPAIR

The genome of mammalian cells is constantly threatened by endogenous metabolic products and exogenous genotoxic agents that can finally lead to a range of nucleotide modifications and different kinds of DNA lesions. The major causes of spontaneous DNA damage as well as that caused by ionising radiation (IR) and chemotherapeutic agents most commonly used in the treatment of cancer are reviewed below.

I.2.1. Endogenous DNA damage

Base loss

DNA is a helical molecule, long and double-stranded composed of units of deoxyribonucleotides. A deoxyribonucleotide is composed of the pentose sugar deoxyribose, one of four nitrogenous bases (adenine, guanine (called purines); cytosine, or thymine (called pyrimidines)), and a phosphate group. The N-glycosyl base sugar bond linking DNA bases with deoxyribose is labile under physiological conditions. Base loss consist in the lost of a purine or a pyrimidine due to hydrolytic cleavage of the glycosyl bond which creates an apurinic or apyrimidinic (AP) site, also called abasic site[35].

Base Modification

Deamination. It is the removal of a primary amino group of nucleic acid bases and its conversion to keto groups. Cytosine can be deaminated to uracil, which is commonly found in the RNA, but its presence in the DNA can be easily detected and repaired. Specially, deamination of 5-methyl cytosine to thymine is potentially mutagenic because if it is not detected by the cell as DNA damage, it remains uncorrected and leads to mutation. Similarly, the deamination of adenine is a potentially mutagenic lesion because hypoxanthine forms a more stable base pair with cytosine rather than thymine[36].

Oxidation. Cellular metabolism is a source of endogenous reactive oxygen species (ROS) which include singlet oxygen, peroxide radicals, hydrogen peroxide and hydroxyl radicals (OH). ROS can also be generated by ionizing or ultraviolet radiation and exogenous chemicals. It is widely described that ROS are can modify DNA bases. Among others,

hydroxyl radicals react with guanine to generate 8-hydroxyguanine, a potentially mutagenic lesion that shows preference for base pairing with adenine rather than cytosine[37].

Methylation. In addition to oxygen, living cells contain several other reactive molecules that have the potential to cause DNA damage. This process involves the addition of a methyl group to specific positions in DNA bases. DNA methylation is a cellular mechanism to regulate gene transcription, for this reason the aberrant methylation is considered DNA damage. The most important of these is probably S-adenosylmethionine (SAM). SAM is a methyl group donor that is used as a co-factor in most cellular transmethylation reactions. SAM can react accidentally with DNA to produce alkylated bases such as 3-methyladenine which blocks replication, and is therefore a cytotoxic DNA lesion[38].

Replication errors

Another major source of potential aberrations in DNA is the generation of mismatches or small insertions or deletions during DNA replication. Particularly highly repetitive sequences are prone to this type of error. Although DNA polymerases are moderately accurate and most mistakes are immediately corrected by polymerase-associated `proofreading' exonucleases nevertheless, the machinery is not always perfect and mistakes do happen[39].

I.2.2. Exogenous DNA damage

I.2.2.1. UV damage

Nucleic acid bases absorb electromagnetic radiation of ultraviolet light (UV) which can induce chemical changes in the DNA. The most frequent

photoproducts are the formation of bonds between adjacent pyrimidines within one strand, which is called pyrimidine dimers. Of these, the most frequent are cyclobutane pyrimidine dimers (CPDs). T-T CPDs are formed readily. CPDs cause extreme distortion of the DNA chain structure which can impair transcription, replication and induce mutations such as C o T or CC to TT transition[40].

I.2.2.2. Chemical damage and cytotoxic induced damage

Many chemical agents can damage DNA and act as carcinogens by modifying DNA bases, frequently by addition of an alkyl group (alkylation). Examples of alkylating agents that humans can be exposed to include: polycyclic aromatic hydrocarbons present in the tobacco smoke, pollution or tar fumes; aromatic amines, used in the chemical and rubber industries; or dimethyl- and diethyl-nitrosamine, in trace amounts in many food products[41].

In spite of this, certain toxic alkylating agents and some types of radiation are commonly used as treatments for cancer patients with the ultimate goal of killing cancer cells, yet paradoxically, they are also known to induce cancer since they can cause genetic changes. Radio- and chemotherapy are used to cause a cytotoxic lesion that might arrest tumour progression, theoretically without affecting normal tissue[41]. In general, the cytotoxic lesions induced by these therapies are DNA strand breaks caused by a variety of mechanisms, including direct DNA damage or indirect DNA damage by repair mechanisms which introduce breaks as a part of the repair process. Some of these therapeutic agents have been used in this thesis and are therefore reviewed below.

Radiotherapeutic agents

Ionising radiation (IR), including X rays, y rays and high energy electrons, interacts with matter by transferring energy to the electrons in the irradiated sample. IR acts indiscriminately on all molecules in the irradiated area, being DNA the critical target of IR-induced cell death. The toxic effect of IR on cells is the result of a direct interaction of radiation with DNA or indirectly through the formation of free radicals. These radicals can efficiently react with the DNA resulting in base damage and subsequent DNA strand breaks, or in adducts causing protein crosslinks[42]. Double Strand Breaks (DSBs) are the main cytotoxic lesion produced by direct interaction of IR with DNA or as repair intermediate. Due to the wide spectrum of lesions introduced into the DNA, IR-induced DNA damage can be repaired by multiple DNA repair pathways.

Chemotherapeutic agents

The most common chemotherapeutic agents act on fast-dividing cells, one of the main features of most cancer cells. These kinds of "cytotoxic" drugs affect cell division, DNA synthesis or function through different mechanisms. The cytotoxic agents more relevant to the work presented in this thesis are discussed below.

Cisplatin

Cisplatin (cis-diammine-dichloro-platinum[II], CDDP) is a platinum derivate (Figure I.3). Cisplatin is one of the most potent chemotherapeutic agents known and it is widely used in a variety of solid tumours, specifically it is approved treat bladder, cervical, ovarian, testicular, head and neck, non-small cell lung cancer and malignant

mesothelioma[43]. Cisplatin displays clinical activity against breast cancer but it is not used routinely for its treatment[44].
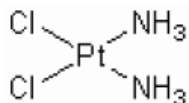
Figure I.3. Structure of cisplatin

Its cytotoxic mechanism of action is mediated by its interaction with the purine bases in the DNA to form DNA adducts, mainly intrastrand crosslinks adducts, but also protein-DNA crosslinks[45]. These DNA lesions are translated in inhibition of DNA synthesis, DNA breaks, suppression of RNA transcription and transduction of these DNA damage signals to downstream effectors activating cell cycle checkpoints, p53, MAPK and finally inducing apoptosis[46].

Doxorubicin

Doxorubicin (also known as Adriamycin or hydroxydaunorubicin), was one of the first two anthracyclines described (together with daunomycin) with high toxicity in mammalian cells *in vitro* and in vivo[47]. Doxorubicin was originally isolated from the bacterium *Streptomyces peucetius var. caesius*[48] (Figure I.4).
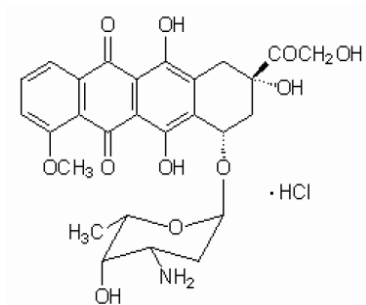
Figure I.4. Doxorubicin structure

Doxorubicin performs its cytotoxic activity through different mechanisms of action, but the main target for doxorubicin is the enzyme Topoisomerase IIα. Topoisomerases I and II (Topo I and II) are enzymes that regulate the strand breakage, rotation and rejoining of DNA to enable DNA transcription, replication, recombination and repair to occur. Due to the specific mechanisms of action of each enzyme, Topo I poisons are associated with SSB whilst Topo II poisons give rise to the formation of DSBs. Mechanistically, doxorubicin has the ability to intercalate DNA inhibiting the progression of TopIIα. Functionally, it stabilizes the TopIIα-DNA complex after it breaks the DNA chain, thus preventing DNA resealing and thereby blocking replication, causing a permanent DNA damage[49,50]. For this reason cells in the S phase of the cell cycle are the most sensitive to the cytotoxic action of doxorubicin and other topoisomerase inhibitors. Moreover, doxorubicin generates ROS which can also induce DSBs, damage membrane lipids and/or activation of apoptotic signalling[51].

I.2.3. DNA repair mechanisms

As described above, cells are continuously under assault from a wide array of DNA-damaging agents. It is essential for the optimal replication of mammalian cells a high-fidelity process that protects, corrects and assures an accurate passage of genomic information to subsequent generations. For this reason, different surveillance systems and DNA repair pathways have evolved to maintain genome integrity, assure cell survival, and prevent cancer.

However, the intrinsic cellular DNA repair mechanisms used to protect the genome can also play a role in the response to radio- and chemotherapy. In this aspect, increased rates of repair of cellular DNA damage represent an important mechanism of resistance to chemo- and radiotherapy. In the context of this thesis, modulation of DNA repair by the use of specific inhibitors has been evaluated as an attractive mechanism to modulate resistance/sensitivity to a number of anticancer agents.

Regardless the cause, upon DNA damage cells can activate systems that induce cell cycle arrest, allowing time enough to the action of the DNA damage response (DDR) to repair the lesion. DDR activates the proper DNA repair pathway, and in the case of irreparable damage, causes apoptosis[52]. Key players in DDR are considered to be the tumour suppressor protein p53, ataxia telangiectasia mutated (ATM), DNA-dependent protein kinase (DNA-PK) and poly(ADP-ribose) polymerase-1 (PARP1)[53]. The roles of PARP1 in DNA damage repair and cell survival have been investigated in the work described in this thesis.

The main pathways to repair single-strand damage, in which the strand without defect can be used as a template to guide the repair of the damage strand, are: Base Excision Repair (BER), Nucleotide Excision Repair (NER) and MisMatch Repair (MMR). Whereas the main mechanisms to repair double breaks (DSB), particularly hazardous to the cell because both strands are damaged and this can lead to genome rearrangements, include Non-Homologous End Joining (NHEJ) and Homologous Recombination (HR).
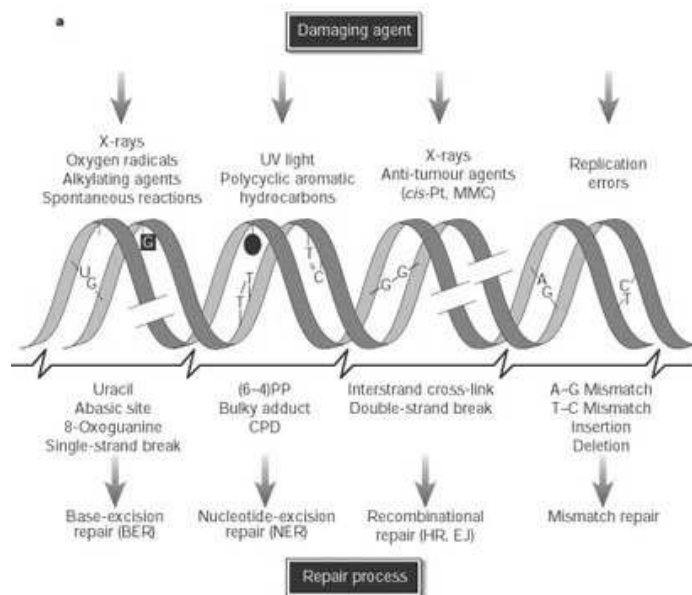
Figure I.5. DNA damage, repair mechanisms and consequences. Adapted from[54].

<u>Base Excision Repair (BER)</u> removes small alterations of bases, mainly acting against lesions due to cellular metabolism which include deamination, methylation or hydroxylation of bases and oxidation or alkylation of nucleotides due to ROS generated either by normal metabolism such as cellular respiration, or environmental stresses such as exposure to oxidizing chemicals, alkylating drugs and IR, or smoking[36]. Briefly, damaged bases are recognized and excised by a DNA glycosylase, generating an AP site which is converted by an AP endonuclease (APE1) into a single nucleotide gap, or single strand break (SSB). The SSB, or longer repair patches, are processed and filled by a DNA polymerase β and finally ligated and sealed by the XRCC1-ligaseIIIα complex[55]. The specific action of PARP1 in SSB repair is described in section "I.1.5.1. PARP1 and DNA repair".

Mismatch Repair (MMR) removes nucleotides misspaired by DNA polymerases and insertion/deletion loops, which are generated during recombination or as a result of slippage during replication of repetitive sequences[56]. Several proteins are involved in MMR, initially MSH complex recognizes the mismatch followed by the interaction with MLH1/MS2 and MLH1/MLH3 complexes[57]. Tumour cells with deficiencies in MMR have mutation frequencies higher than normal cells and present microsatellite instability[58].

Nucleotide Excision Repair (NER) recognizes and removes DNA bulky adducts and helix-distorting base modifications that interferes with DNA base pairing[54]. The most important function of NER is to remove ultraviolet-induced DNA damage, such as pyrimidine dimers, or adducts formed by chemotherapeutic agents such as cisplatin. The main members that act in the NER mechanism are the *Xeroderma pigmentosum* complementation group -A (XPA), -B (XPB), -C (XPC), -D (XPD), -F complex (ERCC1/XPF), -G (XPG) and the transcription factor IIH (TFIIH)[54]. All these proteins collaborate in recognizing and excising the damaged nucleotides and resynthesizing and ligating a new DNA strand.

Homologous Recombination Repair acts on DSB which can be caused by both; environmental stresses, such as ROS, IR, X-Ray and specific antineoplastic drugs such as anthracyclines and other topoisomerase inhibitors; and endogenous factors specially acting during the S-phase of the cell cycle or during replication of a DNA containing SSB or lesions which finally cause collapse of the replication fork[59]. The repair of DSB through this mechanism requires alignment an identical or almost identical sequence which is used as a template for the repair. The templates used in this process are present in late S to G2/M phases of

cell cycle when a sister chromatid or a homologous chromosome are available[60]. HR is a complex process that requires many proteins. Briefly, DSB are immediately and extensively marked by the phosphorylation of H2AX where BRCA1 migrates rapidly[61]. Among the different complexes in which BRCA1 acts as a scaffold protein, the RAD50-MRE11-NSB1 (MRN) complex is recruited initially for the HR repair. This complex possesses 3'-5' exonuclease activity essential for the initial processing of the 3' ends of either side of a DSB[62]. Then BRCA2 recruits and stabilizes RAD51 which act as recombinator mediators allowing the alignment of the 3' ends from the damage strand with the complementary sequence of the homologous chromosome or sister chromatid and further repair of the lesion[63,64]. Finally, and in a very simple description, the 3' end is extended by DNA polymerases and after replication resolvases ends the process by returning each strand to the original chromosome[59]. Failure of DSB repair can lead to many aberrations such as mutations, gross chromosomal rearrangements and cell death.

Non Homologous End Joining is another main pathway to repair DSB. This pathway is important before the cell has replicated its DNA, out of S and G2/M phases, when there is no available template for HR repair. NHEJ is basically the ligation of DNA ends of the DSB without need for homology. NHEJ is an error-prone repair pathway which can generate small insertions and deletions, but can also be error free when a direct ligation of the ends of a DSB occurs[65]. In the case of incompatible ends, the heterodimer Ku80/70, with sequence independent activity, binds to DNA ends and attracts additional proteins for the DNA synthesis and ligation including MRE11, RAD50, NBS1, XRCC4, Artemis and DNA ligase IV (reviewed in [66]).

I.3. ADP-RIBOSYLATION

ADP-ribosylation is a reversible posttranslational modification of proteins catalysed by a group of enzymes nowadays known as ADP-ribosyl transferases (ADPRTs or ARTs). ARTs catalyse the transference of the ADP-ribose units of NAD^+ to target proteins. The molecule of NAD^+ comprises of an ADP-ribosyl moiety that is covalently attached to nicotinamide through a β-N-glycosidic bond [67] (See Figure I.6).
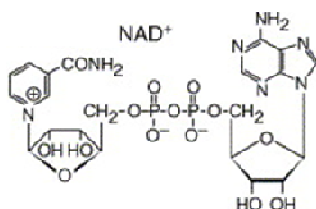
Figure I.6. Structure of NAD+ (Adapted from[67]).

I.3.1. Mono(ADP-ribosylation) and poly(ADP-ribosylation)

ARTs have been found in the nuclei and cytoplasm of many organisms[68]. In general, cytoplasmic ART enzymes form mono-ADPribosyl products, whereas nuclear ARTs are able to form longer homopolymers of ADP-ribose on target proteins, known as poly(ADP-ribosylation).

Mono-ADPribosylation reactions catalyse the transfer and covalent attachment of one ADP-ribose unit from NAD^+ to a specific amino acid residue on suitable acceptor proteins (See Figure I.7).
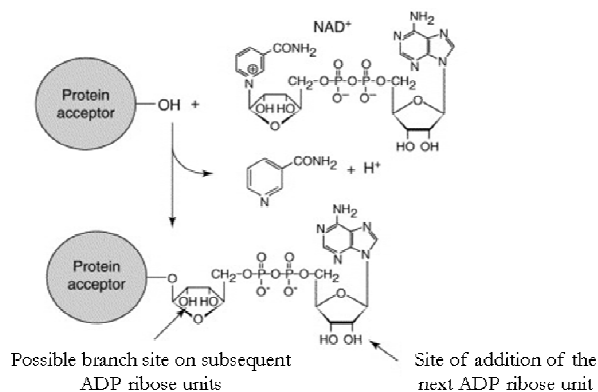
Figure I.7. Mono-ART reaction. (Adapted from[67]). Mono(ADP-ribosylation) reaction consist in the covalent attachment of the ADP-ribose moiety from NAD$^+$ to an acceptor amino acid, mainly glutamate, on the target protein. This figure also indicates the sites of attachment of the next ADP-ribose units for poly(ADP-ribosylation).

Mono(ADP-ribosylation) was first described as a pathogenic mechanism catalysed by the bacterial toxin, diphtheria. Enzymes with mono(ADP-ribosyl transferase) capacity have been found in prokaryotes, eukaryotes and viruses.[69] The residues: glutamate, arginine, asparagine, cysteine, and diphthamide (a post-translationally modified histidine) have been identified as amino acid acceptors of the ADP-ribose moiety.

A group of hydrolases have the capacity to remove the ADP-ribose molecule from acceptor proteins, regenerating free protein. This fact proves the existence of ADP-ribosylation cycles and it is likely that these cycles are involved in regulating protein activities[70].

Poly(ADP-ribosylation), unlike mono(ADP-ribosylation), is the transference of ADP-ribose moieties sequentially to an initial protein-bound ADP-ribose to form long ADP-ribose polymers. ADP-ribose

polymers constitute negatively charged molecules variable in size (from 2 to more than 200 ADP-ribosyl moieties), linear or multibranched and with different rates of synthesis and degradation[71] (Figure I.8).
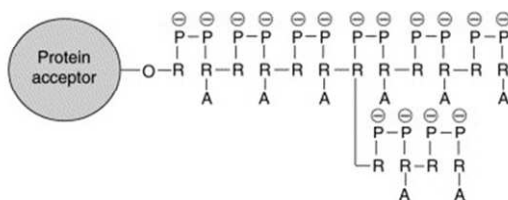
Figure I.8. Structure of poly(ADP-ribose) polymer. This figure shows the overall charge distribution of the poly(ADP-ribose) polymer. R - ribose, P - phosphate and A – adenine (Adapted from [67]).

The poly(ADP-ribosyl) transferase activity was initially referred as poly(ADP-ribosylation). It was first described by Nishizuka *et* al.[72] in 1968 as an activity associated with a chromatin-bond enzyme, the poly(ADP-ribose) polymerase (PARP), later known as PARP1, as other family members were described. First studies purifying PARP1 and assessing its poly(ADP-ribosylation) capacity[73,74], rise to describe that PARP1 is activated upon DNA damage[75,76]. For this reason, historically PARP1 and poly(ADP-ribosylation) have been studied in the context of DNA damage detection and repair. The presence of ADP-ribose-binding consensus motifs on ADP-ribose acceptor proteins overlapping functional or binding domains began to suggest the ability of ADP-ribose-binding to modulate protein activities[77]. Moreover, the discovery of new members of PARPs family evidenced that PARP1 and other described PARPs play a role in diverse biological processes such as the regulation of chromatin structure, genome stability and regulation of transcription.

29

I.3.2. Synthesis and degradation of poly(ADP-ribose) polymers

The synthesis of poly(ADP-ribose) polymers consist in three different but related ART activities:

1. <u>Initiation</u> or transfer of a mono-ADPribose moiety from NAD$^+$ to an acceptor aminoacid in the target proteins.

2. <u>Elongation</u>. Transfer of sequential ADP-ribose molecules glycosidically linked by an α (1"-2') ribosyl-ribose bond to the adenine ribose of the preceding ADP-ribose molecule to form poly(ADP-ribose) linear chains by polyARTs.

3. <u>Branching</u>: transfer of ADP-ribose moieties from NAD$^+$ to the poly(ADP-ribose) chain via a 1"-2" glycoside branch[78].

The degradation of poly(ADP-ribose) chains can be performed by at least three described enzymes. The main enzyme with ability to hydrolyse poly(ADP-ribose) polymers is the poly(ADP-ribose)glycohydrolase (PARG). PARG splits ribose-ribose linkages in the polymer to release ADP-ribose units. The PARG activity can be modulated by many factors such as the length of the polymer, the acceptor protein or the phase of the cell cycle. When the ADP-ribose synthesis is stimulated and the concentration of polymers is high, the activity of PARG is increased, explaining the short-life of these polymers in stimulated conditions (reviewed in [79]). Another structurally unrelated protein with capacity to hydrolize the glycosidic linkages between the ADP-ribose units is the ADP-ribosylhydrolase 3 (ARH3)[80]. Other enzymes that degrade poly(ADP-ribose) polymers are the poly(ADP-ribose) phosphodiesterase which degrades the phosphate bond in mammalian cells and the ADP-

ribosyl protein lyase, which cleaves the remaining ADP-ribose residue on the acceptor protein following PARG action[81]. This cycle of synthesis and degradation of poly(ADP-ribose) polymers is represented in the Figure I.9 below.
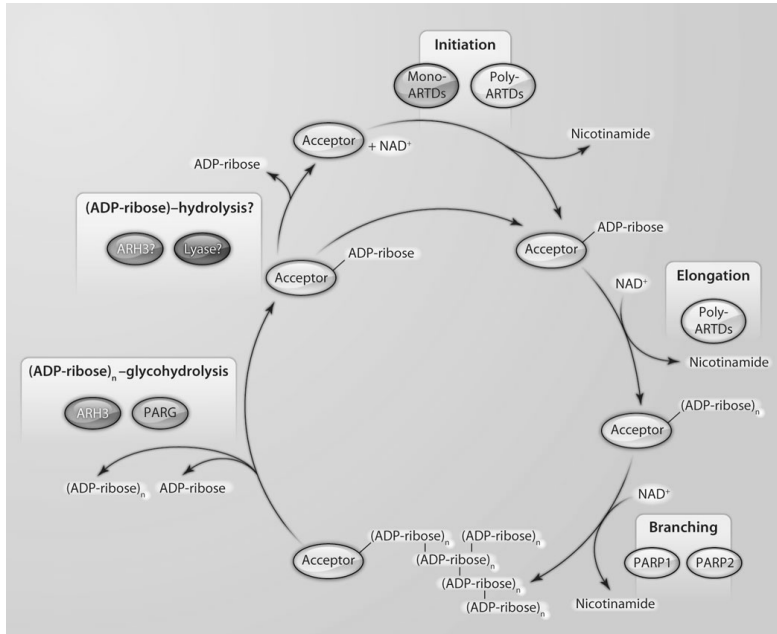
Figure I.9. Cycle of synthesis and degradation of poly(ADP-ribose)polymers. (Adapted from [82]). (Initiation) MonoARTs transfer the first ADP-ribose moiety from NAD^{+} to acceptor proteins. (Elongation) To produce linear chains, polyARTs catalyses the of linear poly(ADPribose) polymer. (Branching) To produce branched chains, polyARTs also catalyses the formation ribose *a(1'''-2'')* ribose linkages leading to the synthesis of a branched poly(ADP-ribose) polymer. (Degradation) Poly(ADP-ribose) polymers are rapidly degraded by PARG or AHR3. The last ADP-ribose residue is removed from the protein by basically an ADP-ribosyl protein lyase. The pyrophosphate bond in mammalian cells can also by degraded by phosphodiesterase.

I.3.3. PARP1 structure

The enzyme poly(ADP-ribose) polymerase-1 (PARP1; also known as ADP-ribosyltransferase-1, ADPRT-1; or Poly(ADP-ribose) synthase-1) is one of the most abundant nuclear proteins present in eukaryotes and the

most studied and founding member of PARPs family. PARP1 is a highly conserved 116kDa nuclear protein made up of 1014 aminoacids[83] which is comprised of three functional domains: the N-terminal DNA-binding domain (DBD), the central automodification domain (AMD) and the C-terminal catalytic domain (CD). These domains are highly conserved across a wide range of vertebrate species[84]. These major domains are divided into subdomains, as described below and illustrated in the figure I.10.
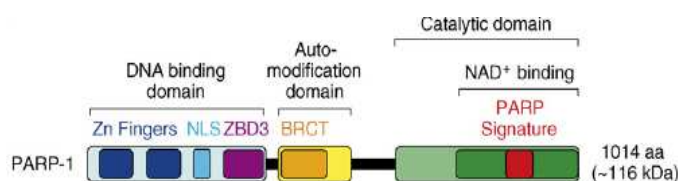
Figure I.10. Schematic representation of the three functional domains of human PARP1. (Adapted from[85]) In this figure there are schematically represented the three main structural and functional domains of PARP1: First, a N-terminal DNA binding domain containing a pair of zinc finger motifs(Zn fingers), a nuclear localization signal (NLS), and a recently identified third zinc-binding domain (ZBD3); second, a central automodification domain containing a BRCA1 C-terminus-like (BRCT) motif, and third a C-terminal catalytic domain (CD) containing a NAD+-binding domain and the highly conserved "PARP signature" motif that characterize the PARP proteins.

The DNA-Binding Domain (DBD)

The 46kDa N-terminal DBD extends from amino acid residues 1 to 373. This domain contains two zinc fingers motifs that bind to DNA, the first zinc finger mediates PARP1 activation by DSB, whereas the second by SSB[86]. Noteworthy is that these zinc finger motifs recognize altered structures in DNA rather than specific nucleotide sequences[86]. A third zinc finger has been recently described as mediator of interdomain interaction upon DNA binding[87]. It has been shown that this domain play a role in homo- and heterodimerization with other proteins including another family member, PARP2[88].

32

This domain also contains a Nuclear Localization Signal (NLS) which constitutes a PARP-1 nuclear homing signal, and a caspase recognition sequence which constitutes a cleavage site for several apoptotic caspases[89], making PARP1 a target for degradation during apoptosis, and thus the detection of its cleavage a useful marker of apoptosis.

The Automodification domain (AMD)

The 22 kDa central AMD extends from the aminoacid residues 374 to 525 in human PARP1. This region contains highly conserved glutamate and lysine residues where ADP-ribose molecules can be covalently attached[90] and modulate the activity of the enzyme[91], being PARP1 itself the major acceptor of ADP-ribose molecules. Several studies show that this domain contains several potential protein-protein binding motifs putatively involved in both homo- and heteromodification reactions believed to be crucial for PARP1 activity[92].

This domain also contains a Breast Cancer Susceptibility protein, BRCA, carboxy-terminal (BRCT) repeat motif. The BRCT motif is also present in other DNA repair and cell cycle checkpoint proteins mediating protein-protein interactions[93,94]. It has been described interaction with repair enzymes and other kind of proteins such as XRCC1[95], DNA ligase II[96], p53[97], NF-kappaB[98], DNA-polymerase α[99] and Oct-1[100] among others.

The Catalytic domain (CD)

The 54kDa C-terminal CD of PARP1 extends from the aminoacid residue 654 to 1014. This domain contains the "PARP signature" motif, a 50 amino acid sequence that is strictly conserved between vertebrates, showing 100% of homology[84]. This domain contains the substrate

(NAD⁺) binding site and mediates the transfer of ADP-ribose molecules to acceptor proteins to form the poly(ADP-ribose) polymer.

I.3.4. The poly(ADP-ribosyl)polymerases family

The presence of residual DNA-dependent PARP activity in embryonic fibroblasts from *PARP1⁻ᐟ⁻* mice led to the discovery of other poly(ADP-ribosyl)ating enzymes[101,102]. After this fact, several new PARPs were identified including PARP2, PARP3, Tankyrases-1 and 2; vault-PARP[102-104].

Up to date, PARP family is constituted by 17 homolog members. The members of the whole family were identified by searching those proteins with homology on PARP signature (GenBank XP_037275 residues 796–1014) on a non-redundant protein database from the National Center of Biotechnology Database (NCBI)[105]. These different members localize at different cellular compartments although the function of many of them remains unclear. PARP1-3 and tankyrases1-2 are primary nuclear (Reviewed in[106]), whereas PARP4, 6, 8, 9, 13-15 can be also found in the nucleus, but not exclusively. The functions of these proteins involve many cellular processes including DNA repair, cell-cycle regulation, proliferation and mitosis (Reviewed in[105-108]).

Based on the characteristics of their catalytic domain, a new classification of the PARP family members in three groups has been suggested[109]:

1- With poly(ADP-ribosyl) transferase activity: PARP-1-5 which conserve the residue Glu988 that indicates PARP catalytic

activity. (PARP5a- and -b are the classically called Tankyrase-1 and -2 respectively)[105].

2- With mono(ADP-ribosyl) transferase activity: PARP-6-8, 10-12, 14-16 which have demonstrated or putative monoADP-ribosyl transferase activity.

3- Lack of reported activity: PARP-9 and 13 which have been reported to be inactive because they lack the NAD+-binding residues and the catalytic glutamate[110].

PARP2 and PARP3 are the two closest members of PARP1 which are also thought to be related to DNA repair.

<u>PARP2</u>

PARP2 (62kDa) is the second member most described, and together with PARP1, the only that described to present polyADP-ribosyl transferase activity upon DNA damage. PARP2 has the highest similarity to PARP1 and for this reason is believed to be functionally similar[102]. In fact, it is postulated that PARP2 is involved in up to 10% of the total poly(ADP-ribose) synthesis activated upon DNA damage, which is likely to reflect a lower abundance and/or lower catalytic activity of this enzyme[88]. PARP2 crystal structure is very similar to PARP1 except in the structure around the acceptor site and the DBD, which may reflect differences in terms of affinity for substrates and/or DNA strand breaks. In this sense, PARP1 has been described to preferentially poly(ADP-ribosylate) the linker histone H1, whereas PARP2 to preferentially modify a core histone[111]. PARP2 and PARP1 can heterodimerize and interact with common nuclear proteins, such as XRCC1, DNA polβ and DNA ligaseIII, involved in different DDR processes[88].

PARP3 consists of a unique N-terminal of 39 amino acids followed by the PARP homology domain (the region identified as the PARP homology domain is the catalytic domain of PARP-1 between amino acids 524 - 1014), being the smallest protein of the PARP family[103]. By proteomic approach, PARP3 was found forming complexes with DNA repair proteins such as DNA-PKcs, PARP1, DNA ligase III, DNA ligase IV, Ku70, and Ku80[112]. Although the previous classification proposed by several authors, recently it has been characterized that PARP3 is a mono(ADP-ribosyl)transferase with ability to ADP-ribosylate itself and histone H1, and with capacity to bind and activate PARP1[113].

I.3.5. Physiological roles of PARP1

As previously mentioned, first studies about the activity of PARP1 showed that its basal catalytic activity increased over 500 times upon stimulation by DNA strand breaks[75]. These studies suggested that PARP1 and its poly(ADP-ribosyl)transferase activity might be involved in many of those cellular processes in which "DNA break" feature is present, including DNA repair, replication, modulation of chromatin structure, recombination, apoptosis, well as genomic stability. Besides, generation and study of PARP1, and other PARPs, mouse deficient models (knockout, KO) and PARP1 knocked-down cell lines has allowed, and is nowadays contributing, to better characterize the functions of this enzyme and its implication in cellular processes. The principal functions of PARP1 described from these types of studies are detailed in this section.

I.3.5.1. PARP1 and DNA repair

The observation that cells treated with DNA damaging agents depleted the intracellular levels of NAD+ [114], led years later to the confirmation by different researchers that this NAD+ depletion coincided with the utilization of this substrate for poly(ADP-ribosylation) upon DNA damage[115]. The first experimental evidence that suggested an implication of PARP1 in the BER mechanism was reported by Creissen et al[116]. This and subsequent studies proposed that PARP1 might has a direct role in DNA repair by regulating the activities of several repair enzymes and facilitating the recruitment to the DNA strand break to repair[117].

Nowadays it is accepted that PARP1 has a critical role in detection and repair of SSB, as part of the BER mechanism[118], but also has been described to be able to bind to DSB[119] playing also a role in the repair of this damage[120,121]. In this context of DNA repair, the study of *PARP1* deficient mice models demonstrate increased sensitivity to DNA damaging agents, specially to alkylating agents and IR to different extents[122,123]. Conclusive evidence for a role of PARP1 in BER was described by Dantzer et al.[124] who demonstrated that upon treatment with methylmethanesulfonate, an alkylating agent and a carcinogen, mouse embryonic fibroblasts (MEFs) derived from *PARP1-/-* mice have a reduced capacity to repair a single abasic site present on a circular duplex molecule. The DNA repair process performed by PARP1 is depicted in the figure I.11 and detailed below.

In the presence of DNA breaks, PARP1, detects the exposed ends of the DNA through its zinc fingers, leading to stimulation of the enzymatic activity of PARP1 and poly(ADP-ribosylation) of acceptor proteins and

itself. X-ray crystallography has demonstrated that the high negative charge of poly(ADP-ribose) polymer in N- and C- terminal tails of histone H1 and H2B collaborates in the relaxation of chromatin and facilitates the access of other proteins of the repair mechanism, as well as serves as an indicator of the severity of the damage to adapt the response in cell cycle arrest or apoptosis[84,125]. Among the hundreds of proteins that can be recruited, XRCC1 binds directly PARP1 and acts as a scaffolding protein that activates other BER components such as DNA polymerase β and DNA ligase III[117] that mediate the DNA repair process. The automodified PARP1, negatively charged, reduces its affinity for DNA and is then released allowing the action of the repair enzymes to seal the DNA strand break. PARP1 is rapidly regenerated following the degradation of poly(ADP-ribose) polymers[83]. Regarding DSB, PARP1 is not essential for HR or NHEJ, but can act in an alternative pathway[96].
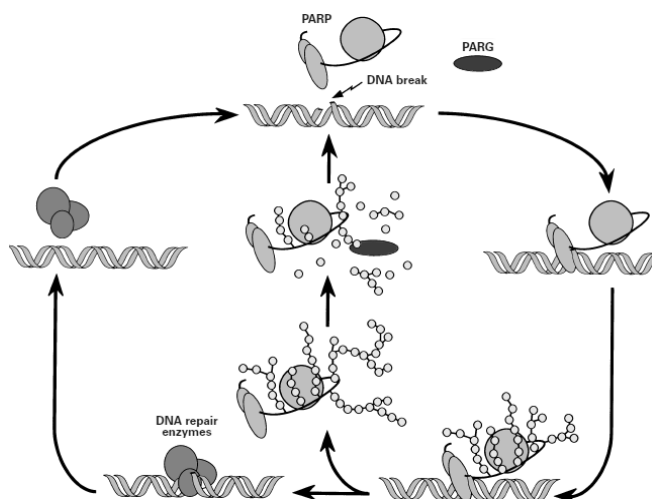
Figure I.11. SSB repair model by PARP1. PARP1 recognizes the SSB and poly(ADP-ribosylates) DNA-bindin proteins, as histones, and itself, relaxing the chromatin structure and facilitating the recruitment of DNA repair enzymes. PARP1 automodification results in loss of affinity for DNA, release from the strand under repair, and inactivation of its catlytic activity. The degradation of the polymer mainly by PARG reactivates PARP1. This diagram does not exclude the possibility that PARP1 acts as a dimer and the repair enzymes are present simultaneously with PARP1. The white beads represents the polyADP-ribose chains (Adapted from[83]).

I.3.5.2. PARP1 and chromatin structure

Nuclear processes such as replication, recombination, DNA repair and transcription require a relaxed chromatin structure to allow the access of the DNA machinery. One mechanism that allows the decondensation of chromatin is the poly(ADP-ribosylation) of histones[126]. In fact, modulation of chromatin structure was one of the first described effects of PARP1 on epigenetic modifications of the genome. In this regard is described that PARP1 blocks the binding of the linker histone H1, a repressive chromatin architectural protein, by poly(ADP-ribosylating) the histone tails[127] or by competing for binding with nucleosomes[128], the basic units of packaging DNA in eukatyotes around a histone protein core[129]. This modification of histones leads to electrostatic repulsion which displaces them from DNA allowing the access of other proteins. Furthermore, PARP1 can also affect chromatin structure, and hence the transcription, by other mechanism such as increasing the recruitment of HMGB1[130], a chromatin architectural protein that enhances transcription.

I.3.5.3. PARP1 and genomic stability

To study the role of PARP1 in the surveillance and maintenance of genomic stability many models of PARP1 deficient mice and PARP1 depleted cell lines has been used. First studies with PARP1 depleted HeLa cell lines observed alterations in cell morphology, chromatin structure and DNA repair mechanisms suggesting the involvement of PARP1 in genomic stability[131].

In this context, studies with PARP1 depleted mice found that PARP1 is important in processes such as chromosome segregation, telomeres

integrity and DNA recombination, whose defects might lead to genomic instability and cancer. Some experimental results in this regard have described that *PARP1*^{-/-} cells from different tissues exhibit telomere shortening and increased frequencies of chromosome fusions and aneuploidy[132] and that PARP1 localizes peri/centromeric heterochromatic region[133] allowing the maintenance of centromeric heterochromatin structure.

I.3.5.4. PARP1 and cell death

In contrast to the survival role of PARP1 in a context of mild DNA damage by facilitating the repair of DNA lesions, PARP1 collaborate in promoting cell death in the presence of extensive DNA damage. Depending on the cell type, the strength, duration and type of genotoxic stimuli PARP1 may facilitate cell death by apoptosis or by necrosis[134]. A schematic representation of these three cell fates is represented in the figure I.12.

Many studies have shown that PARP1 is cleaved during apoptosis by caspase-3 and -7[135,136] in two fragments that separate the DNA binding domain from the catalytic domain, thus inactivating PARP1. PARP1 cleavage is a useful marker of apoptosis. The aim of cleaving PARP1 in a situation of DNA damage is to prevent its overactivation and preserve the cellular energy for certain ATP dependent steps of apoptosis. Other studies have shown that PARP1 also play a role in caspase-independent apoptotic cell death by triggering the translocation of AIF (Apoptotic Inducing Factor) from the mitochondria to the nucleus which mediates the classical DNA fragmentation in apoptotic cell death[137].

In the presence of more severe DNA damage, PARP1 hyperactivation leads to necrotic cell death. This overactivation results in a massive poly(ADP-ribose)polymer synthesis which implies large NAD^+ consumption[138]. Because NAD^+ is required in many metabolic pathways, cells attempt to recover NAD^+ levels through a reaction that, in excess, depletes the levels of ATP and finally induces necrotic cell death[139]. It is also suggested that other factors such as the intracellular acidification caused by the increase of H^+ ions, product of NAD^+ catabolism, may collaborate in necrotic cell death[140]. Besides this energy depletion, the high levels of ADP-ribose molecules generated in the degradation of poly(ADPribose) polymers by PARG may be further hydrolysed by other enzymes into phospho-ribose and AMP. This results in a dramatic increase in the cellular AMP:ATP ratio which, by specific pathways, can induce cell autophagy[141]. The role of PARP1 in necrosis is consistent with the fact that PARP1 depletion protects from disease models characterized by necrotic cell death such as stroke, myocardial infarction or ischemia-reperfusion injury.
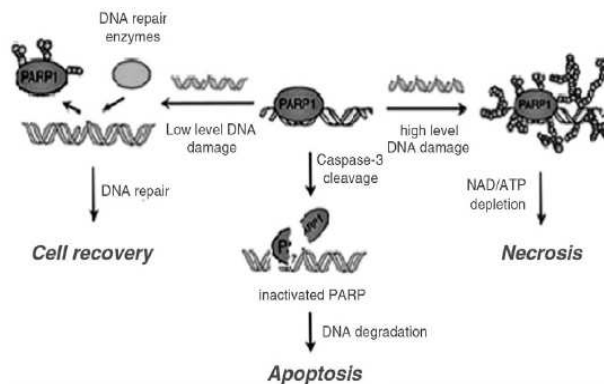
Figure I.12. Survival, apoptosis or necrosis, the three cell fates depending on the level of DNA damage. In low DNA damage conditions, poly(ADP-ribosylation) collaborates in DNA repair and survival of the cell; in more intense genotoxic stimuli the apoptotic pathway might be activated; whereas massive DNA damage may induce excessive PARP1 activation depleting cellular NAD^+/ATP and cell death by necrosis. Adapted from[142].

I.3.5.5. PARP1 and transcription

Many studies describe the role of PARP1 in the regulation of gene transcription and its implication in the regulation of cellular processes. As many as four modes of transcription regulation by PARP1 has been described including modulation of chromatin structure and composition, enhancer binding, transcriptional coregulation and insulation (Represented in the figure I.13).
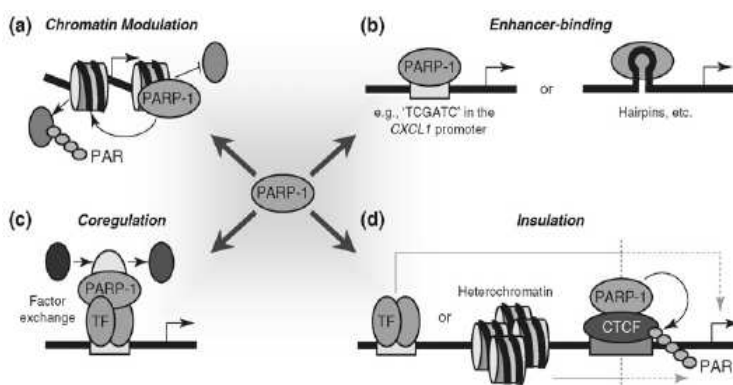
Figure I.13. Modes of transcription regulation by PARP1. PARP1 regulates transcription in at least four modes: (a) Modulating chromatin structure by modifying histones, binding to nucleosomes or regulating its composition; (b) Acting as a classical enhancer-binding factor, by binding to specific sequences or structures in the DNA; (c) Acting as a classical co-activator/repressor, by promoting the recruitment or release of stimulatory factors; (d) As a component of insulators, by limiting the effects of enhancers on promoters or preventing spread of heterochromatin.

The role of PARP1 in the regulation of <u>chromatin structure</u> to alter the accessibility of proteins that mediates gene transcription has been commented previously.

PARP1 can also act as a classical <u>enhancer-binding factor</u> through its binding to specific sequences or DNA structures in the regulatory regions of target genes. For example, PARP1 gene expression is autoregulated by direct binding of PARP1 protein to hairpins in its promoter region[143]. Other studies show that PARP1 can bind to specific sequences upstream of the CXCL1 promoter region and inhibits its expression by preventing the binding of the transcription factor NFkappaB[144].

Regarding the <u>coregulator function</u> of PARP1, diverse mechanisms which vary depending on the activator or the regulated gene have been described. This promoter specific coregulator function, that can be either coactivation or corepression, has been shown for different sequence-specific DNA-binding transcriptional regulators. In some studies, the coregulatory activity does not require PARP1 enzymatic activity, as shown with NFkappaB[98], Oct-1[100], B-Myb[145], RAR[146] and HTLV Tax-1[147], whereas in others it is necessary, as occurs with HES1[148], Sp1[149], NFAT[150,151] and Elk1[152]. In other studies in vitro, poly(ADP-ribosylation) inhibits the binding to DNA of transcription factors such as NFkappaB, YY1[153] and TBP[83]. When acting as a coregulator, PARP1 can behave as a promoter specific "exchange factor", promoting the release of inhibitory factors and the recruitment of stimulatory factors during signal-regulated transcriptional responses. Different studies show this function of PARP1[130,146,148].

Finally, several studies show that PARP1 can act as a component in <u>insulator function</u>. Insulators are DNA elements that organize and protect the genome in regulatory units that prevent distal enhancers from activating a promoter, or block the spread of heterochromatin preventing the silencing of a gene[154]. In this regard PARP1 has been implicated, for example, in poly(ADP-ribosylation) of CTCF, a ubiquitous DNA-binding

protein that plays a role at insulators, collaborating in the preservation of insulator function of CTCF[155].

Regarding factors that can modulate PARP1, many signalling pathways affect PARP1-dependent transcriptional process. Signals such as cytokines, heat shock proteins and kinases (CaM kinase IIδ and ERK2)[148,152] can finally result in post-translational modification of PARP1 by auto-pADPribosylation[152], acetylation[156], or phosphorylation[157].

Among the different genes that by these mechanisms may be regulated directly or indirectly by PARP1, we highlight two genes of interest in this thesis: HER2 (ErbB2) and EGFR. Literature on this specific topic is not abundant and is briefly detailed below.

Kitamura et al.[158] showed that PARP1 and HER2 are highly expressed in rheumatoid synovial cells. Taking into account that HER2 is an important target gene of NFkappaB, and PARP1 can coregulate this transcription factor, they demonstrated that PARP1 binds to NFkappaB and activates the transcription of *ERBB2* gene, probably by stabilizing the transcription complex, whereas the depletion of PARP1 with siRNA, reduced HER2 expression in synovial cells[158].

Regarding the regulation of EGFR expression by PARP1, a study in hepatocarcinoma cell lines showed that PARP inhibition in tumour xenografts and cell lines, and PARP1 knockdown with siRNA produced a reduction in the expression of EGFR among other tumour-related genes such as MDM2 and HIF2α[159], suggesting a coregulation of NFkappaB by PARP1 behind these genes modulations.

I.3.5.6. PARP1 in inflammation and angiogenesis

Many studies show that PARP1 plays a role in important processes such as inflammation and angiogenesis whose alteration is frequently linked with the development and progression of cancer.

Regarding the inflammatory response, it is widely described that PARP1 regulates the expression of various proteins related with the development of inflammatory cell injury[160]. Much of PARP's role in this process is as transcriptional coregulator of NFkappaB to coactivate the expression of AP-1 and proinflammatory target genes such as *iNOS*, *ICAM-1*, *MIP-1a* and *C3*[161]. Studies in *PARP1-/-* mice show protection from inflammatory injury as a result of impaired transcription of NFkappaB pro-inflammatory target genes[162], as well as decreased expression of cytokines, adhesion molecules and reduced tissue infiltration with phagocytes in various resistance models of inflammation[161]. In addition, PARP1-induced necrotic cell death releases intracellular components to the surrounding tissues that also collaborate in promoting inflammation.

Regarding angiogenesis, several studies links PARP1 with this function by means of transcription regulation of key genes in this process. Different studies showed that inhibition of PARP1 induced antiangiogenic effect by reducing the vascular endothelial growth factor (VEGF)-induced proliferation, VEGF expression *in vitro* or impairing the blood vessel neo-formation in response to antiangiogenic stimuli *in vivo*[163] [164]. Moreover, *PARP1-/-* mice displays defects in growth factor-induced angiogenesis[165]. Studies with PARP1 depleted cell lines inoculated in xenografts also show a reduced expression of angiogenesis markers and of proinflammatory mediators[166].

I.4. PARP1 IN CANCER

I.4.1. PARP1 in *in vivo* models of cancer

Given the relationship between PARP1 and the surveillance of the genome, and taking into account that *PARP1⁻/⁻* show an increased spontaneous genomic instability and higher sensitivity to DNA assaults, it is logical to link missregulation of PARP1 and cancer.

By studying the role of PARP1 in chemical-induced carcinogenesis studies, PARP1 deficient models and in combination with deficiencies in other essential genes, the field of PARP's research is attempting to define the implication of this enzyme in cancer.

I.4.1.1. Chemical carcinogenesis

Studies with animal models of carcinogenesis induced with chemicals revealed that PARP inhibition sensitizes to carcinogenic drugs. In this regard, the PARP inhibitor 3-aminobenzamide (3-AB) sensitized liver to carcinogenesis induced by diethylnitrosamine[167], phenobarbital[168]. 3-AB also accelerated skin tumours in UV light exposed mice[169], and induced pancreatic β-cell tumours upon streptozotocin or alloxan treatment in rats[170]. Furthermore, PARP1 deficient mice treated with the carcinogenic agent nitrosamine also showed an increase in formation of sarcomas and adenomas[171]. However, it is worth noting that the underlying mechanism of carcinogenesis in PARP1 KO mice and PARP inhibitor treated mice may be different, since in the model of PARP1 inhibited, the enzyme is still present and can be bound to DNA strand breaks blocking the access of other repair enzymes, whereas in *PARP1⁻/⁻* model PARP1 protein is

absent and no interferes with other enzymes or alternative mechanisms of repair.

I.4.1.2. Tumour susceptibility in *PARP1* knockout models

PARP1 KO mice develop normally, are fertile and exhibit higher genomic instability, but in spite of this it is not prone to develop tumours[122,123,172], suggesting that other alterations apart from the genomic instability resulting from the absence of PARP1 are required to cause oncogenesis. In addition, several studies have shown that the genetic background and even the strain of the mice model appear to play a relevant role in tumour incidence and spectrum in mice. In this line, *PARP1^{-/-}* on specific mice background exhibited, in low frequency and late onset, higher tumour incidence and wide spectrum of tumours, mainly adenomas, carcinomas and hepatocellular carcinomas [172-174].

I.4.1.3. Tumour susceptibility in *PARP1* KO models in different genetic backgrounds

In agreement with the cooperation of PARP1 with other DNA repair molecules, when in *PARP1* KO mice other essential molecules, such as p53, Ku80 and DNA-PKc, are also removed, higher incidence of tumours of wide spectrum and in an earlier onset is observed[174-178]. In the case of *PARP1^{-/-} P53^{-/-}* and *P53^{+/-},* high frequency of mammary gland, prostate, uterus, liver, brain and skin carcinomas were detected. When PARP1 deficiency was combined with DNA-PK or Ku80, mice developed tumour lymphomas with a high incidence.

The results from these and other studies suggest that the molecular mechanisms of malignant transformation by PARP1 deficiency in mice might be due to telomere dysfunction and a resulting chromosomal instability that would facilitate the loss of tumour suppressor genes and oncogene activation.

I.4.2. PARP1 in human cancer

Although PARP1 in animal models appears to protect against carcinogenesis-induced, it remains unclear the role of PARP1 in human cancers. Studies on patterns of expression of PARP1 protein, mRNA and gene status in human tumour samples and cancer cell lines that are contributing to elucidate this question are reviewed below.

I.4.2.1. *PARP1* gene status, mutations and polymorphisms

One hallmark of cancer is the activation of oncogenes and the inactivation of tumour suppressor genes which might disrupt essential processes as cell division and differentiation leading to development of cancer. Regarding tumour suppressors, the mutation of one allele and the loss of the other allele ("Loss Of Heterozygosity, LOH") are the initial mutational events for cancer to develop.

PARP1 gene is located at position 1q41-42, consists of 23 exons and spans approximately 43kb[179]. Based on its described functions and the results in carcinogenesis-induced animal models, *PARP1* could be considered as tumour suppressor, but to date genetic studies on copy number alterations in mammary carcinomas have not reported any LOH

of *PARP1* gene[180]. Whereas, contrary to the previous hypothesis, the amplification of the chromosome 1q, where *PARP1* localizes, is frequently found[181-183].

In terms of mutations in *PARP1* gene and according to the Catalogue Of Somatic Mutations In Cancer (COSMIC) from Sanger Institute[184], mutations in this gene does not appear to be really frequent. Only 12 distinct mutations (1 deletion and 11 substitutions) have been described in a total of 720 unique samples and uploaded to the database to date, including samples in breast (2), lung (3), ovary (2), skin (3) and upper aerodigestive tract (2).

Moreover, while a mutation is defined as any alteration in the DNA sequence somatically acquired (present in the tumour sample but absent in the normal tissue), a single nucleotide polymorphism (SNP) is a single base alteration in any genetic location at which at least two different sequences are found and are present in at least 1% of the population[185]. When a polymorphism is located in the coding region of a gene sometimes it could affect features of the expressed protein. Therefore, polymorphisms in *PARP1* gene could affect its transcription, the enzymatic activity or even the mRNA stability as well as the resulting protein expression levels.

In this context, several studies have associated SNP in *PARP1* gene and cancer. The most described SNP in *PARP1* gene is the T2444C that results in an amino-acid *Val762Ala* located in the PARP1 catalytic activity domain[186]. This variant exhibits a 30-40% decrease in enzymatic activity and a reduced interaction with XRCC1[187,188]. Studies in breast show that the SNP *Val762Ala* does not associate with higher risk of

breast cancer, probably due to the limited sample size of theses studies[189,190], but associates with higher risk to develop prostate cancer[187], oesophageal[191] and lung cancer[192]. In the case of breast cancer, it has been reported other polymorphisms situated upstream near the transcription initiation site where multiple promoter elements and binding site of transcription factors are located which might influence the transcription efficiency of *PARP1*[189,193,194].

I.4.2.2. PARP1 mRNA and protein expression in human samples

Beyond the animal or cellular models, to study the expression and activity of a given protein directly in human tissues and associate with the clinicopathological data of the samples allow to further describe in a more realistic manner the role of a protein in vivo.

The study of PARP1 expression in human samples has been mainly performed by using genetic approaches to determine: gene amplification, by Comparative Genomic Hybridization arrays (aCGH), and mRNA levels (by qRT-PCR and gene expression microarrays). There are fewer studies describing the levels of PARP1 protein, by Western Blot (WB) or by IHC, and/or its enzymatic activity (by enzymatic assays or immune detection of polyADP-ribose).

Expression in non-tumour tissues

In most of the non-tumour tissues PARP1 expression is low. In the Ossovskaya et al.[195]. study, PARP1 levels assessed by microarray analysis in histologically normal tissues exhibited low and uniform expression across a variety of tissues including breast, endometrium, lung, ovary, skin, colon, prostate and stomach among others. Only lymphoid tissues,

such as lymph node, B lymphocytes adenoids, thymus and spleen exhibited higher expression of PARP1 compared with other normal tissues, probably due to the increased frequency of recombination and genetic events during differentiation of B-cells where PARP1 is required[195]. Other previous studies show similar results regarding expression in normal tissues[196].

Expression in tumour tissues

mRNA expression studies

In the case of human tumours, the expression of PARP1 is mainly upregulated compared with normal tissues. In one of the first studies performed with primary human breast carcinomas (n=35), PARP1 mRNA was overexpressed in 57% (20/35) of tumour samples, and in those tumours with the highest PARP1 expression, the 70% (7/10) presented PARP1 locus amplification[197]. Amplification of the PARP1 locus has been also described in hepatocellular carcinoma[198]. In terms of mRNA overexpression, enhanced levels of PARP1 might be a common characteristic of human malignant lymphoma[199] and colorectal cancer[180] compared with adjacent non-tumoral tissue.

In the previously cited Ossovskaya et al.[195] study a wide variety of primary human cancers were also analyzed including breast, endometrium, lung, ovary and skin cancers, and non-Hodgkin's lymphoma, and was confirmed that PARP1 mRNA was elevated in many human primary malignancies compared with normal tissues. In the case of breast cancer samples, 30% of the Infiltrating Ductal Carcinoma (IDC) demonstrated a significant upregulation of PARP1 mRNA.

Another recent meta-analysis carried out in a large public retrospective gene expression data set from breast cancers reported that PARP1 mRNA was overexpressed in over 50% of the samples and the overexpression was associated with basal subtype and with poor metastasis-free survival and Overall Survival (OS)[200]. Other studies also associates overexpression of PARP1 and poor prognosis as in the case of ovarian carcinoma[201] and melanoma[202]. As an exception, there is another study of pancreatic adenocarcinoma in which PARP1 does not appear to be a marker of poor prognosis[203].

Protein expression and enzymatic activity studies

Less studies have determined the levels of PARP1 protein and its enzymatic activity in a single and exhaustive study.In Ewing's sarcoma cells a study with these characteristics was performed. In these cells, high levels of PARP1 mRNA correlated with high levels of PARP1 protein and high enzymatic activity[204]. Which are the mechanisms that could contribute to the upregulation of PARP1 levels, not only in Ewing's sarcoma, but also in other cases of tumours with PARP1 overexpression, is an important question to be answered. No gross amplifications or rearrangements of the gene were observed by the authors[204]. In this line Soldatenkov et al.[205] identified multiple binding motifs for the ETS transcription factors in the promoter region of PARP1 gene, which causes an increase of the mRNA transcription of PARP1, this correlation was observed not only in Ewing's sarcoma cells but also in other cell lines such as cervical carcinoma (HeLa), lung carcinoma (A4573) and laryngeal squamous carcinoma (SQ-20B) cell lines. Enhanced PARP1 enzymatic activity has been also reported in tumour tissues compared with non-tumour adjacent tissue in hepatocellular carcinomas[206], colon carcinomas[207], cervical cancer[208] and non-Hodking lymphoma[209].

Although other studies associated low poly(ADP-ribose)polymer formation with breast, colon, lung[210] and laryngeal cancer[211].

Few studies have analyzed PARP1 protein levels in tumours. Increased expression of PARP1 by Western Blot has been found in hepatocellular carcinoma compared with non-tumour portions, being greater in the less differentiated tumours[212]. PARP1 overexpression by IHC has been also reported in intestinal adenomas of patients with familial adenomatous polyposis[213], early stage of colorectal carcinogenesis[180], ovarian carcinoma[201] and melanoma[202].

To understand the meaning of PARP1 mRNA, protein and activity levels in cancer and to elucidate whether its overexpression, specifically in breast, is a cause or a consequence of the development of human cancer is one of the main goals of this thesis.

I.4.3. PARP inhibition as a target in breast cancer

Observing that PARP1 is dramatically activated upon DNA damage caused by IR and DNA-alkylating agents, great interest appeared in generating PARP inhibitors and examining the effects of these in combination with DNA-damaging agents as a strategy to potentiate the cytotoxicity of these treatments and sensitize cancer cells. Moreover, PARP inhibitors were considered not only likely to be useful in the treatment of diseases related to genomic integrity, but also in the treatment of stress and inflammatory responses, where PARP1 overactivation is one of the causes of these diseases.

Therefore, the development of PARP inhibitors has become a valuable clinical tool.

I.4.3.1 PARP inhibitors

The vast majority of the PARP inhibitors act as competitive inhibitors of the enzyme by mimic the nicotinamide moiety of NAD^{+}, thus blocking its binding to the PARP catalytic domain and preventing the poly(ADP-ribosylation) of proteins and the automodification, with the consequent effects of this alteration (reviewed in[214]).

The development of PARP inhibitors began more than 30 years ago. Initially were used only for research purposes to study the function of PARP, later on, with the growing interest in using PARP inhibitors for therapeutic treatments many new and improved inhibitors were developed by different pharmaceutical companies and entered in clinical trials in humans.
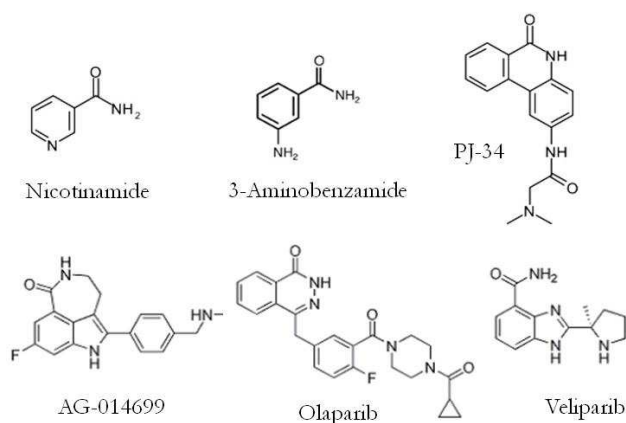
Figure I.14. Structures of the main PARP inhibitors from the three generations. Chemical structures of nicotinamide, 3-Aminobenzamide, PJ-34, AG-014699, olaparib and veliparib.

The classical or first generation of PARP inhibitors exhibit very low potency and exert non-specific effects. Nicotinamide, one of the products of PARP1 NAD^+ catalysis, was the first compound to be described as a PARP inhibitor[215]. But this product weakly inhibits PARP and interferes with many cellular pathways where NAD^+ is used[216]. Analogues of nicotinamide, such as benzamide and 3-subtitute analogues were the next to be developed[217]. These inhibitors showed increased specificity and potency at millimolar concentrations, but it was an improved analogue, the 3-aminobenzamide (3-AB), with enhanced solubility in water and an IC_{50} in vitro in the micromolar range[218], the first PARP inhibitor to be extensively characterized.

For the next generation of PARP inhibitors developed in the 1990', several structural requirements for inhibiting PARP with greater specificity and potency were elucidated[219]. These second generation of inhibitors are classified as analogues of benzamides and include compounds with different biochemical, pharmacokinetic and PARP selectivity properties, such as phenanthridines (PJ-34), only used in research[220].

The third generation PARP inhibitors are mostly derived from the 3-AB structure and exhibit improved potency and pharmacokinetics[221]. These new generation includes different types of molecules such as benzimidazoles (ABT-888 or veliparib)[222], dihydroisoquinolinones (INO1001)[223], pthalazinones (AZD-2281 or olaparib)[224], tryciclic indoles (AG-014699)[225] as well as other recent structural derivates or not disclosed structures (BSI-201 or iniparib). These inhibitors exhibit different chemical structures and bioavailability, having in general a short-half life which requires frequent doses[222]. Most of them are been tested

tested in clinical trials. Surprising finding was that one of the putative
PARP inhibitors (iniparib) that underwent phase III clinical testing was
later on reported that did not inhibit PARP1/2 activity. This exemplifies
the insufficient preclinical and translational work available prior to a
clinical trial design.

I.4.3.2. Therapeutic rational for targeting PARP

The inhibition of PARP in vivo is thought to exert its antitumoral effects
through at least two different and complementary effects:

- Synthetic lethality
- Chemosensitization.

These two approaches have been studied preclinically in different types
of cancer and different generations of PARP inhibitors as discussed in
the following sections and depicted in the figure I.15 below.
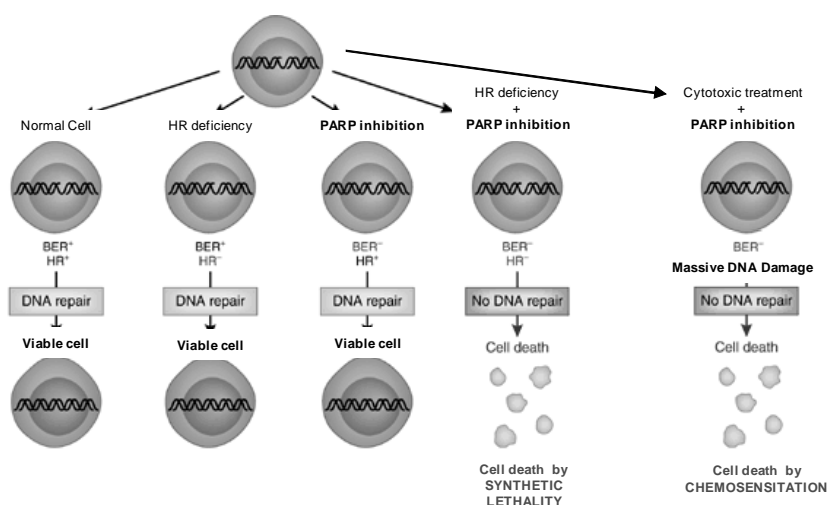
Figure I.15. PARP inhibitors as treatment for cancer. Two approaches for
cancer treatment with PARP inhibitors: Synthetic lethality: The inhibition of Base
Excision Repair (BER) with PARP inhibitors causes cell death in those cells with
deficiencies in the Homologous Recombination (HR) repair. Chemosensitation: The
DNA damage and cell death induced with cytotoxic treatments is potentiated with
PARP inhibitors. (Adapted from[226]).

I.4.3.2.1. Synthetic lethality. The single agent approach

The concept of synthetic lethality was first described in 1946 in genetically modified organisms, in which 2 non-lethal genetic mutations are not critical for cell survival when occur individually, but result lethal when both occur in the same cell[227].

Taking into account that many tumour cells carry specific genetic lesions or defects in essential pathways, many studies in cancer therapy are trying to find which could be the "synthetic lethal partners" in these tumour cells (reviewed in[228]). The application of this concept in the clinic should lead to more selective tumour cell death, whereas non-tumour cells should not suffer major side effects of cancer therapy as occurs with chemotherapy, as well as allowing treatments with large therapeutic windows.

In the context of PARP inhibitors, the synthetic lethal effect occurs when a cell with deficiencies in HR repair is treated with a PARP inhibitor. In these cells, persistent SSBs, which cannot be repaired because of the presence of the inhibitor, will result in DSBs during DNA replication. These DSBs, that in normal cells can be efficiently repaired, in cells with HR deficiencies cannot. The accumulation of DSB is fatal for these cells which result in chromatid instability, cell cycle arrest and eventually cell death[229].

BRCA1/2 deficiency

The classical synthetic lethal partners in PARP inhibition are BRCA1 and BRCA2 proteins which, as described previously, play important roles in

cell cycle control, transcription regulation and DSB repair by HR, and therefore in the maintaining genomic stability (reviewed in[230]).

Recent studies are trying to describe the mechanisms which might explain the synthetic lethality behind the specific targeting of BRCA-deficient cells with PARP inhibitors. One possibility explaining this strong relation between PARP inhibition and BRCA is that PARP1 is also involved in HR repair at replication forks, hence the absence of both is critical for the cell[231].

Preclinical research has been conducted to prove the hypothesis of synthetic lethality. Two pivotal studies demonstrate this concept. On one hand, Farmer et al. showed that the decrease of PARP1 levels with RNA interference causes a higher reduction in clonogenic survival in BRCA1- and BRCA2-deficient embryonic stem cells compared with wild type cells[232]. This result suggested that PARP inhibitors might have similar effects. In this line, clonogenic survival assays demonstrated that *BRCA1*-/- and *BRCA2*-/- cell lines were extremely more sensitive to potent PARP inhibitors (KU0058684 and KU0058948), in contrast to wild type (*BRCA*+/+) or heterozygous (*BRCA*+/-)[232]. In the other hand, Bryant et al similarly observed that PARP inhibitors (NU1025 and AG14361) were dramatically cytotoxic in the V-C8 BRCA2-deficient cell line compared to the wild-type V79 cell line[233]. Furthermore, depletion of BRCA2 mRNA with RNA interference in MCF7 and MDA-MB-231 also led to high sensitivity to PARP inhibition. In addition, xenograft models with V-C8 BRCA2-deficient cell line also presented significant response to AG14361[233]. More recent studies show that BRCA1/2-deficient mammary tumors, and derived cell lines, are more sensitive to PARP inhibition (with olaparib) than proficient cell lines[234,235].

Moreover, it should be noted that the selective sensitivity of BRCA1/2-deficient cells is dependent on the specificity and potency PARP inhibitor used. This may explain controversial results obtained with a BRCA2-deficient pancreatic cancer cell line, CAPAN-1, which was sensitive to KU0058948, but not to less potent and less specific PARP inhibitors such as 3-AB and NU1025[236,237].

These studies reflect no selective effect of PARP inhibitors on BRCA1^{+/-} or BRCA2^{+/-} cells lines. Considering that the normal tissue in BRCA-deficient patients is heterozygous for the mutation, whereas tumour does not express the functional protein due to LOH, this might support that the effects of PARP inhibitors might be restricted to the tumours.

Unfortunately, it has been observed that tumours with frame-shift BRCA1/2 mutations can restore the expression and HR function of these proteins through secondary intragenic mutations that restores the open reading frame. This recovery of BRCA function/expression results in a mechanism of acquired resistance to PARP inhibitors and chemotherapy (commented in[238]).

BRCAness phenotype

In addition to BRCA-mutants, which represent most of the hereditary breast and ovarian cancers, a large proportion of sporadic breast cancers (and other cancers) exhibits other mechanisms of BRCA deficiency and/or other defects in HR repair components. This phenomenon has been described as "BRCAness"[239]. These BRCA-like sporadic tumors have become another potential target for PARP inhibitors, assuming that they might respond similarly to the aforementioned synthetic lethality.

In this context, several mechanisms have been described in the inactivation of BRCA pathway in these BRCA-like tumors:

BRCA1 gene can be inactivated by promoter methylation. In fact, 10-15% of sporadic tumours harbour BRCA1 promoter methylation which correlates with undetectable BRCA1 expression[240,241]. Other possible, and less referenced, mechanism responsible for low BRCA1 protein expression might be by inhibition of transcription and translation of BRCA1 gene. In this line, it has been described that overexpression of HMGA1 proteins, which act as architectural proteins enhancing or inhibiting gene transcription, or ID4, a negative regulator of BRCA1, can result in downregulation of the BRCA1 promoter activity[242,243]. Alternatively, several microRNAs (miR) have been also implicated in the inactivation of BRCA1. miR, which are able to negatively regulate mRNA translation by binding to the 3' untranslated region (3'UTR), are implicated in cancer. In addition, polymorphisms in this region have been associated with higher susceptibility to specific cancers. In the case of BRCA1 gene, variants in the 3'UTR region and specific miR have been associated with a reduced BRCA1 activity and sporadic breast cancer[244,245]. In this line, a recent study demonstrates that miR-182-mediated downmodulation of BRCA1 reduces DNA repair capacity and sensitizes cells to PARP inhibition[246].

In the case of BRCA2 it is unclear whether its function is disrupted in sporadic cancers. No evidence for epigenetic silencing by hypermethylation of its promoter has been observed in breast cancer[247]. In contrast, a potential mechanism for BRCA2 inactivation is the overexpression of *EMSY* gene, which has been implicated in suppression of BRCA2 transcription regulation activity[248]. Overexpression of the

EMSY gene has been reported in 13% of sporadic cancer correlating with worse survival[248].

Studies of gene-expression profiling of breast tumors have found that most of the BRCA1-mutated breast cancers associate with basal-like intrinsic subtype, suggesting a similar aetiology for both[26,249]. Taking into account that the microarray defined basal-like intrinsic subtype overlaps up to 80% with the IHC defined TNBC, it has been observed that BRCA1-mutated, basal-like and TNBC share clinical and pathological similarities, including high rates of p53 mutation, aneuplody, high pathological grade and relative sensitivity to DNA damaging agents as shown in the table I.1 (reviewed in [250]). These findings led to suggest a possible rationale use of PARP inhibitors in TNBC subtype

.

Table I.1. Shared clinic-pathologic features between Hereditary BRCA-1 breast cancer and triple negative/Basal-like breast cancer.

Clinico-pathologic Characteristics	Hereditary BRCA1 Breast Cancer	Triple Negative/Basal-like Breast Cancer
ER/PR/HER2 status	Negative	Negative
TP53 status	Mutant	Mutant (Up to 80%)
BRCA1 status	Mutational Inactivation	Diminished Expression (?)
Gene-expression patterns	Basal-like	Basal-like
Tumor Histology	Poorly-differentiated (high grade)	Poorly-differentiated (high grade)
Chemosensivity to DNA-damaging chemotherapy	Highly sensitive	Likely sensitive
Genome-wide Aneuploidy	Yes	Yes

Some preclinical studies supported this hypothesis. A study working with cell lines representing the different subtypes of breast cancer showed that BRCA-mutated and basal-like breast cancer cells were defective in BER upon oxidative DNA damage and this defect conferred sensitivity to a PARP inhibitor[251]. In a parallel study using the same panel of cell lines, the basal-like cells were sensitive to platinum and gemcitabine which

synergized when were combined with a PARP inhibitor, a fact that did not occur with luminal cells[252]. Given these results, TNBC were included in clinical trials with PARP inhibitors, regardless of BRCA or BRCAness status.

Expanding the rationale of synthetic lethality beyond BRCA1/2, it is possible that deficiencies in those genes with non-redundant functions in DSBs repair could make cells sensitive to PARP inhibitors. In this line, in the previously mentioned study of Bryant et al, defects in XRCC2 and XRCC3 also conferred high sensitivity to PARP inhibition[233]. Furthermore, disruption in other critical HR repair components such as: RAD51, RAD54, DSS1, RPA1, NSB1, ATM, ATR, CHK1, CHK2, FANCD, FANCA, FANCC, or Aurora-A overexpression, has been shown to hypersensitize to PARP inhibition[253-255].

I.4.3.2.2. Chemosensitization. A combined approach with cytotoxic therapies

The other therapeutic rational approach for targeting PARP is to combine it with cytotoxic therapy (i.e. DNA damaging agents, or IR). As commented in the beginning of the section "PARP inhibition as target for breast cancer", the use of these inhibitors in combination with DNA damaging agents was one of the first applications tested in cancer cells. Remember that DNA damaging agents exert their antitumoral effects if the DNA damage induced in the tumour cells cannot be repaired and ends up causing cell death. However, to some extent, cells have the ability to repair the DNA damage caused by genotoxic stress, leading to partial resistance to chemotherapy. For this reason, to target a key component in

DNA repair, PARP, is a good approach for reducing resistance and enhancing antitumoral effects of cytotoxic therapy.

There is a large body of evidence demonstrating that preclinical and clinical PARP inhibitors sensitize to chemotherapies. The first studies with non-clinical PARP inhibitors reported positive results when combined with different types of DNA-damaging chemotherapeutic agents (reviewed in [256]). Experimental data in this regard reported sensitization to: topoisomerase I inhibitors when combined with 3-AB or more specific inhibitors[257,258]; topoisomerase II inhibitors, including doxorubicin, which showed to sensitize p53-deficient breast cancer cell lines[259]; platinum compounds combined with nicotinamide *in vitro* and *in vivo*[260]; as well as great effects in combination with methylating agents such as temozolomide or *N3*-adenine.

Later, clinical PARP inhibitors have been combined in tumour cell lines and in xenograft models with cytotoxic therapy including alkylating agents (cyclophosphamide and temozolomide), platinums (cisplatin and carboplatin), topoisomerase inhibitors (irinotecan and topotecan) and anthracyclins (doxorubicin)[222,225,258,261-263], confirming and improving the results obtained with the previous generations of PARP inhibitors.

In this context, Evers et al. established a panel of BRCA2-deficient/proficient mammary tumor cell lines that were treated with the clinical PARP inhibitor, olaparib, in combination with 11 different classes of cytotoxic agents including alkylating, antimetabolites, spindle poisons, a topoII inhibitor and a histone deacetylase inhibitor. Combination of olaparib with these drugs reflected additive effect (in BRCA-proficient) and synergistic effect (in BRCA-deficient), being the most potent

combinations those with drugs that directly induces DSBs (cisplatin, mitomycin C, temozolomide and methylmethane sulfonate)[234].

Further recent experimental data with olaparib in other types of cancers reports cytotoxicity in mantle cell lymphoma deficient in ATM and p53[264]; sensitization of BRCA-1 associated breast cancer mice models to topotecan[265]; radiosensitization in medulloblastoma cell lines[266], in p53 mutant pancreatic cancer cells in combination with Chk1 inhibitors[267], in lung tumour xenografts[268] and synergism in combination with 5-fluorodeoxyuridine in ovarian cancer cells[269].

Beyond the combinations with chemotherapeutic agents or radiation, studies combining PARP inhibitors with targeted therapies in BRCA-proficient cancers are less abundant, but have also demonstrated sensitization effects. Johnson et al.[270] showed that BRCA1 needs to be phosphorylated by the Cyclin-dependent kinase 1 (Cdk1) for efficient formation of BRCA1 foci. Depletion or inhibition of Cdk1 in BRCA1-wild type cancer cells resulted in deficient HR repair, sensitized to PARP inhibition (AG014699) *in vitro* and *in vivo*, and prolonged survival in mouse model of lung adenocarcinoma. Therefore, defective function of Cdk1 creates a state of BRCAness that can be efficiently targeted with PARP inhibitors. Another study in head and neck cancer cells with EGFR overexpression observed that treatment with an antibody against EGFR (cetuximab) reduced the HR and NHEJ repair capacity of these cells. Combination of cetuximab with PARP inhibition (ABT-888, veliparib) induced persistence of DNA damage and sensitization of these cells to the targeted therapy[271], suggesting that this combination also could be useful in other cancers with EGFR overexpression.

I.4.3.2.3. Clinical trials with PARP inhibitors

Based on the preclinical data demonstrating synthetic lethality in BRCA1/2-deficient cancers and other DNA-repair deficiencies, and sensitization with chemotherapy, PARP inhibitors were tested in clinical trials. The first clinical data proving efficacy of a PARP inhibitor on BRCA1/2-mutation carriers comes from the phase I clinical trial with olaparib[272]. For this reason and for the cytotoxic potency observed *in vitro* olaparib was the preferred PARP inhibitor selected in this work.

Olaparib

Also called AZD-2281, from AstraZeneca Pharmaceuticals, is a selective and potent oral inhibitor with an in vitro IC_{50} in the nanomolar range that has demonstrated single agent activity against BRCA1/2-mutated cancers. Initially, this first-in-human clinical trial with olaparib in BRCA1/2-mutation carriers enrolled 60 patients with a wide range of advanced tumours that were followed by prospective enrichment limited to patients with BRCA1/2 mutations during cohort expansion. Olaparib was generally well tolerated with dose-limiting toxicities resolved with drug discontinuation. With a maximum tolerated dose (MTD) of 400mg twice daily, the most common drug-related toxicities were: grade1-2 fatigue, nauseas and low-incidence of myelosupression. Importantly, adverse effects did not differ between BRCA1/2-mutation carriers and non-carriers, supporting the predictions from preclinical data. The expansion cohort for BRCA1/2-mutation carriers consisted in 22 patients with primary breast, ovarian and prostate cancers. Whereas no objective tumour response was observed in BRCA1/2-mutation non-carriers, 12/19 (63%) BRCA-mutation carriers had clinical benefit, and 9 of these (47%) had objective response by using Response Evaluation Criteria In

Solid Tumours (RECIST)[273], including a complete response in a patient with BRCA2-mutated breast cancer and durable responses over 1 year.

Further proof-of-concept for this synthetic lethal approach has been provided by two open-label, multicenter, phase II studies with olaparib in germline BRCA1/2-mutation carriers with advanced breast and ovarian cancers (ICEBERG-1 and -2 respectively). In the ICEBERG-1 presented by Tutt et al.[274], 54 patients were recruited in two non-randomized sequential dose cohorts comparing olaparib at 100mg and 400mg (MTD) twice daily. As in the phase I study, olaparib was well tolerated with mainly mild to moderate nausea, fatigue and haematological events previously observed. This study reported an objective response rate (ORR) of 41% (11/27) in the cohort that received 400mg olaparib twice daily, including 1 RECIST complete response (CR) and 10 RECIST partial responses (PRs), and a median of progression-free survival (PFS) of 5.7 moths. In contrast, the cohort that received 100mg of olaparib twice daily presented 22% (6/27) of ORR, 6 RECIST PRs and a median of 3,8 months. These results indicate that higher doses of olaparib appear to be more efficacious, however, it is noteworthy that patients who received the lower dose of olaparib had poorer prognostic features than those in the higher dose cohort.

Despite the promising results from phases I and II obtained with olaparib, negative results were reported in more recent clinical trials in BRCA mutated breast cancer. Furthermore, olaparib has been ineffective in TNBC.

The discordant result have coasted doubts on the continued clinical development of olaparib, and, at present, industry sponsored clinical trials appeared to be halted.

Iniparib

Beyond the use of PARP inhibitors in BRCA1/2-mutated cancer, as mentioned, TNBC has been the other main focus among the sporadic breast cancers included in these clinical trials. Regarding this issue, the largest amount of data comes from the clinical trails with iniparib (BSI-201). Iniparib, from BiPar/Sanofi-Aventis, was initially described as a PARP inhibitor, but recent studies have now described it as a small molecule with low PARP inhibitory activity. In contrast with the rest of PARP inhibitors, iniparib is not a NAD^+ competitive inhibitor and even modulates other molecules rich in cysteines[275,276].

Initially, the phase I for dose evaluation was performed in combination with topotecan, gemcitabine, temozolomide, irinotecan and carboplatin-paclitaxel in advanced solid malignancies. Adverse effects similar to those described with the chemotherapy regimens and evidence of activity in breast cancer were described[277]. Subsequent phase II study assessed the activity of iniparib in combination with gemcitabine and carboplatin in 123 patients with metastatic TNBC. The addition of iniparib to gemcitabin/carboplatin improved clinical benefit rate from 34% to 56%, prolonged the PFS from 3.6 to 5.9 months and increased the OS from 7.7 to 12.3 months with no apparent significant differences in toxicity[278].

These encouraging results lead to a rapid confirmatory phase III study[279]. In this clinical trial, 519 patients with metastatic TNBC were enrolled and randomly assigned to receive carboplatin/gemcitabine regimen alone or

in combination with iniparib. Although this study demonstrated a consistent safety profile, it did not achieve statistical significance for the co-primary end-points OS and PFS. Further analysis to explain these discouraging results are being carried on.

This failure triggered a slowdown in the development of clinical trials in the field. Recently, after reporting that iniparib was not a bonafide PARP inhibitor, the interest in this class of small molecules from different pharmaceutical companies has reawakened expecting that the disappointing results of iniparib in TNBC might not be translated to the other types of PARP inhibitors.

Other combinations of chemotherapy with PARP inhibitors in metastatic TNBC are currently limited. Some evidence of activity was detected in a combination of olaparib with paclitaxel, but this trial was stopped early due to toxicities (mainly neutropenia)[280].

R.4.3.3. The need of biomarkers of PARP inhibitor sensitivity

Clinical data has clearly demonstrated the activity of PARP inhibitors in germline BRCA-mutation carriers, but this subtype of hereditary cancers represents a small percentage of all types of cancers. Now, the challenge remains in identifying those groups of patients with HR repair deficiencies, different from BRCA-mutations, most likely to respond to PARP inhibition and/or those key targets of HR repair susceptible to be inhibited in combination with PARP inhibitors. This purpose requires the development of validated and readily applicable screening assays to delineate molecular determinants of response.

Currently there are an increasing number of DNA-repair proteins described that could be potential synthetic lethal partners of PARP inhibition[281]. Approaches as high-throughput siRNA screenings silencing these genes related with DNA repair and testing the sensitivity of transfected cells to PARP inhibition have identified known and novel determinants of PARP inhibition response[282]. Other approaches have defined the gene expression profile by Affymetrix technology, the protein expression and the mutational status of DNA repair genes in large panels of cell lines and have associated these baseline profiles with the sensitivity to olaparib. These kinds of approaches try to identify those candidate gene transcripts or potential signatures that predict sensitivity to PARP inhibition with olaparib[283].

Currently, γH2AX and RAD51 foci formation are being evaluated as potential clinical biomarkers. γH2AX foci formation has been used preclinically and clinically to determine the extent of DNA damage[284], whereas RAD51 foci formation has demonstrated to be useful for assessing the HR repair pathway integrity in vitro. A large prospective study quantified γH2AX, BRCA1, conjugated ubiquitin and RAD51 foci to assess the HR repair competence in paired tumour biopsies from breast cancer patients prior and after receiving neoadjuvant treatment. Proficient DNA repair based in these 4 biomarkers correlated with drug resistance, according to the hypothesis that DNA damage response competence predicts lower sensitivity to DNA damaging agents[285].

Identification and validation of candidate biomarkers to robustly predict responders to PARP inhibition as a single agent or in combination with chemotherapy, radiotherapy or targeted therapies will be the key for optimal selection of patient population.

OBJECTIVES

OBJECTIVES

The general objectives of this PhD thesis were to provide further translational background to help to understand the role of PARP, and particularly PARP1, in breast cancer, and to explore combination treatments of PARP inhibition with standard therapies that might expand the field.

The specific objectives of this thesis were:

1.   To characterize PARP1 in human breast tumours and explore its association with clinicopathological and molecular features.

2.   To describe *in vitro* and *in vivo* the effects of chemical inhibition of PARP to potentiate biological and cytotoxic therapies in breast cancer cells.

3.   To assess *in vitro* and *in vivo* the effects of genetic downmodulation of PARP1 in breast cancer cells.

RESULTS

R.1. PARP1 EXPRESSION IN PRIMARY BREAST TUMOUR SPECIMENS

To study the role of PARP1 in breast cancer we focused in two aspects, first, the expression of PARP1 in the development or progression of breast cancer, and second, the potential that it has as target. We first evaluated by immunohistochemistry (IHC) the expression of PARP1 protein in series of breast tumour specimens (n=330) with clinical follow-up and determining whether different expression levels were associated with clinicopathological features.

Patients included in the study

We worked in close collaboration with two additional hospitals to achieve a large patients sample size to conduct PARP1 studies. Surgical resection specimens from primary breast tumours and mammoplasties were obtained from Parc de Salut Mar Biobank (MARBiobanc, Barcelona, Spain), Fundación Jiménez Díaz Biobank (Madrid, Spain) and València Clínic Hospital Biobank (València, Spain). Tumour specimens from formalin-fixed paraffin-embedded (FFPE) blocks were retrospectively selected from consecutive breast cancer patients diagnosed between 1998 and 2000, which had the following criteria: infiltrating carcinomas, operable, no neoadjuvant therapy, enough available tissue and clinical follow-up. TNM (tumor–node–metastasis) staging was classified using the American Joint Committee on Cancer (AJCC) staging system. Histological grade was defined according Scarff–Bloom–Richardson modified by Elston[286]. ER and PR were determined by IHC establishing positivity criteria in ≥1% of nuclear tumour staining[20]. HER2 amplification was assayed by FISH[23]. Ki-67 was studied by IHC[287].

Patients referred to genetic counselling were studied for BRCA1 and BRCA2 gene status by direct sequencing. The study was approved by the Ethics Committees of the three hospitals.

A total of 330 infiltrating carcinomas were collected and Tissue MicroArrays (TMA)[288] were constructed using a tissue arrayer by a highly trained technician (Sílvia Menéndez). All breast cancer cases were histologically reviewed by Dr. Rojo (pathologist) and the most representative area of tumour cells (neoplastic epithelial cells) were carefully selected and marked on the Haematoxylin and Eosin slide and sampled for TMA blocks. Complete sections of infiltrating carcinoma (N = 153), adjacent histological normal tissue (N = 25), ductal hyperplasia lesions (N = 75) and ductal carcinoma in situ (DCIS) (N = 102) from the same specimens were assayed. A cohort of 42 patients with previously known BRCA status was also studied for PARP1. Normal breast tissue specimens (N=50) obtained from noncancerous mammoplasties were included.

R.1.1. Protein expression

R.1.1.1. PARP1 protein staining assay validation

First, we assessed the specificity of PARP1 IHC assay FFPE pellets from wild type (WT) and PARP1 gene KnockOut (KO) derived murine embryonic fibroblast cell line (MEFs), parental and PARP1 shRNA knocked-down human breast cancer cells, and kidney or liver tissues from wild type and PARP1 KO mice kindly provided by José Yélamos. All assays revealed a nuclear staining in the wild type and parental samples (**Fig. R.1**).
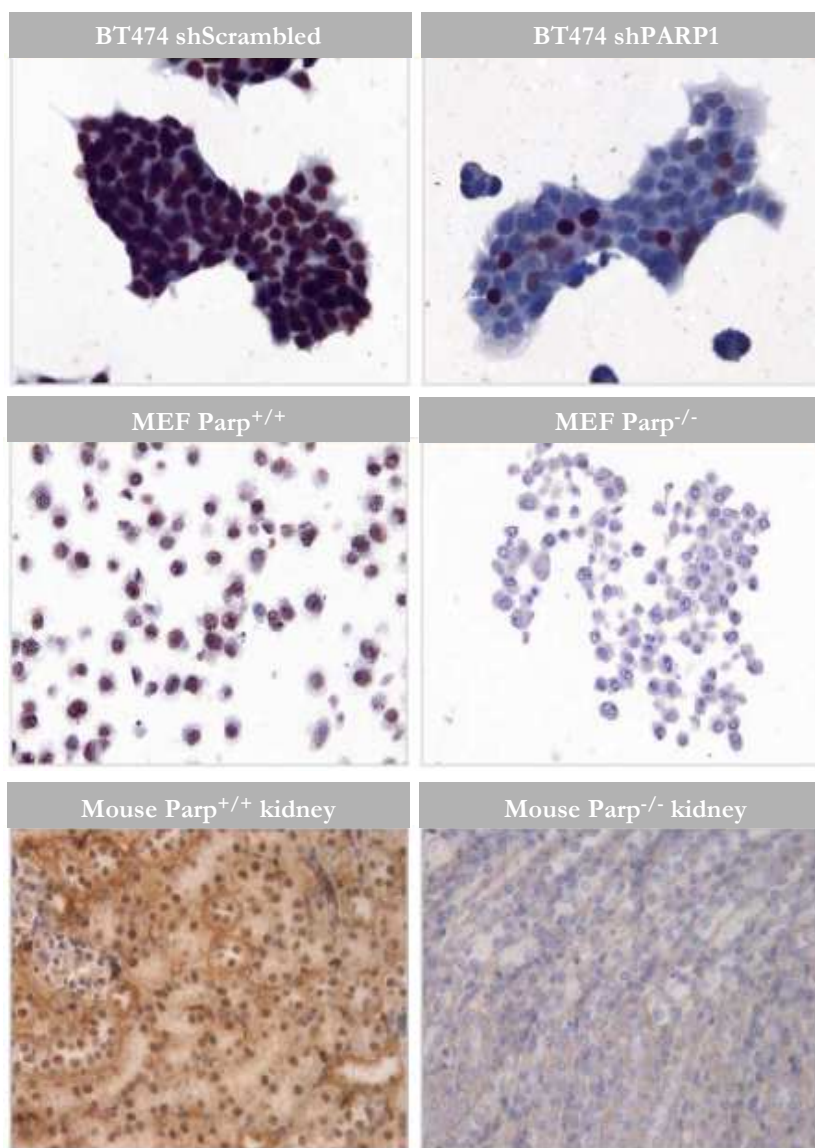
Figure R.1. Validation of PARP1 antibody for immunohistochemistry (IHC).
The specificity of the pattern of staining was determined using FFPE cell pellets
from parental and PARP1 knockdown using shRNA BT474 human breast cancer
cells, wild type and PARP1 gene knockout Mouse Embryonic Fibroblasts (MEF)
and renal tissue from wild type and PARP1 knockout mice. In all cases, a nuclear
PARP1 expression was observed.

By using the same anti-PARP1 antibody a single band corresponding to the expected size of PARP1 (at ~116kD) was detected by WB from corresponding cell lysates prepared from the above indicated cells (**Fig. R.2A**). The nuclear subcellular localization of PARP1 observed by IHC in the FFPE cell pellets and tissues was confirmed by WB of nuclear/cytoplasmatic protein extracts from BT474 cell line (**Fig. R.2B**). Further confirmation was performed in a set of 20 paired fresh frozen and FFPE samples which were processed in parallel by WB and IHC (**Fig. R.3A**). We obtained highly concordant results between the assays (p<0,001, R^2=0,965) (**Fig. R.3B**). To validate the use of Tissue Microarray technology (TMA) for PARP1 testing by IHC, we compared the staining results from 153 infiltrating carcinomas assayed in TMA cores and their corresponding complete tissue sections. The concordance was highly significant (p=0,002, R^2=0,757) (**Fig. R.3C**).
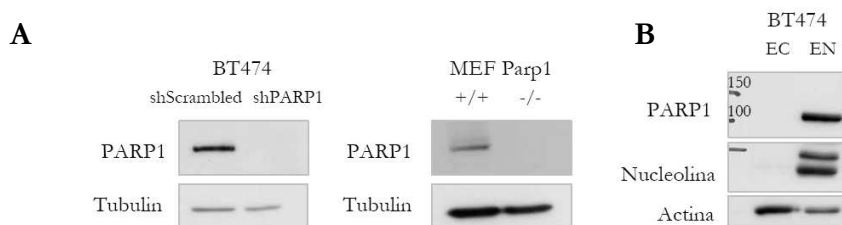
Figure R.2. Validation of PARP1 antibody for immunohistochemistry (IHC) by western blot. A. 20μg of total protein from cell lysates from parental and knockdown BT474 cells (left) and wild type and knockout MEFs (right) were subjected to WB and confirmed the specificity of the antibody, observing a single band at the known molecular weight for the target (116 kDa). β-tubulin was used as loading control. **B**. Subcellular nuclear localization of PARP1 was confirmed by WB of Nuclear extracts (EN) and cytoplasmic extracts (EC) and PARP1 detection. Nucleolin and actin were used as loading controls for nuclear and cytoplasm extracts, respectively.

A
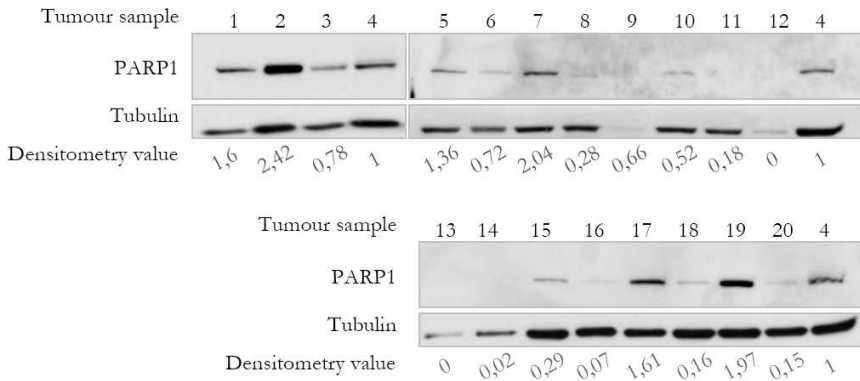
B
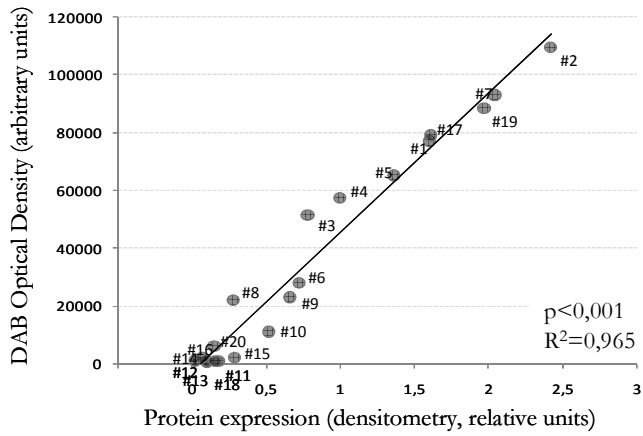
C
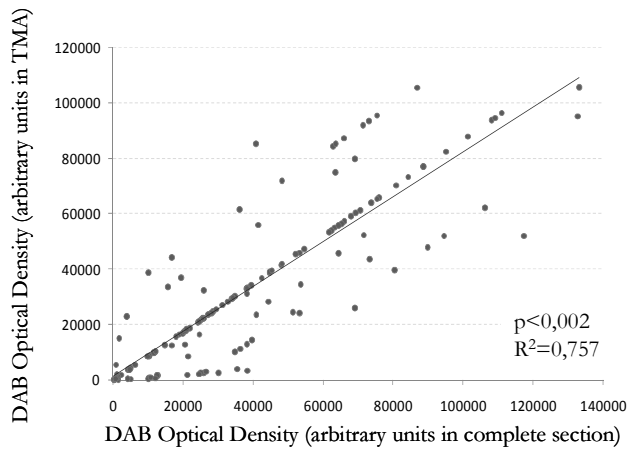
Figure R.3. Correlations of PARP1 antibody by immunohistochemistry (IHC), western blot and TMA. A. 40µg of total protein from 20 frozen OCT-included human breast cancer tumours cell lysates were subjected to WB that showed single band of the expected molecular size for PARP1. Levels of protein expression were densitometred, normalized to GAPDH densitometry values and expressed as a ratio relative to tumour #4. **B**. Correlation between the PARP1 DAB intensity by IHC and correspondent protein levels by WB, the concordance was significant (p<0,001, R^2=0,965). **C**. Correlation of PARP1 DAB intensity by IHC between 153 infiltrating carcinomas assayed in TMA cores and their corresponding complete tissue sections. The concordance was highly significant (p=0,002, R^2=0,757).

R.1.1.2. PARP1 protein expression in normal and pathological breast

Breast ductal and lobular epithelial cells, either from mammoplasty specimens or from histological normal tissue adjacent to cancer, exhibited diffuse and weak PARP1 staining in the nuclei as shown in the following **figure R4**. In stromal cells and lymphocytes, nuclear PARP1 staining was commonly detected.
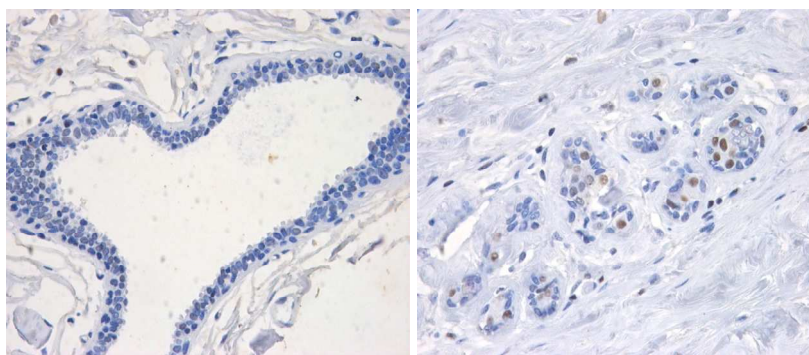
Figure R.4. PARP1 expression in normal breast tissue. Representative images from normal mammary tissue (breast lobular, left, and ductal, right, epithelial cells surrounded by stroma) showing diffuse and weak PARP1 staining.

In usual ductal hyperplasia, the expression was similar to normal breast epithelium. All cases (but one) of ductal hyperplasia had no PARP1 overexpression according to the cut-off point described in methods. In contrast, in a 33,3% of DCIS, PARP1 was overexpressed, more frequently observed in high grade DCIS and comedocarcinomas. The pattern of PARP1 staining was exclusively nuclear and diffusely present in the examined tumour areas, ranging different degrees of intensity (**Fig. R.5**).
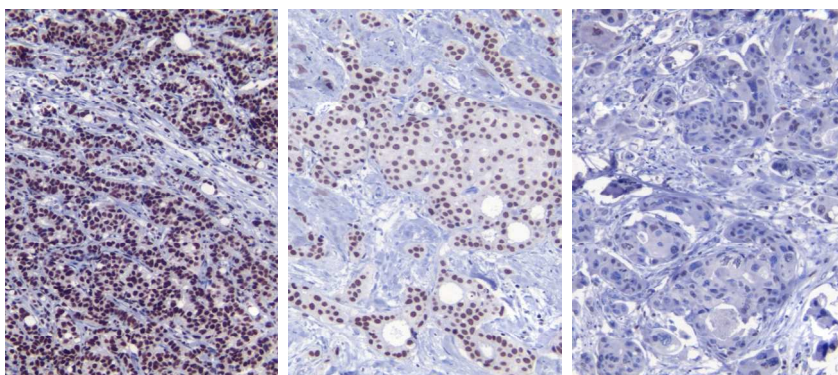
R.5. PARP1 staining in breast tumour tissue. Representative images from three breast tumour tissues exhibiting PARP1 overexpression (left), PARP1 medium expression (medium), PARP1 low expression (right).

In those specimens with infiltrating carcinoma associated to DCIS, the *in situ* component had on average a score of ~50% higher than the adjacent infiltrating counterpart, but the difference was not statistically significant (p=0.081). In the entire series, PARP1 was overexpressed, according to the cut-off defined in methods, in 103 of the 330 (31.2%) of infiltrating carcinomas (**Fig. R.6**).
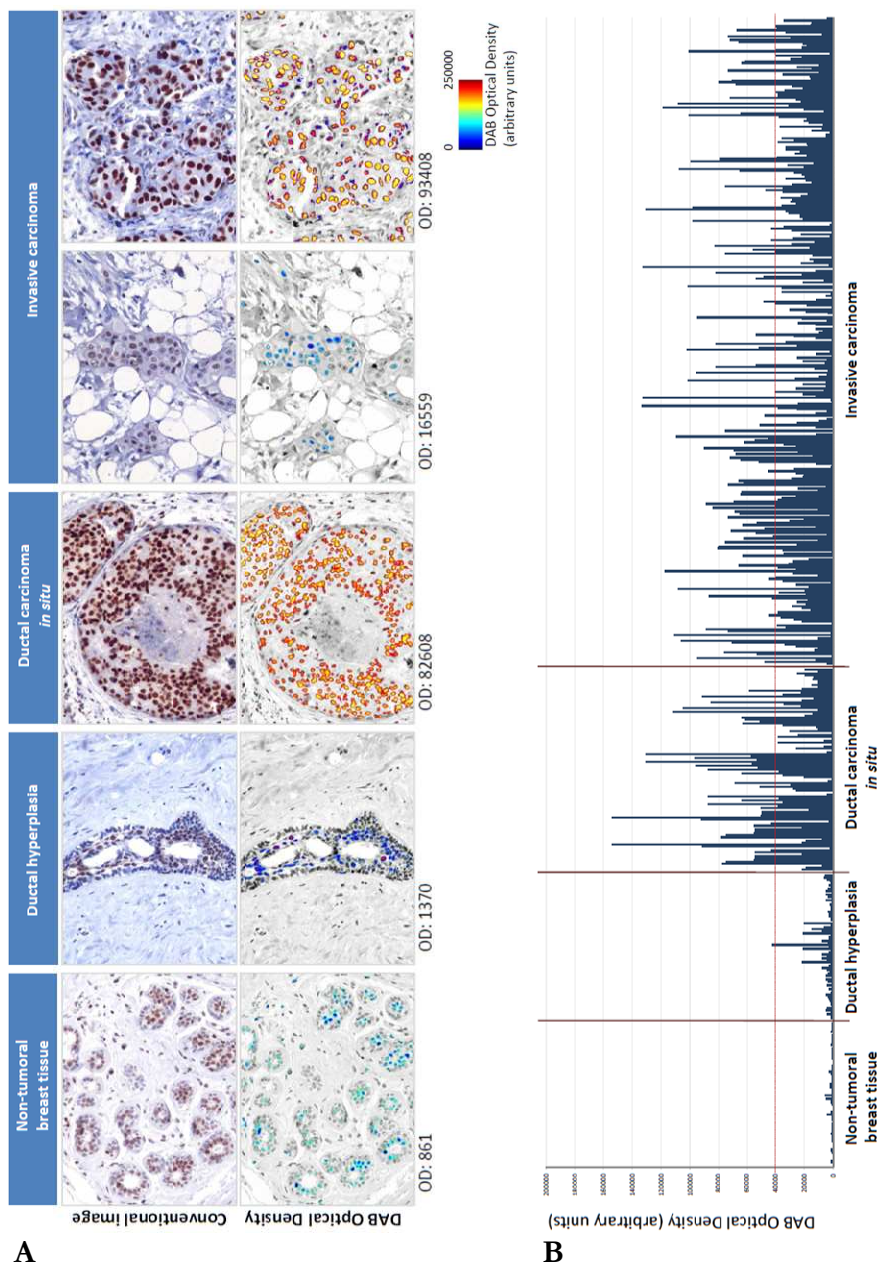
Figure R.6. PARP1 quantitative expression assay in breast tissues by means of a specific IHC signal intensity scanning method (See Methods for details) **A**. Upper panel, Representative PARP1 IHC pictures from normal breast with low expression, ductal hyperplasia with low expression, a DCIS overexpressing PARP1 and invasive carcinoma (one non-overexpressing and one overexpressing PARP1). Lower panel, Individual components of each IHC picture were recolorized in a component image; hematoxylin was turned to gray and diaminobenzidine (DAB)

was converted to a quantitative pseudo-color scale (lower panel). DAB intensity determined in the nuclear subcellular compartment, based on a colocalization with hematoxylin dye and pixel aggregation algorithm, was converted from transmission to quantitative optical density (OD) units, reflecting directly the abundance of PARP1 in the specimen. DAB OD values are indicated in the bottom. **B**. Quantitative representation of DAB OD for PARP1 expression for each normal breast, ductal hyperplasia, DCIS and invasive carcinoma specimens. OD units ranged from 29 to 133.094. The dotted red line indicates PARP1 overexpression threshold (optical density of 39.970).

R.1.1.3. PARP1 protein expression and clinicopathological features in breast cancer patients

Clinicopathological characteristics of the entire series (n=330) of patients with infiltrating breast cancer and their relationship with PARP1 overexpression are shown in **Table R.1**. By the time of the analysis, the median follow-up time was 103 months (range 8-250). A total of 65 (19,7%) patients had a relapse and 43 (13%) had died. Adjuvant chemotherapy had been administered to 270 (81,8%) patients [combination chemotherapy with cyclophosphamide, metotrexate and fluorouracil (CMF) in 72 and anthracycline-based chemotherapy in 198]. Adjuvant hormonal therapy was prescribed to women with hormone-receptor positive disease (237 patients, 71,8%).

The following characteristics were significantly associated to PARP1 overexpression: tumour grade III (p=0,01); negative estrogen receptors (ER) (p<0,001); triple negative status (p<0,001); absence of administration of hormonal therapy (p=0,012). Histological type, progesterone receptor (PgR), HER2 amplification, primary tumour size, lymph node metastasis, proliferation (as assayed by Ki-67 staining), were not significantly related to PARP1 overexpression. Despite being statistically more frequent in triple-negative tumours, PARP1

overexpression was also present in a proportion of hormone receptor-positive (24,4%) and HER2-amplified (30,6%) breast cancers.

Table R.1. Baseline characteristics according to PARP1 expression.

Characteristics	Complete series (n=330) No. of patients	%	PARP-1 non-overexpression (n=227) No. of patients	%	PARP-1 overexpression (n=103) No. of patients	%	P
Age (median, range)	58, 26-90		58, 28-90		58, 26-83		
Menopausal status							0.864
Premenopausal	95	28.8	66	29.1	29	28.2	
Postmenopausal	235	71.2	161	70.9	74	71.8	
Tumor size, mm							0.226
≤20	176	53.3	128	56.4	48	46.6	
21-50	117	35.5	74	32.6	43	41.7	
>50	37	11.2	25	11.0	12	11.7	
Tumor grade							0.010
I	53	16.1	43	18.9	10	9.7	
II	150	45.5	108	47.6	42	40.8	
III	127	38.5	76	33.5	51	49.5	
Lymph nodes							0.172
None	194	58.8	141	62.1	53	51.5	
1-3	80	24.2	54	23.8	26	25.2	
4-9	38	11.5	22	9.7	16	15.5	
>9	18	5.5	10	4.4	8	7.8	
Histology							0.620
Ductal	274	83.0	189	83.3	85	82.5	
Lobular	39	11.8	28	12.3	11	10.7	
Others	17	5.2	10	4.4	7	6.8	
Estrogen receptor							<0.001
Negative	86	26.1	45	19.8	41	39.8	
Positive	244	73.9	182	80.2	62	60.2	
Progesterone receptor							0.104
Negative	123	37.3	78	34.4	45	43.7	
Positive	207	62.7	149	65.6	58	56.3	
HER2 status							0.859
Negative	264	80.0	181	79.7	83	80.6	
Positive	66	20.0	46	20.3	20	19.4	
Triple negative phenotype							<0.001
No	273	82.7	201	88.5	72	69.9	
Yes	57	17.3	26	11.5	31	30.1	
Proliferation (Ki-67)							0.265
Low proliferation (<20%)	274	83.0	192	84.6	82	79.6	
High proliferation (≥20%)	56	17.0	35	15.4	21	20.4	
Adjuvant chemotherapy							0.484
No	60	18.2	39	17.2	21	20.4	
Yes	270	81.8	188	82.8	82	79.6	
Adjuvant hormonotherapy							0.012
No	93	28.2	54	23.8	39	37.9	
Yes	237	71.8	173	76.2	64	62.1	

Abreviations: HER2, human epidermal growth receptor 2

We also assayed PARP1 expression in a serie of 42 specimens from patients with known BRCA1/2 gene status that had been referred to the genetic counselling unit. In wild-type BRCA (n=15) tumours, PARP1 overexpression was detected in 7 (46,7%), whereas in BRCA-mutated cases (n=27, 23 in BRCA1, 4 in BRCA2), PARP1 overexpression was

present in 8 (29,6%), but no significant association was observed between the two variables (p=0,270).

R.1.1.4. PARP1 protein overexpression and patient outcome

Receiver-operator curve (ROC) was used to determine the optimal cut-off point based on relapse end point for PARP1 expression[289]. The area under the curve (AUC) for PARP1 was 0,809 (95% CI 0,743-0,875). Examination of the coordinates of the curve indicates that an optimal cut-off point for PARP1 was 39.970. At this value, the sensitivity of the test was 79,7%, with a specificity of 80,2% (**Fig. R.7**).
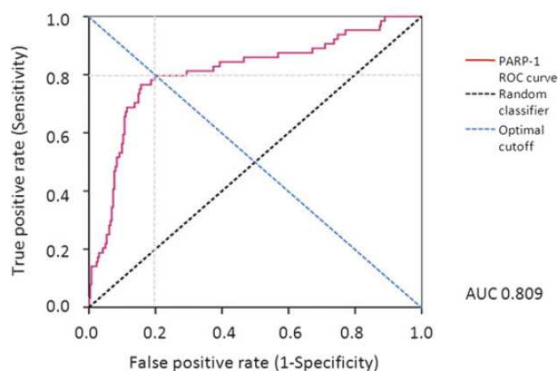
Figure R.7. Receiver operating curve (ROC) for determining PARP1 expression. ROC was used to determine the optimal cut-off point for PARP1 expression that corresponds to the intersection between the red dotted line (PARP1 expression levels) and the blued dotted line (that accounts for sensitivity and specificity). The PARP1 optical density according to ROC data at this intersection point was 39.970. At this value, the sensitivity of the test was 79.7%, with a specificity of 80.2%, and was used to define overexpression.

We compared the difference in outcome between patients. The primary endpoints of our study were Disease-Free Survival (DFS) and Overall

Survival (OS). OS was defined as the time from the date of surgery to the date of death from any cause, or last follow-up. DFS was considered from the date of surgery to the date of any primary, regional or distant recurrence, as well as the appearance of a secondary tumour or DCIS. DFS and OS analysis showed a higher risk of relapse or death respectively, in patients with PARP1 overexpression (**Fig. R.8.A** and **R.8.B**; log-rank test p<0,001, and **Table R.2** and **Table R.3**). These associations were also observed in the analysis performed in the subset of patients treated with chemotherapy (CMF or anthracycline-based, n=248; p<0,001 for both DFS and OS), in patients treated with anthracycline-based adjuvant chemotherapy (n=176; p<0,001 for both DFS and OS) or in patients treated with hormonal therapy with or without chemotherapy (n=237; p<0,001 for DFS and p=0,008 for OS).

The hazard ratio (HzR) for relapse in patients with PARP1 overexpressing tumours was 8,87 (IC 95%; 5,05-15,59). Kaplan-Meier curves for relapse and log-rank test comparisons also showed that primary tumour size (p=0,007), axillary lymph node involvement (p<0,001), hormone receptor (ER- and/or PR-positive versus both negative) status (p=0,033), and HER2 (p=0,023) were associated with the risk of relapse (**Table R.2**). The HzR for death in patients with PARP1 overexpressing tumours was 7,24 (IC 95%; 3,56-14,75). Kaplan-Meier survival curves for OS and log-rank test comparisons also showed that primary tumour size (p=0,015), tumour grade (p=0,03), axillary lymph node involvement (p<0,001), hormone receptor status (p=0,03), triple negative phenotype (p=0,039) and adjuvant chemotherapy (p=0,011) were associated with the risk of death (**Table R.2** and **Table R.3**).
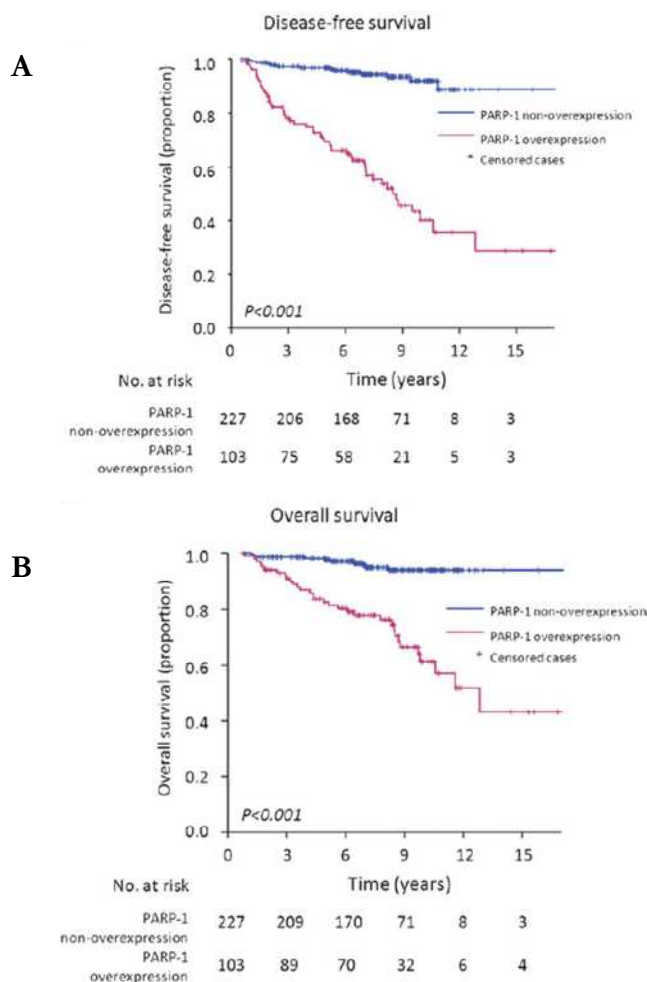
Figure R.8. PARP1 overexpression threshold and prognostic significance in the cohort of 330 breast cancer patients. A. Association between PARP1 expression and disease-free survival. B. Association between PARP1 expression and overall survival. P-values were calculated with use of the log-rank test and survival curves by Kaplan–Meier analysis.

A multivariate analysis was performed including all the baseline clinicopathological factors with p-values lower than 0,1 (**Table R.2** and **Table R.3**). In this analysis, PARP1 overexpression retained its adverse prognostic role for relapse (p<0,001) and death (p<0,001). The HzR for

relapse in patients with PARP1 overexpressing tumours was 10,05 (IC 95%; 5,42-18,66) and for death was 1,82 (IC 95%; 1,32-2,52). Other independent prognostic factors were lymph nodes (p=0,038) for DFS and adjuvant chemotherapy (p<0,001) for OS.

Table R.2. DFS analysis in patients with PARP1 expression.

Variable	Univariate (n=330)			Multivariate (n=330)		
	HR	95% CI	P	HR	95% CI	P
Age			0.158			-
Premenopausal	1.00			-		
Postmenopausal	1.51	0.85 to 2.66		-		
Tumor size, mm			0.007			0.086
≤20	1.00			1.00		
21-50	1.99	1.15 to 3.43		1.56	0.86 to 2.82	
>50	2.73	1.35 to 5.51		2.52	1.04 to 6.11	
Tumor grade			0.065			0.401
I	1.00			1.00		
II	1.04	0.46 to 2.31		1.56	0.74 to 2.53	
III	0.73	0.79 to 3.78		1.93	0.61 to 2.01	
Lymph nodes			<0.001			0.038
None	1.00			1.00		
1-3	1.71	0.95 to 3.09		1.28	0.69 to 2.39	
4-9	1.66	0.78 to 3.56		1.33	0.32 to 2.03	
>9	4.91	2.37 to 10.17		2.86	1.23 to 5.67	
Histology			0.603			-
Ductal	1.00			-		
Lobular	0.89	0.33 to 2.35		-		
Others	1.25	0.41 to 3.86		-		
Hormonal receptor status			0.033			0.624
Negative	1.00			1.00		
Positive	0.58	0.35 to 0.96		0.77	0.26 to 2.23	
HER2 status			0.023			0.341
Negative	1.00			1.00		
Positive	1.71	1.08 to 2.71		1.47	0.68 to 2.22	
Triple negative phenotype			0.072			0.511
No	1.00			1.00		
Yes	1.66	0.95 to 2.89		1.83	0.43 to 5.46	
Proliferation (Ki-67)			0.714			-
Low proliferation (<20%)	1.00			-		
High proliferation (≥20%)	1.14	0.59 to 2.31		-		
Adjuvant chemotherapy			0.631			-
No	1.00			-		
Yes	0.95	0.51 to 3.72		-		
Adjuvant hormonotherapy			0.124			-
No	1.00			-		
Yes	1.28	0.89 to 1.96		-		
PARP-1			<0.001			<0.001
Non-overexpression	1.00			1.00		
Overexpression	8.87	5.05 to 15.59		10.05	5.42 to 18.66	

Abbreviations: DFS, disease free survival; HR, hazard ratio; CI, confidence interval; HER2, human epidermal growth factor receptor 2

Table R.3. OS analysis in patients with PARP1 expression.

Variable	Univariate (n=330)			Multivariate (n=330)		
	HR	95% CI	P	HR	95% CI	P
Age			0.072			0.089
Premenopausal	1.00			1.00		
Postmenopausal	1.64	0.80 to 3.35		1.28	0.96 to 1.70	
Tumor size, mm			0.015			0.646
≤20	1.00			1.00		
21-50	2.02	1.01 to 4.06		1.11	0.71 to 1.85	
>50	3.33	1.43 to 7.71		1.31	0.53 to 2.38	
Tumor grade			0.030			0.103
I	1.00			1.00		
II	2.11	0.62 to 7.21		1.15	0.81 to 1.64	
III	3.16	0.94 to 10.61		1.49	1.01 to 2.21	
Lymph nodes			<0.001			0.074
None	1.00			1.00		
1-3	1.81	0.85 to 3.88		1.55	0.73 to 3.28	
4-9	1.93	0.75 to 4.99		1.61	0.64 to 3.02	
>9	6.84	2.99 to 15.64		1.89	1.05 to 3.52	
Histology			0.191			-
Ductal	1.00			-		
Lobular	0.80	0.24 to 2.67		-		
Others	1.60	0.43 to 5.99		-		
Hormonal receptor status			0.030			0.218
Negative	1.00			1.00		
Positive	0.57	0.31 to 1.03		0.73	0.43 to 1.21	
HER2 status			0.256			-
Negative	1.00			-		
Positive	1.43	0.77 to 2.63		-		
Triple negative phenotype			0.039			0.132
No	1.00			1.00		
Yes	2.01	1.04 to 3.86		1.55	0.88 to 2.72	
Proliferation (Ki-67)			0.203			-
Low proliferation (<20%)	1.00			-		
High proliferation (≥20%)	1.23	0.91 to 1.68		-		
Adjuvant chemotherapy			0.011			<0.001
No	1.00			1.00		
Yes	0.44	0.24 to 0.67		0.35	0.32 to 0.52	
Adjuvant hormonotherapy			0.173			-
No	1.00			-		
Yes	0.83	0.63 to 1.09		-		
PARP-1			<0.001			<0.001
Non-overexpression	1.00			1.00		
Overexpression	7.24	3.56 to 14.75		1.82	1.32 to 2.52	

Abreviations: OS, overall survival; HR, hazard ratio; CI, confidence interval; HER2, human epidermal growth factor receptor 2

CI, confidence interval; HER2, human epidermal growth factor receptor 2; HR, hazard ratio; OS, overall survival

R.1.2. Gene status and mRNA levels

Genomic techniques as Fluorescent In Situ Hybridization (FISH) or even quantitative Reverse-Trascription PCR (qRT-PCR) are more robust and reproducible techniques between labs than the classical IHC. If these associations between PARP1 protein levels and patient outcome could be also reproduced with mRNA levels or gene amplification status of PARP1 it represent a clinically easy way to screen breast cancer specimens for PARP1 expression, as occurs in the determination of HER2 in breast cancer[23]. On the other hand, lack of correlation between protein levels, mRNA levels and/or gene amplification could indicate a complex regulation of PARP1 or even alterations in this regulation.

R.1.2.1. PARP1 gene gains and patient outcome

Given the results obtained at PARP1 protein level, we wondered whether we could observe any correlation between *PARP1* gene gains and PARP1 protein expression as defined by IHC analysis. We also assessed the correlation between the genetic findings with patient clinical outcome.

For this purpose we applied the Fluorescent In Situ Hybridization (FISH) technique to 156 breast tumours that were included in our TMA using. For this approach we used a bacterial artificial chromosome (BAC) clone labeled with Green 5-Fluorescein representing the gene of interest from the region 1q41-q42 probe which includes the *PARP1* locus. We established as a positive condition of altered *PARP1* gene those cases with more than two copies of the gene (taking into account that two copies are strictly a gain, not an amplification of the gene) (**Fig. R.9A**).
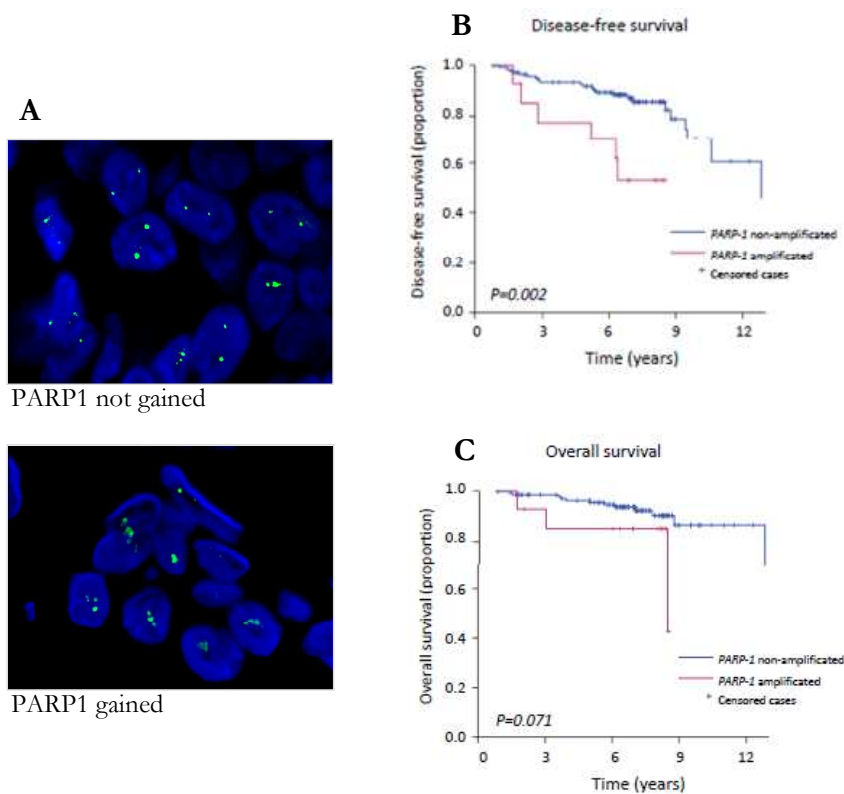
Figure R.9. PARP1 gains by FISH and prognostic significance in the subset of 156 breast cancer patients. A. Representative immunofluorescence of PARP1 gene not-gained (left) and gained (right) detected by FISH. **B.** Association between PARP1 gained and disease-free survival. **C.** Association between PARP1 gained and overall survival. P-values were calculated with use of the log-rank test and survival curves by Kaplan–Meier analysis.

Out of 156 cases analyzed by FISH about 10% (15/156) of the cases showed gains of *PARP1* gene locus. Although no centromeric probe was used to discard that the detected gains were not polysomies, aCGH analyses mentioned below suggested that these gains were real since no polysomies were found. Moreover, when we studied the correlations between *PARP1* gene status and PARP1 protein expression we found that among PARP1 overexpressing cases, only a 23% showed *PARP1* gene gains, whereas 76% did not present any degree of gain, suggesting a

possible accumulation of PARP1 protein. In addition, we found that gains in PARP1 gene were associated with poor DFS (p=0,002), but not with OS (p=0,071) (**Fig. R.9B, C**).

R.1.2.2. PARP1 mRNA expression and correlation with protein levels

Published studies, such as in Ewing's sarcoma cells, high levels of PARP1 protein correlate with high levels of PARP1 mRNA[204]. We asked whether in our set of fresh breast tumours (n=20) PARP1 protein levels assessed by WB correlated with respective mRNA levels assessed by qRT-PCR. No significant correlation was found (R^2=0,19; p=0,028) (**Fig. R.10**). In this case, the overexpression of PARP1 protein was associated to high levels of PARP1 mRNA only in the half of the cases analyzed, suggesting that in the other half of the PARP1 overexpressed tumours some alteration in the regulation of the protein could be occurring. More tumour specimens are required to confirm this result and further studies are needed to describe which differences might exist in the PARP1 protein between the distinct overexpressed tumours.
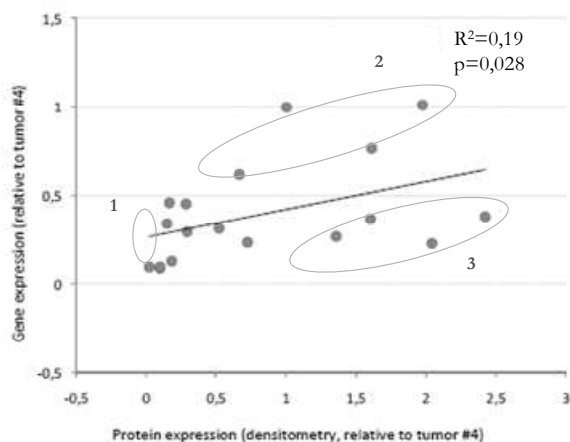
Figure R.10. Correlation of PARP1 protein and mRNA levels in fresh breast tumours. Correlation between the PARP1 protein levels assessed by WB and correspondent mRNA expression assessed by qRT-PCR did not show a significant correlation by Chi-squared test ($R^2=0,19$; $p=0,028$). Three groups are surrounded indicating, first, those tumours with low PARP1 protein and mRNA levels, second, those tumours with high expression of PARP1 protein and mRNA, and third, those tumours in which high levels of PARP1 protein does not correlate with mRNA levels.

R.1.2.3. PARP1 status, DNA repair genes and genomic instability in breast cancer specimens

It is well-known that genomic instability (GI) plays a pivotal role in tumour development and progression. Concerning breast cancer, many studies using microarray Comparative Genomic Hybridization (aCGH) have demonstrated associations between profile of chromosomal alterations and clinicopathological features of breast cancers[290,291]. In this work we wondered whether PARP1 protein expression or the alterations, defined as gains or losses, in DNA repair genes were associated with GI in breast tumour specimens.

For this purpose 10 breast cancer specimens (5 with high levels and 5 with low levels of PARP1 protein expression) were analyzed by aCGH applying the SNP 6.0 array performed by the Microarray Analysis Service (SAM) at IMIM. The GI index was obtained from the percentage of altered genome (taking into account all the altered regions, gains and losses). In addition to the GI index, for each sample was specifically determined the number of gains and losses in each gene locus from a panel of 160 DNA repair genes[281]. Losses were defined as Loss of Heterozigozity (LOH), whereas the sum up of gains and losses were defined as "gene alterations".

First of all, we compared the genomic imbalance profile between low and high PARP1 protein expression groups. All tumour samples showed altered regions. The percentage of altered genome (median of the altered megabase pairs per group) in low PARP1 protein expression and high PARP1 protein expression group was 8.9 (0,7-22,5) and 13,4 (0,14-36,3) respectively; the percentage of gained genome was 2,1 (0,1-16,3) and 11,1 (0,1-21,1) and the percentage of lost genome was 0,1 (0-8,9) and 2,3 (0,1-15,2), respectively. The absolute number of aberrations in low PARP1 protein expression and high PARP1 protein expression group was 354 and 877, respectively. The absolute number of gains was 283 and 628, and the absolute number of losses was 71 and 249 for low PARP1 protein expression and high PARP1 protein expression groups, respectively.

On average, there were 56,6 and 125,6 altered regions/case in low PARP1 protein expression and high PARP1 protein expression group, respectively. Also it was observed 70.8 and 175.4 gained regions/case and 14,2 and 49,8 lost regions/case.

When both groups were compared, we did not find statistical significant differences in any of the studied parameters: percentage of altered genome (p=0,6); percentage of gains (p=0,4); percentage of losses (p=0,6); total aberrations (p=0,3); total gains (p=0,2) and total losses (p=0,2). Non-significant differences could be explained for the date dispersion and the low number of studied cases; however, we were able to detect a non-significant tendency of high PARP1 protein expression cases and more genomic instability.
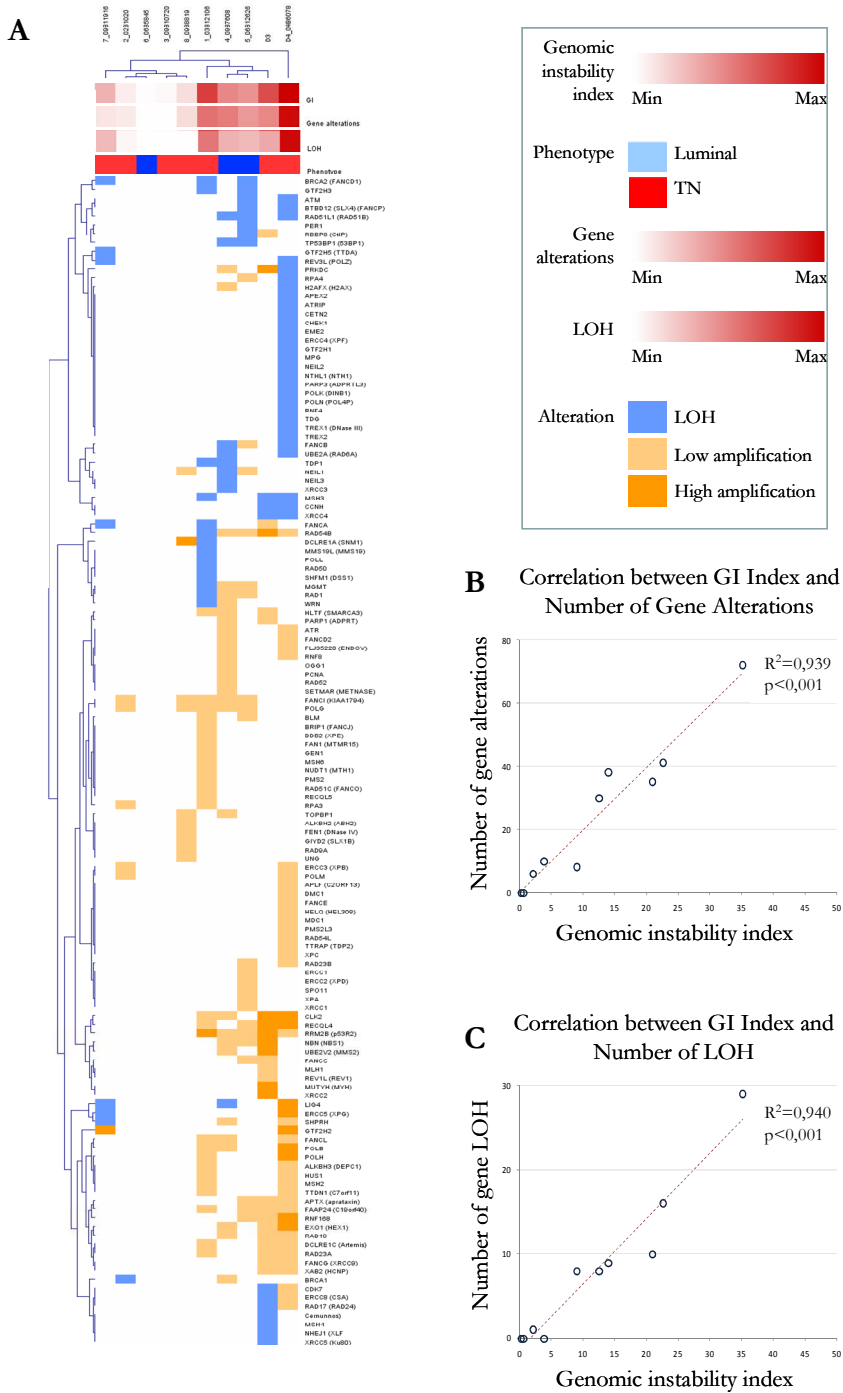
Figure R.11. Genomic instability in breast cancer tumours. A. Map representing gains and losses in a panel of 160 DNA repair genes in 10 breast tumour specimens based on data analysis from aCGH. Colors mean different gene alterations: Blue,

Loss of Heterozigozity (LOH); yellow, low amplification; and orange, high amplification. Degrees of Genomic Instability (GI) Index, Gains and Losses, and IHC phenotype of each sample is specified at the top of the map. **B**. Correlation between GI index and gene alterations by Chi-squared test show significant correlation ($R^2=0,939$, $p<0,001$). **C**. Correlation between GI index and LOH by Chi-squared test show significant correlation ($R^2=0,94$, $p<0,001$).

Moreover, when we assessed the number of gene alterations and LOH in the genes from the panel of DNA repair we found a clear and high statistically significant correlation with the GI index ($R^2=0,939$, $p<0,001$; and $R^2=0,94$, $p<0,001$, respectively) (**Fig. R.11**). Despite the limited number of studied cases, this result might suggest that alterations in DNA repair genes, and not only the levels of PARP1, could be giving rise to these levels of genomic instability.

R.2. PARP1 EXPRESSION IN BREAST CANCER CELL LINES

In parallel to the studies evaluating PARP1 in breast tumours, another main goal during my PhD thesis was to characterize *in vitro* the role of PARP1 by chemical inhibition of PARP enzymatic activity or genetic downmodulation of *PARP1* gene in a panel of human breast cancer cell lines (BCCL). First of all, we characterized PARP1 basal protein and mRNA levels, and enzymatic activity in each cell line. We also examined *PARP1* gene status and genomic instability in those cells. Finally, we looked for possible associations between these variables.

R.2.1. Basal expression levels of PARP1 protein correlates with PARP enzymatic activity, but not with basal pADPr or basal PARP1 mRNA.

The panel of BCCL used for the study consists in 7 different cell lines each of which represents a different subtype of breast cancer as described in the Kao J. study[292] and on the American Type Culture Collection (ATCC) product information sheet. These cells are commonly used as a model in breast cancer studies. Three of them (MDA-MB-231, MDA-MB-468 and HCC1937) are classified as Basal-like molecular subtype by transcriptome signature and Triple-Negative (TN) by IHC. MDA-MB-231 and MDA-MB-468 are BRCA1/2-proficient cells, and HCC1937 is BRCA1-mutant. BT474, SKBR3 cell lines represent the molecular ErbB2 overexpressing subtype and HER2+ by IHC. MDA-MB-453 is defined as TN, and although low expression of ER/PgR is considered molecularly Luminal B. Finally, MCF7 cell line is considered a Luminal A and Hormone receptor positive cell line. This information is summarized in the table below (**Table R.4**).

Table R.4. Molecular and IHC subtypes classification of the BCCLines panel.

Cell line	Molecular subtype	HER2	ER	PgR	IHC subtype
MDA-MB-231	Basal-like	-	-	-	Triple-negative
MDA-MB-468	Basal-like	-	-	-	Triple-negative
MDA-MB-453	Luminal B	+	-	-	Triple-negative
SKBR3	ErbB2	+++	-	-	HER2+
BT474	ErbB2	+++	+	+	HER2+
MCF7	Luminal A	-	+	+	Hormone Receptor +
HCC1937*	Basal-like	-	-	-	Triple-negative

* BRCA1 mutant

As previously performed in IHC analysis of breast cancer tumours, we wondered if there are specific BCCL subtypes that are associated with different PARP1 protein expression. When we assessed basal PARP1 protein levels by WB, we did not find any clear association with a specific subtype. The expression of PARP1 was variable among TN cells. MDA-MB-231 and MDA-MB-468 showed lower expression levels of PARP1 compared with the other cell lines from the panel (0,14 and 0,23 densitometric value of PARP1 protein normalized by tubulin, respectively), whereas MDA-MB-453 and HCC1937 cells showed higher expression levels (0,59 and 0,36 densitometric value of PARP1 normalized by tubulin, respectively). The Hormone positive cell line MCF7 presented one of the lowest levels of the protein (0,18 densitometric value of PARP1 protein normalized by tubulin). In contrast, both HER2+ cell lines, SKBR3 and BT474, showed high expression of PARP1 (0,39 and 0,79 densitometric value of PARP1 protein normalized by tubulin, respectively) (**Fig. R.12.A**). In this panel it appeared that cell lines with expression or overexpression of HER2 tended to exhibit the highest levels of PARP1 protein (BT474, SKBR3 and MDA-MB-453), followed by the basal-like/TN and BRCA1-mutated cell line, HCC1937.

Next, we analyzed the expression levels of PARP1 mRNA by qRT-PCR in this panel. Similar to our findings in breast cancer tumours tested, we did not observe a significant correlation between PARP1 mRNA and protein levels (R=0,34, p=0,5) (**Figure R.12.B-C**).
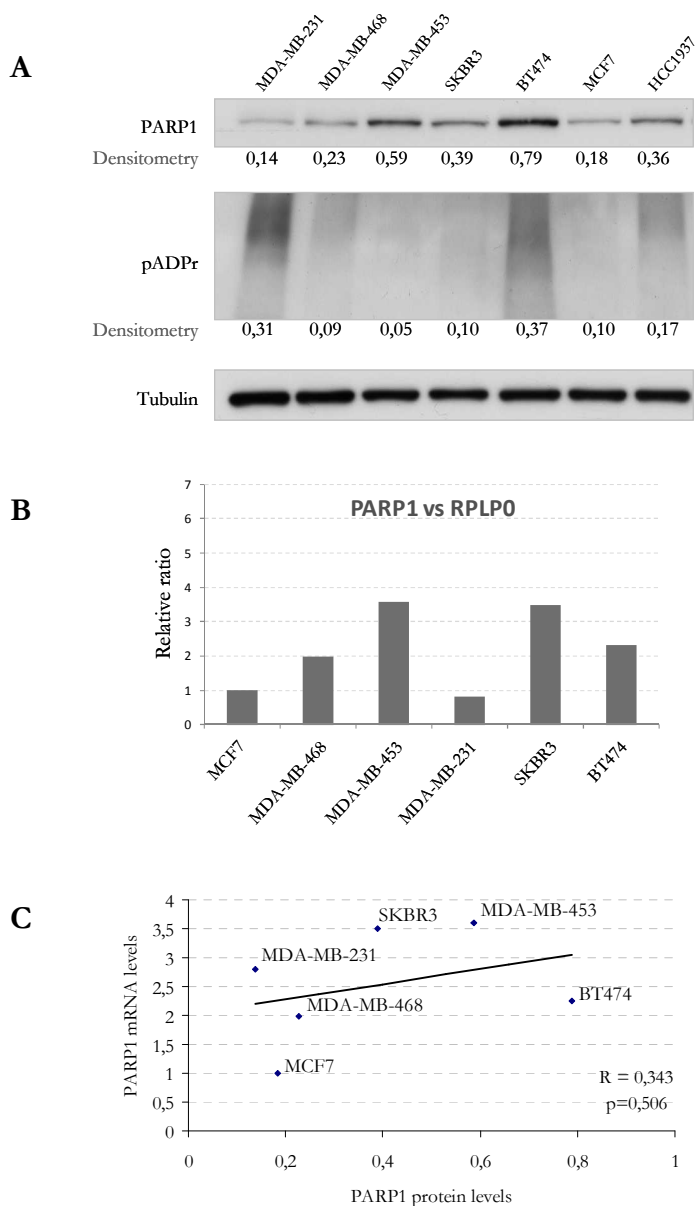
Figure R.12. Basal PARP1 and pADPr protein levels and correlation with basal PARP1 mRNA levels. A. 20µg of total protein from cell lysates of BCCL were subjected to WB for assessing PARP1 and poly(ADP-ribose) (pADPr) basal protein levels. β-tubulin was used as loading control. Densitometry values of PARP1 and pADPr protein levels were normalized with the respective β-tubulin densitometry values and expressed below each panel. **B.** PARP1 mRNA levels. mRNA from BCCL was isolated, reverse-transcribed and subjected to qRTPCR using gene-specific primers for PARP1 and normalized with the housekeeping,

RPLP0. **C.** Correlation between PARP1 mRNA and PARP1 protein levels from BCCL in basal conditions showed no significant correlation by Chi-square test ($R^2=0,343$, $p=0,5$).

Furthermore, we wanted to determine whether the basal levels of PARP1 protein correlated with the amount of poly(ADP-ribosylated) proteins or the enzymatic activity assessed by an enzymatic assay. This assay combines a poly(ADP-ribosylation) reaction and ELISA method to direct detect poly(ADP-ribosylation) of coated histones in a well.

We investigated the pattern of poly(ADP-ribosylation) of cellular proteins. Cell lysates were analysed by WB using an anti-poly(ADP-ribose)polymer (anti-pADPr antibody). As shown in the **figure R.12A**, the poly(ADP-ribosylation) reaction (pADPr polymer formation) was detected as a typical smear for this type of posttranslational modification. The levels of PARP1 did not correlate with the amount of pADPr determined by WB ($R=0,278$; $p=0,54$) (**Fig. 13A**). Similar non-correlating results were obtained from the analysis of breast cancer specimens (n=4) (**Figure R.13B**). On the other hand, the enzymatic activity showed a statistically significant tendency to correlate with PARP1 protein content ($R=0,849$ $p=0,016$) (**Fig. R.13C-D**). Therefore, these results suggest that the enzymatic assay might be a more reliable technique to assess PARP enzyme activity than determining the levels of pADPr. Polymers of pADPr are present only transiently, because can be rapidly synthesized and degraded. If these data could be replicated in human tumour tissues, it might be important to better understand the role that PARP1 levels are playing in breast tumour specimens. I.e., in determining if PARP1 is active or just accumulated in the tumours. In fact this type of PARP

enzymatic activity assay has been used in pharmacodynamics assessment of PARP inhibitors in clinical trials[293].

A

B

C

D
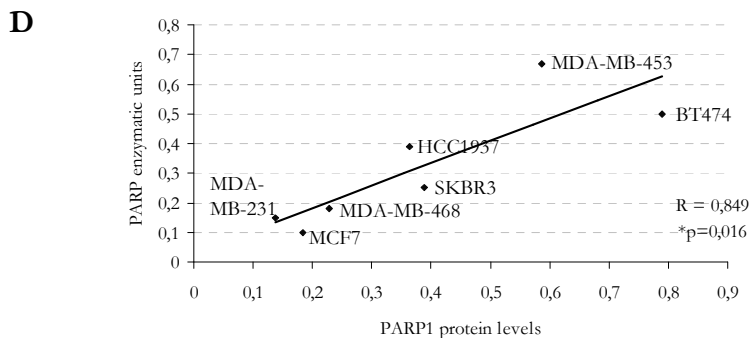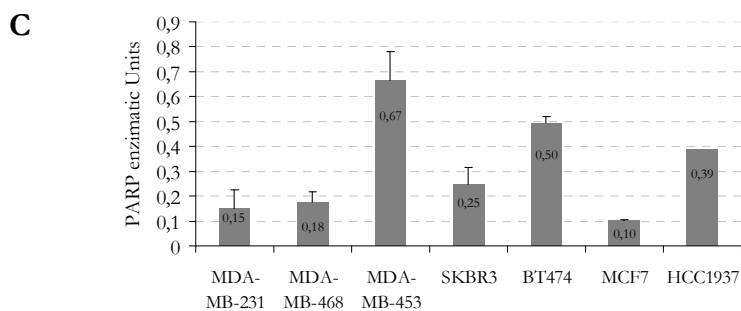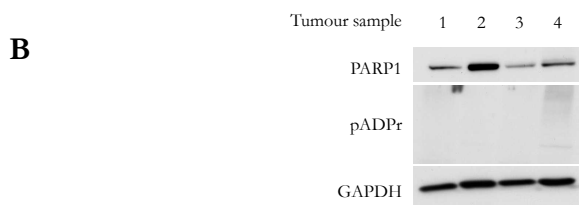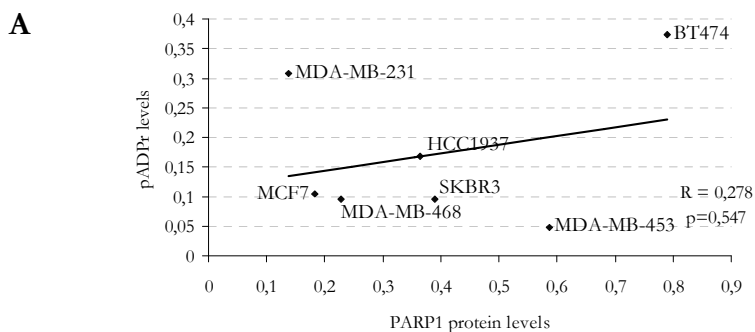
Figure R.13. PARP enzymatic activity and correlation with PARP1 protein levels. A. Correlation between pADPr and PARP1 protein levels from BCCL in basal conditions assessed by WB showed no significant correlation by Chi-square test (R^2=0,27, p=0,54). **B.** 40μg of total protein from 4 frozen OCT-included human breast cancer tumours cell lysates were subjected to WB for assessing PARP1 and poly(ADP-ribose) (pADPr) basal protein levels. GAPDH was used as loading control. **C.** 5ug of protein from cell lysates of BCCL in basal conditions were subjected to PARP enzymatic activity assay and expressed as PARP enzymatic units. **D.** Correlation between PARP enzymatic units and PARP1 protein levels showed significant correlation assessed by Chi-squared test (R^2=0,849, p=0,016).

R.2.2. PARP1, DNA repair genes and genomic instability in breast cancer cell lines.

As previously performed in breast tumour specimens, we estimated the number of gains of *PARP1* gene in the panel of BCCLs. In this occasion we analyzed the alterations in the locus of *PARP1* gene in the chromosome 1q by aCGH array to determine the copies of the gene. For this analysis in BCCL we also applied the SNP 6.0 array performed by the Microarray Analysis Service (SAM) at IMIM. We observed that those cells with higher PARP1 protein levels had significantly more copies of the *PARP1* gene locus (R=0,856; p=0,029) (**Fig. R.14**).
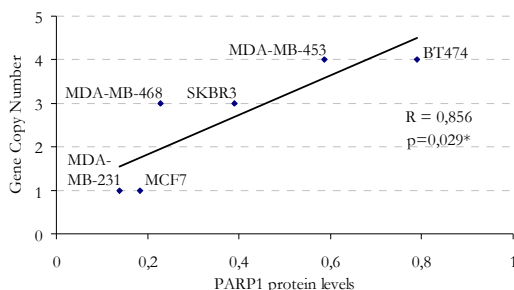
Figure R.14. Correlation between *PARP1* gene gains and PARP1 protein levels. *PARP1* gene gains assessed by aCGH and PARP1 protein levels assessed by WB from BCCL in basal conditions showed significant correlation by Chi-squared test (R^2=0,856, p=0,029).

As in the case of breast tumour samples, we wanted to characterize in the panel of cell lines whether the levels of PARP1 protein or the alterations in DNA repair genes correlated with the GI index. The study was performed in the same manner as described previously.

All cell lines showed altered regions and the GI index ranged from 15,3 to 32,5. The GI index average was higher than in tumour samples, but the highest absolute values were similar. In this case, we observed no correlation between PARP1 protein levels and the GI index. Furthermore, when we assessed the number of gene alterations and LOH of the genes in the panel DNA repair, we found a higher absolute number of aberrations compared with tumor samples, but neither gene alterations nor LOH correlated with the GI index ($R^2=0,175$, p=0,019; and $R^2=0,002$, p=0,173, respectively) (**Fig. R.15**). This result suggests that in this panel of cell lines the alterations in the DNA repair genes do not explain the genomic instability values. Probably in cell lines, the enzymatical and mechanical stress of being in culture and periodically trypsinized induce an accumulation of alterations in the genome that are not caused only by the alterations in DNA repair genes, thus not correlating with the genomic instability index.

Figure R.15. Genomic instability in breast cancer cell lines. A. Map representing the gains and losses in a panel of 160 DNA repair genes in 6 BCCL. Colors mean different gene alterations: Blue, Loss of Heterozigozity (LOH); yellow, low amplification; and orange, high amplification. Degrees of Genomic Instability (GI) Index, Gains and Losses, and PARP1 protein levels of each cell line are specified at the top of the map. **B.** Correlation between GI index and gene alterations. **C.** Correlation between GI index and LOH. B. and C., showed no correlation by Chi-squared test.

(Next page)

Figure A: Genomic instability index, Gene alterations, LOH, PARP1 expression heatmaps. Alteration legend: LOH, Low amplification, High amplification.
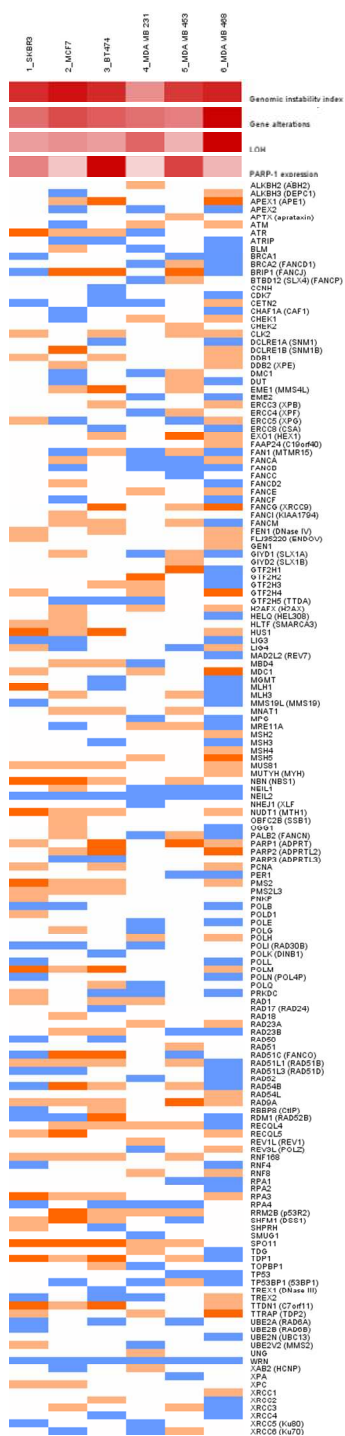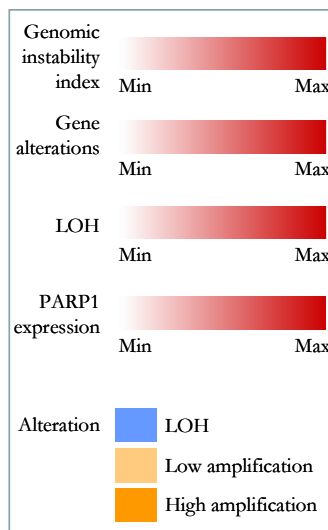
Figure B: Correlation between GI Index and Number of Gene Alterations. R² = 0,175, p = 0,019.
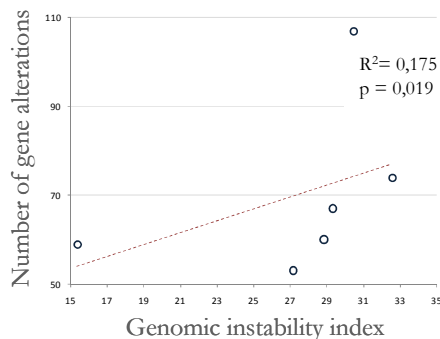
Figure C: Correlation between GI Index and Number of LOH. R² = 0,002, p = 0,173.
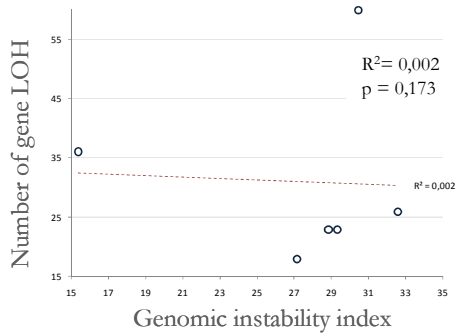
R.3. CHARACTERIZATION OF THE EFFECTS OF PHARMACOLOGICAL INHIBITION OF PARP IN BREAST CANCER CELL LINES

As demonstrated in the first clinical trial with olaparib, PARP inhibitors have a synthetic lethality effect in BRCA1/2-mutated tumours[272]. We wanted to study whether the different subtypes of BCCLs, including a BRCA1-mutant, had different sensitivities to different PARP inhibitors alone or in combination with different types of therapies. We wanted to explore which breast cancer subtypes might benefit from this therapy, alone or in combination.

For this purpose we used two commercially available PARP inhibitors:

• PJ34, a widely used inhibitor of PARP activity in preclinical models.

• Olaparib, which has completed phase II clinical trials for breast cancer.

R.3.1. Effects of PARP inhibitors as single agents

R.3.1.1. PJ34 and olaparib effectively inhibit PARP activity

First of all, we confirmed that PJ34 and olaparib were able to block PARP activity by both, the detection of pADPr by WB and enzymatic activity quantification by PARP enzyme activity assay. Both inhibitors were able to block the pADPribosylation of target proteins that accept ADP units (**Fig. R.16A**) and the enzymatic activity of PARPs (**R.16B**). Whereas PJ34 performed well in the micromolar range as also described

in the literature[294], olaparib demonstrated in each functional assay much higher potency in the nanomolar range.
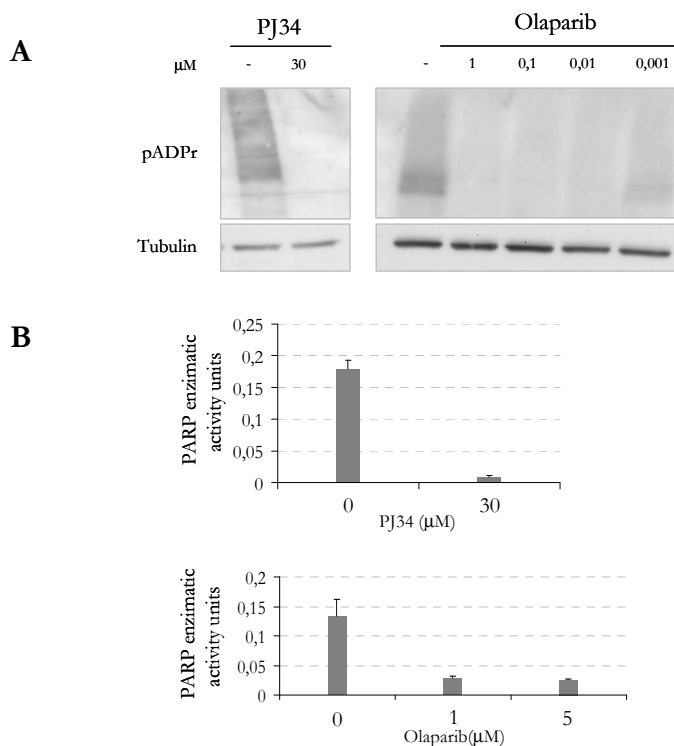
Figure R.16. PARP inhibition by PJ34 and olaparib PARP inhibitors. A. 20μg of total protein from cell lysates of MDA-MB-468 cells treated 90' with 30μM of PJ34 or 1-0,1-0,01-0,001μM of olaparib were subjected to WB to assess the decrease of pADPr protein levels, β-tubulin was used as loading control. **B.** 5μg from cell lysates of MDA-MB-468 cells treated 90' with 30μM of PJ34 (Top) or 1-5μM of olaparib (Bottom) were subjected to PARP enzymatic activity assay and showed decrease in PARP enzymatic activity units.

R.3.1.2. Sensitivities of breast cancer cell lines to PJ34 and olaparib as single agents

Next, we assessed the sensitivity of the panel of BCCL towards PJ34 or olaparib treatments in terms of cell growth capacity.

In parallel, we assessed BRCA1 and BRCA2 protein expression by WB in order to study whether their expression levels could associate with sensitivities to these inhibitors. In addition to BCCL, as control of BRCA2-mutant we included the pancreatic cell line, CAPAN-1 (**Fig. R.17A**). In addition, we confirmed the reported mutations in *BRCA1*[295] and *BRCA2*[296] genes for HCC1937 and CAPAN-1 cell lines, respectively, by direct DNA sequencing. For this approach specific primers for the exon where the mutation localizes were used. (**Fig R.17B**)
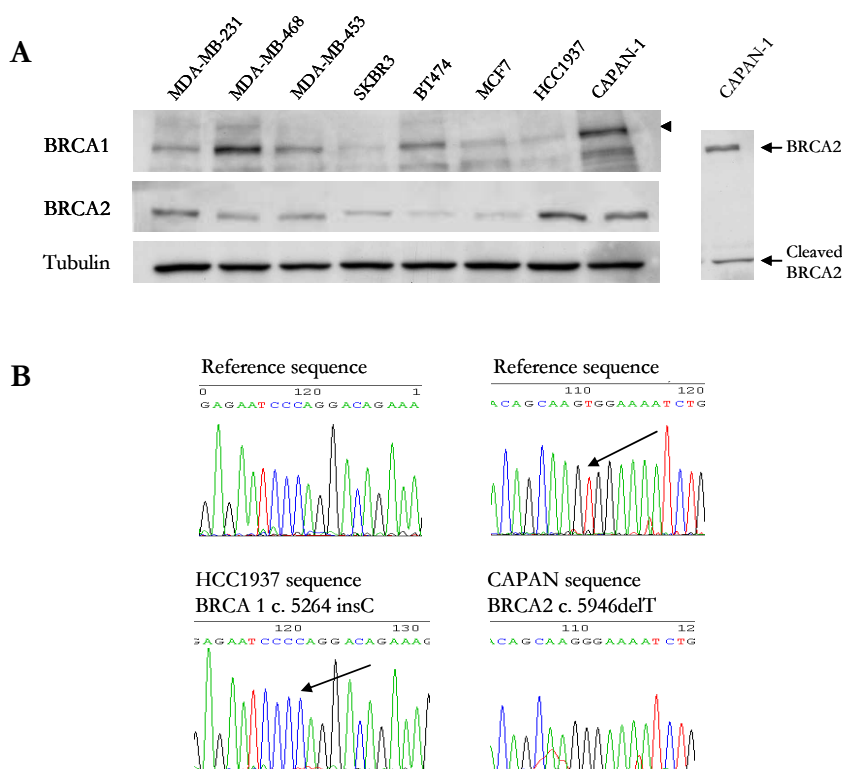
Figure R.17. BRCA1 and BRCA2 in the panel of BCCL panel and CAPAN-1 pancreatic cell line. A. 20μg of total protein from cell lysates of BCCL and CAPAN-1 in basal conditions were subjected to WB to assess BRCA1 and BRCA2 protein levels, β-tubulin was used as loading control. (Continues) **B.** Direct sequencing of DNA extracted from HCC1937 and CAPAN-1 cells was used to assess the presence of mutations in *BRCA1* and *BRCA2* genes, respectively. Graphs shows reference sequences (upper panels) and the obtained sequences (lower panels), arrow indicates the localization of the mutated nucleotide.

109

All BCCL responded in a dose-dependent manner to 48h treatment with PJ34 (0-30μM) assessed by MTS assay, whereas no effect was observed in the 48h treatment with olaparib (0-20μM) using the same assay in three BCCL (**Fig R.18A-B**). Then, we decided to assess the sensitivity to olaparib by clonogenic assay using a longer-term treatment (10 - 20days). Using this sensitive assay we observed that all BCCL responded in a dose-dependent manner to olaparib (0 - 0,5 - 1μM) (**Fig R.18C**). In both cases we observed a spectrum of sensitivities.

C

D
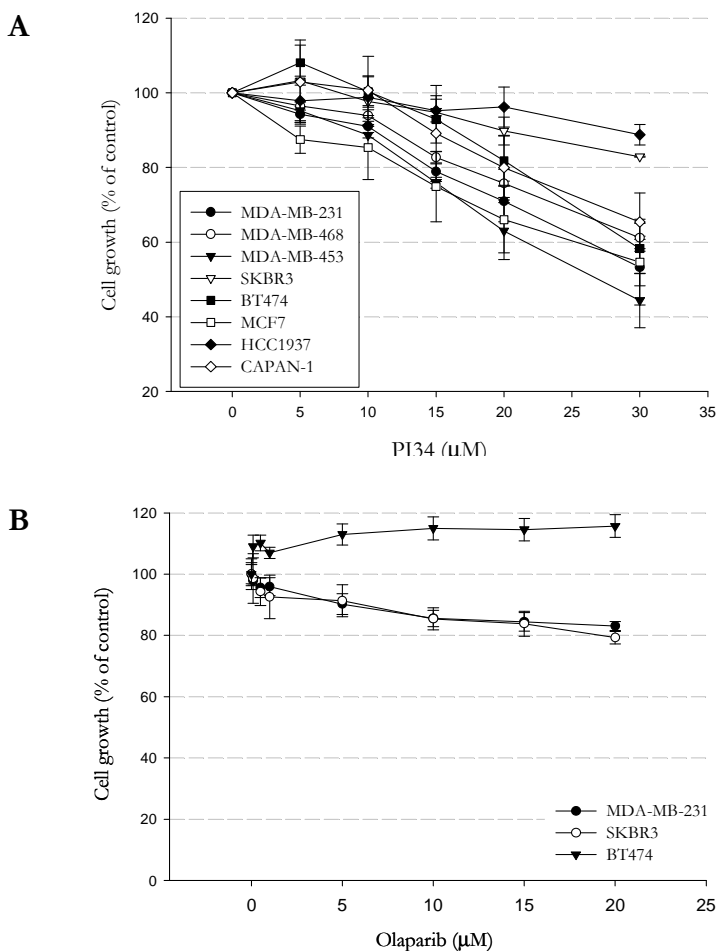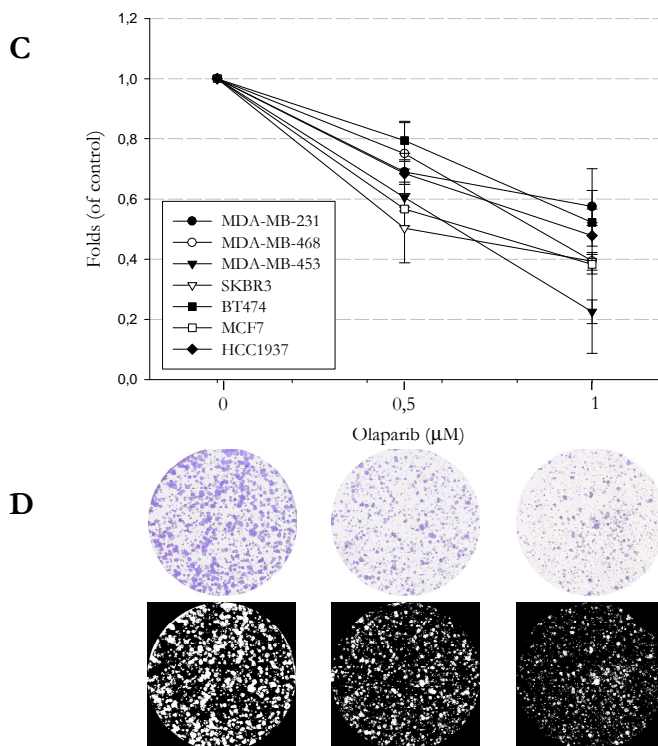
Figure R.18. Sensitivity of BCCLines to PJ34 and olaparib treatments.
Sensitivity to PJ34 (**A**) and olaparib (**B**) treatments for 48h assessed by MTS assay.
Each data point represents the mean ± s.d. percent cell growth inhibition of three
independent experiments, compared to controls at 100%.. **C**. Sensitivity to olaparib
long-term treatment assessed by clonogenic assay. Cells were seeded at low density,
treated during 10-20 days with olaparib (0,5-1μM) and the resultant colonies were
stained and analyzed by ImageJ. Each data point represents the mean ± s.d. folds
cell growth inhibition of three independent experiments, compared to controls at 1
fold. **D**. Representative images of stained colonies (top) and respective ImageJ
processed images (bottom).

All cell lines tested, including BRCA-mutant as well as BRCA-proficient
cell lines, exhibited decrease in cell growth upon PARP inhibitor
treatments.

In our hands, HCC1937 was the most resistant cell line in front of PJ34 treatment, and the third less sensitive to olaparib. Arranging the cells in a scale from the most to the least sensitive in front of the highest dose tested with each inhibitor we can observe the distribution depicted in the following figure (**Fig. R.19**).

More sensitive		More sensitive	
	MDA-MB-453		**MDA-MB-453**
	MDA-MB-231		**MCF7**
	MCF7		**SKBR3**
PJ34	**BT474**	Olaparib	**MDA-MB-468**
	MDA-MB-468		**HCC1937**
	CAPAN-1		**BT474**
	SKBR3		**MDA-MB-231**
Less sensitive	**HCC1937**	Less sensitive	
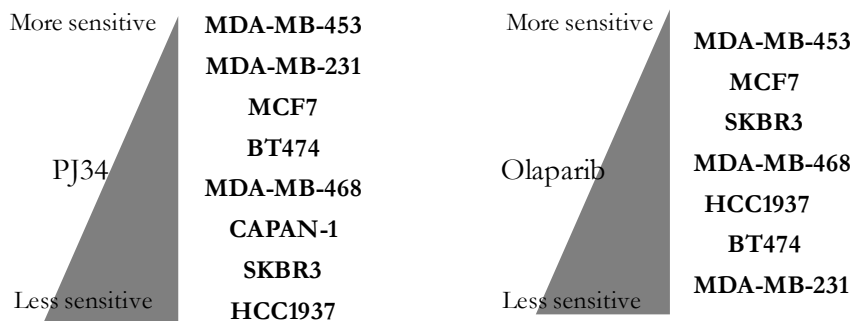
Figure R.19. Scale of sensitivities of BCCLines to PJ34 and olaparib treatments. BCCL are arranged from the most sensitive to the less sensitive to the higher dose of PJ34 (30μM, 48h), assessed by MTS (left), and to the higher dose of olaparib (1μM, 10-20days) assessed by clonogenic assay (right).

MDA-MB-453 was found to be the most sensitive cell line to both inhibitors, while the rest of cells responded very different, in terms of sensitivity, to each drug. In part, it could be explained because PJ34 is less potent and less specific than olaparib, and some effects might be caused by other mechanisms beyond the inhibition of PARP.

Taking into account only the effects on viability with olaparib we did not observe any correlation between PARP1, pADPr, or BRCA1/2 levels/mutational-status and sensitivity to the inhibitor, as single agent, in the cells of the panel. We cannot rule out that the observed effects on cell growth non-specific (i.e. no mediated by PARP inhibition) since the

concentrations required to observe effects were in the micromolar range. It was intriguing the lack of synthetic lethality in BRCA-mutated cells, but the results were replicated in independent experiments and the mutation confirmed in cultured cells.

R.3.2. Effects on cell survival of olaparib in combination with chemotherapy

The use of PARP inhibitors could sensitize tumours cells to different DNA damaging therapies. For this reason, we tested olaparib in combination with different chemotherapies (doxorubicin and cisplatin) using the clonogenic assay.

As performed in the clonogenic assay to test olaparib as a single agent, cells were treated continuously with olaparib (1 - 0,5μM) during 10-20 days. 24 hours before the end of the experiment cells were treated with doses of doxorubicin or cisplatin corresponding to the IC_{25} and IC_{50} values for 48h and analysed for colony formation by staining with crystal violet.

Olaparib sensitized all BCCL to doxorubicin and cisplatin (**Fig. R.20**). All combination treatments reached statistical significance. In contrast to olaparib alone, the presence of a mutated BRCA gene determined higher sensitization to the combined treatment with chemotherapy. The HCC1937 cell line was sensitized most efficiently to both drugs (cisplatin and doxorubicin) upon combination with olaparib.

The second and third cell lines most efficiently chemosensitized in combination with the PARP inhibitor were SKBR3 cells, apparently with low levels of BRCA1 and BRCA2 protein content, and MCF7, with relative low levels of BRCA2. The chemosensitization presented as fold decrease relative to olaparib treatment and the statistical significance level in the panel of BCCL are summarized in **Table R.5**. It is noteworthy that in these combinations with olaparib, basal-like/TN cell lines were not, in general, the most chemosensitized cell lines in the panel. In the case of MDA-MB-453 and MDA-MB-468 the dose of olaparib used for the clonogenic assay was 0,5μM, instead of 1μM used in the rest of cells. The dose was reduced in order to detect quantifiable colonies in the combined conditions.

Figure R.20. Chemosensitizing effects of olaparib combined with chemotherapeutic agents on clonogenic survival. Cells were seeded at low density, treated during 10-20 days with olaparib (1μM, and 0,5μM in the case of MDA-MB-453/468) and the last 24h cells were treated with doses of doxorubicin or cisplatin around IC_{25}-IC_{50} values. The resultant colonies were stained and analyzed by ImageJ. Each bar represents the mean ± s.d. folds cell growth inhibition of three independent experiments, compared to controls at 1 fold. ANOVA One-way was used for statistical analysis. Bars: Black (Chemotherapy), white (Olaparib), grey (combined treatment).

(Next page)

114
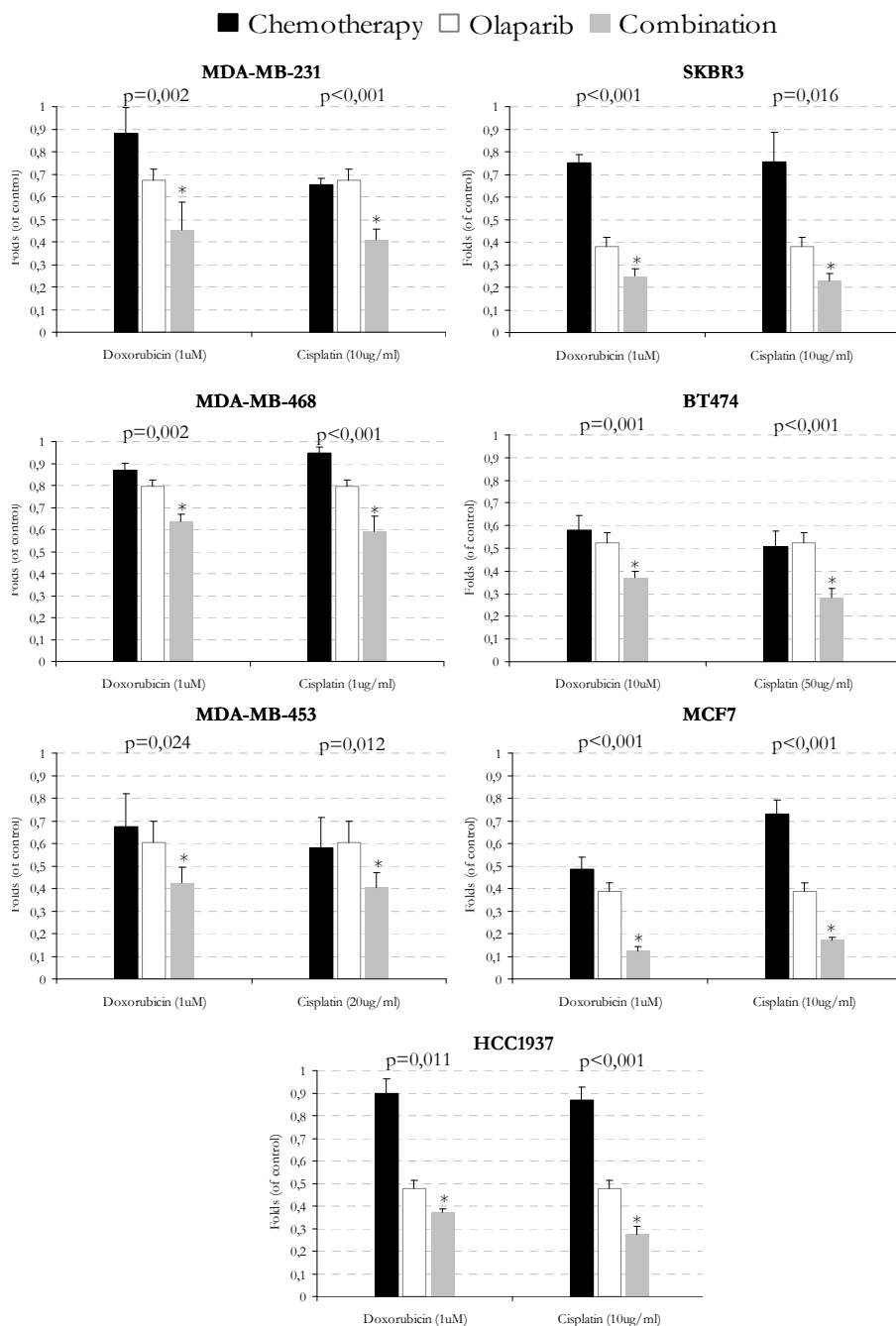
Table R.5. Folds of chemosensitizations upon combination of doxorubicin or cisplatin with olaparib.

	Doxorubicin	p	Cisplatin	p
MDA-MB-231	0,45	0,002	0,2	<0,001
MDA-MB-468	0,24	0,002	0,35	<0,001
MDA-MB-453	0,25	0,02	0,17	0,01
SKBR3	0,51	<0,001	0,53	0,01
BT474	0,22	0,001	0,22	<0,001
MCF7	0,36	<0,001	0,56	<0,001
HCC1937	0,52	0,001	0,6	<0,001

R.3.3. Effects of olaparib in combination with a targeted therapy (trastuzumab)

As stated in the introduction, combinations of PARP inhibitors with other targeted therapies are less common than their combination with chemotherapy, but is another potential approach in specific subtypes of cancer patients.

In the literature only a few examples exist whereby the chemical inhibition of PARP activity or abrogation of *PARP1* gene modulates the expression levels of HER2 and EGFR in cancer cell lines[158,159].

We asked whether this was the case for olaparib in our HER2+ cell lines. If affirmative, then we could explore whether it sensitized cells to anti-HER2 therapy (trastuzumab).

R.3.3.1. Molecular effects of olaparib on HER2 and EGFR

Olaparib downmodulated HER2 and EGFR in SKBR3 and BT474

As a first approach we decided to treat our HER2+ cell lines (BT474 and SKBR3) with 1-5µM of olaparib during 24, 48 or 72 hours. These concentrations were chosen because nearly all available data showed that these doses are below the maximum achievable dose in normal clinical use and thus to achieve a clinical significance of these results[297]. WB analysis of lysates from control and olaparib treated cells revealed that the expression of both receptors, HER2 and EGFR, decreased in a dose- and time- dependent manner in both cell lines (**Fig. R.21A**).

A   **B**
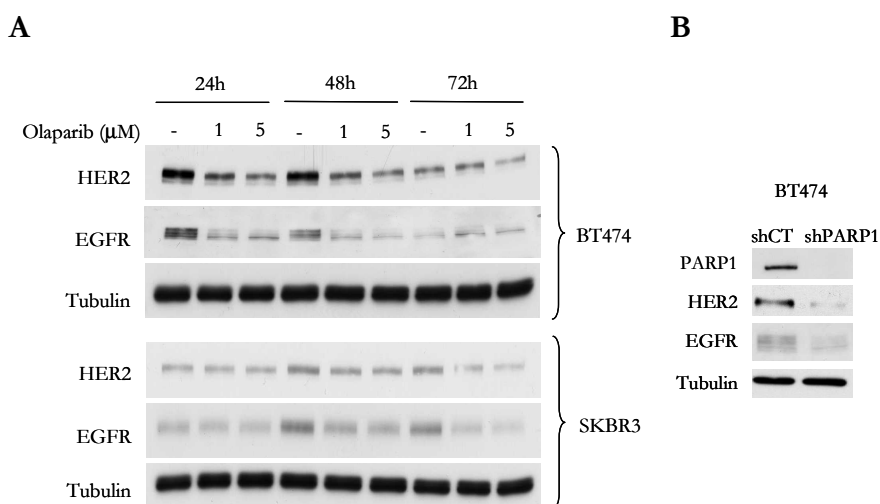
Figure R.21. Olaparib treatment modulates EGFR and HER2 levels in BT474 and SKBR3. A. 5-20µg of total protein from cell lysates of BT474 (Top) and SKBR3 (Bottom) cells treated 24-48-72h with 1-5µM of Olaparib were subjected to WB to assess HER2 and EGFR protein levels, β-tubulin was used as loading control. **B.** PARP1, EGFR and HER2 protein levels assessed by WB from BT474 cells stably depleted for PARP1 (shCT, control, shPARP1, PARP1-depleted).

To determine whether this modulation was mainly due to PARP1 inhibition by olaparib, or to additional effects of the drug, we stably

knocked-down PARP1 expression in BT474 by lentiviral transduction of shRNA of PARP1 and a scrambled sequence in the case of the control. Genetic silencing of PARP1 in BT474 also tended to downmodulate the protein levels of HER2 and EGFR (**Fig. R.21B**).

Olaparib slightly enhanced the receptor downmodulation of trastuzumab

In light of these results, we hypothesized that the addition of olaparib to trastuzumab treatment could sensitize HER2+ cells to the downregulatory actions of this antibody. As shown in the densitometries of the WB, the concomitant treatment with olaparib (1-5μM) and trastuzumab (1-10μg/mL) slightly downmodulated the protein levels of total HER2, EGFR, and the surrogate downstream proteins phospho-Akt (Ser473) and phospho-Erk (Thr202/204) more than each drug alone in BT474. In the case of SKBR3, we only observed an enhanced decrease in EGFR levels (**Fig.R.22**).

Figure R.22. The addition of olaparib to trastuzumab treatment slightly enhanced the downmodulation of HER2-EGFR-Akt-Erk axis. Cells were serum starved for 24h and then concomitantly treated 48h with olaparib (1-5μM) and trastuzumab (1-10μg/mL) for BT474 and SKBR3 respectively. 20μg of total protein were subjected to WB to assess HER2, EGFR, phospho-Akt (Ser473), Akt, phospho-Erk (Thr202/204) and Erk protein levels. β-tubulin was used as loading control. Densitometry values of each condition were normalized with the respective β-tubulin and expressed as folds of the control condition below each panel.

(Next page)

	BT474					SKBR3			
Olaparib (µM)	-	+	-	+		-	+	-	+
Trastuzumab (ug/mL)	-	-	+	+		-	-	+	+
HER2									
	1	0.70	0.60	0.45		1	0.72	0.68	0.65
EGFR									
	1	0.39	0.43	0.33		1	0.63	0.63	0.31
pAkt									
	1	0.82	0.38	0.26		1	1.02	0.19	0.23
pErk									
	1	0.66	0.38	0.29		1	0.45	0.49	0.40
Tubulin									
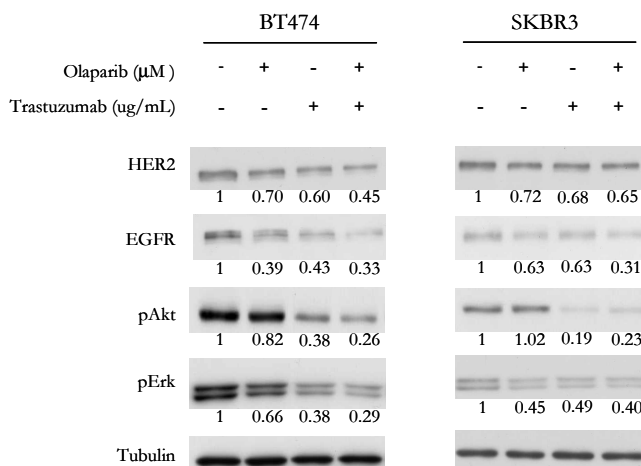
R.3.3.2. Cellular effects of the olaparib – trastuzumab combination

Since HER2 downmodulation is one of the key mechanisms of action of trastuzumab, the molecular results shown in the previous section left the door open to the possibility of potentiating cytotoxic and cell growth inhibitory effects of trastuzumab by combining it with olaparib.

Olaparib sensitized HER2+ cell lines to trastuzumab treatment

In our first approach we tested the effects of combining trastuzumab and olaparib on cell viability by clonogenic assay. Drugs were combined at two fixed optimal concentrations as obtained from previous dose-dependence experiments with each drug. Every three days the media was changed and fresh drug was added. Following treatment, the cells were fixed with methanol and stained with 0,1% crystal violet. For quantification, the plates were scanned, and blue color intensity was determined in each case using the software ImageJ. The drugs effects are

shown as relative values referred to the vehicle treated control that was set to one. Long-term treatments with low concentrations of trastuzumab (1µg/mL) and olaparib (1µM) reduced significantly the clonogenic capacity of BT474 and SKBR3 cells more than each drug alone. (**Fig. R.23**).
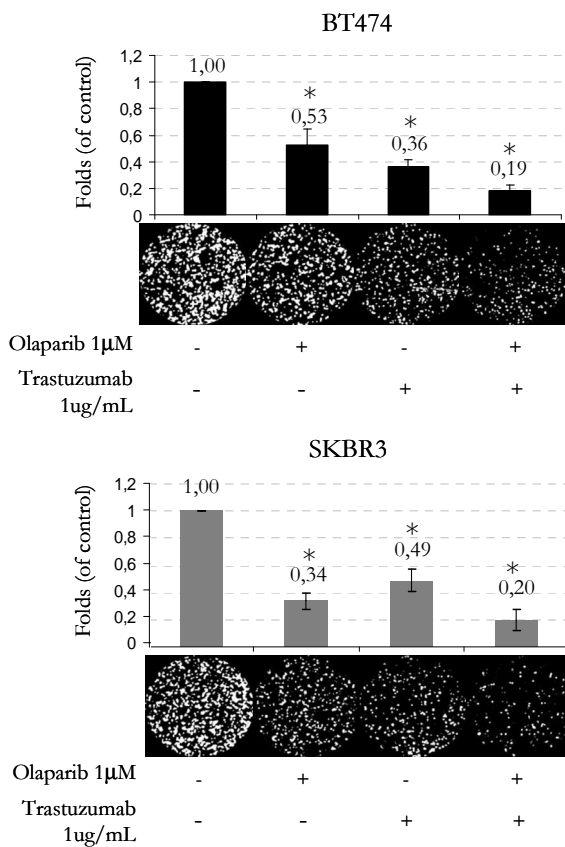
Figure R.23. Effects of olaparib/trastuzumab combination on clonogenic survival of HER2+ cell lines. Cells were seeded at low density, treated during 20days (BT474, top) or 10 days (SKBR3, bottom), depending on its proliferation rate, with olaparib (1µM) and trastuzumab (1µg/mL). The resultant colonies were stained and analyzed by ImageJ. Representative processed images are below each condition. Each bar represents the mean ± s.d. folds cell growth inhibition of three independent experiments, compared to controls at 1 fold. ANOVA One-way was used for statistical analysis.

120

In a second instance, selected combinations were examined in detail using cell cycle analysis. For this approach, HER2+ cells were seeded and 24h later were treated with 5μM of olaparib and 10μg/mL of trastuzumab. After 96h cells were harvested, fixed with 70% methanol and stained with DAPI staining solution to discriminate cells in different phases of the cell cycle based on their DNA content by flow cytometry analysis. This assay showed that the combination, in a statistically significant manner, increased the percentage of apoptotic/death cells defined by subG0/1 phase in SKBR3; while a tendency was detected in BT474. Statistically significant in both cell lines were also the increases detected in the percentage of cells arrested in G2 compared with trastuzumab alone, and in the percentage of cells arrested in G1 compared to olaparib alone. A slight tendency in both cell lines to decrease the number of cells in S-phase in the combinatory condition compared with the drugs alone was also detected (**Fig. R.24A**). These results reflected that the effects of both drugs cooperate significantly in terms of cell cycle effects. In addition, we confirmed these data by WB analysis reproducing the same conditions used in cell cycle analysis by FACS. In this case, we detected an accumulation of p27kip1, a cyclin-dependent kinase inhibitor, and p21, as a maker of G2 cell arrest, indicating a correlation with the data obtained by flow cytometry analysis of the cell cycle (**Fig R.24B**).

Figure R.24. Effects of trastuzumab/olaparib combination on cell cycle. A. Cell cycle analysis by FACS of BT474 (top) and SKBR3 (bottom) cells treated 96h with olaparib (5μM) and trastuzumab (10μg/mL). Each bar represents mean ± s.d. percentage of cells in each phase of the cell cycle of three independent experiments. ANOVA One-way was used for statistical analysis. **B.** 20μg of total protein from lysates of BT474 (left) and SKBR3 (right) treated as in (A.) were subjected to WB to assess levels of cell cycle proteins: CyclinD1, p27 and p21. β-tubulin was used as loading control.

(Next page)

A

BT474

SKBR3

B
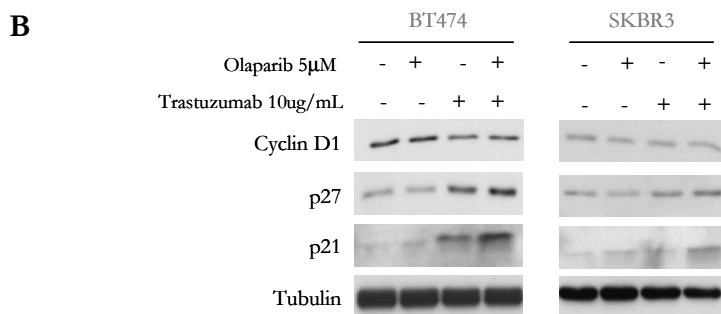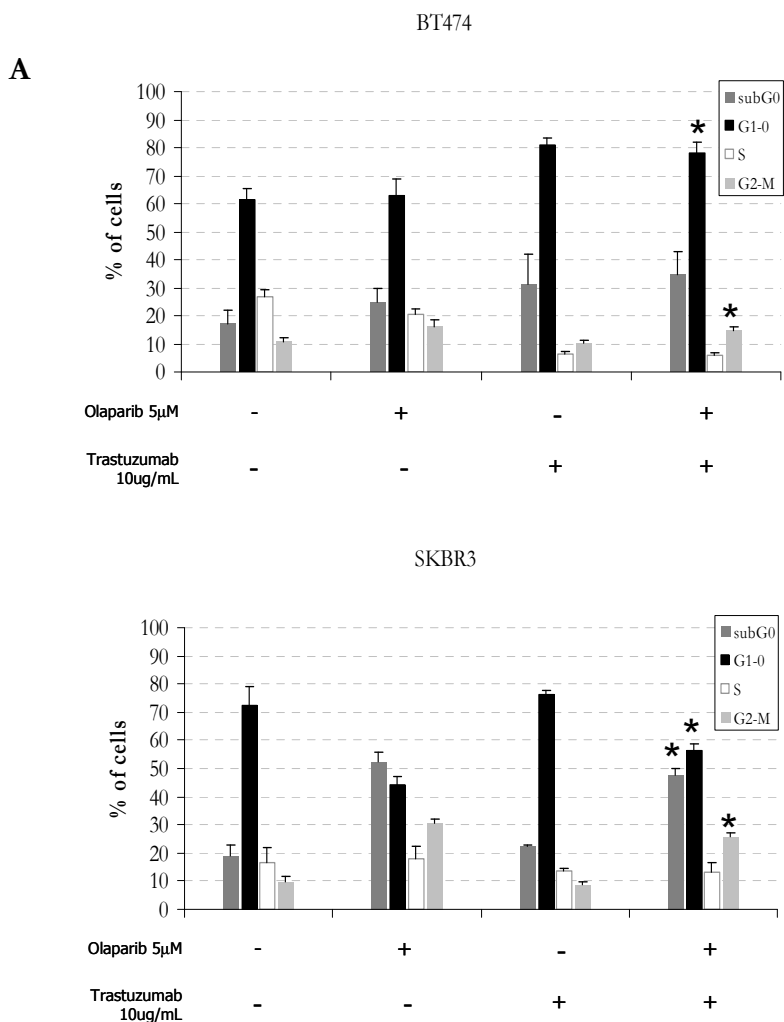
In the view of these results, we aimed to know if this potentiation in terms of cell cycle could lead cells to a less proliferative capacity. For this purpose and in parallel to the previous 96h treatments, manual cell count was performed and a statistically significant reduction in number of cells was detected when both drug were combined (p<0,05) (**Fig R.25A**). Furthermore, these results were confirmed by assessing the antiproliferative effects in response to the combined treatment as compared to each drug alone at 96h with two cell viability assays, based on the total amount of proteins (SRB assay), and the metabolic capacity (MTS assay). Once again, significantly lower levels of proteins and metabolic activity were detected in the combined condition of trastuzumab plus olaparib than that with each drug alone, as shown in the **figure R.25B** for SKBR3.
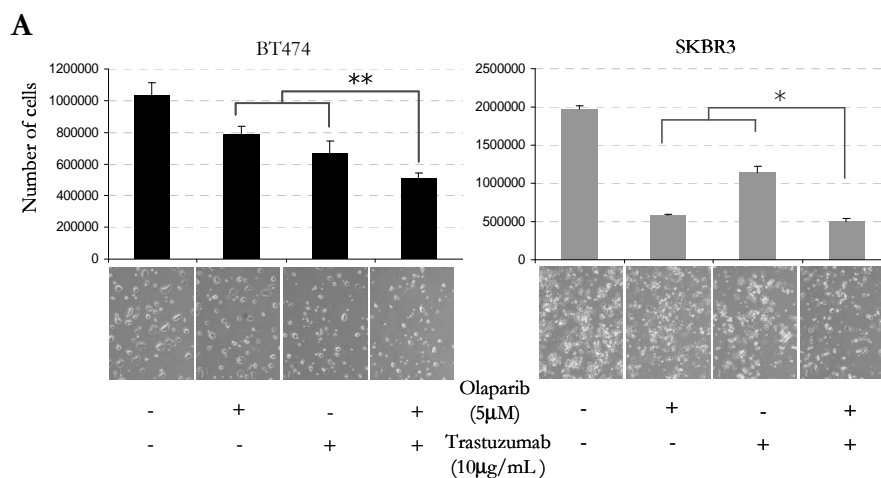
Figure R.25. Cell growth inhibitory effects of olaparib/trastuzumab combination in HER2+ cell lines. A. BT474 (left) and SKBR3 (right) cells were treated 96h with olaparib (5μM) and trastuzumab (10μg/mL) and cell count was performed with Scepter device. (Continues)
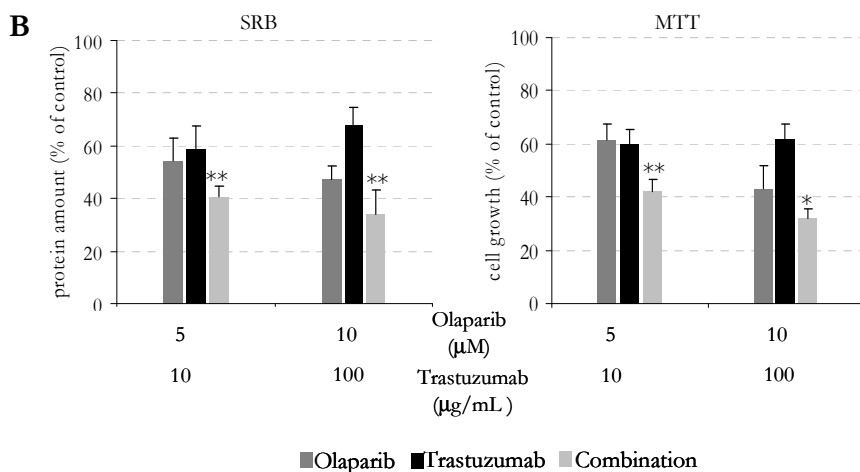
Figure R.25. Continued. B. SKBR3 were subjected to the same treatment described in A.. Cell growth inhibition was assessed by SRB assay (left) and MTS assay (right). Each bar represents the mean ± s.d. percentage of cell growth inhibition of three independent experiments, compared to controls at 100%. ANOVA One-way was used for statistical analysis. Bars: Dark grey (olaparib), black (trastuzumab), grey (combined treatment). * $p<0,05$; ** $p<0,01$

When we performed the same previous assays in a non-HER2+ cell line, MDA-MB-231 cell line, which express low levels of HER2, as expected, no enhanced reduction of clonogenic capacity, total amount of proteins or metabolic capacity were detected when the cells were treated with both drugs (**Fig. R.26 A,B.**). These results further indicated that olaparib was able to enhance the effects of trastuzumab to a greater extent in HER2+ cell lines, probably mainly through alterations in HER2-EGFR signalling pathway, but not in HER2- cells.

A

MDA-MB-231

B

■Olaparib ■Trastuzumab ■Combination
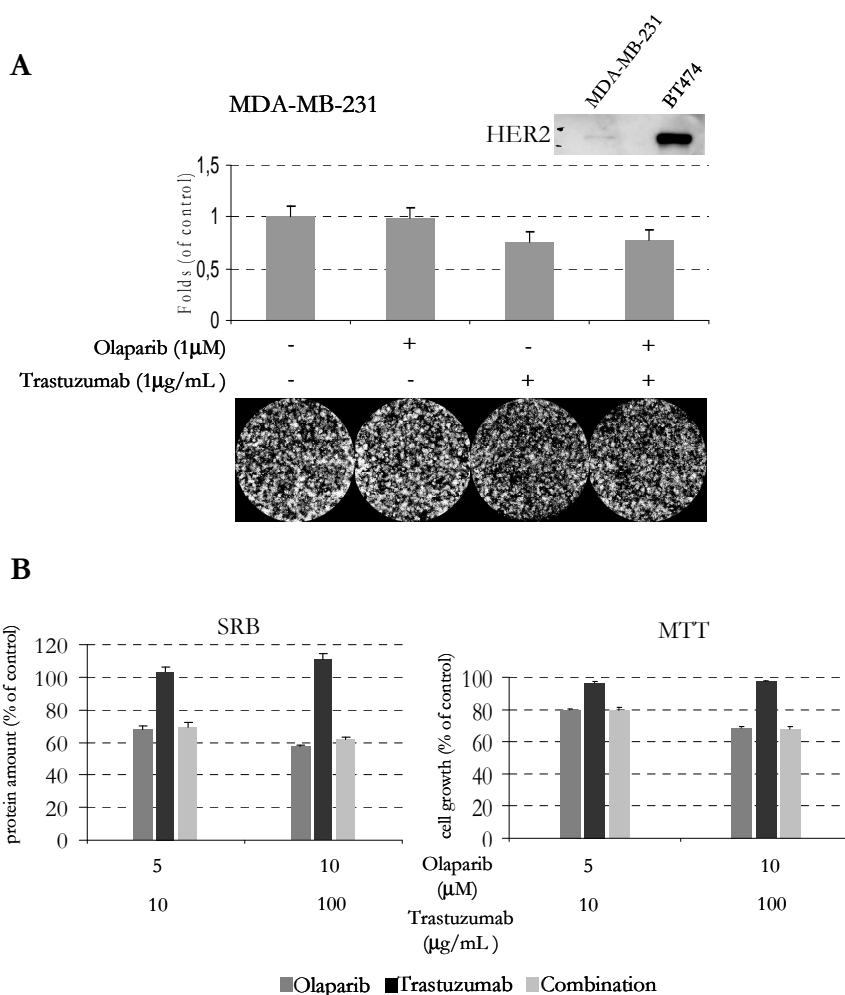
Figure R.26. Cell growth inhibitory effects of olaparib/trastuzumab combination in a non-HER2+ cell line. **A.** Clonogenic assay. MDA-MB-231 cells were seeded at low density, treated during 10 days with Olaparib (1μM) and Trastuzumab (1μg/mL). The resultant colonies were stained and analyzed by ImageJ. Representative processed images are below each condition. Each bar represents the mean ± s.d. folds cell growth inhibition of three independent experiments, compared to controls at 1 fold. (Right panel) WB showing HER2 protein levels in MDA-MB-231 and BT474 cells **B.** MDA-MB-231 cells were treated 96h with Olaparib (5μM) and Trastuzumab (10μg/mL). Cell growth inhibition was assessed by SRB assay (left) and MTS assay (right). Each bar represents the mean ± s.d. percentage of cell growth inhibition of three independent experiments. Bars: Dark grey (Olaparib), black (Trastuzumab), grey (combined treatment).

Effects of olaparib-trastuzumab combination in DNA damage by γH2AX detection and comet assay.

Based on information from other previous studies reporting that the inhibition of EGFR and HER2 may modulate the response to DNA damage through the inhibition of DNA repair and the induction of DNA strand breaks[271,298-300] we hypothesized that one of the mechanisms that might explain, at least in part, the greater activity of the combination could be that induced significantly higher levels of DNA damage and subsequent cell death than trastuzumab or olaparib alone.

We performed the experimental set-up following the same schedule and doses described in our cell cycle experiments. We determined the amount of DNA damage using two techniques: IF assessment of phosphorylated-histone H2AX (Ser 139) (γH2AX) foci and detection of different types of DNA aberrations and/or strand breaks by Comet assay.

For the analysis of the formation of γH2AX foci, indicative of DNA double-strand breaks, by manual count, first we elaborated a scale of γH2AX foci per nucleus that would allow us to more accurately classify cells into more than two categories ("positive" or "negative" cases) according to their amount of DNA damage. (**Fig. R.27**).
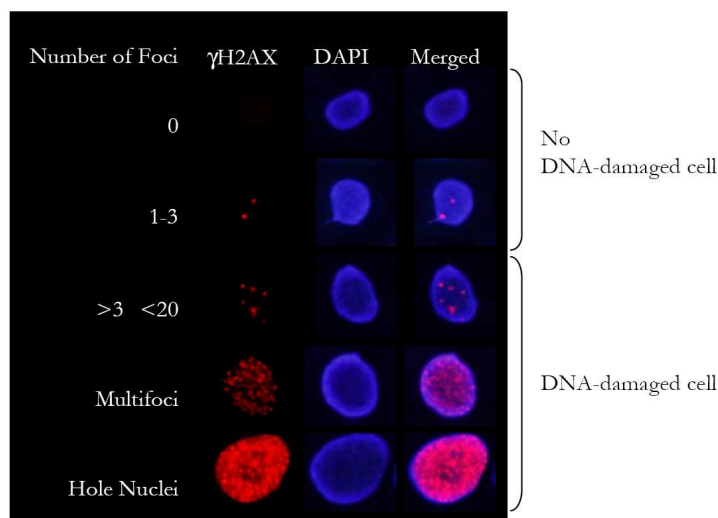
Figure R.27. Scale of γH2AX foci per nucleus. Immunofluorescent images of cells stained with H2AX and DAPI representing a range of DNA damage into 5 cathegories.

Based on this scale, when we considered all those cells ≥4 focis (including the cathegories: more than 3-foci, multifoci and hole nucleus) as cells positive for DNA-damage, we observed that: olaparib induced a marked increase in cells with damaged DNA in both HER2+ cells and especially in SKBR3 cells. Interestingly, data from our study had pointed that SKBR3 was more sensitive to olaparib than BT474; in lesser extent trastuzumab also increased the percentage of cells positive for DNA-damage especially in BT474, which in previous experiments exhibited greater sensitivity to this drug than SKBR3. Also, the combination of olaparib-trastuzumab increased the percentage of cells DNA damaged cells in a statistically significant manner in both cell types (BT474 p=0,005; SKBR3, p=0,04) (**Figure R.28A, B**). When we observed the distribution of positive DNA-damaged cells into the different categories the increase of DNA-damaged cells in the combination compared with the drugs alone was mainly due to an increase in the percentage of cells considered "multifoci", indicating that a large proportion of positive cells

showed a large amount of DNA damage. Besides, we determined the amount of γH2AX by WB, confirming higher increase of this marker when both drugs were combined (**Figure R.28C**).

A
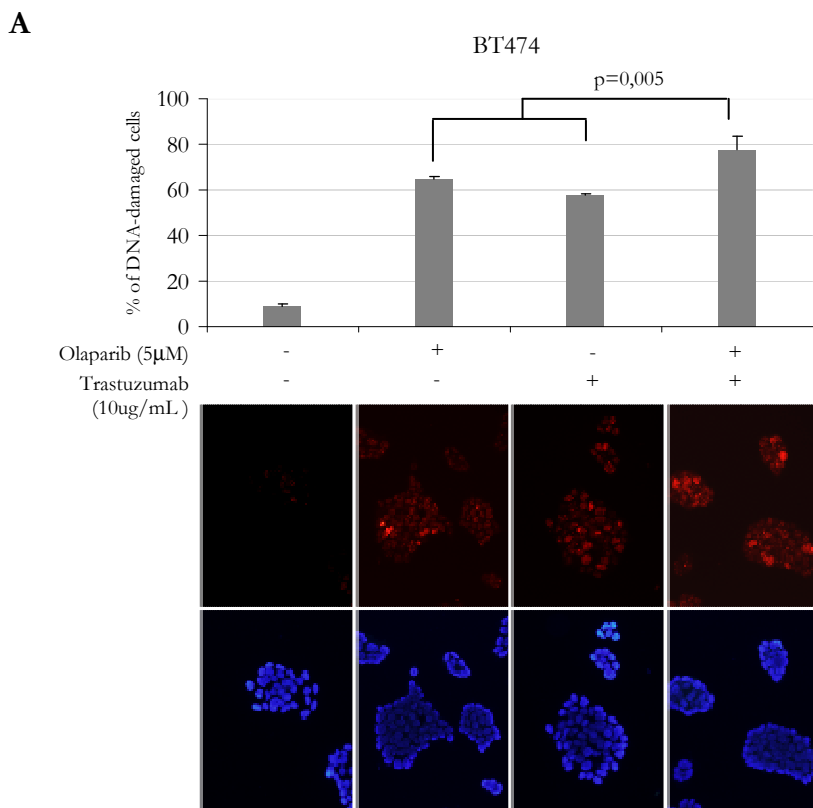
Figure R.28. Effects of olaparib/trastuzumab treatment on DNA damage assessed by γH2AX foci in HER2+ cells. Double strand break DNA damage after 96h of Olaparib (5μM) and trastuzumab (10μg/mL) treatment in BT474 (**A**) and SKBR3 (**B**) cell lines was assessed by immunofluorescence (IF) staining for γH2AX-foci. Those nuclei with ≥4 γH2AX-foci were considered "positive DNA-damaged cell". Each bar represents the mean ± s.d. of percentage of DNA-damaged cells. About 100-200 cells in each condition in three independent experiments were analyzed. ANOVA One-way was used for statistical analysis. Below each graph are included representative IF images from each condition, γH2AX (Top) and DAPI (Bottom).

SKBR3

B

Olaparib (5μM)	-	+	-	+
Trastuzumab (10ug/mL)	-	-	+	+

C

	BT474				SKBR3			
Olaparib 5μM	-	+	-	+	-	+	-	+
Trastuzumab 10ug/mL	-	-	+	+	-	-	+	+
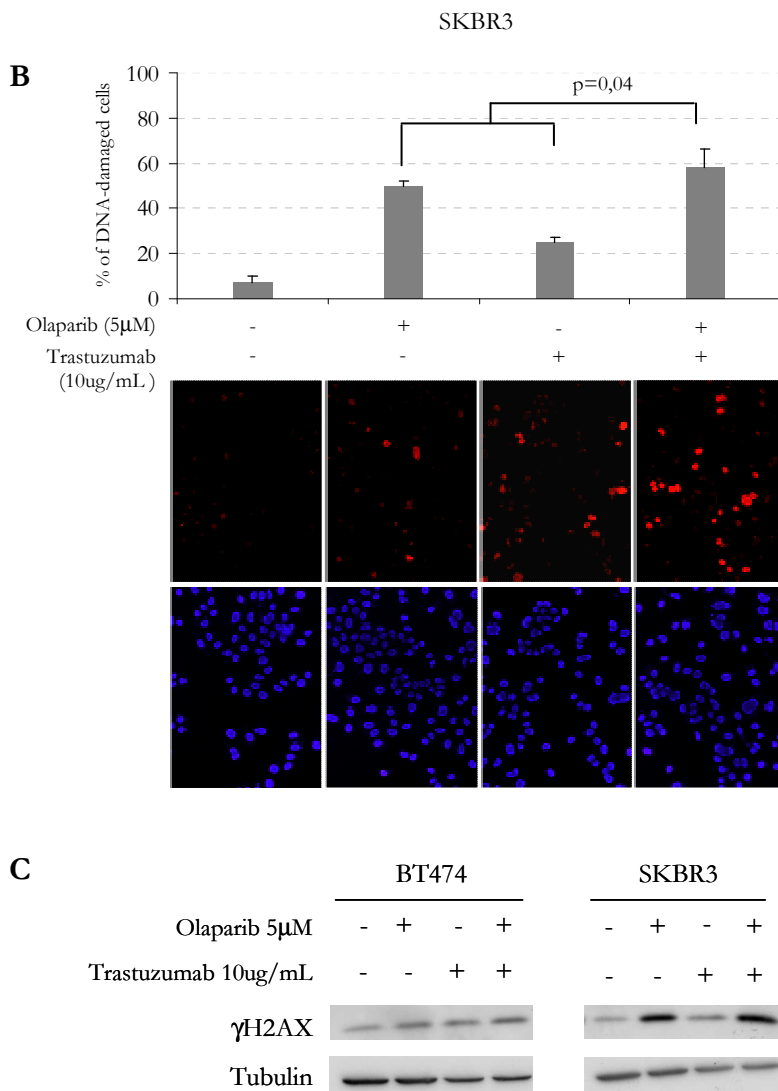
Figure R.28. Continued. C. Confirmation of DNA-damage induction. 20μg of total protein from cell lysates from BT474 (left) and SKBR3 (right) cells treated 96h with Olaparib (5μM) and Trastuzumab (10μg/mL) were subjected to WB to assess levels of γH2AX. β-tubulin was used as loading control.

The other technique used to assess the amount of DNA damage was the Comet Assay. This approach allows the detection of DNA strand breaks and aberrations based on the ability of DNA fragments to migrate out of

the nucleoid faster than intact DNA upon the application of an electric field. The immunofluorescence image of the obtained comets in each treatment was analyzed by ImageJ software to quantify the amount of DNA in the tail.

As in the previous approach we detected an increase in the amount of damaged DNA, i.e. in the amount of DNA in the tail, in all the conditions compared to control. Each drug alone induced increase of damaged DNA in both cell lines, being greater in the olaparib treated cells. The combination of olaparib and trastuzumab increased significantly the amount of damaged DNA in BT474 and SKBR3 cells (p<0,05) (**Figure R.29A, B**)

.

A

B
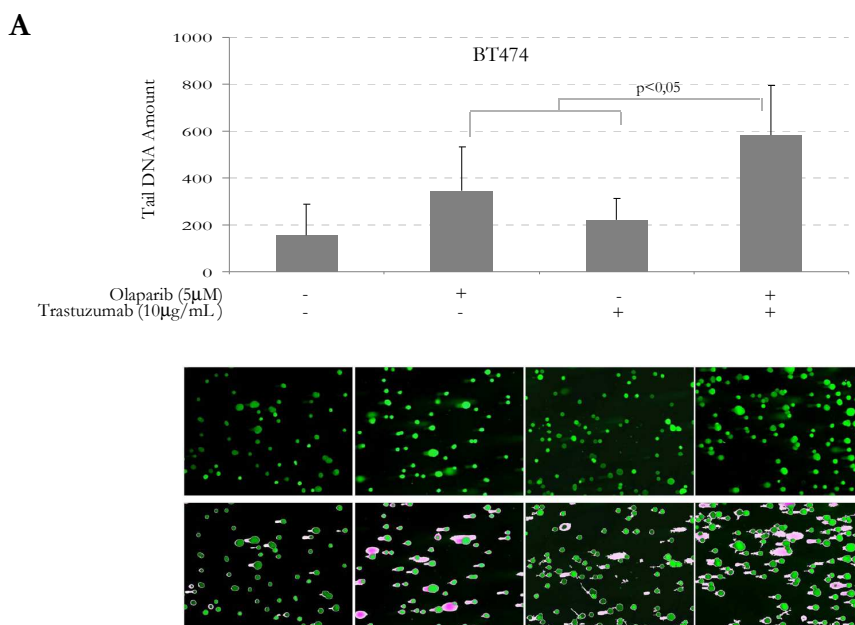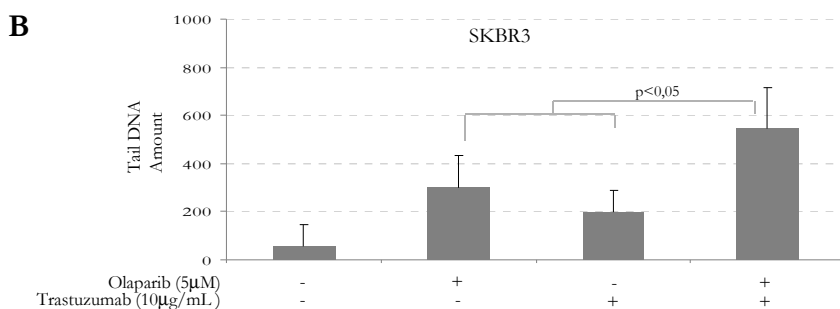
Figure R.29 Comet assay. Effects of olaparib/trastuzumab treatment on DNA damage assessed by Comet Assay in HER2+ cells. DNA damage after 96h of olaparib (5μM) and trastuzumab (10μg/mL) treatment in BT474 (**A**) and SKBR3 (**B**) cell lines was assessed by Comet Assay. IF images were analyzed with ImageJ determining the amount of fluorescence (DNA) in tails versus nuclei. Each bar represents the mean ± s.d. amount of DNA in tails. More than 200 cells in each condition in three independent experiments were analyzed. ANOVA One-way was used for statistical analysis. Below BT474 graph are included representative IF images from each condition; IF (Top), processed images (Bottom).

R.3.3.3. *In vivo* effects of the olaparib - trastuzumab combination

We generated a standard tumour xenograft model with the parental BT474 cell line because they are the only HER2+ breast cancer cellular model cell tumorigenic in nude mice within the panel. Forty Balb/C nude mice were inoculated subcutaneously (s.c.) with BT474 cells mixed with matrigel into the right flank. Biodegradable time-release estrogen-pellets (0,72mg, 60day release) were implanted subcutaneously on the back of each mouse one day before tumour cell inoculation. Tumour growth was periodically analyzed by measurement with a digital calliper and the tumour volume in mm^3 was estimated by the formula: [Volume = (Length * Width^2)/2]. To note, BT474 cells from different laboratories differ for the potential to form tumours in nude mice. As reported by other authors[301] the original parental BT474 had a low tumorogenic rate in xenograft model. In this experimental system, estrogens are needed for

its optimal implantation and growth. However, the estradiol pellet could cause urinary trait obstruction problems, and thus urine retention and ultimately death[302]. Initially, the model was designed to allocate the forty mice of 10 animals each group into four groups. As a consequence of the side-effects of the estrogens pellets, of the forty mice that started in the study only 25 reached the experimental endpoint and were included in the data set for analysis. Mice bearing subcutaneous proliferative tumours were distributed homogenously when tumours reached a volume between 150-250mm^3 into experimental and control groups with approximately equal volumes per group at the beginning of the treatment: Control, olaparib, trastuzumab and olaparib plus trastuzumab. olaparib (50mg/kg) was inoculated intraperitoneally (i.p.) daily, whereas a low dose of trastuzumab (0,3mg/kg) was inoculated i.p. every four days. Combination-therapy group received both drugs at the same doses. Trastuzumab and olaparib vehicles solvents (IgG1 Kappa 0,3mg/kg and 10% 2-hydroxy-propyl-β-cyclodextrine/PBS, respectively) were also inoculated in the olaparib group and trastuzumab group, respectively, according to the schedule shown in the **Table R.6** below.

Table R.6. Treatment schedule for the study of the Olaparib-Trastuzumab combination in subcutaneous xenograft models of BT474.

Groups (final n)	Doses	Schedule
Control (n=6)	Olaparib vehicle	i.p. every day
	Trastuzumab vehicle	i.p. every 4 days
Olaparib (n=6)	50mg/kg	i.p. every day
	Trastuzumab vehicle	i.p. every 4 days
Trastuzumab (n=5)	0,3mg/kg trastuzumab	i.p. every 4 days
	Olaparib vehicle	i.p. every day
Combination (n=8)	50mg/kg Olaparib	i.p. every day
	0,3 mg/kg trastuzumab	i.p. every 4 days

After five weeks of treatments, the olaparib treated group presented tumour growth delay compared to the control group. Trastuzumab, even at the relatively low dose used, achieved clear delay of the tumour volumes as expected. Finally, the group that received both drugs exhibited a slightly enhancement in the tumour growth inhibition compared with either group alone. Despite this enhancement, the differences between the indicated conditions were not statistically significant (p=0,86 between trastuzumab alone and in combination; p=0,29 between control and olaparib). This may be explained in part due to the relatively final low number of mice per group, the slow growth of the parental cell line, or true lack of additive effects (**Fig. R.30**).
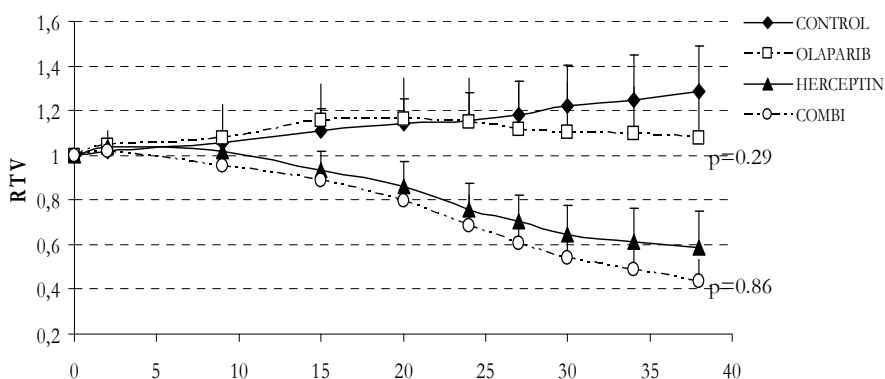
Figure R.30. Effects of olaparib/trastuzumab combination *in vivo*. BT474 cells were implanted subcutaneously in flank of Balb/C nude mice, treatments started when tumour reached ~200mm³. Olaparib, trastuzumab and respective vehicles were intraperitoneally injected at doses and schedules indicated in table R.6. above. Tumour was measured periodically with a digital calliper. Tumour growth is expressed as volume relative to the initial volume (Relative Tumour Volume, RTV). Each data point represents the mean ± s.d. folds RTV growth of tumours from each group of mice compared to controls at 1 fold of RTV. Student *t-test* was used to compare each pair of conditions.

After five weeks of treatment, tumour-bearing mice were sacrificed and tumours were prepared for IHC. Different markers were used to assess

various cellular processes: Proliferation (as the percentage of and Ki-67 or phospho-H3 positively stained tumour cells nuclei); the tumour-associated angiogenesis (as determined by microvessel density measurement, MVD, through the average of CD31-stained vessel tubular structures), apoptosis (as the percentage of cleaved-caspase3 stained cells) and DNA damage (as the percentage of cells with presence of nuclear γH2AX-foci). In terms of proliferation, the combination of olaparib-trastuzumab significantly reduced Ki-67 positive tumour cells compared to trastuzumab alone (p=0,003), and significantly reduced the phospho-H3 positive tumour cells compared to olaparib alone (p=0,017). The angiogenesis evaluated as MVD was not significantly modulated. The apoptosis was significantly increased in the tumours from the combination group compared with the single agent treatment groups (Olaparib vs. combination: p=0,008; Trastuzumab vs. combination: p=0,036), whereas the amount of DNA-damaged cells with positive staining of γH2AX-foci was greater, near the signification, with the combined treatment than with trastuzumab or olaparib alone (p=0,056 and p=0,053 respectively). These in vivo observations appeared to support our in vitro data. Regarding PARP1, we have not found any differences in the expression of the PARP protein in the three treatment groups compared to the control group (**Fig. R.31**).
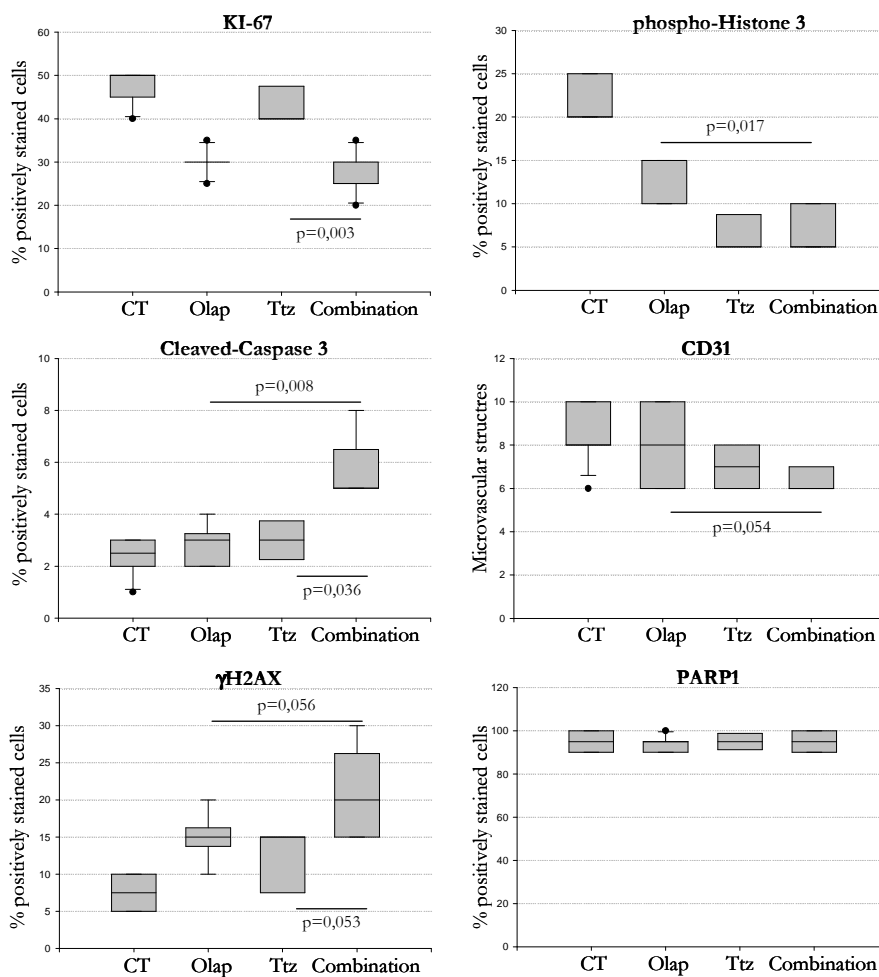
Figure R.31. Effects of olaparib − trastuzumab treatments *in vivo* assayed by IHC. Box plot graphs indicating the IHC results for Ki-67, phospho-H3, CD31, cleaved-caspase3, γH2AX and PARP1 staining in mice tumours of each group of treatments. ANOVA One-way was used for statistical analysis.

R.4. CHARACTERIZATION OF THE EFFECTS OF GENETIC DOWNMODULATION OF PARP1

As stated in the introduction, the actions of PARP1 are not only restricted to its capacity to poly(ADP-ribosylate) proteins, and exerts multiple functions in the cell by binding to different molecules and structures. Furthermore, our funding of worse prognosis in breast cancer women overexpressing PARP1, suggested that PARP1 was a marker or cause of this poor outcome.

For this reason, we decided to further explore the role of PARP1 in breast cancer and we genetically abrogated the expression of PARP1 in three BCCL representing different molecular phenotypes: BT474 (HER2+), MCF7 (Hormone receptor positive) and MDA-MB-231 (Triple-Negative).

R.4.1. *In vitro* effects of stable knockdown of PARP1

The downmodulation of PARP1 protein expression was carried out by lentiviral transduction of shRNA of PARP1 or scrambled shRNA sequence in the case of the control. Transduced cells were culture in fresh medium for 2 days before puromycin selection (0,5μg/mL). Cells were maintained under selection until all control cells were dead. After selection, cells were then allowed to grow for at least two weeks in a healthy pool and frozen stocks were generated of the pool of stable cell lines.

WB of cell lysates from these stably silenced-cell lines showed an almost complete reduction of PARP1 protein compared with parental cells. However, only a slight reduction in the amount of pADPr was detected (**Fig. R 32A**). This result might be due to the redundant or compensatory activity of other PARPs present in these cells. On the other hand, the PARP enzymatic assay showed a clear lower specific activity in shPARP1 cells compared with their respective control cells (**Fig. R.32B**). To assess the PARP enzymatic activity in these cells we used a kit that determines the capacity of PARP enzymes present in whole cell lysates to incorporate biotinylated poly(ADP-ribose) onto histone proteins coated wells by colorimetric measurement. Taking into account that histone H1 is the most abundant histone present in this commercially available kit and PARP1 is among all PARP family members, the enzyme with the highest affinity for histone H1, this could explain the differences observed in the decrease of PARP activity assessed by the presence of pADPr by WB, that allow to detect a wide spectrum of poly(ADPribosylated) proteins, or by the enzymatic assay, that is designed to mainly detect poly(ADPribosylation) of histone H1.
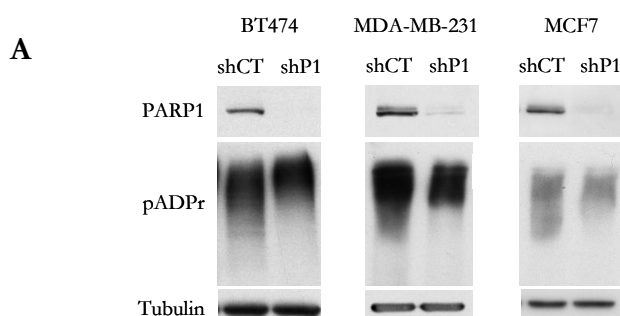
Figure R.32. Stable knockdown of PARP1 in BT474, MCF7 and MDA-MB-231 cell lines. A. PARP1 depletion was performed by lentiviral transduction of shRNA of PARP1 (shPARP1) or scrambled sequence (shCT) in the case of control. 20μg of total protein from cell lysates of each pair shCT/shPARP1 cell lines in basal conditions were subjected to WB to assess PARP1 and pADPr protein levels, β-tubulin was used as loading control. (Continues)
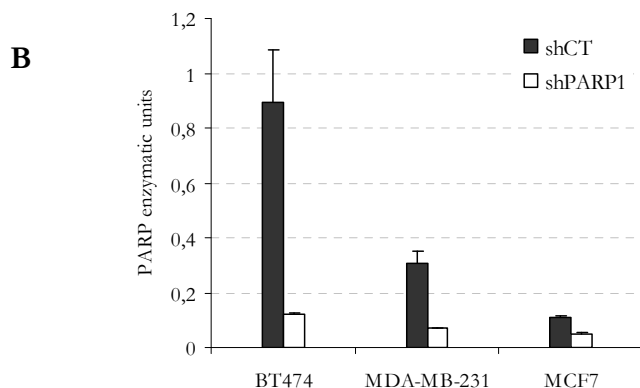
Figure R.32. Continued. B. 5ug of protein from cell lysates of each pair shCT/shPARP1 cell lines in basal conditions were subjected to PARP enzymatic activity assay and expressed as PARP enzymatic units. Each data point represents the mean ± s.d. PARP enzymatic units of three independent experiments.

R.4.1.1. Cellular effects of stable knockdown of PARP1

Knockdown of PARP1 gene in BCCLs did not affect their proliferation rate in any of the three cell lines in cell culture (**Fig R.33A**). In contrast, the anchorage-dependent colony formation capacity was clearly reduced in all genetically modified cells (**Fig. R.33B**). In addition, when we performed the anchorage-independent colony formation assay in soft agar with the only cell line suitable for this test, MCF7, we observed that shPARP1-MCF7 cells had less capacity to form colonies in soft agar causing 2,2 and 0,8 folds decrease in the number of colonies with size >100μm and <100μm respectively, compared to parental cells (**Fig R.33D**). Furthermore, in the unique cell line with capacity of invade or migrate assessed by the transwell assay, MDA-MB-231, we found that shPARP1-MDA-MB-231 cells exhibited a statistically significant increase in migration capacity which occurs via chemotaxis (p=0,001) but a similar invasive capacity compared with its control (**Fig R.33C**).

A

B

C

D
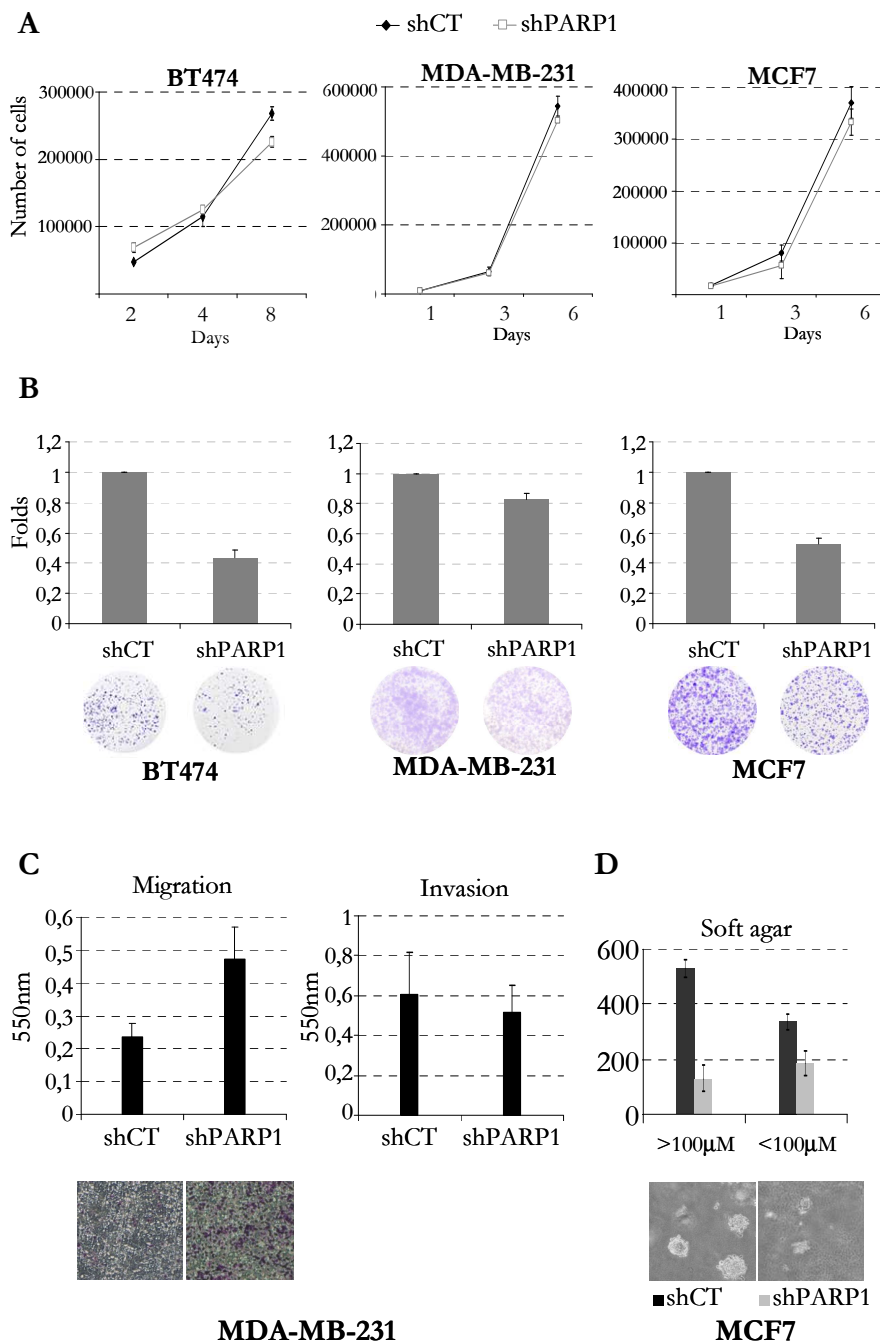
Figure R.33. Cellular effects of stable knockdown of PARP1. A. Proliferation curves. Each pair of shCT/shPARP1 cell line was manually counted in three time points. Each data point represents mean ± s.d. cell number of three independent

experiments. **B.** Clonogenic assay. Cells were seeded at low density and maintained during 10-20 days, resulting colonies were stained and analyzed by ImageJ. Each bar represents the mean ± s.d. folds cell growth of three independent experiments, compared to shCT at 1 fold. In A and B: Left, BT474; medium MDA-MB-231, right, MCF7. **C.** Transwell migration (left) and invasion (right) assays. shCT/shPARP1-MDA-MB-231 cells were seeded and allowed to migrate or invade during 6h or 24h, respectively, through transwell inserts. Each bar represents mean ± s.d. of the OD 550nm of three independent experiments. **D**. Anchorage-independent colony formation. shCT/shPARP1-MCF7 cells were seeded and counted after 21days, Each bar represents the mean ± s.d. number of colonies of three independent experiments

In addition, we tested the sensitivity of each pair of PARP1-silenced and parental cell lines towards different chemotherapeutic drugs (CDDP, Doxorubicin and Docetaxel) and to the PARP inhibitor PJ34. Cells were treated with concentrations within the IC_{50-25} values at 48h and cell viability was evaluated by MTS assay (**Fig R.34**). We did not observe sensitization to any of the therapies in any of the three PARP1-silenced cell lines, except in the case of shPARP1-BT474. These cells were found to be more sensitive to PJ34 treatment than were its counterpart shCT cells, and although somehow contraintuitive appeared to be more resistant to the DNA damaging agent CDDP than the respective parental cells shCT-BT474. Although this point has not been experimentally demonstrated in this thesis, a possible explanation for this effect that was opposite to the expected direction might be a higher rate of necrotic cell death upon CDDP treatment in shCT cells. The hypothesis is that these shCT cells attempts to repair the massive DNA damage induced by CDDP, and then PARP1 becomes activated upon DNA damage and poly(ADP-ribosylates) acceptor proteins, which consumes large amounts of NAD^+, resulting in depletion of cellular ATP, and subsequent necrotic cell death by energy depletion. Whereas in the shPARP1 cells, the result of CDDP produced DNA damage causes cell death by apoptosis, the almost complete absence of PARP1 could prevent excessive ATP

consumption that can cause necrotic cell death, finally resulting in less sensitivity to CDDP at 48h compared with shCT-BT474.
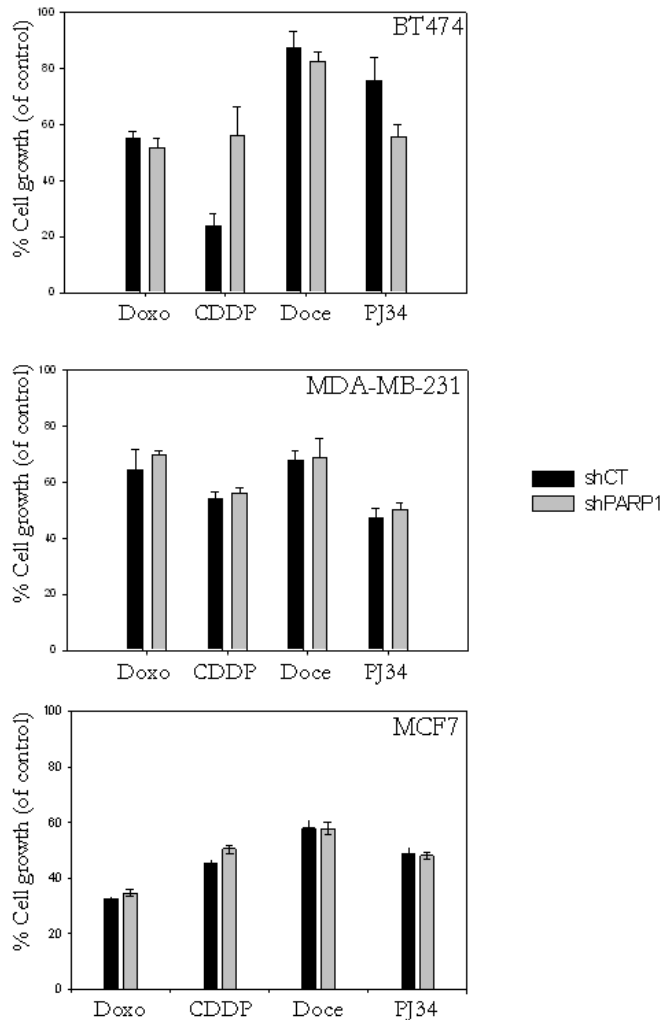
Figure R.34. Sensitivity of shCT versus shPARP1 cell lines to different chemotherapeutic drugs and PJ34. Sensitivity of each parir of cell lines to Doxorubicin, CDDP, Docetaxel and PJ34 treatments for 48h assessed by MTS assay. Each data point represents the mean ± s.d. percent cell growth inhibition of three independent experiments, compared to controls at 100%.

R.4.1.2. Molecular network effects of stable knockdown of PARP1

In an attempt to determine whether the downmodulation of PARP1 could reveal a distinct or similar gene coexpression patterns and networks in the three different silenced molecular subtypes of cell cancer cell lines. We analyzed the changes in the expression levels of 18 708 genes in each pair of cell lines by microarray analysis with the Affymetrix Human Exon 1.0 ST GeneChip. The microarray hybridization procedure and data filtering were performed by the Microarray Analysis Service (SAM) at IMIM All list of genes differentially expressed were compared in pairs. For the analysis of changes in gene expression we set an adjusted p-value threshold of 0,05.

Total cellular RNA was isolated by RNeasy Kit. RNA extraction was performed in triplicate from cells grown under identical conditions. RNA Integrity Number (RIN) values were determined by Bioanalyzer, indicating that all the samples were of high quality.

With this statistical adjustment, the number of genes with significant expression changes between shPARP1 and their control cells were 165, 79 and 59 in BT474, MDA-MB-231 and MCF7 cells respectively. In shPARP1-BT474, compared with controls, 104 were upmodulated and 61 downmodulated; in shPARP1-MDA-MB-231, 59 were upregulated and 20 downmodulated; finally in shPARP1-MCF7, 12 were upregulated and 47 were downmodulated (**Table R.7**). These data suggested that PARP1 is acting mainly as a coactivator of transcription in MCF7, whereas seem to primarily act more as a transcriptional correpressor in BT474 and MDA-MB-231 cells.

142

Table R.7. Number of genes with altered expression in each silenced cell line

	Upmodulated	Downmodulated	Total
BT474	104	61	165
MDA-MB-231	59	20	79
MCF7	12	47	59

All the significant differentially expressed genes were represented in a heatmap (**Figure R.35**). In this case, genes consistently upmodulated in the shPARP1 cells compared with their shCT pair are red and genes consistenly downmodulated are green. We observed few genes commonly dysregulated in PARP-depleted cells. Moreover, the expression of some common genes was altered in the opposite direction between the cell lines.

Figure R.35. Heatmap of expression changes in 303 genes altered upon PARP1 silenciation in BCCL. Horizontal rows shows individual genes; vertical columns represent each silenced-cell line (From left to right: BT474, MDA-MB-231, MCF7). Color intensity means degree of gene expression modulation. Colors means: Green, downmodulation; red, upmodulation, black, no change.

(Next Page)

-2.0 1:1 2.0

poly (ADP-ribose) polymerase 1
secretoglobin, family 1D, member 2
purinergic receptor P2Y, G-protein coupled, 10
protein kinase, cAMP-dependent, regulatory, type II, beta
LIM domain only 3 (rhombotin-like 2)
secretoglobin, family 2A, member 2
breast cancer and salivary gland expression gene
gastrin-releasing peptide receptor
potassium large conductance calcium-activated channel, subfamily M, alpha member 1
secretogranin: KF-hand calcium binding protein
spectrin, beta, non-erythrocytic 1
systemyl isoleucine receptor 1
homeobox B13
degenerative spermatocyte homolog 1, lipid desaturase (Drosophila)
low density lipoprotein receptor-related protein 2
SG12 overlapping transcript (non-protein coding)
parathymosin
parvalbumin
anoctamin 1, calcium activated chloride channel
cysteine-rich secretory protein 3
flavin containing monooxygenase 5
3-hydroxy-3-methylglutaryl-CoA synthase 2 (mitochondrial)
5G motif containing GTPase activating protein 2
enkilgin homolog (mouse)
homogentisate 1,2-dioxygenase
tumor necrosis factor (ligand) superfamily, member 15
heat shock 60kDa protein 1 (chaperonin)
LY6/PLAUR domain containing 6
GTP binding protein 2
solute carrier family 34 pseudogene 52
anemia (n-9 oxidation state) methyltransferase
serpin peptidase inhibitor, clade A (alpha-1 antiproteinase, antitrypsin), member 1
deleted in malignant brain tumors 1
solute carrier family 38, member 8 (monocarboxylic acid transporter 7)
nucleoporin 210kDa
phospholipase C, beta 4
solute carrier family 4, sodium bicarbonate cotransporter, member 4
LY6/PLAUR domain containing 6B
adenylate kinase 5
treslin
collagen, type XII, alpha 1
GULP, engulfment adaptor PTB domain containing 1
dedeltase, rodelihronine, type II
glycine receptor, alpha 3
integrin, beta 8
neuropeptide Y receptor Y1
solute carrier family 14 (urea transporter), member 1 (Kidd blood group)
myelin basic protein
SLAIN motif family, member 1
protein phosphatase 1, regulatory (inhibitor) subunit 3C
hydroxyprostaglandin dehydrogenase 15 (NAD)
talophilin 2
chromosome 10 open reading frame 81
poliovirus receptor-related 3
lysoxokinase (Lynoxomine hydrolase)
cerebellar degeneration-related protein 1
tin? homolog A (C. elegans)
plasiniin homology domain containing, family H (with MyTH4 domain) member 2
tissue factor pathway inhibitor (lipoprotein-associated coagulation inhibitor)
glucan (1-4-alpha-), branching enzyme 1
latent transforming growth factor beta binding protein 1
low density lipoprotein receptor-related protein 12
roundabout, axon guidance receptor, homolog 1 (Drosophila)
putative homeodomain transcription factor 1
FAT tumor suppressor homolog 1 (Drosophila)
syntaxin 2
transient receptor potential cation channel, subfamily C, member 1
phosphodiesterase 5A, cAMP-specific
paternally expressed 10
nuclear factor I/X
TRF-beta activated kinase 1/MAP3K7 binding protein 2
transmembrane protein with EGF-like and two follistatin-like domains 1
coiled-coil domain containing 109A
dpy-19-like 2 (C. elegans)
acyl-CoA dehydrogenase family, member 11
fibronectin 1
hemicentin 1
endomucin
transin-associated factor A
family with sequence similarity 8, member C
CCR4-NOT transcription complex, subunit 6
procollagen-lysine, 2-oxoglutarate 5-dioxygenase 2
hydroxyacid dehydrogenase-like hydrolase domain containing 1A
cosmin, actin binding protein, 2A
nuclear receptor subfamily 4, group A, member 2
limb bud and heart development homolog (mouse)
sialin, RhoGEF kinase
anthrax toxin receptor 1
hypothetical FLJ36979
glucose-3-phosphate dehydrogenase 1-like
cannidin to macrophage differentiation-associated
adrenergic, beta, receptor kinase 2
conlexion homolog 4 (Drosophila)
folate hydrolase (prostate-specific membrane antigen) 1
carbonese protein V
prelisorin-induced protein
arachidonate 15-lipoxygenase, type B
anoctamin 2
CDKN1 domain containing 6
bactericidal/permeability-increasing protein-like 1
Homo sapiens cDNA clone IMAGE:4800770.
solute carrier family 9 (sodium/hydrogen exchanger), member 2
chromosome 7 open reading frame 41
LIM domain only 4
diacylglycerol kinase, delta 130kDa
PBZ domain containing 2
Ras association (RalGDS/AF-6) domain family member 8
ankyrin repeat and sterile alpha motif domain containing 6
alska homolog 2 (Xenopus laevis)
coiled-coil domain containing 3
upstream binding protein 1 (LBP-1a)
olfactomedin-like 1
lymphocyte cytosolic protein 1 (L-plastin)
6-hydroxydopamine (serotonin) receptor 1F
odd, odd OdHer-in homolog 1(Drosophila)
myelin protein zero-like 2
phospholipase C, beta 1 (phosphoinositide-specific)
SLIT and NTRK-like family, member 6
myosin ID
synovial sarcoma, X breakpoint 1
heat shock 22kDa protein 8
achaete-scute complex homolog 1 (Drosophila)
ectonucleotide triphosphate diphosphohydrolase 1
laminin, alpha 3
fibronectin leucine rich transmembrane protein 3
glycoprotein, alpha-galactosyltransferase 1 pseudogene
ribosomal protein S8 kinase, 90kDa, polypeptide 1
cystin B2
MAS-related GPR, member X4
calbindin 2
neurexin 1
sorting nexin 10
ectonucleotide pyrophosphatase/phosphodiesterase 5 (putative function)
caspase 1, apoptosis-related cysteine peptidase (interleukin 1, beta, convertase)
synaptotagmin I
nuclear protein, transcriptional regulator, 1
interleukin-27 beta
gamma-aminobutyric acid (GABA) A receptor, alpha 3
trimethylysine hydroxylase, epsilon
mucin 15, cell surface associated
tumor necrosis factor (ligand) superfamily, member 18
tubby like protein 3
cystatin S
Fc fragment of IgG, low affinity IIa, receptor (CD32)
sprouty homolog 3 (Drosophila)
T-bfR-induced factor homeobox 2-like, Y-linked
family with sequence similarity 46, member C
SET binding protein 1
Kruppel-like factor 13
serine/threonine protein kinase MST4
very low density lipoprotein receptor
proteolipid protein 1
ribosomal protein S6 kinase, 90kDa, polypeptide 2
2',3'-oligoadenylate synthetase 1, 40/46kDa
SPANX family, member B1
neogenin homolog 1 (chicken)
phosphoglucerate dehydrogenase
family with sequence similarity 189, member A
mal, T-cell differentiation protein 2
sel-1 suppressor of lin-12-like 3 (C. elegans)
family with sequence similarity 43, member A
synovial sarcoma, X breakpoint 9
androgen receptor
P. antigen family, member 5 (prostate associated)
prostaglandin E2 receptor negative regulator
nsh homeobox 2
serpin peptidase inhibitor, clade B (ovalbumin), member 2
cystatin SN
multiple C2 domains, transmembrane 2
solute carrier family 2 (facilitated glucose transporter), member 3
laminin, gamma 2
cystatin SA
SPAN1 family, member E
solute carrier family 16, member 1 (monocarboxylic acid transporter 1)
myelin protein zero-like 3
SLIT and NTRK-like family, member 1
vimin-like 1
calcitonin receptor
kallikrein-related peptidase 11
Rho-related BTB domain containing 3
neuropeptide Y receptor Y5
syndecan 2
diacylglycerol kinase, alpha 80kDa
golgi membrane protein 1
peroxisome proliferator-activated receptor gamma
family with sequence similarity 5, member B
fibrinent box P2
prostectathn 11 Y-linked
insulin receptor substrate 1
phospholipase C, epsilon 1
synaptotagmin-like 5
family with sequence similarity 38, member B
RAS guanyl releasing protein 1 (calcium and DAG-regulated)
family with sequence similarity 169, member A2
ras homolog gene family, member D
synovial sarcoma 2 (chaplain)
GDNF family receptor alpha 1
solute carrier family 7 (cationic amino acid transporter, y+ system), member 2
ankyrin repeat domain 29
B-cell CLL/lymphoma 2
glypican 6
cyclin-dependent kinase 8
protocadherin 11 Y-linked
patched domain containing 1
plasma glutamate carboxypeptidase
G protein-coupled estrogen receptor 1
G protein-coupled receptor 115
phospholipase A2, group XV/I
inhibitor of DNA binding 1, dominant negative helix-loop-helix protein
multiple EGF-like-domains 9
peptidylglycine alpha-amidating monooxygenase
v-akt murine thymoma viral oncogene homolog 3 (protein kinase B, gamma)
Rho-related BTB domain containing 1
TIMP metallopeptidase inhibitor 2
beta-site APP-cleaving enzyme 1
bone morphogenetic protein 7
erythrocyte membrane protein band 4.1-like 1
LIM and senescent cell antigen-like containing domain protein 1
guanine nucleotide binding protein (G protein), alpha inhibiting activity polypeptide 1
solute carrier family 9 (sodium/hydrogen exchanger), member 6
growth regulation by estrogen in breast cancer-like
SATB homeobox 2
SRY (sex determining region Y)-box 9
insulin-like growth factor binding protein 4
spermatogenesis associated, serine-rich 2-like
cadherin 2
related RAS viral (r-ras) oncogene homolog
UDP-N-acetyl-alpha-D-galactosamine:polypeptide N-acetylgalactosaminyltransferase 4 (GalNAc-T4)
serine/threonine kinase 10
microtubule-associated protein 1B
glutamic-oxaloacetic transaminase 1, soluble
plexin A2
Down syndrome cell adhesion molecule
melanoma cell adhesion molecule
basic helix-loop-helix family, member e41
HIT ligand
desmuttie
heparan sulfate 6-O-sulfotransferase 2
bradykinin receptor B1
nephroblastoma overexpressed gene
PBZ and LIM domain 3
inhibitor of DNA binding 3, dominant negative helix-loop-helix protein
cathepsin D
sterile alpha motif domain containing 4A
transmembrane and tetratricopeptide repeat containing 1
glypican 3
diphtokinein, alpha
CO22 molecule
heat shock 70kDa protein 4-like
LON peptidase N-terminal domain and ring finger 2
desmoplakin-2
solute carrier family 4, sodium borate transporter, member 11
septin-40
integrin, alpha 6
solute carrier family 25 (mitochondrial oxodicarboxylate carrier), member 21
catepdermin 2
transmembrane protease, serine 11E
cysteine rich transmembrane BMP regulator 1 (chordin-like)
prokocalytom-like
aryl hydrocarbon receptor
cathepsin C
RNA binding motif protein 24
fibromodulin
fibronectin type III domain containing 3B
glypican 4
Rap guanine nucleotide exchange factor (GEF)-like 1
granulin
prostate androgen-regulated mucin-like protein 1
visinin
mucin-like 1
pyrimidinergic receptor P2Y, G-protein coupled, 4
vimentin
fukin domain containing 1
thioredoxin interacting protein
tubulin small leucine rich primarlycan homolog (Xenopus laevis)
synaptotagmin-like 4
transmembrane protein 74
HSA1324
zinc finger protein 491

All those genes with altered expression in the three silenced cell lines were represented in a Venn's diagram (**Figure R.36**) where is shown that only two genes, apart from PARP-1, are in common between all of them, whereas there are thirteen in common between MCF7 and BT474 cell lines, and four in common between the rest of comparisons.
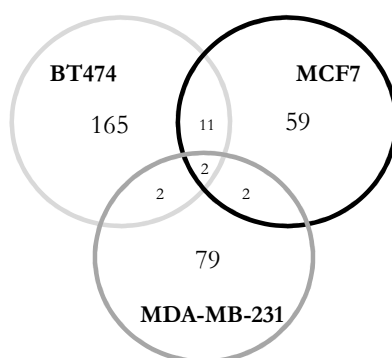
Figure R.36. Venn's diagram. Each circle represents those genes differentially expressed upon PARP1 depletion in each cell line. Crossed areas represent those genes differentially expressed in common between the different cell lines.

For the functional analysis of the changes in gene expression we set a less restrictive non-adjusted p-value threshold of 0,05. To analyze the most relevant signalling pathways, networks and functions that were modified upon PARP1 knockdown we used the Ingenuity pathway analysis software (IPA). Among the alterations in cellular functions and associated networks, "Cellular Movement", "Cell death" and "Inflammation" were the top altered networks common between the three cell lines. This result might be consistent with the alteration in migration experimentally characterized in shPARP1-MDA-MB-231 cell line. "Cellular growth and Proliferation" and "Cellular Development" and were top altered

networks common between BT474 and MDA-MB-231. "Cell to Cell Signalling" and "Interaction" were top altered network common in MCF7 and MDA-MB-231. Among the top altered canonical pathways, there was no common pathway between the three cell lines, but it is noteworthy that HER2 signalling was between the top altered pathways detected in shPARP1-BT474 cell line. In the **figure R.37** are represented the heatmaps of each top altered network common between the three cell lines, and "Cellular growth and Proliferation" network common between BT474 and MDA-MB-231, containing the genes differentially expressed in each network.

The validation of selected genes of these microarray analyses is being currently performed.

Figure R.37. Heatmaps of Top altered networks common between the three silenced-cell lines. "Cell death", "Cell movement" and "Inflammation" are in common between the three cell lines, "Cell Growth and Proliferation" is Top network in common between BT474 and MDA-MB-231. Horizontal rows shows individual genes; vertical columns represent each silenced-cell line (From left to right: MCF7, BT474, MDA-MB-231,). Color intensity means degree of gene expression modulation. Colors means: Green, downmodulation; red, upmodulation, black, no change.

(Next Page)

Inflammation

Cell death   Cell movement   Cell growth Proliferation
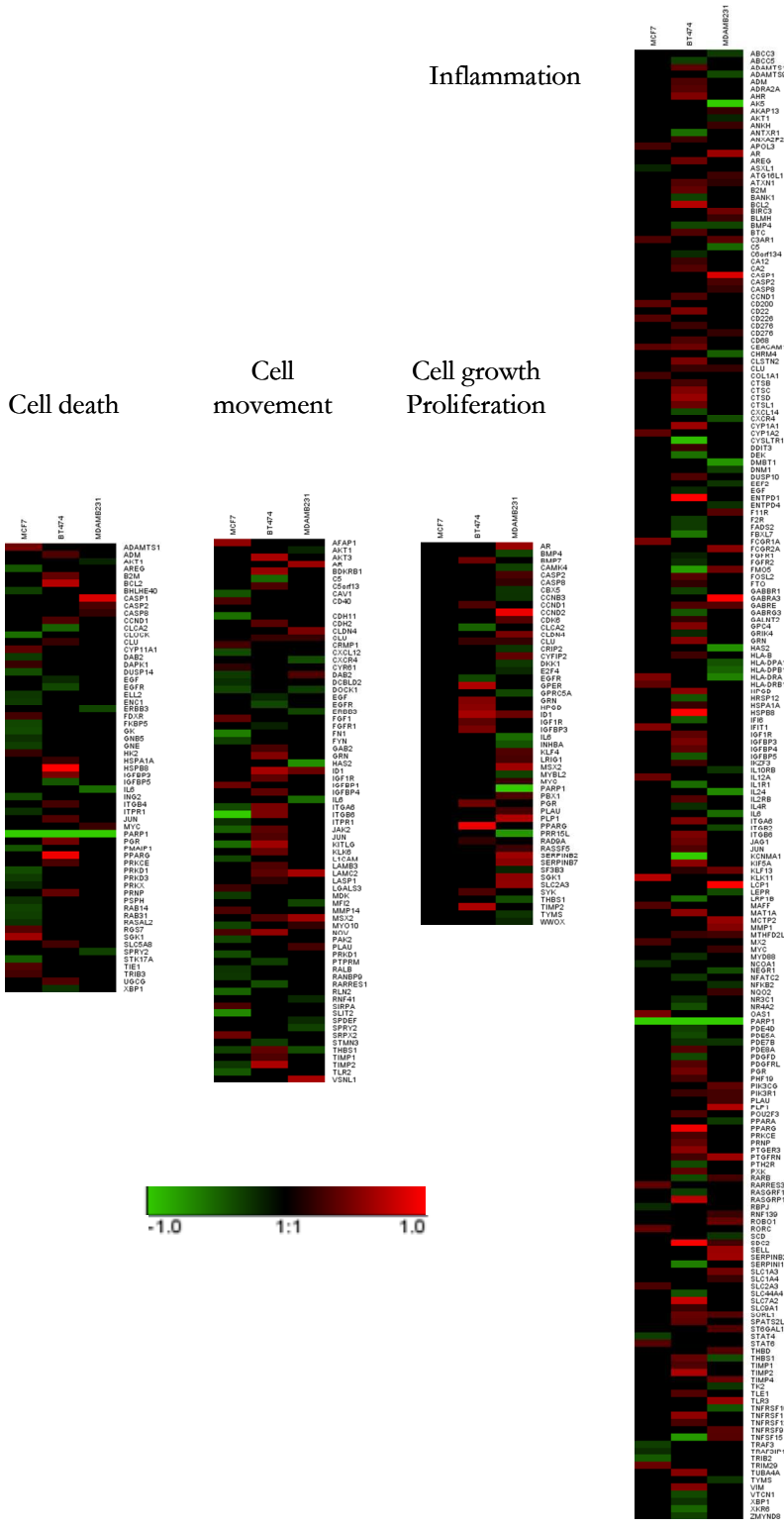
R.4.2. *In vivo* effects of stable knockdown of PARP1

Since different important pathways are modulated upon the depletion of PARP1 in the three BCCL tested but in distinct manner depending on each cell line, we investigated whether this specific modulation of gene expression could influence the ability to grow *in vivo* using a subcutaneous (s.c.) xenograft mouse model.

R.4.2.1. Characterization of the xenograft model with MCF7 shCT and shPARP1 cell lines

Ten athymic nude mice were inoculated s.c. with MCF7-shCT and MCF7-shPARP1 cells, into the right and left flanks respectively (**Fig R.38A**). Biodegradable time-release estrogen-pellets (0,72mg, 60day release) were implanted subcutaneously on the back of each mouse one day before tumour cell inoculation. Tumour growth was periodically analyzed by measurement with a digital calliper and the tumour volume in mm³ was estimated by the formula: [Volume = (Length * Width²)/2]. All of them developed tumours on both flanks.

At the endpoint of the experiment, mice were sacrificed and the final tumour volume and weight were measured. MCF7-shPARP1 cells exhibited less ability to grow *in vivo* than the control cells. The average MCF7-shPARP1 tumour volume was 71% significantly smaller (p=0,02) than that of MCF7-shCT group. Average weight of MCF7-shPARP1 tumours was also 65,8% significantly less (p=0,01) than those of MCF7-shCT tumours (**Fig.R.38B**).
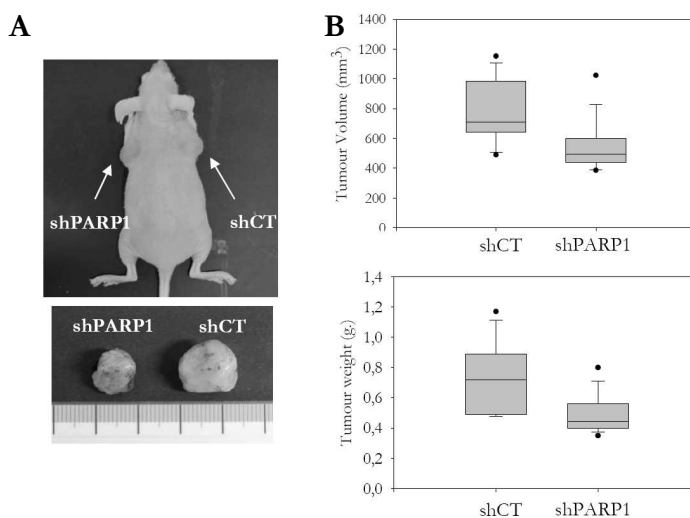
Figure R.38. Xenograft model with MCF7-shCT versus cell lines. A. Photograph of a representative mouse with MCF7-shCT and MCF7-shPARP1 cells subcutaneously inoculated at right and left flanks respectively (Top), and photograph of the excised tumours from the same animal (Bottom). **B.** Box plot graphs indicating mean ± s.d. tumour volumes (Top) and tumour weights (Bottom) from MCF7-shCT and MCF7-shPARP1 tumours.

The excised tumours from mice were divided into three parts: One portion was formalin-fixed and processed for histology, another portion of each specimen was embedded in OCT blocks and frozen on dry-ice in cryomold for future isolation of protein and total RNA. We checked whether PARP1 was still downmodulated in the MCF7-shPARP1 tumours. IHC analysis of PARP1 protein expression revealed that the silencing of the gene had been effective (**Fig. R39A**).

In this model, the remaining portion of each fresh tumour was immediately disgregated and lysed at 4°C to assess the PARP enzymatic activity in protein extracts from each fresh tumour.

Using a colorimetric commercial kit, the enzymatic assay reflected clearly that those protein extracts from shPARP1 tumours had less PARP activity than their respective pair control (**Fig R.39B**).
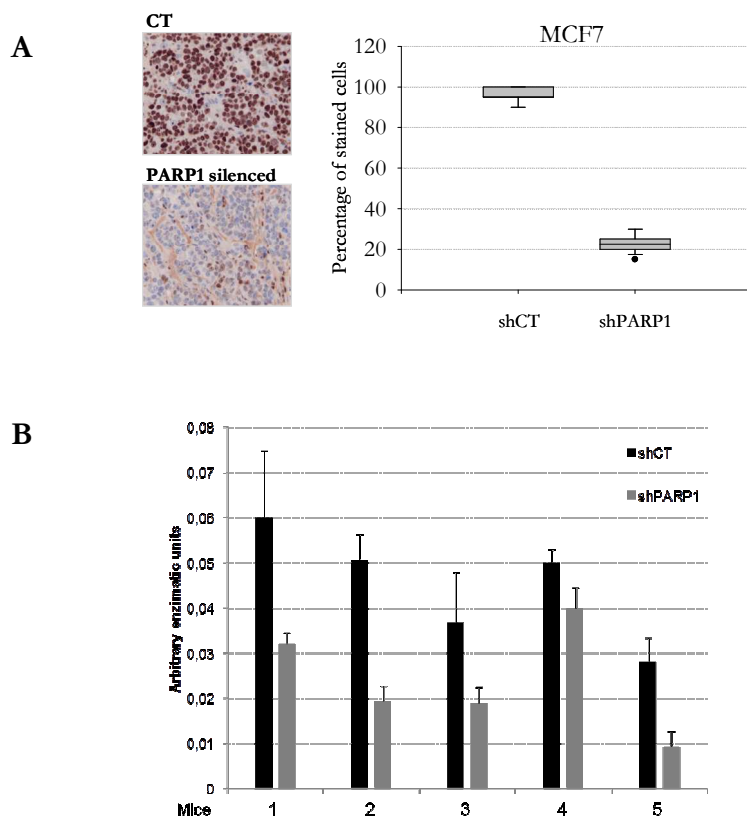
Figure R.39. IHC and enzymatical confirmation of PARP1-stably depletion in tumours from xenograft model with MCF7-shCT versus MCF7-shPARP1 cell lines. A. Representative IHC of PARP1 staining of MCF7 tumours (left) and Box plot graph (right) indicating the IHC results for PARP1 staining in MCF7-shCT and MCF7-shPARP1 tumours. **B.** Enzymatic assay. 5µg from from freshly disgregated shCT/PARP1-MCF7 tumours were subjected to PARP enzymatic activity assay and showed decrease in PARP enzymatic activity units.

Representative images of the IHC markers used to study proliferation, apoptosis and angiogenesis in these tumours and graphs with the results are shown in the **figure R.40**. Immunohistochemical staining of

150

proliferation markers Ki-67 and phospho-Histone H3 (p-H3) from the same tumour sample exhibited different patterns. Ki-67, which is a marker of actively cycling cells, showed similar percentage of stained cells in both group of tumours, while p-H3, which is a sensitive marker for cells in mitosis, was significantly decreased (p=0,002) in MCF7-shPARP1 tumours as compared to the control MCF7-shCT tumours. These results suggest that the downmodulation of PARP1 could be interfering in the proper mitosis progression and faithful chromosomal segregation process in tumour cells. The MVD was slightly lower in MCF7-shPARP1 tumours, but it was not significant (p=0,23). The apoptosis determined cleaved-caspase 3 staining and the γH2AX DNA-damage marker were significantly increased in PARP1 downmodulated tumours (p=0,037 and p=0,004 respectively). The results observed with proliferation and apoptosis markers are consistent with the lower volume and weight of shPARP1 tumours compared with shCT tumours.

151
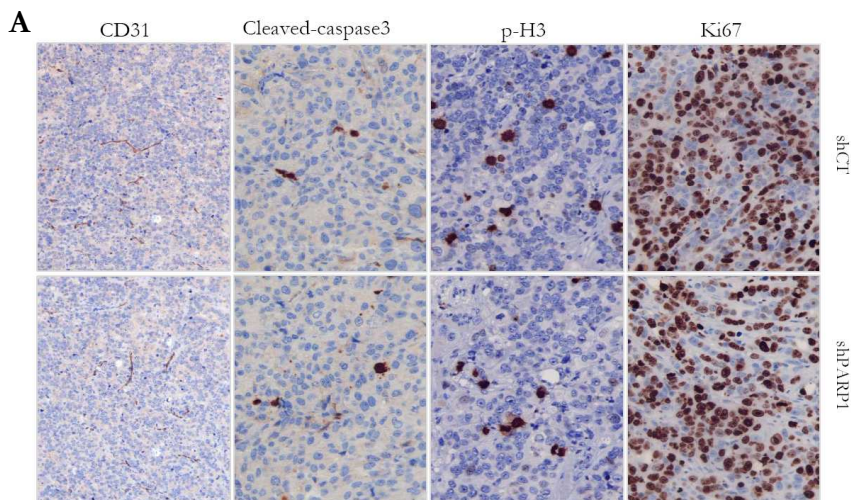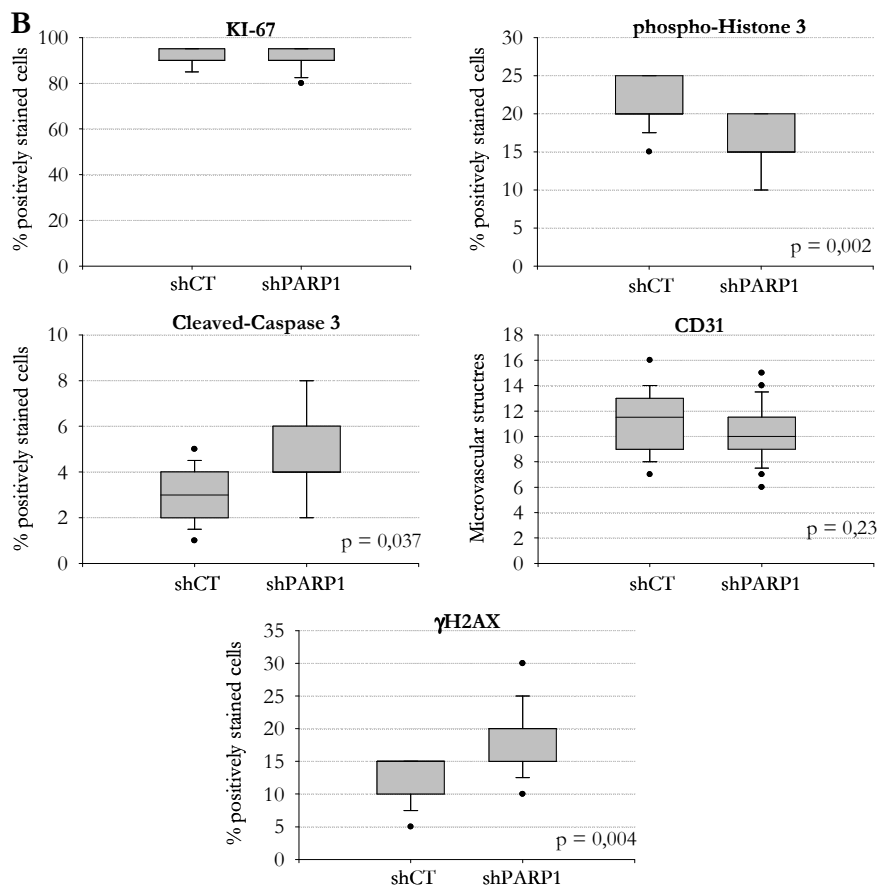
Figure R.40. IHC analysis of tumours from xenograft model with MCF7-shCT versus MCF7-shPARP1 cell lines. A. Representative IHC images of Ki67, phospho-H3, Cleaved-caspase 3 and CD31 stainings of MCF7-shCT and MCF7-shPARP1 tumours. **B.** Box plot graphs indicating the IHC results for Ki-67, phospho-H3, cleaved-caspase3, CD31, and γH2AX staining in MCF7-shCT and MCF7-shPARP1 mice tumours of each group of treatments. Student *t-test* was used for statistical analysis.

R.4.2.2. Characterization of the xenograft model with BT474 shCT and shPARP1 cell lines.

As in the previous model, 10 Balb/C nude mice were inoculated s.c. with BT474-shCT and BT474-shPARP1 cells with matrigel into the right and left flanks respectively (**Fig R.41A**). Also in this case, biodegradable time-release estrogen-pellets (0,72mg, 60day release) were implanted subcutaneously on the back of each mouse one day before tumour cell inoculation. Tumour volume was followed by periodic measurement with digital calliper and the tumour volume was estimated with the formula commented in the previous models. Nine of them developed tumours and one was sacrificed because of the side-effects of estrogen-pellets.

At the endpoint, BT474-shPARP1 cells exhibited greater capacity to grow *in vivo*. The average volume of BT474-shPARP1 tumours was 76,4% significantly larger (p=0,043) than the BT474-shCT tumours, if we take into account the average weight, BT474-shPARP1 tumours were 74,4% significantly heavier (p=0,046) than the BT474-shCT tumours (**Figure R.41B**). The results were opposite to what we observed in MCF7 cells.
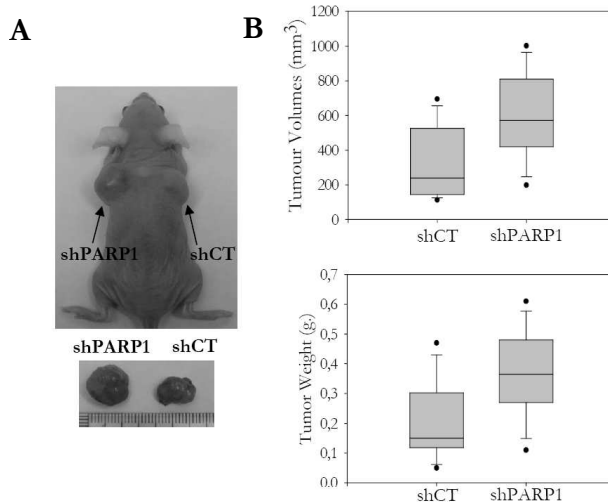
Figure R.41. Xenograft model with BT474-shCT versus BT474-shPARP1 cell lines. A. Photograph of a representative mouse with BT474-shCT and BT474-shPARP1 cells subcutaneously inoculated at right and left flanks respectively (Top), and photograph of the excised tumours from the same animal (Bottom). **B.** Box plot graphs indicating mean ± s.d. tumour volumes (Top) and tumour weights (Bottom) from BT474-shCT and BT474-shPARP1 tumours.

In this model, tumours were excised from mice and divided into two parts: one portion was formalin-fixed and processed for histology and another portion of each specimen was embedded in OCT blocks and frozen on dry-ice in cryomold for future isolation of protein and total RNA. We checked whether PARP1 was still downmodulated in the BT474-shPARP1 tumours. IHC analysis of PARP1 protein expression revealed that the silencing of the gene had been effective (**Fig. 42A**).

The IHC study of proliferation, apoptosis and angiogenesis markers in these tumours is shown in the **figure R.42B**. Immunohistochemical staining of proliferation markers Ki-67 and phospho-H3 showed an increase in proliferation in the shPARP1 tumours which was statistically significant in the case of phospho-H3 (p=0,002). The angiogenesis assessed by the presence of CD31-stained tubular structures within the tumour showed a tendency to increase in the shPARP1 tumours, but it was not significant (p=0,14). The results with these markers of proliferation and angiogenesis were consistent with the greater volume and weight of BT474 - shPARP1 tumours compared with BT474 - shCT tumours. In terms of apoptosis assessed by cleaved-caspase-3 and DNA-damage assessed by γH2AX significant increase in BT474-shPARP1 tumours was detected with both markers (p=0,000 and p=0,008). Although it could seem an opposite result from expected of the tumour volumes, in the one hand the absence of PARP1 in the shPARP1 tumours might be the cause of the higher γH2AX staining, on the other

hand these higher levels of DNA damage could be inducing apoptosis in a higher percentage of cells that would explain the increase in cleaved-caspase 3 staining in the BT474-shPARP1 tumours compared with BT474-shCT tumours.
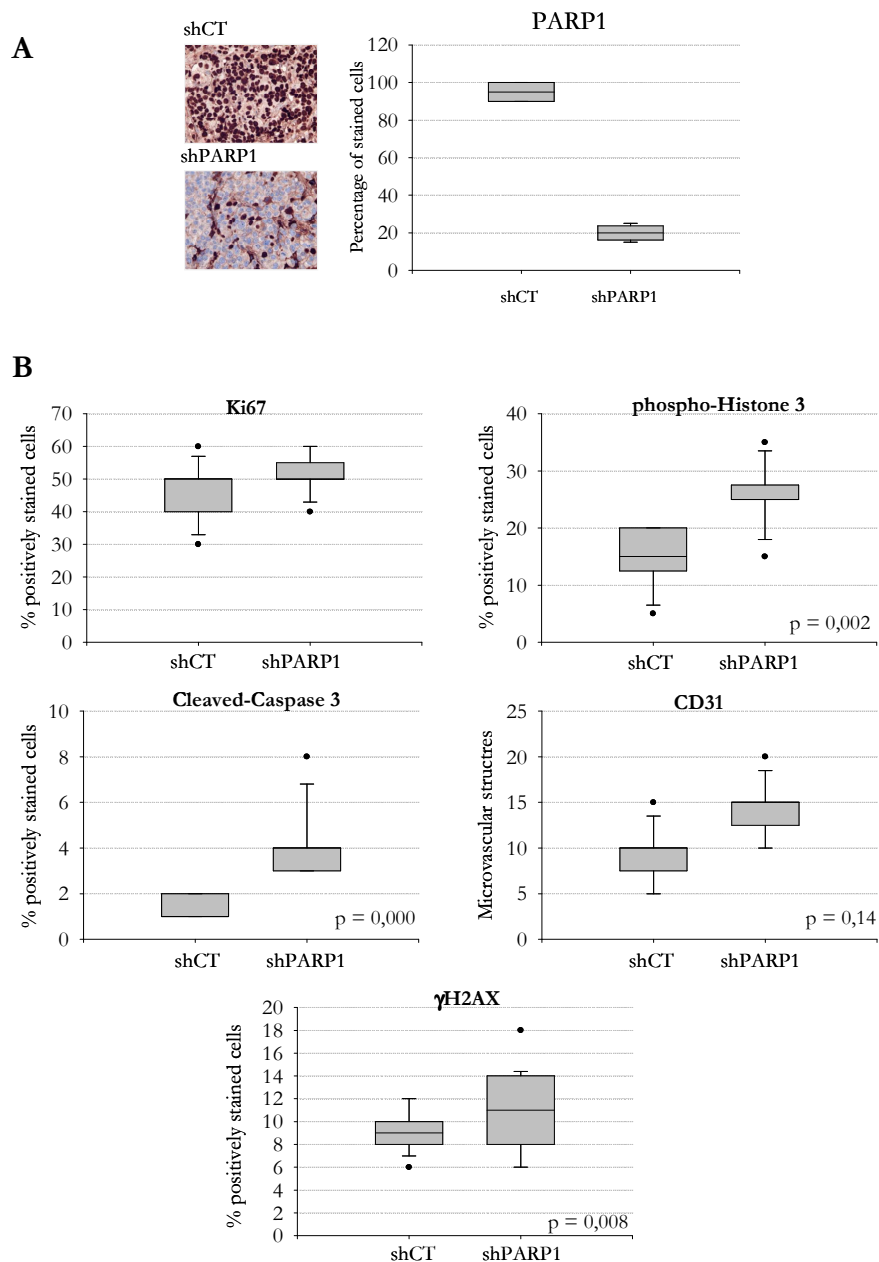
Figure R.42. IHC analysis of tumours from xenograft model with BT474-shCT versus BT474-shPARP1 cell lines. A. representative IHC of PARP1 staining of BT474 tumours (left) and Box plot graph (right) indicating the IHC results for PARP1 staining in BT474-shCT and BT474-shPARP1 tumours. **B.** Box plot graphs indicating the IHC results for Ki-67, phospho-H3, cleaved-caspase3, CD31, and γH2AX staining in BT474-shCT and BT474-shPARP1 mice tumours of each group of treatments. Student *t-test* was used for statistical analysis.

R.4.2.3. Preliminary characterization of the xenograft model with MDA-MB-231 shCT and shPARP1 cell lines.

The xenograft model with MDA-MB-231 shCT and shPARP1 cell lines has been also performed and the first preliminary results are reported in this last section of results.

As in the previous models, 10 Balb/C nude mice were inoculated s.c. with MDA-MB-231-shCT and MDA-MB-231-shPARP1 cells with matrigel into the right and left flanks respectively (**Fig R.43A**). Tumour volume was followed by periodic measurement with digital calliper and the tumour volume was estimated with the formula commented in the previous models. All of them developed tumours.

At the endpoint, MDA-MB-231-shPARP1 cells exhibited greater capacity to grow *in vivo,* as in the case of BT474-shPARP1 cells. The average volume of tumours was 63,9% significantly larger (p=0,019) than the MDA-MB-231-shCT tumours, if we take into account the average weight, MDA-MB-231-shPARP1 tumours were 64,4% significantly heavier (p=0,047) than the MDA-MB-231-shCT tumours (**Fig. R.43B**).
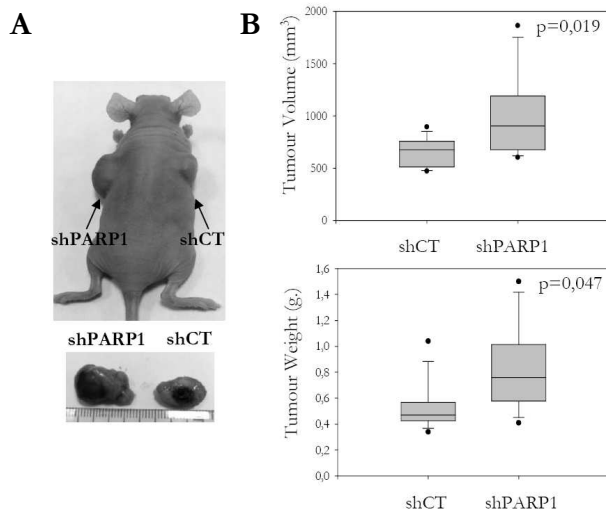
Figure R.43. Xenograft model with MDA-MB-231-shCT versus MDA-MB-231-shPARP1 cell lines. A. Photograph of a representative mouse with MDA-MB-231-shCT and MDA-MB-231-shPARP1 cells subcutaneously inoculated at right and left flanks respectively (Top), and photograph of the excised tumours from the same animal (Bottom). **B.** Box plot graphs indicating mean ± s.d. tumour volumes (Top) and tumour weights (Bottom) from MB-231-shCT and MDA-MB-231-shPARP1tumours.

DISCUSSION

DISCUSSION

In the present work we have aimed to shed some light on the current knowledge of the role that PARP1 plays in breast cancer. For this purpose, the study has been divided into two main parts. First, we started studying the expression of PARP1 directly in clinical primary breast tumour samples. Afterwards, we started the second part that consisted both in *in vitro* and *in vivo* work with a panel of breast cancer cell lines and xenografts models. In this second part, we focused in two main experimental points: On one hand, the comprehensive characterization of the cellular and molecular effects of olaparib, a PARP inhibitor that exhibited good activity in clinical trial. On the other hand, providing new data to further describe the role of PARP1 in the different subtypes of breast cancer by genetic depletion of the levels of the protein present in the cells.

Our interest in this field aroused by some encouraging results obtained in clinical trials with PARP inhibitors involving breast cancer patients over the recent years[272,274], and at the same time the yet poorly characterized PARP1 protein expression, the main target of these new inhibitors, in breast tumour specimens. Moreover, the role of PARP1 expression and its possible association with clinical outcomes was not fully explored by the time this PhD project started.

By then, there was already available an extensive literature devoted to studies of PARP1 and PARP inhibitors in human cancer cell lines (reviewed in the introduction section), but most of the oldest works used relatively non-specific PARP inhibitors in combination with chemo/radiotherapy. More recently, increasing number of studies have

examined a synthetic lethal strategy of PARP inhibitors with any deficiency in other genes implicated in HR pathway. But to our knowledge, no study to date on breast cancer, beyond characterizing inhibition of PARP in cells HR-deficient, has characterized the chemical inhibition and genetic silencing of PARP1 in cell lines representing major subtypes of breast cancer, aiming to decipher if PARP1 might play different roles in each of the different subtypes and the potential therapeutic implications of these data.

Overexpression of PARP1 protein in human breast cancer

In most human tissues, the expression of PARP1 is low[195,197]. On the contrary, PARP1 expression is frequently upregulated in human tumours compared with normal non-malignant tissues (their histologically normal counterparts). Examples include reports describing PARP1 mRNA levels in breast[197,200], ovarian, endometrial and lung cancer[195]. Same type of data is available from malignant lymphoma[199], melanoma[202] and early stage of sporadic colorectal cancer[180]. Studies assessing PARP1 protein levels are less frequent, but tumour tissues also exhibited overexpression of PARP1 protein as reported in hepatocellular carcinoma[212], early stage of colorectal cancer[180], ovarian carcinoma[201] and melanoma[202]. These overexpressed mRNA/protein levels of PARP1 in all these tumours suggest a role for PARP1 in cancer.

In breast cancer there have been two large studies recently published assessing the mRNA expression levels of PARP1. The study of Gonçalves et al[200] combined the analysis of 12 microarray expression data sets public available together with their expression database of 326 invasive breast cancer samples profiled with Affymetrix oligonucleotide

microarrays, resulting in a total of 2485 invasive breast cancers informative for meta-analysis. They analyzed correlation between PARP1 mRNA expression and molecular subtypes and clinicopathological parameters and the results revealed that: (i) PARP1 mRNA was higher in basal breast cancers, although overexpression was also found in other subtypes; (ii) PARP1 overexpression was associated with a worse prognosis, in terms of metastasis-free survival and overall survival (iii) and PARP1 expression retained its prognostic value in a multivariate analysis in the group of patients who has not received any adjuvant chemotherapy. In addition, PARP1 mRNA overexpression and gain/amplification at the PARP1 gene locus analyzed using array-based comparative genomic hybridization (aCGH) were significantly associated. Moreover, in the Ossovskaya et al.[195] study, PARP1 mRNA expression was significantly higher in infiltrating ductal breast cancer compared with normal breast tissue. Specifically, higher degree of PARP1 upregulation was more frequent in breast tumours negative for ER, PR or HER2 receptors. Further IHC analysis in a small subset of these breast samples showed that the upregulation PARP1 gene expression was consistent with increased protein expression in triple-negative breast cancer.

Contrary to the two articles described above, in the present study we did not focused on the study of PARP1 transcripts, instead PARP1 protein expression was assessed by an immunohistochemical assay in a set of 330 breast cancer specimens from patients with clinical follow-up. Among the family members of PARP, we focused particularly on PARP1 because is the most abundant member of the family and the major player in SSB repair through the BER pathway.

Moreover, we decided to study PARP1 protein expression instead of mRNA for various reasons. First, PARP1 protein levels can be upregulated by several factors other than mRNA overexpression. These factors include genomic gains or amplifications of the PARP1 gene, polymorphisms or post-transcriptional modifications. PARP1 mRNA overexpression has been clearly demonstrated in breast tumour specimens (n=18) in the Ossovskaya et al. study[195], in Ewing's sarcoma[204] and in colorectal cancer[180]. This PARP1 mRNA overexpression could be attributed to increased transcription rate driven by the transcription factor ETS[205,303] or changes in mRNA stability[304]. Genomic gains/amplification in PARP1 gene[197,200] can also underlie PARP1 protein upregulation, although this is not true in all the cases[204]. Polymorphisms in the promoter region of the PARP1 gene[189] might also influence the rate or efficiency of gene transcription and thus PARP1 expression. One example is a microsatellite polymorphism consisting of a variable number of CA repeats (CA)n located close to the binding site of the transcription factor YinYang-1 that could contribute to the upregulation of PARP1 expression[153,305]. Post-transcriptional modifications of PARP1 protein, due to alterations in the PARP1 protein processing by caspases-3/7, as a result of modulations in caspase activities[306], automodification (i.e. auto-poly(ADP-ribosylation) of PARP1[307] or some Single Nucleotide Polymorphisms (SNPs) of PARP1 gene[187,189], may reduce PARP1 catalytic activity or interfere in the protein stability and final levels. Finally, the number of identified genetic mutational PARP1-variants of PARP1 in human cancer cell lines is increasing, although have not been functionally characterized[308].

Secondly, studying PARP1 protein rather than mRNA would be also advantageous because PARP1 protein expression is directly correlated,

although only modestly, with activity in peripheral blood mononuclear cells from healthy volunteers and patients with solid tumours[309]. The last reason why we studied PARP1 protien comes from the fact that IHC approaches may be easily applied in a routine clinical setting than other tests, albeit all may be useful.

As stated in Results section, in order to determine PARP1 protein in tumour specimens from patient, first we performed an exhaustive PARP1 staining assay validation. Once we confirmed the specificity of PARP1 IHC assay we processed the samples. We found that PARP1 overexpression occurred in about a third of both ductal carcinomas in situ and infiltrating carcinomas. The upregulation of PARP1 at early stages of breast malignant transformation is consistent with findings in other tumours[180,212,213,310]. In infiltrating carcinoma, PARP1 overexpression was significantly associated to higher tumour grade, ER negative tumours, triple negative phenotype and patient outcome.

We were able to achieve these results and at the same time, one study came up showing that PARP1 overexpression was significantly higher in BRCA1-mutated cancer. This study by Domagala et al.[311] assayed the expression of PARP1 in 130 BRCA1-mutated and 594 BRCA1-non-related breast cancers and found that high PARP1 nuclear expression was significantly associated with BRCA1-mutated status in basal-like and triple-negative breast cancers. These results suggest that the deficiency in an essential mechanism of DNA repair tend to be compensated by the activity of alternative repair mechanisms, i.e. PARP1 upregulation. To note, 7% and 18,5% of BRCA1-mutated cancers exhibited no-expression or low PARP1 nuclear expression, respectively. In this line, we assayed the association of PARP1 protein overexpression with BRCA1/2 gene

status in a small set of tumours (n=42), independent from our series, but we did not find any significant association probably due to the small size of the subset studied. Apart from this, it is noteworthy that in our study PARP1 overexpression was also present in a fraction of HER2 and ER positive breast cancers. Another recent study spell out that HR pathway is commonly defective in triple negative breast cancer, but also in other subtypes[312].

Taken together, our results of high expression of PARP1 across all subtypes of breast cancer are consistent with the results reported by others[195,200,311] and support the notion that PARP inhibitors may play a role in triple-negative/basal-like, but also suggest potential applications in a larger fraction of breast cancer patients including other molecular subtypes.

The results of this work provide novel evidence on nuclear PARP1 protein overexpression as a promising prognostic factor for relapse and death. The multivariate analysis showed that PARP1 overexpression was an independent prognostic factor for both disease-free (HzR 10.05) and overall survival (HzR 1.82). These results are in agreement with the study of Gonçalves et al[200] that assessed PARP1 mRNA expression in breast cancer, also our results are in agreement with previous studies in ovarian cancer and melanoma showing that nuclear PARP1 staining was a poor prognostic factor[201,202]. Conversely, it has been recently reported that in pancreatic cancer high nuclear PARP1 expression is associated with improved survival[313].

Of course, the retrospective nature is the principal weakness of our study, but we were aware that there are other limitations as the lack of

information on the possible relationship between PARP1 expression and response to PARP inhibitors. However, we believe it would be very interesting to assess the expression of PARP1 protein in tumour samples from patients enrolled and with long-term follow up in clinical trials of PARP inhibitors in order to ascertain its suitability for further consideration as predictive factor for response.

Insights in the mechanisms of PARP1 overexpression in human breast cancer

We decided to explore the potential underlying reasons of PARP1 overexpression in breast cancer.

In this line, in a subset of our patient samples (n=156) we assessed *PARP1* gene status by FISH. We observed that those samples with a genomic gain of *PARP1* gene exhibited relatively higher levels of PARP1 protein than those without PARP1 gene alterations. Conversely, not all PARP1 protein-overexpressing tumours showed gain at *PARP1* gene locus. Similarly, when we assessed the correlation between the levels of PARP1 mRNA by qRT-PCR and protein in a representative subset of samples (n=20), we found a subgroup of samples in which high PARP1 mRNA combined with high protein tumoral levels, but there was also other subgroup with low PARP1 mRNA transcript levels and high PARP1 protein. Results from both assays suggest that some aberrant accumulation of PARP1 protein may occur, although these findings would need to be confirmed in a larger series of breast tumour samples. To determine whether accumulated protein is still functional and the reasons behind this massive accumulation may help to understand the role of of PARP1 overexpression in these tumours.

One possible explanation for a high protein content in some tumours could be a reduction in the level of PARP1 cleavage by caspases, which is a marker of early apoptosis, hence suggesting imbalances in the apoptotic process that might predispose cells to acquire alterations in gatekeeping genes leading to tumour progression (i.e. mutations within apoptotic effectors genes in metastatic breast cancer[314]). This mechanism of PARP1 accumulation has been suggested in malignant melanoma[315]. In fact, evasion of apoptosis is one of the hallmarks of cancer[6] which in addition could represent a resistance-mechanism to chemotherapeutic agents as described in the development of lymphomas[316] or malignant melanomas[317]. In this line, it has been reported that in highly cisplatin-resistant melanoma cell lines, PARP1 cleavage is strongly reduced[318].

Moreover, angiogenesis and promoting survival are two important roles reported for PARP1. Therefore, if this accumulated PARP1 is functional it might favour the worse prognostic of patients with PARP1-overexpressing tumours.

Regarding angiogenesis, several studies show that PARP1 can regulate this process. Experimental data demonstrates that *PARP1* KO mice display defects in angiogenesis upon growth factor stimulation[165], as well as PARP inhibitors exhibit antiangiogenic effects *in vitro* and *in vivo* by reducing the expression of VEGF, reducing the VEGF-induced proliferation or impairing the formation of neovasculature in response to specific stimuli[163,319,320]. In addition, stable depletion of *PARP1* gene reduces *in vivo* melanoma growth and increases chemosensitivity in xenograft models through diminished neo-vasculature formation within the tumour[166]. Effects of PARP1 on angiogenesis have been also reported through modulation of the hypoxia inducible growth factor 1 α

(HIF-1α) expression, a transcription factor involved in tumour progression that can mediate the new vessels formation in response to hypoxia[321]. PARP inhibitors or the absence of PARP1 is reported to prevent the induction of this transcription factor[322].

On the other hand, PARP1 expression is related to survival. This may be related to its direct role in DNA repair in response to DNA damage, but also by its reported role as cofactor of transcription factors related to cell survival such as NFkappaB. NFkappaB is frequently constitutively overexpressed in several human tumours, such as breast cancer, and its nuclear activation correlates with tumour progression and resistance to chemotherapy[323-325]. It has been reported by several authors that PARP1 is required for specific NFkappaB transcriptional activity[98,326]. Accordingly, experimental data shows that the absence of PARP1 in *PARP1-/-* cells drastically reduces the NFkappaB transcriptional activity, while the restoration of PARP1 in these cells restores the NFkappaB-dependent gene activation. Recent publications report that inhibition of PARP1 in murine colon carcinoma cells downregulates the expression of metastasis-related genes and proliferation at least in part through regulation of NFkappaB transcriptional activity[327].

Other hypothesis that would explain the role of PARP1 in cancer is the presence of SNPs affecting the enzymatic activity or the ability to interact with its target proteins. In this regard, the PARP1 SNP that results in the Val762Ala variant exhibits a 30-40% decrease in enzymatic activity and a reduced interaction with XRCC1[187,188]. Although a pair of studies carried in breast cancer did not associate this polymorphism with higher risk of breast cancer[189,190], it has been associated with higher risk of prostate, oesophageal and lung cancers[187,191,192]. Other polymorphism reported in

breast cancer is located in near the transcription initiation site and therefore likely linked to alteration of the transcription[189], but this affirmation has not been proven.

As commented above in the association of PARP1 levels with BRCA1/2 mutations, and beyond the discussed functions of PARP1 that could collaborate in carcinogenesis, PARP1 could be a marker of genomic instability. Supporting this fact, PARP1 might be overexpressed to compensate increased rates of DNA damage due to alterations in DNA repair pathways. This might explain why triple-negative and basal-like breast cancers (usually presenting the unstable BRCAness phenotype) tend to exhibit higher levels of PARP1. Such hypothesis is consistent with recent published data in which PARP1 expression, thus higher instability, correlated with response to neoadjuvant chemotherapy[328], as well as its expression together with other repair genes (*RAD51*, *CHEK1*, *FANCA*) was used to differentiate the triple-negative breast cancers that are sensitive to anthracyclines and resistant to taxane-based chemotherapy[329]. Conversely, Bieche et al[197] pointed that low levels of PARP1 are the cause of genomic instability in the breast tumours analyzed. This study found an association between *PARP1* gene overexpression with low genetic instability (15/35), although the results of this study should be interpreted with caution due to the limited number of samples included and the mixture of mRNA from tumour cells and stromal benign cells (n=35).

In this context, we analyzed genome-wide of genomic instability in 10 breast tumour specimens assessed by aCGH. Then we look into a possible association between the levels of PARP1 protein, genomic instability profile and gene alterations/LOH in a list of DNA repair and

170

repair related genes. We found a non-significant tendency to higher genomic instability in high versus normal PARP1 protein expression tumours. These observations are in agreement with recent published articles[200,328] that defend the view that higher levels of PARP1 may reflect a regulatory response to genomic instability. Furthermore, when we studied the association between the GI index and the gene alterations/LOH in the panel of DNA repair genes we found a statistical significant correlation, suggesting that the alterations in these genes could be the cause of the levels of genomic instability observed. If these results were confirmed in larger series of breast tumour samples, this panel of genes might be useful to better describe the genomic instability profile of tumours. In this field, other studies based on aCGH and other features (such as telomere length) to describe genomic instability confirm these results. Fridlyand et al.[330] described that not only genes related with the genomic maintenance are contributors of chromosomal instability but also other pathways (such as Retinoblastoma/EF2 pathway). Even in a recent paper, which includes some of the genes of our panel, the definition of a Copy Number Aberration profile is able to further subdivide breast cancer subtypes[331].

PARP1 in human breast cancer cell lines

In the second part of this thesis we worked with a panel of human breast cancer cell lines representing the various subtypes. Prior to the experimental strategy with chemical and genetic inhibition of PARP1, we characterized its expression at protein level by western blot. These cancer cell lines exhibited different levels of PARP1 protein. However, non-tumour cell lines were not included to compare the levels between tumour and non-tumour cell lines. Among the tumour cells included in

the panel half of the triple-negative cell lines (2/4) exhibited high levels of PARP1, that together with BT474, HER2 overexpressing, and MDA-MB-453, with high HER2 levels, cell lines were those with the higher levels of PARP1 compared with the rest of the panel. Other reasons for PARP1 upregulation in other subtypes such as HER2+, apart from the HR status or the mechanisms previously described, may be related to functional connections with proteins reported to regulate PARP1 posttranscriptional such as extracellular-signal-regulated kinases (ERK)[157]. These data reflect similar results to those found in breast tumour patients. In addition, PARP1 protein correlated with PARP1 gene copy number but not with its mRNA expression, as in breast tumours, suggesting that some of the hypothesis discussed above in breast tumour samples (such as deficient cleavage of PARP1 by apoptosis imbalance, alterations in the transcription or stability of the mRNA, or posttranscriptional modifications altering the protein stability) could explain the alteration of this ratio.

In addition, we assessed whether the levels of PARP1 protein correlated with PARP activity, which could help to explain if there is an accumulation of inactive PARP1, as occurs with p53-mutant protein that can be accumulated at high levels inactive in the cells[332]. When we assessed the activity of PARP in cell lysates measured by the amount of pADPr polymer formation by WB, we did not find any correlation, whereas when the functional state was assessed with an enzymatic assay that tests the capacity of PARPs to poly(ADP-ribosylate) the coated histones in a well, we found a positive correlation. Positive correlations between PARP1 protein and activity have been also found in colon cell lines[333], but contrast with more recent data from Zaremba et al.[305], however, this study compared cell lines from different cancer origins and

used a different PARP activity assay. On the one hand, in the panel used, the different results obtained with both techniques could be due to different reasons: (i) pADPr assessed by WB reflects the whole poly(ADP-ribosylating) activity of all the PARPs in the cell, whereas the enzymatic assay could be biased to mainly reflect PARP1 protein activity. In this assay, the histone H1, one of its main targets in vivo, is the most abundant histone coated in the wells, therefore resulting in better correlation with PARP1 protein levels. (ii) Poly(ADP-ribosylation) is a highly dynamic process and the long chains of ADP polymer can be rapidly degraded/synthesized. The detection of this marker by WB can be biased due to the processing of the cells to obtain the lysates, whereas the enzymatic assay directly assesses the catalytic capacity of PARPs. On the other hand, these results suggest that the enzymatic assay might be a more suitable technique to determine in breast tumour samples whether the overexpressed PARP1 protein in tumours is active or accumulated.

In this context of PARP activity in cells, Gottipati et al.[334] reported that PARP activity is hyperactivated in HR-defective cells. Accordingly to our results, the BRCA1-mutated HCC1937 cell line exhibits high levels of enzymatic activity, although not the highest. It should be noted that the study of Gottipati et al. uses isogenic cells with different BRCA-mutational status.

The results obtained in terms of genomic instability showed that PARP1 levels in cells do not associate with their GI index, probably due to the limited number of cell lines (n=6). Moreover, unlike breast tumour samples, in cell lines the number of gene alterations/LOH did not correlate with GI index. Working with cell lines is usually used as a preclinical approach, but not all the results can always be extrapolated *in*

vivo. In fact, it is well known that cell lines suffer cytogenetic alterations during culture passages[335,336]. This might explain this lack of correlation between gene alteration and GI index in this panel of cell lines.

Antitumor effects of PARP inhibitors in non BRCA-mutated related breast cancer cell lines

PARP inhibitors, and specifically olaparib, are known to exhibit potent antitumor activity in BRCA-mutated cells[232-235]. The explanation for this great sensitivity in this type of cell lines is the based on the widely accepted concept of the "synthetic lethality". In this case, suppression of the Base Excision Repair by PARP inhibition may result in the degeneration of Single-Strand Breaks into Double-Strand Breaks, which in BRCA-mutated cell lines cannot be efficiently repaired causing the subsequent cell death[337]. But the use of olaparib, and other PARP inhibitors, in BRCA-proficient breast cancers are much less commonly studied.

Regarding this part of the work presented in this thesis, there is only one recent published study by Shimo et al[297] (March 2012), reporting the antitumor effect of olaparib in a panel of different subtypes of non-BRCA-mutated breast cancer cell lines.

For the characterization of olaparib in this panel of BCCL, we included as controls two cell lines expected to be highly sensitive to the PARP inhibitor: a BRCA1-mutant breast cancer cell line (HCC1937) and BRCA2-mutant pancreatic cancer cell line (CAPAN-1). In addition, we compared the effects on cell viability with a PARP inhibitor widely used in preclinical setting, PJ34. In this initial characterization we observed

that same cell lines showed different sensitivities to both PARP inhibitors. During the course of this experimental work it was reported that PJ34 has unspecific effects on molecules unrelated to PARP and part of its antitumor effect are due to PARP1-independent p21 dependent mitotic arrest[338]. Since then in our experimental approaches we evaluated only olaparib, a more potent and specific PARP inhibitor.

Although single agent olaparib did not affect the survival of HCC1937 more than in the rest of the BCCL of the panel, when it was combined with DNA-damaging agents (cisplatin and doxorubicin) the BRCA1-mutated cell line was the most sensitized cell line confirming the data reported in the literature with other cell lines[232,235]. Of note, in published studies when comparing the effects of a PARP inhibitor as single agent on BRCA-mutant cells are most often compared with their isogeneic cell lines, but not with a panel of cell lines with many other possible non-described alterations. Thus, the remaining cell lines of the panel used could have alterations in other proteins, not only in BRCA, involved in HR repair that could be affecting their sensitivity to olaparib as single agent. In this line, defects in proteins involved in DNA repair such as XRCC2, XRCC3[233], ATM, ATR, RAD51, RAD54, CHK1, CHK2, FANCA, FANCC, FANCD[253-255]. As postulated by Shimo et al[297], yet undescribed mechanisms of action of olaparib beyond the synthetic lethality could explain its antitumor effects on BRCA-proficient cell lines.

The rest of cells also showed potentiation when olaparib was added to chemotherapeutic treatments. This result might be explained by the "chemosensitization effect" which is another use of PARP inhibitors[339] proven in this panel of cells. Apart from HCC1937, SKBR3, that has low BRCA1 protein expression, also exhibited high degree of sensitization

when combined with olaparib. It has been reported that SKBR3 exhibits low levels of BRCA1 due to aberrant regulation of its transcription[340] and that reduced expression of BRCA1 increases the sensitivity to PARP inhibitors[246] which would be in the line of these results. Similarly, triple-negative cell lines, supposedly owning a BRCAness phenotype, also were chemosensitized as pointed out in the literature[252].

Olaparib effects on HER2+ cell lines. Novel combination with anti-HER2+ targeted therapy

The clinical use of PARP inhibitors in breast cancer is at a very initial stage and but due to some big failure in clinical trials that were poorly planned, the future development of PARP inhibitors in cancer therapy is highly debated. The interest in developing PARP inhibitors as therapeutics agents in breast cancer was based in two non-excluding lines of research: the improvement in the identification of more patients that can benefit from this therapy; and the rational discovery of suitable therapies to be combined and potentiated with PARP inhibitors. Currently, combinations with other targeted therapies is one of the new areas of study in the field of PARP inhibitors[270,271,297].

On one hand, we have seen that olaparib has antitumour effects on BRCA-profient cells. On the other, several studies report that the inhibition or the genetic downmodulation of PARP1 expression may alter the expression of numerous key genes in cancer cell lines. In this sense, modulation of HER2 and/or EGFR expression by PARP1 has been reported in rheumatoid synovial and hepatocellular carcinoma cells, respectively[158,159]. These studies suggests that PARP inhibition may block its ability to coactivate NFkappaB, among others transcription factors.

This causes a downmodulation in the expression of certain NFkappaB target genes directly related to the process of carcinogenesis, such as HER2 and EGFR.

On this basis we decided to study the effects of olaparib in two HER2+ breast cancer cell lines, BT474 and SKBR3. First, we observed that olaparib was able to downmodulate HER2 and EGFR expression in both cell lines. Regardless of the mechanism, we decided to combine for the first time a PARP inhibitor with an anti-HER2 targeted therapy, trastuzumab. The addition of olaparib to trastuzumab treatment slightly decreased the expression of the receptors and their surrogate downstreams more than each drug alone. In contrast, published data reports that olaparib may increase levels of pErk[297,341], but we have to take into account that the experiments are always shorter (1-12h), whereas we have used longer treatments (48-96h). In terms of cellular effects, olaparib sensitized HER2+ cells to trastuzumab as shown by decrease in the anchorage-dependent clonogenic capacity, the metabolic capacity, the cellular amount of proteins, the cell proliferation, and increase in cell cycle arrest and cell death. Same assays performed in a non-HER2+ cell line showed no potentiation with the combined therapy, suggesting that effects of both drugs in EGFR/HER2 pathway might be driving this enhancement in the antitumoral effects.

Moreover, we studied the effects of both drugs on DNA damage by γH2AX-foci detection and Comet assay. γH2AX-foci is widely used as a marker of DSB[342], whereas the Alkaline version of Comet assay is able to detect both single- and double-strand breaks, as well as abasic sites and sites where excision repair is taking place[343]. Confirming previous published data with other PARP inhibitors[232,233], we observed that

olaparib was able to induce DNA damage in both BRCA-proficient cells. In this case, SKBR3 exhibited higher levels of DNA damage, which might be explained by its lower expression of BRCA1. Moreover, trastuzumab also induced an increase in DNA damage, being greater in the more sensitive cell line to this therapy, BT474. In agreement with this result, previous studies show that trastuzumab increases the frequency of DNA strand breaks as a "pre-apoptotic" event in SKBR3 and BT474, but not in non-HER2+ cells[299]. As reported by several authors, this is consistent with the partial inhibition of DNA damage repair after treatment with different chemotherapies or radiation[298,300,344]. In addition, studies of gene expression show that trastuzumab downmodulates the expression of repair genes[345], as well as HER2 depletion also results in downregulation of DNA repair mechanisms[346]. All these data support the role of HER2 signaling in the proper regulation between DNA repair, cell cycle and apoptosis.

In this line, similar results were obtained with a distinct PARP inhibitor, ABT-888, in combination with anti-EGFR targeted therapy, cetuximab, in head and neck cancer cells[271]. In this study it is described that the repair deficiency induced by cetuximab results in persistent DNA damage upon ABT-888 treatment that finally enhances cell death. In another study with glioblastoma cells, the overexpression of an oncongenic variant of EGFR, EGFRvII, induced increased levels of ROS, DNA-strand breaks and genome instability. This event caused hyper-dependency of these cells on a variety of DNA repair genes, among them PARP1. Sensitivity to PARP inhibitors correlated with the levels of EGFR activation and oxidative stress[347].

In this work we went a step further and tested whether olaparib might enhance the fully recognized antitumour effects of the anti-HER2 antibody, trastuzumab, *in vivo*. The clinical activity of trastuzumab is attributed to the internalization and degradation of cell surface receptor HER2, cell cycle arrest in G1, apoptosis, inhibition of DNA repair, as well as other effects described *in vivo* such as inhibition of angiogenesis and activation of antibody-dependent cellular cytotoxicity[348]. These effects together with other properties described about PARP inhibitors *in vivo*, such as inhibition of angiogenesis[163,164] or vasoactivity, which increases vessel perfusion of drugs and thus therapeutic response[349], might widen the effects of the drug combination *in vivo*.

The xenograft model performed with the parental BT474 cell line reproduced the data obtained *in vitro*. Compared with control, olaparib slightly reduced tumour growth, showing by the first time in vivo effects of a PARP inhibitor in a HER2+ cell line. Consistent with the literature[350], the low dose of trastuzumab largely decreased tumour volumes, whereas the group that received both drugs exhibited a greater decrease in final tumour volumes. The difference of mean tumour volumes between trastuzumab alone and in combination was not statistically significant perhaps due to the limited number of mice, but we consider that the results were consistent with the *in vitro* results. Accordingly, the markers of proliferation (Ki67 and phosphor-H3) showed a clear decrease upon olaparib and trastuzumab treatments that were potentiated when combined. In terms of angiogenesis, in this model olaparib did not decrease the microvessel density as much as expected by the reported antiagiogenic effects of PARP inhibitors, whereas trastuzumab induced greater decrease in the formation of new vasculature. It would be interesting to test the expression of angiogenic

markers to further confirm these results. As observed in vitro, olaparib alone induced DNA-damage, trastuzumab exhibited a tendency, whereas the combination enhanced the increase of DNA-damage close to signification, supporting the reported role of both drugs on the accumulation of unrepaired DNA damage. The apoptosis assessed by cleaved-caspase 3 was clearly upregulated when both drugs were combined, likely as a result of the sum of effects, not only DNA damage, but also the rest of the effects described for trastuzumab. We are currently performing additional in vivo experiments in more tumorigenic BT474 cells in collaboration with the group of Dr. Arribas to hopefully confirm and extent the results observed in parental BT474 cells.

Since SKBR3 cells do not form tumours in mice, it would be interesting to further validate this novel therapeutic strategy with other HER2+ tumorigenic cell lines. We plan to do this is a near future. Currently, apart from the combination of a PARP inhibitor with cetuximab or the one described in this work, combinations with other targeted therapies, such as histone deacetylases inhibitors in hepatocellular carcinoma[351] or CDK1 inhibitors in breast cancer BRCA-proficient cells[270] are the new proposals in this field.

Insights of the role of PARP1 in non BRCA-mutated breast cancer subtypes

Another common approach used for studying protein functions consist in the genetic modulation of its expression followed by phenotypic, molecular and functional characterization of the manipulated cells *in vitro* and in animal models. In the latter part of this PhD work, we knocked-down the expression of PARP1 in three BRCA-proficient breast cancer

cell lines representing three histopathological subtypes: BT474 (HER2+), MCF7 (ER+) and MDA-MB-231 (TN). For that, we used lentiviral-based RNA interference and after selecting in medium containing puromycin, all three PARP1-silenced cell pools showed an almost complete and stable abrogation of PARP1 protein expression compared with their respective control cells. To the best of our knowledge, regarding breast cancer cells there is only published data on MCF7 cells stably depleted of PARP1 and PARG[352]. Coincidently, our depleted cell lines showed only a slight reduction in pADPr levels. The remaining levels of pADPr could be explained by the presence of other PARPs with polyADP-ribosylating capacity in the three subtypes.

When we tested the sensitivity of PARP1-silenced cells relative to parental cells towards different chemotherapies (cisplatin, doxorubicin, agents that damage DNA directly, and docetaxel, a microtubule disrupting agent), we observed that, opposite to those results normally reported in KO cells lines and animal models[122,123,166], absence of PARP1 did not chemosensitize any of the three manipulated cell lines. This fact might be explained by several reasons:

- Other PARPs may compensate for the absence of PARP1 in these cells. However, no increase in PARP2 or PARP3 gene expression was detected compared to control cells by microarray analysis. In future experiments we should measure the enzyme activity of PARP under these treatment conditions.

- The deletion of PARP1 protein may have different spectrum of effects than pharmacological inhibition of its enzymatic activity. Different studies report that the inhibited PARP1, due to the lack of auto-poly(ADP-riboylation) activity of itself (automodification), cannot be released from DNA and is accumulated at damaged sites

blocking the action of the repair enzymes[353]. Whereas in the absence of PARP1, other alternative repair mechanisms may be used to repair the DNA damage. As seen in the results, pharmacological inhibition of PARP1 sensitizes cells to chemotherapy, while PARP1-depletion in these cell lines does not sensitize to chemotherapy probably due to the presence of alternative repair mechanisms that counteracts the lack of PARP1 and are able to repair the damage induced by chemotherapies tested.

- The duration of the treatments. Controversial data have been obtained regarding the sensitivity of BRCA2-mutated CAPAN-1 cells towards PARP inhibitors. Theses discrepancies have been attributed to differences in the full culture time period of the experiments[236,237]. Even in our work, when we characterized the effects of olaparib at clinical relevant doses on cell survival, the MTS assay at 48h was not useful to discriminate and characterize the different sensitivities between the panel of cell lines, and we needed to use long-term clonogenic assay. In the case of chemotherapeutic treatments on PARP1-depleted cell lines, to test cell survival upon 48h of treatment could be insufficient to discriminate sensitivities. In this line, other studies with PARP1-silenced cell lines use long-term clonogenic assays[166]. To test the sensitivity of these cells at longer treatments would provide more information in this regard.

Regarding cellular effects, the stable knockdown of PARP1 had no effect on cell proliferation, which is in agreement with the data published in MCF7[352] and also in melanoma cells stably depleted for PARP1[166]. Notably, the anchorage-dependent clonogenic capacity was reduced in the three silenced cells compared to their controls. PARP1 depletion greatly reduced also the capacity of MCF7 to grow in soft agar. Similar

effects were previously reported in PARP1 depleted liver cancer cells[159]. It is likely that PARP1 is required for cells to grow under the more stressful conditions of a clonogenic assay, which measures tumour survival as single cells by plating the cells at low density compared to the optimal condition of standard MTS assay. These results support a role of PARP1 in at least some breast cancer processes.

Moreover, depletion of PARP1 did not alter the invasion capacity of MDA-MB-231 cells, but increased their chemotactic migratory behaviour in the transwell migration assay. We were interested in ascertain in whether this effect was subtype-specific, but we were not able to adress this issue because in our hands neither BT474 nor MCF7 cells had the ability to migrate or invade *in vitro* in our transwell migration and invasion assays. Our results in MDA-MB-231 cells are controversial since most of the published data shows that PARP1 depletion or PARP inhibition leads to a decrease in cell motility. However the majority of these studies used models of inflammation in which PARP1 regulates the expression of inflammatory mediators, chemokines and/or adhesion molecules such as MIP-1α[354], TNF-α, IL-12, iNOS or ICAM-1[355]. Other migration studies were performed with growth factor stimulated endothelial cells[165]. In hepatocellular carcinoma cell lines the decrease in migration upon PARP inhibition or depletion was justified by the modulation of tumour-related gene expression[159].

To better understand these and other observed effects as a result of PARP1-knockdown in breast cancer, we studied the gene expression profiles of the three PARP1-depleted cells relative to their parental counterparts by microarray analysis. Regarding the data about migration obtained with MDA-MB-231 cells, we observed that PARP1-silencing

induced opposite changes in the expression of a series of genes inducers of migratory response in tumour cells. On the one hand, PARP1 depletion induced downmodulation of genes such as Interleukine-6 and the chemokine receptor type-4[356,357]. However, in line with our experimental observations, PARP1-depletion also induced upregulation of metastasis-related genes such as L-plastin and urokinase plasminogen activator[358]. This is only a preliminary observation that reflects the complexity to interpret which are the relevant changes provided by microarray data analysis. Overall, based on current and reported results, the regulation of migration by PARP1 might be dependent on the cell type, the experimental model and the stimulus for migration. Currently, we are validating by qRT-PCR selected genes from these analyses to confirm their changes in expression upon PARP1-silencing.

The next step was to try to analyze this microarray data in a global perspective and not by genes in isolation. For this purpose we performed functional analysis using the Ingenuity Pathway Analysis (IPA) software to identify the functions, pathways and networks most relevant to our data. This analysis revealed that in fact the functional cathegorie "Cellular Movement" was among the top altered functions in the three PARP1-depleted cell lines. The functions "Cell Death" and "Inflammation" were also commonly altered in all cells. Notably, "Cellular Growth and Proliferation" was a top altered network common between BT474 and MDA-MB-231. Of course, the depletion of PARP1 in MCF7 cells also induced changes in genes related with proliferation, but the overall significance of these changes based on IPA analysis was not relevant, thus it was not one of the top altered networks in this cell line.

The changes in gene expression between the three PARP1-silenced cell lines exhibited few genes in common as showed in the Venn's diagram in the Results section (See Figure R.36). The analysis and interpretation of data to decipher whether PARP1, beyond its DNA repair function, has a specific role in each subtype of breast cancer or, on the contrary, plays a similar role is complex. In an attempt to elucidate this question we are currently collaborating with the group of Albert Oliveras from the Universitat Politècntica de Catalunya to perform a network analysis of genes from their expression profiles.

Finally, to further characterize the effects of PARP1-silencing in three different subtypes of breast cancer cells, we studied their tumorigenic capacity in a subcutaneous xenograft model. There are few studies about the ability of PARP1-depleted cancer cells to form tumours *in vivo*. In the case of the melanoma cell line, B16, the depletion of PARP1 reduced the *in vivo* growth of the cells[166].

In our work the depletion of PARP1 decreased the tumorigenic capacity of MCF7 cells, while in an apparently counterintuitive manner, increased the tumorigenic capacity of both BT474 and MDA-MB-231 cells. This finding highlights the importance of combining *in vitro* and *in vivo* models to better understand tumour biology, and to explore different cancer subtypes. In the IHC study of xenografted tumours, the expression of the proliferation marker phopho-H3 was lower in tumours from shPARP1-MCF7 cells compared with their paired control, whereas the same marker was highly expressed in tumours from shPARP1-BT474 cells, compared with their controls. These staining patterns might explain the differences in tumour final volumes obtained in each case. Regarding the extent of DNA damage, as expected by its role in genome stability, the knockdown

of PARP1 induced an increase in percentage of cells with nuclear γH2AX in both models, as well as also increased in the percentage of cells staining positively for apoptotic marker cleaved-caspase3, relative to control shRNA transduced tumours. Qualitatively, the increase of the latter marker and the DNA-damage marker appears to occur in overlapping areas, so non-damaged cells in the BT474 model may equally have a higher rate of proliferation. It would require the analysis of serial samples to confirm this observation. Tumour samples from the MDA-MB-231 animal model are under analysis.

From these results, it is likely to hypothesize that the genes regulated by PARP1 in each model are so distinct that its depletion might involve the different observed outcome depending on the cellular subtype. Which particular genes essential for driving the different tumorigenic capabilities typical for a particular xenograft model is still an important question that needs to be solved.

Reviewing the literature, that faithfully recapitulate many of the genetic features described for the cell lines used as models for breast cancer subtypes, we observed that p53 is mutated in BT474 and MDA-MB-231 cells, whereas is wild-type in MCF7. The results from several tumour susceptibility studies in *PARP1-/- P53-/-* double null mutant mice are controversial. On the one hand, Tong et al[173,175] showed that p53 mutations in PARP1 deficient mice accelerate the onset and shortens the latency of mammary tumorigenesis in female mice. On the other hand, Conde et al[359] found that the double –mutant increased the tumour latency compared to *P53-/-* mice. In addition, *PARP1-/- P53-/-* oncogenic fibroblast delayed tumour formation compared with *PARP1+/+P53-/-*. Despite the differences, the two studies similarly showed that double-

mutant exhibit higher degree of genomic instability compared with either single mutant. In the line of the studies of Tong et al., BT747 and MDA-MB.231 PARP1-depleted cell lines that harbour p53 mutations appeared to display more tumorigenic capacity. Moreover, based on the higher degree of genomic instability of *PARP1$^{-/-}$ P53$^{-/-}$* double-mutants, we might hypothesized that secondary mutations associated with culture passage and during *in vivo* growth could have activated specific oncogenes in BT474 and MDA-MB-231 PARP1-silenced cells, which may explain the increased tumorigenic capacity of these. Supporting this hypothesis, PARP1-silenced melanoma cell line, B16, which have reduced *in vivo* growth capacity[166], harbours wild-type p53[360]. Profiling of genomic aberrations and gene alterations in these tumours could shed light to this unsolved question.

To sum up, we described that PARP1 protein overexpression was associated poor prognosis and was more common in triple negative breast cancer, but also detected in some ER positive and HER2 positive breast cancers. Regarding the results from preclinical models, a PARP inhibitor, olaparib, had effects in cell survival in different breast cancer subtypes and enhanced antitumour effects of trastuzumab in HER2 positive cells. Finally, preliminary results pointed to the existence of specific roles of PARP1 in different molecular subtypes of breast cancer.

CONCLUSIONS

CONCLUSIONS

1. PARP1 overexpression occurs in early malignant transformation of breast (DCIS).

2. PARP1 overexpression is associated with Triple-Negative breast cancer, high tumour grade; and is also present in a proportion of HER2 overexpressing and hormone receptor positive breast cancers.

3. PARP1 overexpression independently predicts for poor DFS and OS in patients with early breast cancer.

4. PARP1 overexpression tends to associate with higher genomic instability in human breast tumours; and genomic instability correlates with more alterations in DNA repair genes in human breast tumours.

5. PARP inhibition chemosensitizes BRCA-proficient breast cancer cells to doxorubicin and cisplatin.

6. Olaparib downmodulates HER2 and EGFR protein expression in HER2 positive breast cancer cells.

7. Olaparib potentiates trastuzumab effects in HER2 positive breast cancer cells *in vitro* and *in vivo*.

8. PARP1 contributes to physiological cellular effects including anchorage-dependent, independent clonogenic capacity and migration of breast cancer cells.

9. PARP1 is involved in the expression profile of genes related with cell movement, cell death and inflammation, and its expression can determine the tumorigenic capacity of three different molecular subtypes of breast cancer cells.

MATERIAL AND METHODS

M.1. Cell lines

Seven human breast cancer cells: MDA-MB-231, MDA-MB-468, MDA-MB-453, SKBR3, BT474, MCF7, HCC1937 and a highly transfectable derivative cell from Human Embryonic Kidney, 293T, were obtained from the American Type Culture Collection, ATCC. One pancreatic cancer cell, CAPAN-1, was generously donated by C de Bolós group. And MEFs WT and PARP1 KO were generously donated by J. Yélamos group. All cells were cultured at 37ºC with 5% CO_2. MCF7, CAPAN-1, MEFs and 293T cell lines were mantained in DMEM (Invitrogen), HCC1937 was maintained in RPMI (Invitrogen) and the remaining cells in DMEM/F12 (Sigma). All the media were supplemented with 10% of Foetal Bovine Serum (FBS) (Invitrogen), 2mM L-glutamine (Invitrogen), 100units/ml of Penicillin-Streptomicin Solution (Invitrogen).

M.2. Drugs

Olaparib (AZD-2281, Selleck Chemicals) was resuspended at 10mM in DMSO, aliquoted and stored at -20ºC for the in vitro assays. For the in vivo assays, every day of treatment was freshly solubilised in DMSO (Sigma) at 100mg/mL, and diluted to a working solution of 10mg/mL in PBS containing 10% (w/v) 2-hydroxy-propyl-beta-cyclodextrin (Sigma).

Trastuzumab (Herceptin, Roche) was resuspended at 20mg/mL in PBS, aliquoted and stored at 4ºC up to two weeks for the in vitro assays. For the in vivo, each day of treatment the previous solution in PBS was diluted in physiological serum to a working solution of 50µg/mL.

Cisplatin (Calbiochem) was resuspended fresh each treatment at 10mg/mL in DMSO.

Doxorubicin (Sigma) was resuspended at 10mM in water aliquoted and stored at 4ºC up to a month preserved from light.

Docetaxel (Sigma) were resuspended at 10mM in DMSO, aliquoted and stored at -20ºC.

M.3. Cell proliferation and viability

Different complementary techniques were used to assess the proliferation and survival of cells upon distinct kinds of treatments.

M.3.1. MTS assay

MTS is a colorimetric method based on the metabolic capacity of cells for the quantification of the viable cells in a plate. For this technique we used the *MTS-CellTiter 96 Aqueous Non-Radioactive Cell Proliferation Assay Kit* (Promega). MTS is a tetrazolium salt that is bioreduced by cells into a formazan product. The conversion of MTS into aqueous, soluble formazan is accomplished by dehydrogenase enzymes found in cells that are metabolically active. The amount of formazan product measured by the amount of 490 nm absorbance is proportional to the number of living and active cells in culture.

We performed the MTS assay in 96-well flat-bottomed plates (Corning). 10^4 cells or less, depending on its proliferation rate and/or time of treatment, were seeded in 100µl of drug free medium and incubated for 24h before drug treatment. 100µl of various 2X drug concentration (1X final concentration) were added for 48h or 96h. For the measurement, 80µl of medium from each well were substracted and 20µl of MTS solution were added. The plate was further incubated for 1 - 3 hours protected from light. The amount of soluble formazan produced, by cellular reduction of the MTS, was measured by the absorbance on a microplate spectrophotometer at 490nm (test wavelength) and 630nm (reference wavelength, background). The percentage of surviving cells was estimated by dividing the [A490nm -

A690nm] of treated cells by the [A490nm-A690nm] of control cells. Approximate IC50 values were determined from the dose response curve. A minimum of three technical replicates were performed.

M.3.2. SRB Assay

SRB is a colorimetric method based on the determination of total biomass by staining the cellular proteins with Sulforhodamine B (SRB). For this technique we used the *In Vitro Toxicology Assay Kit, Sulforhodamine B based* (Sigma). SRB is a dye that has the ability to bind to basic aminoacid residues in proteins from trichloroacetic acid (TCA)-fixed cells in an electrostatical and pH dependent manner. In mild acidic conditions SRB binds to cellular proteins, whereas in mild basic conditions it can be unbinded, solubilized and the resultant absorbance can be measured. Changes in the amount of dye incorporated by the cells in the culture are proportional with changes in the number of cells (total biomass). This indicates the degree of cytotoxicity caused by the test material. Cells were seeded and treated as described for MTS assay.

The assay was performed as described in the manufacturer's protocol. Once treated, cells were fixed by adding 50µl/well of TCA and incubating 1 hour at 4ºC. Once fixed, plates were washed 5 times with water to remove TCA, serum, and proteins not contained in the cells, and air dried. 100µl of SRB solution were added to each well and incubated for 20 minutes at room temperature (R.T.). After staining, the unbound dye was removed by washing 5 times with 1% acetic acid and air dried. The incorporated dye was solubilized by adding 200µl/well of 10mM Tris Base and measured by reading the absorbance on a microplate spectrophotometer at 490nm (test wavelength) and 630nm (reference wavelength, background). The percentage of surviving cells was determined as described in the MTS assay. A minimum of three technical replicates were performed.

M.3.3. Viable cell counting

For proliferation curves and specific experiments the density of viable cells was counted manually using Trypan Blue or automatically using the Scepter 2.0 Handheld Automated Cell Counter. In both methods, cells were carefully trypsinized avoiding leaving any cell attached to the plate. Each condition was counted at least in duplicate in at least 3 independent experiments.

Manual cell count was performed with a classical Neubauer chamber using Trypan Blue staining to discriminate non-viable cells, blue-stained, from viable cells, which has an intact membrane that excludes the dye.

Automatic cell count was performed with a Scepter 2.0 Handheld Automated Cell Counter. This system employs the Coulter principle in handheld format. The device allowed the count of any particle that passed through the orifice within the cell diameter range between 6-25μm, displaying a histogram of size distribution. Density of the viable cell population was obtained by adjusting the range of sizes that excluded the aberrantly large or small cells and debris from the count. The same range was applied for all the conditions in a same experiment.

M.3.4. Anchorage-dependent Clonogenic Assay

Clonogenic assay or colony formation assay is an in vitro cell survival assay based on the ability of a single cell to grow into a colony attached on a plastic surface.

Clonogenic ability was evaluated by plating 6 x 10^3 single cells in 60 mm diameter dishes in triplicate. After 24 hours of attachment period, cells were continuously exposed to different concentrations of drugs or solvent for 1-3 weeks. The medium, containing drugs or solvents, was replaced with fresh

medium and fresh treatments every 48 hours. At the end of the experiment, cells were washed with PBS and stained 1 hour with Violet Cristal solution (0,06% Crystal Violet -Sigma-, 10% ethanol, 10% acetic acid) which has the ability to bind and stain DNA. Stained cells were scanned and the images of each plate were analysed with Java ImageJ software. Briefly, each image was converted to 8-bit type and the same threshold adjustment was applied for all the conditions compared. Particles with size from 10-infinite were analyzed and the area fraction covered by colonies was the value used for the data analysis. Folds of survival were calculated by dividing the area fraction of the colonies formed in each condition by the area fraction of the colonies in the control plate, thus giving to the control condition the value of one fold. Each experiment was performed at least in triplicate.

M.3.5. Anchorage-independent Soft Agar Colony Formation Assay

Anchorage-independent growth is one of the hallmarks of malignant cell transformation. In general, normal (non-tumoral) cells are anchorage-dependent, whereas malignant (tumoral) cells can have the ability to grow unattached. The soft agar colony formation assay is a common and accurate method to determine the capacity of cells to grow independently of anchorage and to test whether specific treatments or genetic modifications modulates the anchorage-independent capacity of a given cell line.

In this assay, 2×10^4 single cell suspensions were seeded and grown in a 0,35% top agar layer (1,5mL) on top of a 0,7% bottom agar layer (1mL), that prevented cells from reaching and attaching to the plastic. 0,5mL of culture medium and the required treatments were added to the plates every 3 days during 21 days. The number and size of colonies were assessed by light microscope inspection at 20X magnification. Colonies bigger than 50μm

were counted and the data were expressed as number of colonies larger and smaller than 100μm. In our panel, the only cell line with capacity to grow independent from anchorage was the MCF7 cell line.

M.4. Cell Cycle by flow cytometry

The analysis of cell cycle was performed by flow cytometry. This approach allows discriminating cells in different phases of the cell cycle based on their DNA content. First, permeabilized single cells are stained with a fluorescent dye that binds stoichiometrically to the DNA, i.e. that the amount of incorporated dye is proportional to the amount of DNA. Thereafter, the stained cells are measured in a flow cytometer that reads at specific wavelength the total fluorescent emission from cell, which is considered as a measurement of the cellular DNA content. Based on the fact that DNA is duplicated during the S phase of the cell cycle, distinct phases are recognized in proliferating cell populations: G_2 and M phases (after S phase) have twice amount of DNA than G_0 and G_1 phases (before the S phase), whereas S phase have an intermediate amount.

In this assay, cell media, PBS from the washings and trypsinized cells from each condition were harvested and centrifuged 8 minutes at 1500 rpm. 1-2 x 10^6 cells were resuspended in 300μl of PBS and gently pipetted to obtain a single cell suspension. Cell suspension was fixed by adding dropwise 700μl of 100% cold ethanol and keeped at 4ºC for at least 24h. Fixed cells were centrifuged 2 minutes at 10 000 rpm, the supernatant containing the ethanol was decanted and the cell pellet was resuspended in 1mL of PBS by gently pipetting to maintain the single cell suspension. PBS cell suspension was centrifuged 5 minutes at 10 000 rpm, and the wash was repeated twice. Finally, cell pellet was resupended in 1mL of DAPI staining solution (50ng/mL in PBS) and incubated 2 days at 4ºC protected from light. Stained samples were analyzed using a Beckton Dickinson LSR flow cytometer with

Cell Quest software. For fluorescence excitation it was used the UV light laser at the wavelength nearest to 359nm. Sample running, data acquisition and interpretation was performed under supervision of the flow cytometry core facility staff.

M.5. Cell migration and invasion

M.5.1. Cell migration

Cell migration capacity was assessed using the widely accepted Boyden Chamber assay based in the capacity of cells to migrate through the microporous (8µm pore size) of a polycarbonate membrane insert in response to a chemoattractant or specific treatments.

The transwell migration capacity was assessed with the *QCM Chemotaxis Cell Migration Colorimetric Assay* (Millipore). Following the manufacturer's recommendations, 500µl of 10% FBS medium were added to each lower chamber well of a 24-well plate. Required inserts were placed in each well and 300µl of FBS-free medium containing $2,5 \times 10^5$ cells were added to the insert. After 6 hours of incubation at 37ºC and 5% CO_2 in an incubator, cell suspension of the insert was pipetted-out and non-migratory cells that remained in the interior of the insert were gently removed with a cotton-tipped swap. Cells migrated to the bottom of the insert membrane were fixed and stained with Crystal Violet solution for 20 minutes and washed with water several times to rinse. The stain from the underside of the insert was extracted in a well containing 200µl of 10% acetic acid for 15 minutes at R.T. 100µl of the dye mixture were transferred to a 96-well microtiter plate and the optical density (OD) was read at 550nm in a multiwell plate reader. The migration capacity was expressed as absorbance units. Each migration experiment was performed at least in three independent replicates.

M.5.2. Cell invasion

Invasion through the extracellular matrix (ECM) is an important step in tumour metastasis that involves adhesion and proteolysis of molecules from the basement membrane of blood vessels to invade other tissues. The invasion capacity was assessed using the *QCM ECMatrix Cell Invasion Colorimetric Assay* (Millipore). This kit is based on the capacity of cells to migrate through an invasion chamber that consists, as in the migration assay, in an insert with 8μm pore size polycarbonate membrane that in this case is covered with a thin layer of dried ECMatrixTM. This ECM occludes the pores and blocks the migration of non-invasive cells, whereas the invasive cells migrate through the ECM and arrives to the bottom of the polycarbonate membrane. The protocol was basically the same as for the migration assay (see previous point M.5.1), except for two steps: First, the ECM layer was rehydrated for 1 – 2 hours with 300μl of warm FBS-free media and, once rehydrated, carefully removed before adding the FBS-free cell suspension to the insert. And second, the incubation was prolonged for up to 24h hours at 37ºC, 5% CO_2 in the incubator before the staining.

M.6. DNA damage analysis

M.6.1. Immunofluorescence detection γH2AX focis

The formation of DSB induces the phosphorylation of thousands of molecules of H2AX adjacent to the break on serine 139 (γH2AX). The detection of γH2AX foci by immunofluorescence (IF) has been widely applied as a measure of DSB. For γH2AX foci detection, 18750 cells were seeded in each well of a 8-multichambered slide (Lab-Tek II Slide, Nunc) in 300μl of media. 24h hours later, treatments were added. After the treatments, media was carefully removed and attached cells were fixed 30

minutes with 4% paraformaldehyde (PFA) (Sigma) and permeabilized 10 minutes with 0,3% Triton X-100 (Sigma) in PBS. Between each step, cells were washed twice for 5 minutes with PBS. Once fixed, cells were blocked during 10 minutes with 400μl/well of 10% Bovine Serum Albumine (BSA), to avoid the unspecific binding of primary antibody. Cells were washed twice with TBS-T (The receipt of TBS-T is detailed in section M.8.2 Western Blot) and incubated 1 hour R.T. with 300μl/well of γH2AX antibody (Cell Signalling) diluted 1:300 in antibody diluent (DAKO). Cells were washed three times in TBS-T and incubated 30 minutes protected from light with 300μl/well of Alexa anti-rabbit 555 (Invitrogen) diluted 1:700 in antibody diluent. After the final incubation, cell were washed twice with TBS-T, the plastic chamber was carefully detached from the slide, each condition was stained and mounted with 5μl of DAPI Counterstain II (Abott Molecular) and the entire slide was covered with a coverslip avoiding the formation of air bubbles. γH2AX foci/DAPI stained cells were detected on an Olympus BX61 Motorized Fluorescence Microscope under the appropriate filters. For the data acquisition, 10 different fields from each well were photographed at 10X magnification for γH2AX and DAPI staining. For the data analysis, the nucleus of 100 – 300 cells were evaluated for γH2AX foci presence and classified in a scale depending on the amount of focis consisting in 5 categories: 0 foci; 1-3 focis; [>3 ,<20] focis, multifoci [>20]; and hole nucleus staining. The categories were determined by the personal observation that the greater the number of focis in a nuclei, the greater the size of the nuclei. Thus, being important to discriminate cells not only by the presence of γH2AX foci, indicating DNA damage, but also by the different amount of DNA damage between cells and conditions. Data was expressed in both manners: as percentage of cells in each category in each condition; and percentage of cells with/without DNA damage (considering DNA-damaged cells those with more than 3 foci in the nuclei). Each condition was

seeded in duplicated wells and the data analysis was performed from at least three independent experiments.

M.6.2. Comet assay

Comet assay or single cell gel electrophoresis assay is an effective method for evaluating DNA damage in cells. This assay is based on the ability of denatured and cleaved DNA fragments to migrate out of the nucleoid faster than undamaged DNA under the application of an electric field. The evaluation of the DNA comet tail shape and migration pattern provides many data about DNA damage. Specifically the Alkaline Comet assay, used in our experiments, is more sensitive than Neutral comet assay, and is able to detect SSB and DSB, as well as other DNA aberrations.

For the experiments the *CometAssay® Kit* (Trevigen) was used. The protocol was performed according the manufacturer's recommendations. Plates with treated cells and the medium were gently scraped on ice, transferred to an ice cold centrifuge tube, counted, pelleted and washed once with ice cold 1X PBS. 1×10^5 cells/mL (in cold 1X PBS) were combined with pre-warmed aliquots of molten LMAgarose at 37ºC at a ratio of 1:10. Immediately 50μl of cells/agarose mixture were pipetted onto pre-warmed CometSlide and spread over the sample area. Slides were placed flat at 4ºC protected from light for 30 minutes to ensure the gelling of the agarose and the adherence to the slide. Once gelled, slides were carefully immersed on prechilled Lysis Solution for 60 minutes at 4ºC in the dark. Next, the excess buffer was drained and the slides were carefully immersed in freshly prepared Alkaline Unwinding Solution (pH>13, 200mM NaOH, 1mM EDTA) at R.T. for 40 minutes. For the following step of electroforesis, the CometAssay® ES tank was previously chilled at 4ºC room. The slides were placed in the correct sense and ~700mL of fresh prechilled Alkaline Solution (pH>13, 200mM

NaOH, 1mM EDTA) were added. Electroforesis was performed at 20-21 volts, 220mA, for 30 minutes. The excess of electroforesis solution was drained from the slides and were immersed twice in ice cold dH_2O for 5 minutes each and once in ice cold 70% ethanol for 5 minutes. Slides were dried at ≥45ºC for 20 minutes until the shape of the agarose drop disappeared and all the cells were brought in a single plane to facilitate the observation. Each sample of the slides was stained with 100ul of diluted SYBR Green I (1:10 000 SYBR Green I in TE Buffer [10mM Tris-HCl pH7,5, 1mM EDTA]) for 5 minutes at 4ºC. The excess of SYBR solution was gently removed by tapping and the slides were allowed to dry completely at R.T. at dark. The samples were observed under an Olympus BX61 Motorized Fluorescence Microscope with fluorescein filter. For the data acquisition, 10 different fields from each sample were photographed at 4X magnification. For the data analysis, around 100 comets from each sample were analyzed with Comet Assay IV software (Perceptive Instruments). The percentage of DNA in the tail area by the whole DNA area and the comet tail length (from the center of the DNA head to the end of the DNA tail) were the parameters used for the data analysis. Each experiment was performed at least in triplicate.

M.7. Lentiviral transduction of short hairpin RNA for PARP1 stable knockdown in BCCL.

To stably downmodulate PARP1 expression in our BCCL we performed lentiviral transduction using *MISSION$^{®}$ shRNA* for PARP1, TRC Number: TRCN0000007931 (Sigma). This lentiviral vector was a pLKO.1-puro with different features represented in the following vector map:

Figure M.1. pLKO.1-puro vector map. Features of lentiviral vector for shRNA expression from Sigma website[361].

The indicated region in the figure M.1 contains the shRNA insert for PARP1 with the sequence below:

CCGGGCTTCACATATCAGCAGGTTACTCGAGTAACCTGCTGATATGTGA AGCTTTTT

In the case of the Control shRNA, the same vector containing a non-target sequence was used. All the vectors needed for the lentiviral transduction were generously donated by J. Baulida group.

3×10^6 293T packaging cells were plated in 10mL of media in P100 plates for producing the lentiviral particles. 24 hours later ans for each P100, 10μg of the transfer vector (shPARP1 or shControl) were cotransfected with the viral envelope vector pVSV-G (2μg), the retrotranscriptase vector pRSV (2μg) and the packaging vector pRRE (6μg). Total DNA was added to a volume of 150mM NaCl up to 1500μl and finally 78μl of Polyethylenimine 1mg/mL (PEI) (PolyScience Inc.) were used as transfection reagent mixed with the total DNA and the NaCl. The mixture was incubated 15 minutes at R.T. and added to the medium of 293T plates. 24 hours later, the medium was replaced with 5,5mL of fresh medium, in order to concentrate the

lentiviral particles produced by the transfected 293T cells, and in parallel the cells to be transduced were seeded (1,7 x 10^6 in 10mL of medium in P100). The medium from 293T containing the viral particles was collected at 48 hours and 72 hours post-transfection, filtered with 0,22μm filters, supplemented with 8μg/ml of polybrene (Sigma) and added to the medium of BCCL to be transduced. 24h after the second transduction, the medium of infected cells was replaced with fresh medium and puromycin (0,5μg/mL) for antibiotic selection. The selection ended when no viable cells were in the control non-transduced cells plate. This control was always performed in each transduction for each cell line. The dose of puromycin needed for the selection of each cell line was determined previously with a puromycin curve from 0 – 4 μg/mL in non-transduced cells treated for a week. PARP1 knockdown was confirmed by determination of PARP1 protein levels by Western Blot.

M.8. Protein analysis

M.8.1. Protein extraction

For <u>whole cell protein extracts</u>: Cell culture plates were lysed by scrapping on ice-cold in Lysis buffer (1% Igepal CA-630 [Nonidet P-40 buffer], 50mM Tris-HCL pH7,4, 150mM NaCl, 5mM EDTA, 5mM NaF, 2mM Na3VO4, 1mM PMSF, 5μg/mL Leupeptin and 5μg/mL Aprotinin). After shaking during 20min at 4ºC, the samples were centrifuged (10min, 13200rpm, 4ºC) and the supernatant was aliquoted and stored at -20ºC.

For <u>nuclear/cytosol fractionated cell protein extracts</u>: Cell culture plates were scrapped on ice in 1mL of cold 1X PBS. Cells were centrifuged (3 minutes, 2000rpm, 4ºC), cell pellet was resuspended in 400μl of Buffer A (consisting in: 20mM Hepes pH8, 10mM KCl, 0,15mM EDTA pH8, 0,15mM EGTA pH8, 0,15mM Espermidin, 0,15mM Espermin, protease inhibitors, 1mM

DTT and 1,2% Triton X-100), passed through a syringe to separate cytoplasm from intact nuclei, and confirmed this separation under a light microscope. 80μl of Sucrose Restore Buffer were added to the suspension and centrifuged (5 minutes, 5 000 rpm, 4ºC). The supernatant was centrifuged again (15 minutes, 14 000 rpm, 4ºC) to obtain the cytosolic fraction and kept at -20ºC, whereas the pellet was resuspended in 50μl of Buffer B (consisting in: 20mM Hepes pH8, 50mM NaCl, 25% Glicerol, 0,15mM EDTA pH8, 0,15mM EGTA pH8, 15mM MgCl$_2$, protease inhibitors and 1mM DTT), centrifuged (15 minutes, 5 000 rpm, 4ºC). The obtained pellet was resuspended in 40μl of Buffer C (Buffer B + 400mM KCl), shaked 30 minutes at 4ºC and centrifuged (5 minutes, 10 000 rpm, 4ºC). The supernatant was the nuclear fraction, and was kept at -20ºC.

For tissue whole protein extract: Fresh tissues where frozen in OCT and kept at -80ºC until needed. For the lysates, 4 tissue slides of 16μm from each sample were obtained in a cryostat and immediately lysed in 100μl of the lysis buffer described above. After 5 freezing/thawing cycles transferring each sample from liquid N$_2$ to 37ºC water, tissue lysates were processed as cell lysates, shaking on ice, centrifuging and aliquoting the supernatant.

Protein quantification was performed with *Bio-Rad DC Protein Assay* (Bio-Rad) which is based on the Lowry Assay. A standard curve with BSA was used to determine the protein concentration of our samples.

M.8.2. Western Blot (WB) Analysis

For the lysate sample preparation, an equal amount of protein (20–40 μg) was mixed with 2X Laemmli Buffer (1:1 dilution) and 5% of β-mercaptoethanol and heated at 95ºC for 5 minutes. Prepared samples were

loaded and separated on 8% or 12% SDS–PAGE gels, and then transferred to a PVDF membrane (Biorad). Transferred PVDF membrane was blocked 1 hour in 5% non-fat milk in TBST (50 mM Tris.HCl pH 7,4, 150 mM NaCl, 0,1% Tween 20) at R.T, prior to overnight incubation at 4ºC with the primary antibody diluted in TBST with 5% of BSA or milk (according to manufacturer's indications). Horseradish peroxidase-conjugated secondary antibodies were used for the subsequent 1 hour at R.T. incubation in 5% non-fat milk in TBST. Target proteins were visualized after enhanced chemiluminescence treatment of membranes with ECL reactives (Amersham) for 1 minute and subsequent exposure to X-ray film (Fujifilm).

The following primary antibodies were used: PARP1 (Clone A6) (generously supplied by J. Yélamos group), poly(ADP-ribose) (pADPr, BD Pharmigen or ACRIS), HER2 (Biogenex), CyclinD1 (Neomarkers) and BRCA1, BRCA2, EGFR, phospho-Akt (Ser473), phospho-Erk (Thr202/204), p27, p21 and γH2AX (Ser139) (all of them from Cell Signalling).

Immunoblotting with β-tubulin (Sigma) was done to confirm equal protein loading for cell extracts, GAPDH (Santa Cruz) for tissue extracts, and nucleolin (Sigma) and actin (Sigma) for nuclear/cytosol fractioned extracts.

M.8.3. Immunohistochemistry (IHC)

IHC was performed at Pathology service of Hospital del Mar with the technical help of Silvia Menendez. The tissues (mainly human and xenograft-mice tumours) analyzed in this work were basically Formalin-Fixed Paraffin-Embedded (FFPE). For the IHC procedure, tissue sections of 3μm thick from FFPE tissues were placed on positively charged glass slides and dried. Automated deparaffinization and antigen retrieval was performed using *Dako*

PT Link instrument. The slides were stained in the *Dako Autostainer Plus* with the *Flex Plus 3,3'-diaminobenzidine (DAB) kit.* Counterstaining was performed with hematoxylin, dehydrated with increasing concentrations of ethanol and xylene and mounted with dibutyl phthalate xylene (DPX) avoiding bubbles under the cover slip and dried at R.T. overnight.

The specifically optimized conditions of antigen retrieval and staining for each antibody used in our samples are described in the following table M.1 (for PARP1, a more extended description is detailed in M.8.3.1):

Table M.1. Antigen retrieval and staining conditions of antibodies used for IHC.

Antibody	Antigen Retrieval	Dilution	Incubation	Peroxidase	Secondary antibody
Ki-67 (DAKO)	pH6	1:100	30'	5'	Envision Flex
Cleaved-caspase 3 (C.S.)	pH9	1:100	60'	5'	Envision Flex Plus
Phospho-Histone 3 (C.S.)	pH9	1:100	60'	5'	Flex Plus Rb / Envision Flex
CD-31 (S.B.)	pH9	1:200	60'	5'	Flex Plus Rb / Envision Flex
γH2AX (C.S.)	pH9	1:150	60'	5'	Flex Plus Rb / Envision Flex
PARP1 (clone A6)	pH9	1:300	60'	5'	Flex Plus Ms / Envision Flex

…….C.S.: Cell Signalling; S.B.: Spring Bioscience.

For each staining and each antibody a set of control slides was run in parallel. Positive tissue controls were specimens, processed in the same manner as the specimens to be tested, with a known positive expression of the specific protein to be stained, whereas negative tissue controls were cell types with a known negative expression of the protein to be stained. Non-specific negative reagent control were the slides from the mice or patient specimens to be tested incubated with a non-specific negative reagent to

determine non-specific background staining and to help in the interpretation of specific staining.

Expression of the studied proteins in human and mice specimens was assessed by Federico Rojo. The quantification of the proliferation markers (Ki-67 and phospho-H3), the apoptotic protein cleaved-caspase 3 and the DSB marker γH2AX was assessed by estimation of positively stained cells for the antibody tested versus the total of tumour cells and expressed as percentage of tumour cells stained in each field studied. CD31 was used as a specific marker of endothelial cells to confirm the presence of microvessels. The evaluation of microvessels density (MVD) was assessed applying to the ocular an eyepiece graticule containing 25 randomly positioned dots which was rotated so that the maximum of points were on or within the vessels of the different fields studied in each sample. Instead of counting the individual microvessels, the overlaying dots were counted and expressed as average of microvascular structures. The quantification of PARP1 staining was performed by computerized measurement and has been extensively described in the next point M.8.3.1

M.8.3.1. PARP1 immunostaining and quantification

Immunostaining was performed using 3μm tissue sections, placed on plus charged glass slides in a *Dako Link platform*. After deparaffinization, heat antigen retrieval was performed in pH 9 EDTA-based buffered solution (Dako). Endogenous peroxidase was quenched by 0.03% hydrogen peroxide. PARP1 antibody was used for 30 minutes at R.T., 1:300 dilution, followed by incubation with an anti-mouse Ig dextran polymer coupled with peroxidase molecules (Flex+, Dako). Sections were then visualized with DAB and counterstained with hematoxylin. PARP1 antibody sensitivity (1:300) had been calculated in a range of crescent dilutions of primary antibody from

1:50 to 1:3000. Specificity was determined using wild type and PARP1 gene knockout mouse embryonic fibroblasts (MEF) and parental and knocked-down BT474, MCF7 and MDA-MB-231 human breast cancer cells using PARP1 shRNA. Specificity was also shown in kidney and liver tissue specimens from wild type and PARP1 knockout mice. Formalin-fixed cell pellets were processed as described for IHC and results confirmed by WB from whole lysates. In addition, a set of 18 paired fresh frozen and FFPE samples was processed by western blot and IHC. Sections from the same specimens incubated with normal mouse IgG2 (X0943, Dako) instead primary antibodies were used as non-specific negative reagent controls.

The quantification of PARP1 immunostaining was scored by a computerized measurement set up with the experience of Dr. Rojo. Nine representative images from each specimen were acquired at 10-nm wavelength intervals between 420 and 700 nm using a DM2000 Leica microscope equipped with the *Nuance FX Multispectral Imaging System* (CRI Inc). Before acquiring a spectral dataset of an image, an autoexposure routine was performed while imaging a blank area of slides to determine the exposure time necessary to approximately 90% fill the device wells at each wavelength to compensate for variations in source intensity, filter transmission efficiency and camera sensitivity. A library of pure DAB and Hematoxylin dye colors was created and used to unmix the colors from image cubes using the *Nuance 1.6.4* software. A cube (stack of images taken at the different wavelengths) of reference was then acquired for each new case, followed by spectral imaging of three representative tissue fields using the same exposure times. After deconvolution of the images, the spectral data was flat fielded to compensate for unevenness in illumination and background was filtered. The positive signals were converted from transmission to optical density units by taking the negative log of the ratio of the sample divided by the reference cube using a Beer law conversion. A computer-aided threshold was set, which

creates a pseudo-color image that highlights all of the positive signals. Analysis yielded quantitative data of PARP1 from the average intensity of regions of interest. Only the nuclei of epithelial cells (normal and malignant), but not stromal cells or lymphocytes, were automatically detected by setting distinct size threshold and confirmed by a pathologist. Each case was calculated for the mean value of the signal intensity of all regions of interest for statistical analysis. The output of the computerized measurement produced a continuous data ranging from 29 to 133,094 for PARP1 expression.

M.8.4. PARP enzymatic activity assay

For the assessment of PARP enzymatic activity in cells or fresh tumours we used the *HT Universal Colorimetric PARP Assay Kit* (Trevigen). This kit tests the capacity of the PARP enzyme present in our samples to incorporate biotinylated poly(ADP-ribose) onto histone proteins coated in a 96-well strip well format by colorimetric measurement. The protocol was performed according the manufacturer's recommendations.

For processing cells, plates with treated cells were harvested by gentle trypsinization and centrifuged (10 minutes, 400g, 4ºC). The cell pellet was resuspended in 1mL of ice-cold 1X PBS and the cell suspension was centrifuged again (10 seconds, 10 000g, 4ºC). For the preparation of extract, the pellet was resuspended in 5-10 pellet volumes of cold 1X PARP Buffer (0,4mM PMSF, 0,4mM Aprotinin/Leupeptin/Ortovanadate, 0,4M NaCl and 1% NP-40) and incubated vortexing 30 minutes on ice. The cell lysates were centrifuged (10 minutes, 10 000g, 4ºC) and the supernatants were quantified and kept at -80ºC.

For processing tissues, in our case the fresh tumours from xenografts were washed with cold 1X PBS to remove blood and debris, minced on a petri dish on ice into small pieces with a scalpel and disaggregated in cold 1X PBS with a homogenizer on ice. The homogenized tumour was passed through a 100μM disposable sieve with 20mL of cold 1X PBS to a 50mL conical tube, mixed by inverting several times and let stand up on ice for 1 minute to allow large aggregates of tissue to settle out of the suspension. Cell suspension was carefully recovered, centrifuged (10minutes, 400g, 4ºC) and the cell pellet resuspended in 1mL of cold 1X PBS and centrifuged again (12 seconds, 10 000g, 4ºC). For the preparation of extracts, cell pellets were processed as previously described for cell line suspensions.

For the ribosylation reaction, coated histones of the strip wells needed were previously rehydrated during 30 minutes at R.T. with 50μl/well of 1X PARP Buffer. In parallel, always on ice, we prepared a PARP Standard curve with serial dilutions of PARP-HSA units (1 - 0,5 - 0,25 - 0,125 - 0) and the cell extracts using 5μg of proteins. Each sample was equated with 1X PARP Buffer to 25μl. Samples were distributed, 25μl/well of 1X PARP cocktail were added to each well and the plate was incubated covered with parafilm for 60 minutes, R.T.. Strip wells were washed twice with 200μl/well of 1X PBS + 0,1% Triton X-100 and twice with 200μl/well of 1X PBS + 0,1% Triton X-100. For the detection, 50μl/well of Strep-HRP were distributed in each well, incubated 60 minutes R.T., followed by two pairs of washes as in previous steps and 50μl/well of pre-warmed TACS-Saphire were finally distributed and incubated 10 minutes in the dark. The plate was measured by reading the absorbance on a microplate spectrophotometer at 630nm. For the data analysis, the absorbance of each sample was intrapolated in the PARP Standard curve to obtain the PARP enzymatic units of activity. Each

sample was assayed in triplicates and a minimum of three technical replicates were performed.

M.9. Nucleic acid analysis

M.9.1. DNA extraction

DNA extraction was performed with QIAamp DNA Mini Kit (Qiagen) according the manufacturer's recommendations. For DNA extraction from cultured cells, plated cells were gently scraped with the medium, centrifuged, resuspended in 200µl of 1X PBS and added to microcentrifuge tubes with 20µl of proteinase K. 200µl of provided Buffer AL were added to the samples, vortexed for 15 seconds and incubated 10 minutes at 56°C. After a brief spin, 200µl of 100% ethanol were added to the samples, vortexed for 15 seconds again and briefly centrifuged. The mixtures were applied to QIAamp mini spin column and centrifuged 8000rpm for 1 minute. The filtrates were discarded, 500µl of provided Buffer AW1 were added and centrifuged 8000rpm for 1 minute. The filtrates were discarded again, 500µl of provided Buffer AW2 were added and centrifuged at full speed for 3 minutes. Finally, DNA was eluted with 200µl of DEPC water incubated in the column 1 minute and centrifuged 8000rpm for 1 minute.

For DNA extraction from tissues, fresh tissues where frozen in OCT and kept at -80°C until needed. For the DNA extraction, 4 tissue slides of 14µm from each sample were obtained in a cryostat, placed in a microcentrifuge tube with 1mL of 1X PBS, vortexed for 30 seconds and centrifuged at maximum speed 5 minutes R.T. The pellet was resuspended in 180µl of provided Buffer ATL, added to a microcentrifuge tube with 20µl of proteinase K, vortexed and incubated at 55°C with shaking overnight. Next,

200μl of provided Buffer AL were added, vortexed and incubated at 70ºC for 10 minutes. After a brief spin, 210μl of 100% ethanol were added, vortexed for 15 seconds again and briefly centrifuged. From this step, the process with QIAamp columns is the same as in cultured cells. The elution was performed with 70μl of 70ºC heated TE Buffer, incubated 1 minute in the column and centrifuged twice 8 000rpm for 1 minute.

The DNA was kept at 4ºC for short term storage and -20ºC for long term storage. The DNA quantification and purity was measured with NanoDrop ND-1000 spectrophotometer (NanoDrop Technologies).

M.9.2. RNA extraction

RNA extraction/purification was performed with RNeasy Mini Kit (Qiagen) according the manufacturer's recommendations. For RNA extraction from culture cells an extraction with TRIzol (Invitrogen) previous to purification with Qiagen columns was used. Plated cells were washed with 1X PBS, disrupted with $0,1ml/cm^2$ of TRIzol and incubated 5 minutes R.T. $0,02ml/cm^2$ were added to the suspension, incubated 15 minutes R.T., centrifuged (15 minutes, 12 000g, 4ºC) and the aqueous phase containing the RNA was recovered. For RNA $0,05ml/cm^2$ of 100% isopropanol were added to the solution, incubated 10 minutes R.T. and centrifuged (10 minutes, 12 000g, 4ºC). The supernatant was eliminated by decantation, $0,1 ml/cm^2$ of 75% ethanol were added, mixed by inversion and centrifuged (5 minutes, 7500g, 4ºC). The pellet was air dried for ~30 minutes and resuspended in 100μl of DEPC water to proceed with QIAgen columns. 350μl of provided Buffer RLT were added and mixed by pippeting, 250μl of 100% ethanol were also added and all the mixture was placed on a Qiagen column and centrifuged 15 seconds 10 000 rpm. 350μl of provided RW1

were added to the column and centrifuged 15 seconds 10 000 rpm. 10µl of DNAse in 70µl of provided Buffer RDD were added and incubated 15/30 minutes (for cell/tissue RNA extraction). Again, 350µl of provided RW1 were added to the columns and centrifuged 15 seconds. Next, 500µl of RPE were added twice and centrifuged 15 seconds and 2 minutes 10 000 rpm the first and the second time respectively. The RNA elution was performed with 50µl of 50ºC pre-warmed DEPC water, incubated 1 minute in the column and centrifuged 1 minute at maximum speed.

For RNA extraction from tissues, fresh tissues where frozen in OCT and kept at -80ºC until needed. For the RNA extraction TRIzol was not used. Directly, 4 tissue slides of 14µm from each sample were obtained in a cryostat, placed in a microcentrifuge tube with 350µl of provided Buffer RLT (600µl in the case of more than 20mg of sample), homogenized with a syringe and centrifuged 3 minutes at maximum speed. The supernatant was recovered and one volume of 70% ethanol was added, mixed and centrifuged 15 seconds 10 000 rpm. The following steps are the described for RNA extraction from cells. The final elution was performed with 30µl of 50ºC pre-warmed DEPC water.

The RNA was kept -80ºC. The RNA quantification and purity was measured with NanoDrop ND-1000 spectrophotometer (NanoDrop Technologies). The integrity was assessed with the Agilent 2100 Bioanalyzer (Agilent) when RNA was needed for microarray analysis. RNA Integrity Numbers (RIN) greater than 9 was obtained from cell lines

M.9.3. Reverse Transcription quantitative PCR (qRT-PCR)

To study the mRNA expression by quantitative PCR (qPCR), mRNA was reverse transcribed to cDNA with *High Capacity cDNA Reverse Transcription kit* (Applied Biosystems) according to the manufacturer's recommendations. The conditions for cDNA reverse transcription performed in the thermal cycler *Mastercycler® ep* (Eppendorf) were:

1- 1 cycle of 10 minutes at 25ºC
2- 1 cycle of 120 minutes at 37ºC
3- 1 cycle of 5 minutes at 85ºC
4- Storage at 4ºC up to 24 hours, or -20ºC for long-term storage.

For the DNA amplification we used *Lightcycler 408 Probes Master* (Roche) and the amplification was performed in the *Lightcycle 408 Real Time PCR-System* device (Roche). The amplification conditions used were:

1- 1 cycle of 10 minutes at 95ºC (denaturation step)
2- 45 cycles of :   10 seconds at 95ºC
                        30 seconds at 60ºC

The relative expression of each gene was normalized with the expression of the housekeeping gene: RPLP0.

M.9.4. Fluorescence In Situ Hybridization (FISH) for *PARP1* gene

PARP1 gene copy number was determined by FISH on 3 μm sections resulting from the TMA using standard procedures. This determination was carried on by Sandra Zazo under the supervision of Dr. Rojo at Fundación

Jiménez Díaz. A bacterial artificial chromosome (BAC) clone labeled with Green 5-Fluorescein was selected representing the gene of interest from the region 1q41-q42: RP11-831N20 (PARP1) and obtained from the CloneCentral™ Human BAC Clone (Empiregenomics). Results were captured with a fluorescence DM2000 Leica microscope and analyzed with the Nuance FX Multispectral Imaging System. FISH scoring of fluorescence signals was carried out by counting the number of single gene copy in an average of 100 non-overlapping nuclei for each case. Normal number of probe signals of the gene was two signals per nuclei. Amplification was considered when the probe signals were more than two per nuclei. Fewer than two probe signals in more than 50% of the nuclei were considered a loss.

M.9.5. Direct sequencing of BRCA1 and BRCA2

DNA from cell lines was extracted as described in M.9.1. Primers for the detection of mutations in BRCA1 (Exon 20, 5382C (c.5263insC, p.Ser1755fs, STOP1829, BIC) and BRCA2 (Exon 11 c.5946delT) were used. The sequences used were:

BRCA1:

Fw: ATATGACGTGTCTGCTCCAC

Rv: AGTCTTACAAAATGAAGCGG

BRCA2:

Fw: CACCTTGTGATGTTAGTTT

Rv: TTGGGATATTAAATGTTCTGGAGTA

Mutational analysis was performed by direct sequencing with BigDye v3.1. (Applied Biosystems) according to the manufacturer's instructions and analysed on an ABI3730XLSequencer (Applied Biosystems). The sequencing and analysis was performed by Molecular Biology service from Hospital del Mar, by Silvia Pairet and Bea Bellosillo.

M.9.6. Microarray analysis

Microarrays were performed and analyzed by the core facility Microarray Analysis Service (SAM) at IMIM (Hospital del Mar Research Institute). Two types of technologies were used in this work:

SNP array (Comparative Genomic Hybridization, CGH)

CGH arrays were used to analyze genomic instability in human breast tumour specimens and breast cancer cell lines by evaluating copy number changes.

To quantify the genome instability four variables for each chromosome were analyzed: the number of aberrations of each group (total, gains and losses); the % of altered genome (total, gains and losses); the average of aberrations/case (total, gains and losses); the most overlapped region.

Presence of alteration (gains and losses) in regions that contains DNA repair genes was also analyzed.

All samples were hybridized to Genome-Wide Human SNP Array 6.0 array (Affymetrix Inc.), which included more than 906 600 single nucleotide polymorphisms (SNPs) and more than 946 000 probes for the detection of copy number variation. Hybridizations were done according to the manufacturer's protocol (Affymetrix Cytogenetics Copy Number assay). Briefly, 500 ng of total genomic DNA was digested with Nsp I and Sty I restriction enzymes and ligated to adaptors. After, the adaptor-ligated DNA fragments were amplified, fragmented, labeled and hybridized to a Genome-Wide Human SNP Array 6.0 array. Following hybridization, the array was washed, stained and scanned. Microarray data was extracted and visualized using the Affymetrix Chromosome Analysis Suite (ChAS) (Affymetrix Inc).

A total of ten human breast tumour specimens were considered for the study, five with low PARP protein expression and five with high PARP

protein expression. And a total of six breast cancer cell lines were also compared between them.

PARP related DNA genes repair were assessed for gains and losses in all samples in the data obtained from the same array using Affymetrix Affymetrix® Chromosome Analysis Suite (ChAS) Software, using human genome build hg19 and na31 annotations. No filters were considered to study alterations, that is a gain or a lost is considered if at least one probe is altered.

The U Mann-Whitney test was used for analyzing continuous variables (% of altered, gained and lost genome; alterations, gains and losses per sample, protein expression). All the statistical tests were done with the *SPSS 12.0* software (SPSS-IBM). A p-value of ≤0,05 was considered statistically significant and a p-value of ≤0,01 was considered statistically marginal.

The elaboration of the heatmap representing the gains and losses in locus of genes related with DNA repair was performed with Genesis software[362]

Expression arrays

Expression arrays were used to study the gene expression profiles of three pairs of breast cancer cell lines (BT474, MCF7 and MDA-MB-231) knocked-down for PARP1 compared with their control cell line and between them.

All samples were hybridized to Human GeneChip Exon 1.0 ST Array (Affymetrix). This array contains approximately 40 probes covering the length of each of the 18 708 genes contained. These probes are summarized into a single level data point that represents the expression of all the transcripts derived from each gene in a specific cell line at a specific moment. For the study of gene expression, mRNA was extracted

221

from each cell line in basal conditions (48 hours after being cultured in plates), the quality was assessed (RIN>9) and the samples were processed following the manufacturer's protocol.

Briefly, the obtained raw data was background corrected, quantile-normalized and summarized to a logarithmic gene-level. A moderated *t*-statistic model was used to determine those genes differentially expressed between each pair of cell lines (shControl vs. shPARP1). Next, the data was corrected for multiple comparisons using the False Discovery Rate (FDR) and those genes with a new adjusted p-value under 0,05 were considered significant. Hierarchical cluster analysis was performed to test the data aggregation. All data analysis was assessed with R (version 2.11.1) with packages aroma.affymetrix, Biobase, limma and genefilter. The elaboration of the heatmap representing gene expression levels of genes with differential expression was performed with Genesis software Ingenuity Pathway Analysis (IPA) was used to study from our microarray data which functions, pathways and networks were significantly modulated.

M.9.7. Primer designing

Primers for selected genes were specifically generated for validating microarray data and to study the effects of Olaparib in mRNA expression.

First, in the *Universal ProbeLibrary Assay Design Center* (Roche)[363] we introduced the GenBank number of the gene of interest to obtain the probe of Roche and the pair of raw primers to optimize. Next, with the *DNAstar Primer design* software the given primers were improved trying to meet the following characteristics: avoid primer dimer and hairpin

formation; length of each primer between 18-23 mer; length of the amplicon between 90-110 base pairs; melting temperature around 60ºC and equal or similar between primers; preferably ending in "C" or "G" in both 5' and 3' ends; and lack of capacity to bind to other sites in the template. Finally, a BLAST with each of the optimized primers was run to confirm that the homology of each primer for the target gene had the highest score and the lowest E-value, and that the next gene sequences with homology for the primer had an E-value greater than a magnitude of difference. This last step was useful to confirm that the generated primers did not have capacity to bind inespecifically to other sequences in the genome or in the transcriptome different from the gene of interest.

The following primers were designed (sequences on 5' – 3'):

PARP1 (Probe of Roche: #12#)

Forward: GGCGATCTTGGACCGAGTAG

Reverse: GTAATAGGCATCGCTCTTGAAG

EGFR (Probe of Roche: #50#)

Forward: CAAGTGGATGGCATTGGAATC

Reverse: GCTTGGATCCAAAGGTCATC

HER2 (Probe of Roche: #43#)

Forward: GGGCCAAACCTTACGATG

Reverse: CTTGGCCGACATTCAGAGTC

RPLP0 (Probe of Roche: #6#)

Forward: GCAGGTGTTCGACAATGGC

Reverse: CTGGCAACATTGCGGACAC

M.10. Xenograft models

All the animal procedures were performed according to the guidelines of European Community Directive and were approved by the PRBB ethical committee.

All the mice models used in this work consisted in subcutaneous tumour implanted in one or both mice's flanks. Cells were harvested by gentle trypsinization, counted and washed with PBS. Total number of cells to be inoculated for each five mice was resuspended in PBS/Matrigel Growth Factor Reduced (Becton Dickinson) (proportion 1:1), mixed to homogenize the suspension, and preserved on ice during the inoculations. Female 5 weeks old mice from Charles River were used for all the models. Mice strains and millions of cells used for each cell line are specified in the following table:

Table M.2. Mice strains and number of inoculated cells

Cell line	Mouse Strain	Number of Cells	s.c. implantation
BT474	Balb/C nude	$15*10^6$	One flank
BT474 shCT/shPARP1	Balb/C nude	$15*10^6$	Both flanks
MCF7 shCT/shPARP1	Athymic Nude	$10*10^6$	Both flanks
231 shCT/shPARP1	Balb/C nude	$5*10^6$	Both flanks

In the case of BT474 and MCF7 cell lines (which are ER+), 24 hours prior to cell inoculations, 17β-estradiol pellets (0,72mg, 60-day release, from Innovative Research of America) were subcutaneously implanted in the posterior side of the neck between the ears and the shoulders to avoid mice self-manipulation. For pellet implantations and cell inoculations, mice were anesthetized with isofluorane in a *M3000*

Anesthesia Machine Vaporizer Non-rebreathing circuit (ParkLand Scientific) and manipulated in a sterile biological safety cabinet. Tumour growth was measured once or twice weekly with a digital calliper. Tumour volume was calculated based on the formula: [Volume = $(L * W^2)/2$] , where (L)= tumour length and (W)= tumour width. For analyzing the tumour growth, each tumour volume measure was divided by its initial tumour volume (considered the volume registered one measure prior to the onset of tumour growth) to express the growth in folds, in the text called: Relative Tumour Volume (RTV). Once the treatment was finished or before the tumour reached the volume of 1500mm^3, mice were sacrificed with CO_2 inhalation, tumours were extracted and organs were checked to discard the presence of metastasis. A fraction of the tumours was fixed with formalin and paraffin-embedded for immunohistologic staining, another fraction was directly frozen in dry ice and later included in OCT if necessary for protein, mRNA or DNA extraction, and in the case of MCF7 shCT/shPARP1 xenografts, a fresh fraction was preserved at 4ºC and immediately processed to obtain tumour lysates for PARP enzymatic assay.

In vivo treatments were performed as described in results section R.3.3.3.

M.11. Statistical analysis

Statistics for experimental with cell lines

Statistical analysis was carried out with *SPSS v12.0* (SPSS-IBM). Independent sample *t*-test was used to compare shControl cell lines versus shPARP1 cell lines in clonogenic, soft agar assay and migration and invasion assays, as well as to compare shControl versus shPARP1 the final tumour volumes and final tumour weight in xenografts. One-way ANOVA was always used to assess differences in cellular effects between

combined treatments and each drug alone. Tukey's Post Hoc was used to perform pairwise comparison. All the statistical test were performed at the two-sided 0,05 level of significance.

Statistics for PARP1 expression in tumour specimens:

Statistical analysis of PARP1 expression also was carried out with *SPSS v13.0*. We hypothesized that the group of women with tumours non-overexpressing PARP1 would have an 80% 5-year OS and the group overexpressing PARP1 a 65% 5-year OS. The minimal sample needed to detect this difference, with a power of 0,90 and two-sided error α of 0,05, was 241 cases. To correlate PARP1 expression and clinicopathological variables, we used the χ^2 test (Fisher's exact test). OS was defined as the time from the date of surgery to the date of death from any cause or last follow-up. DFS was considered from the date of surgery to the date of any primary, regional or distant recurrence, as well as the appearance of a secondary tumour or DCIS. Univariate analysis was based on the Kaplan– Meier OS and DFS curves using the log-rank test; all predictors with p-values<0,1 were used in multivariate analysis using the Cox proportional hazards model[200]. All the statistical tests were conducted at the two-sided 0,05 level. Receiver operating curve (ROC) was used to determine the optimal cutoff point based on relapse end point for PARP1 expression[289]. As shown in results figure R.6., the cut-off was set for an optical density of 39 970. Specimens with values above this cut-off point were considered as PARP1 overexpressors and specimens with values below non-overexpressors. This work was carried out in accordance with Reporting Recommendations for Tumor Marker Prognostic Studies (REMARK) guideline[364].

BIBLIOGRAPHY

1. WHO. *World Health Organization: The Global Burden Of Disease: 2004 Update*, (World Health Organization, Geneva, 2008).

2. ACS. Global Cancer Facts & Figures. (American Cancer Society, Atlanta, 2011).

3. Jemal, A*., et al.* Global cancer statistics. *CA Cancer J Clin* **61**, 69-90 (2011).

4. Ferlay J, S.H., Bray F, Forman D, Mathers C and Parkin DM. GLOBOCAN 2008 v1.2, Cancer Incidence and Mortality Worldwide: IARC CancerBase (International Agency for Research on Cancer, Lyon, France, 2010).

5. Jemal, A*., et al.* Cancer statistics, 2007. *CA Cancer J Clin* **57**, 43-66 (2007).

6. Hanahan, D. & Weinberg, R.A. The hallmarks of cancer. *Cell* **100**, 57-70 (2000).

7. Kenemans, P., Verstraeten, R.A. & Verheijen, R.H. Oncogenic pathways in hereditary and sporadic breast cancer. *Maturitas* **49**, 34-43 (2004).

8. Thompson, D. & Easton, D.F. Cancer Incidence in BRCA1 mutation carriers. *J Natl Cancer Inst* **94**, 1358-1365 (2002).

9. Greenblatt, M.S., Chappuis, P.O., Bond, J.P., Hamel, N. & Foulkes, W.D. TP53 mutations in breast cancer associated with BRCA1 or BRCA2 germ-line mutations: distinctive spectrum and structural distribution. *Cancer Res* **61**, 4092-4097 (2001).

10. Lakhani. Basal markers and estogen receptor status are powerful predictors of germline BRCA1 mutations in *Proceedings of the Annual Meeting of the American Association for Cancer Research*, Vol. 45 (ed. AACR) (ACCR, 2004).

11. Easton, D.F., Ford, D. & Bishop, D.T. Breast and ovarian cancer incidence in BRCA1-mutation carriers. Breast Cancer Linkage Consortium. *Am J Hum Genet* **56**, 265-271 (1995).

12. Wooster, R*., et al.* Identification of the breast cancer susceptibility gene BRCA2. *Nature* **378**, 789-792 (1995).

13. Gudmundsdottir, K. & Ashworth, A. The roles of BRCA1 and BRCA2 and associated proteins in the maintenance of genomic stability. *Oncogene* **25**, 5864-5874 (2006).

14. Cortez, D., Wang, Y., Qin, J. & Elledge, S.J. Requirement of ATM-dependent phosphorylation of brca1 in the DNA damage response to double-strand breaks. *Science* **286**, 1162-1166 (1999).

15. Venkitaraman, A.R. Cancer susceptibility and the functions of BRCA1 and BRCA2. *Cell* **108**, 171-182 (2002).

16. Clarke, R.B., Howell, A., Potten, C.S. & Anderson, E. Dissociation between steroid receptor expression and cell proliferation in the human breast. *Cancer Res* **57**, 4987-4991 (1997).

17. Russo, J., Ao, X., Grill, C. & Russo, I.H. Pattern of distribution of cells positive for estrogen receptor alpha and progesterone receptor in relation to proliferating cells in the mammary gland. *Breast Cancer Res Treat* **53**, 217-227 (1999).

18. Conneely, O.M., Jericevic, B.M. & Lydon, J.P. Progesterone receptors in mammary gland development and tumorigenesis. *J Mammary Gland Biol Neoplasia* **8**, 205-214 (2003).

19. Effects of chemotherapy and hormonal therapy for early breast cancer on recurrence and 15-year survival: an overview of the randomised trials. *Lancet* **365**, 1687-1717 (2005).

20.   Hammond, M.E.*, et al.* American Society of Clinical Oncology/College Of American Pathologists guideline recommendations for immunohistochemical testing of estrogen and progesterone receptors in breast cancer. *J Clin Oncol* **28**, 2784-2795 (2010).

21.   Smith, I.*, et al.* 2-year follow-up of trastuzumab after adjuvant chemotherapy in HER2-positive breast cancer: a randomised controlled trial. *Lancet* **369**, 29-36 (2007).

22.   Cobleigh, M.A.*, et al.* Multinational study of the efficacy and safety of humanized anti-HER2 monoclonal antibody in women who have HER2-overexpressing metastatic breast cancer that has progressed after chemotherapy for metastatic disease. *J Clin Oncol* **17**, 2639-2648 (1999).

23.   Wolff, A.C.*, et al.* American Society of Clinical Oncology/College of American Pathologists guideline recommendations for human epidermal growth factor receptor 2 testing in breast cancer. *J Clin Oncol* **25**, 118-145 (2007).

24.   Perou, C.M.*, et al.* Molecular portraits of human breast tumours. *Nature* **406**, 747-752 (2000).

25.   Sorlie, T.*, et al.* Gene expression patterns of breast carcinomas distinguish tumor subclasses with clinical implications. *Proc Natl Acad Sci U S A* **98**, 10869-10874 (2001).

26.   Sorlie, T.*, et al.* Repeated observation of breast tumor subtypes in independent gene expression data sets. *Proc Natl Acad Sci U S A* **100**, 8418-8423 (2003).

27.   Stockmans, G., Deraedt, K., Wildiers, H., Moerman, P. & Paridaens, R. Triple-negative breast cancer. *Curr Opin Oncol* **20**, 614-620 (2008).

28.   Sotiriou, C. & Pusztai, L. Gene-expression signatures in breast cancer. *N Engl J Med* **360**, 790-800 (2009).

29.   Osborne, C.K. Tamoxifen in the treatment of breast cancer. *N Engl J Med* **339**, 1609-1618 (1998).

30.   Yarden, Y. & Sliwkowski, M.X. Untangling the ErbB signalling network. *Nat Rev Mol Cell Biol* **2**, 127-137 (2001).

31.   Carter, P.*, et al.* Humanization of an anti-p185HER2 antibody for human cancer therapy. *Proc Natl Acad Sci U S A* **89**, 4285-4289 (1992).

32.   Slamon, D.J.*, et al.* Use of chemotherapy plus a monoclonal antibody against HER2 for metastatic breast cancer that overexpresses HER2. *N Engl J Med* **344**, 783-792 (2001).

33.   Valabrega, G., Montemurro, F. & Aglietta, M. Trastuzumab: mechanism of action, resistance and future perspectives in HER2-overexpressing breast cancer. *Ann Oncol* **18**, 977-984 (2007).

34.   Johnston, S.*, et al.* Lapatinib combined with letrozole versus letrozole and placebo as first-line therapy for postmenopausal hormone receptor-positive metastatic breast cancer. *J Clin Oncol* **27**, 5538-5546 (2009).

35.   Lodish H, B.A., Zipursky SL. *Molecular Cell Biology*, (W. H. Freeman and Company, New York, 2000).

36.   Lindahl, T. Instability and decay of the primary structure of DNA. *Nature* **362**, 709-715 (1993).

37.   Cooke, M.S., Evans, M.D., Dizdaroglu, M. & Lunec, J. Oxidative DNA damage: mechanisms, mutation, and disease. *FASEB J* **17**, 1195-1214 (2003).

38. Sedgwick, B. Repairing DNA-methylation damage. *Nat Rev Mol Cell Biol* **5**, 148-157 (2004).

39. Pray, L. *DNA Replication and Causes of Mutation*, (Nature, 2008).

40. Clancy, S. *DNA Damage & Repair: Mechanisms for Maintaining DNA Integrity*, (Nature, 2008).

41. Fu, D., Calvo, J.A. & Samson, L.D. Balancing repair and tolerance of DNA damage caused by alkylating agents. *Nat Rev Cancer* **12**, 104-120 (2012).

42. Ward, J.F. DNA damage produced by ionizing radiation in mammalian cells: identities, mechanisms of formation, and reparability. *Prog Nucleic Acid Res Mol Biol* **35**, 95-125 (1988).

43. NCI. Cancer Drug Information: Cisplatin. (National Cancer Institute. NIH, 2012).

44. Silver, D.P.*, et al.* Efficacy of neoadjuvant Cisplatin in triple-negative breast cancer. *J Clin Oncol* **28**, 1145-1153 (2010).

45. Pinto, A.L. & Lippard, S.J. Binding of the antitumor drug cis-diamminedichloroplatinum(II) (cisplatin) to DNA. *Biochim Biophys Acta* **780**, 167-180 (1985).

46. Siddik, Z.H. Cisplatin: mode of cytotoxic action and molecular basis of resistance. *Oncogene* **22**, 7265-7279 (2003).

47. Barranco, S.C., Gerner, E.W., Burk, K.H. & Humphrey, R.M. Survival and cell kinetics effects of adriamycin on mammalian cells. *Cancer Res* **33**, 11-16 (1973).

48. Lomovskaya, N.*, et al.* Doxorubicin overproduction in Streptomyces peucetius: cloning and characterization of the dnrU ketoreductase and dnrV genes and the doxA cytochrome P-450 hydroxylase gene. *J Bacteriol* **181**, 305-318 (1999).

49. Fornari, F.A., Randolph, J.K., Yalowich, J.C., Ritke, M.K. & Gewirtz, D.A. Interference by doxorubicin with DNA unwinding in MCF-7 breast tumor cells. *Mol Pharmacol* **45**, 649-656 (1994).

50. Fortune, J.M. & Osheroff, N. Topoisomerase II as a target for anticancer drugs: when enzymes stop being nice. *Prog Nucleic Acid Res Mol Biol* **64**, 221-253 (2000).

51. Mizutani, H., Tada-Oikawa, S., Hiraku, Y., Kojima, M. & Kawanishi, S. Mechanism of apoptosis induced by doxorubicin through the generation of hydrogen peroxide. *Life Sci* **76**, 1439-1453 (2005).

52. Barnes, D.E. & Lindahl, T. Repair and genetic consequences of endogenous DNA base damage in mammalian cells. *Annu Rev Genet* **38**, 445-476 (2004).

53. Watters, D. Molecular mechanisms of ionizing radiation-induced apoptosis. *Immunol Cell Biol* **77**, 263-271 (1999).

54. Hoeijmakers, J.H. Genome maintenance mechanisms for preventing cancer. *Nature* **411**, 366-374 (2001).

55. Freidberg, E.C. (ed.) *DNA Repair and Mutagenesis*, 1118 (ASM Press, Washigton DC, 2006).

56. Harfe, B.D. & Jinks-Robertson, S. DNA mismatch repair and genetic instability. *Annu Rev Genet* **34**, 359-399 (2000).

57. Li, G.M. Mechanisms and functions of DNA mismatch repair. *Cell Res* **18**, 85-98 (2008).

58. Parsons, R.*, et al.* Hypermutability and mismatch repair deficiency in RER+ tumor cells. *Cell* **75**, 1227-1236 (1993).

59. Khanna, K.K. & Jackson, S.P. DNA double-strand breaks: signaling, repair and the cancer connection. *Nat Genet* **27**, 247-254 (2001).

60. Sonoda, E.*, et al.* Sister chromatid exchanges are mediated by homologous recombination in vertebrate cells. *Mol Cell Biol* **19**, 5166-5169 (1999).

61. Paull, T.T.*, et al.* A critical role for histone H2AX in recruitment of repair factors to nuclear foci after DNA damage. *Curr Biol* **10**, 886-895 (2000).

62. Zhong, Q.*, et al.* Association of BRCA1 with the hRad50-hMre11-p95 complex and the DNA damage response. *Science* **285**, 747-750 (1999).

63. Moynahan, M.E., Pierce, A.J. & Jasin, M. BRCA2 is required for homology-directed repair of chromosomal breaks. *Mol Cell* **7**, 263-272 (2001).

64. Davies, A.A.*, et al.* Role of BRCA2 in control of the RAD51 recombination and DNA repair protein. *Mol Cell* **7**, 273-282 (2001).

65. Moore, J.K. & Haber, J.E. Cell cycle and genetic requirements of two pathways of nonhomologous end-joining repair of double-strand breaks in Saccharomyces cerevisiae. *Mol Cell Biol* **16**, 2164-2173 (1996).

66. Pardo, B., Gomez-Gonzalez, B. & Aguilera, A. DNA repair in mammalian cells: DNA double-strand break repair: how to fix a broken relationship. *Cell Mol Life Sci* **66**, 1039-1056 (2009).

67. Smith, S. The world according to PARP. *Trends Biochem Sci* **26**, 174-179 (2001).

68. Shall, S. ADP-ribosylation of proteins: a ubiquitous cellular control mechanism. *Biochem Soc Trans* **17**, 317-322 (1989).

69. Aktories, K. Clostridial ADP-ribosylating toxins: effects on ATP and GTP-binding proteins. *Mol Cell Biochem* **138**, 167-176 (1994).

70. Takada, T., Okazaki, I.J. & Moss, J. ADP-ribosylarginine hydrolases. *Mol Cell Biochem* **138**, 119-122 (1994).

71. de Murcia, G., Jacobson, M. & Shall, S. Regulation by ADP-ribosylation. *Trends Cell Biol* **5**, 78-81 (1995).

72. Nishizuka, Y., Ueda, K., Honjo, T. & Hayaishi, O. Enzymic adenosine diphosphate ribosylation of histone and poly adenosine diphosphate ribose synthesis in rat liver nuclei. *J Biol Chem* **243**, 3765-3767 (1968).

73. Yamada, M., Miwa, M. & Sugimura, T. Studies on poly (adenosine diphosphate-ribose). X. Properties of a partially purified poly (adenosine diphosphate-ribose) polymerase. *Arch Biochem Biophys* **146**, 579-586 (1971).

74. Okayama, H., Edson, C.M., Fukushima, M., Ueda, K. & Hayaishi, O. Purification and properties of poly(adenosine diphosphate ribose) synthetase. *J Biol Chem* **252**, 7000-7005 (1977).

75. Benjamin, R.C. & Gill, D.M. ADP-ribosylation in mammalian cell ghosts. Dependence of poly(ADP-ribose) synthesis on strand breakage in DNA. *J Biol Chem* **255**, 10493-10501 (1980).

76. Durkacz, B.W., Omidiji, O., Gray, D.A. & Shall, S. (ADP-ribose)n participates in DNA excision repair. *Nature* **283**, 593-596 (1980).

77. Pleschke, J.M., Kleczkowska, H.E., Strohm, M. & Althaus, F.R. Poly(ADP-ribose) binds to specific domains in DNA damage checkpoint proteins. *J Biol Chem* **275**, 40974-40980 (2000).

78. Althaus, F.R. & Richter, C. ADP-ribosylation of proteins. Enzymology and biological significance. *Mol Biol Biochem Biophys* **37**, 1-237 (1987).

79. Davidovic, L., Vodenicharov, M., Affar, E.B. & Poirier, G.G. Importance of poly(ADP-ribose) glycohydrolase in the control of poly(ADP-ribose) metabolism. *Exp Cell Res* **268**, 7-13 (2001).

80. Oka, S., Kato, J. & Moss, J. Identification and characterization of a mammalian 39-kDa poly(ADP-ribose) glycohydrolase. *J Biol Chem* **281**, 705-713 (2006).

81. Boulikas, T. Poly(ADP-ribose) synthesis and degradation in mammalian nuclei. *Anal Biochem* **203**, 252-258 (1992).

82. Hottiger, M.O.*, et al.* Progress in the function and regulation of ADP-Ribosylation. *Sci Signal* **4**, mr5 (2011).

83. D'Amours, D., Desnoyers, S., D'Silva, I. & Poirier, G.G. Poly(ADP-ribosyl)ation reactions in the regulation of nuclear functions. *Biochem J* **342 (Pt 2)**, 249-268 (1999).

84. de Murcia, G. & Menissier de Murcia, J. Poly(ADP-ribose) polymerase: a molecular nick-sensor. *Trends Biochem Sci* **19**, 172-176 (1994).

85. Kraus, W.L. Transcriptional control by PARP-1: chromatin modulation, enhancer-binding, coregulation, and insulation. *Curr Opin Cell Biol* **20**, 294-302 (2008).

86. Gradwohl, G.*, et al.* The second zinc-finger domain of poly(ADP-ribose) polymerase determines specificity for single-stranded breaks in DNA. *Proc Natl Acad Sci U S A* **87**, 2990-2994 (1990).

87. Langelier, M.F., Servent, K.M., Rogers, E.E. & Pascal, J.M. A third zinc-binding domain of human poly(ADP-ribose) polymerase-1 coordinates DNA-dependent enzyme activation. *J Biol Chem* **283**, 4105-4114 (2008).

88. Schreiber, V.*, et al.* Poly(ADP-ribose) polymerase-2 (PARP-2) is required for efficient base excision DNA repair in association with PARP-1 and XRCC1. *J Biol Chem* **277**, 23028-23036 (2002).

89. Kaufmann, S.H., Desnoyers, S., Ottaviano, Y., Davidson, N.E. & Poirier, G.G. Specific proteolytic cleavage of poly(ADP-ribose) polymerase: an early marker of chemotherapy-induced apoptosis. *Cancer Res* **53**, 3976-3985 (1993).

90. Tao, Z., Gao, P. & Liu, H.W. Identification of the ADP-ribosylation sites in the PARP-1 automodification domain: analysis and implications. *J Am Chem Soc* **131**, 14258-14260 (2009).

91. Lindahl, T., Satoh, M.S., Poirier, G.G. & Klungland, A. Post-translational modification of poly(ADP-ribose) polymerase induced by DNA strand breaks. *Trends Biochem Sci* **20**, 405-411 (1995).

92. Buki, K.G., Bauer, P.I., Hakam, A. & Kun, E. Identification of domains of poly(ADP-ribose) polymerase for protein binding and self-association. *J Biol Chem* **270**, 3370-3377 (1995).

93. Bork, P.*, et al.* A superfamily of conserved domains in DNA damage-responsive cell cycle checkpoint proteins. *FASEB J* **11**, 68-76 (1997).

94. Loeffler, P.A.*, et al.* Structural studies of the PARP-1 BRCT domain. *BMC Struct Biol* **11**, 37 (2011).

95. Beernink, P.T.*, et al.* Specificity of protein interactions mediated by BRCT domains of the XRCC1 DNA repair protein. *J Biol Chem* **280**, 30206-30213 (2005).

96. Audebert, M., Salles, B. & Calsou, P. Involvement of poly(ADP-ribose) polymerase-1 and XRCC1/DNA ligase III in an alternative route for DNA double-strand breaks rejoining. *J Biol Chem* **279**, 55117-55126 (2004).

97.   Malanga, M., Pleschke, J.M., Kleczkowska, H.E. & Althaus, F.R. Poly(ADP-ribose) binds to specific domains of p53 and alters its DNA binding functions. *J Biol Chem* **273**, 11839-11843 (1998).

98.   Hassa, P.O., Covic, M., Hasan, S., Imhof, R. & Hottiger, M.O. The enzymatic and DNA binding activity of PARP-1 are not required for NF-kappa B coactivator function. *J Biol Chem* **276**, 45588-45597 (2001).

99.   Dantzer, F., Nasheuer, H.P., Vonesch, J.L., de Murcia, G. & Menissier-de Murcia, J. Functional association of poly(ADP-ribose) polymerase with DNA polymerase alpha-primase complex: a link between DNA strand break detection and DNA replication. *Nucleic Acids Res* **26**, 1891-1898 (1998).

100.   Nie, J.*, et al.* Interaction of Oct-1 and automodification domain of poly(ADP-ribose) synthetase. *FEBS Lett* **424**, 27-32 (1998).

101.   Shieh, W.M.*, et al.* Poly(ADP-ribose) polymerase null mouse cells synthesize ADP-ribose polymers. *J Biol Chem* **273**, 30069-30072 (1998).

102.   Ame, J.C.*, et al.* PARP-2, A novel mammalian DNA damage-dependent poly(ADP-ribose) polymerase. *J Biol Chem* **274**, 17860-17868 (1999).

103.   Johansson, M. A human poly(ADP-ribose) polymerase gene family (ADPRTL): cDNA cloning of two novel poly(ADP-ribose) polymerase homologues. *Genomics* **57**, 442-445 (1999).

104.   Smith, S., Giriat, I., Schmitt, A. & de Lange, T. Tankyrase, a poly(ADP-ribose) polymerase at human telomeres. *Science* **282**, 1484-1487 (1998).

105.   Ame, J.C., Spenlehauer, C. & de Murcia, G. The PARP superfamily. *Bioessays* **26**, 882-893 (2004).

106.   Hassa, P.O. & Hottiger, M.O. The diverse biological roles of mammalian PARPS, a small but powerful family of poly-ADP-ribose polymerases. *Front Biosci* **13**, 3046-3082 (2008).

107.   Schreiber, V., Dantzer, F., Ame, J.C. & de Murcia, G. Poly(ADP-ribose): novel functions for an old molecule. *Nat Rev Mol Cell Biol* **7**, 517-528 (2006).

108.   Hakme, A., Wong, H.K., Dantzer, F. & Schreiber, V. The expanding field of poly(ADP-ribosyl)ation reactions. 'Protein Modifications: Beyond the Usual Suspects' Review Series. *EMBO Rep* **9**, 1094-1100 (2008).

109.   Hottiger, M.O., Hassa, P.O., Luscher, B., Schuler, H. & Koch-Nolte, F. Toward a unified nomenclature for mammalian ADP-ribosyltransferases. *Trends Biochem Sci* **35**, 208-219 (2010).

110.   Aguiar, R.C., Takeyama, K., He, C., Kreinbrink, K. & Shipp, M.A. B-aggressive lymphoma family proteins have unique domains that modulate transcription and exhibit poly(ADP-ribose) polymerase activity. *J Biol Chem* **280**, 33756-33765 (2005).

111.   Oliver, A.W.*, et al.* Crystal structure of the catalytic fragment of murine poly(ADP-ribose) polymerase-2. *Nucleic Acids Res* **32**, 456-464 (2004).

112.   Rouleau, M.*, et al.* PARP-3 associates with polycomb group bodies and with components of the DNA damage repair machinery. *J Cell Biochem* **100**, 385-401 (2007).

113.   Loseva, O.*, et al.* PARP-3 is a mono-ADP-ribosylase that activates PARP-1 in the absence of DNA. *J Biol Chem* **285**, 8054-8060 (2010).

114.   Roitt, I.M. The inhibition of carbohydrate metabolism in ascites-tumour cells by ethyleneimines. *Biochem J* **63**, 300-307 (1956).

115. Whish, W.J., Davies, M.I. & Shall, S. Stimulation of poly(ADP-ribose) polymerase activity by the anti-tumour antibiotic, streptozotocin. *Biochem Biophys Res Commun* **65**, 722-730 (1975).

116. Creissen, D. & Shall, S. Regulation of DNA ligase activity by poly(ADP-ribose). *Nature* **296**, 271-272 (1982).

117. Masson, M*., et al.* XRCC1 is specifically associated with poly(ADP-ribose) polymerase and negatively regulates its activity following DNA damage. *Mol Cell Biol* **18**, 3563-3571 (1998).

118. Dantzer, F*., et al.* Base excision repair is impaired in mammalian cells lacking Poly(ADP-ribose) polymerase-1. *Biochemistry* **39**, 7559-7569 (2000).

119. D'Silva, I*., et al.* Relative affinities of poly(ADP-ribose) polymerase and DNA-dependent protein kinase for DNA strand interruptions. *Biochim Biophys Acta* **1430**, 119-126 (1999).

120. Audebert, M., Salles, B., Weinfeld, M. & Calsou, P. Involvement of polynucleotide kinase in a poly(ADP-ribose) polymerase-1-dependent DNA double-strand breaks rejoining pathway. *J Mol Biol* **356**, 257-265 (2006).

121. Wang, M*., et al.* PARP-1 and Ku compete for repair of DNA double strand breaks by distinct NHEJ pathways. *Nucleic Acids Res* **34**, 6170-6182 (2006).

122. de Murcia, J.M*., et al.* Requirement of poly(ADP-ribose) polymerase in recovery from DNA damage in mice and in cells. *Proc Natl Acad Sci U S A* **94**, 7303-7307 (1997).

123. Masutani, M*., et al.* Function of poly(ADP-ribose) polymerase in response to DNA damage: gene-disruption study in mice. *Mol Cell Biochem* **193**, 149-152 (1999).

124. Dantzer, F*., et al.* Involvement of poly(ADP-ribose) polymerase in base excision repair. *Biochimie* **81**, 69-75 (1999).

125. Realini, C.A. & Althaus, F.R. Histone shuttling by poly(ADP-ribosylation). *J Biol Chem* **267**, 18858-18865 (1992).

126. Boulikas, T. Poly(ADP-ribosylated) histones in chromatin replication. *J Biol Chem* **265**, 14638-14647 (1990).

127. Huletsky, A*., et al.* The effect of poly(ADP-ribosyl)ation on native and H1-depleted chromatin. A role of poly(ADP-ribosyl)ation on core nucleosome structure. *J Biol Chem* **264**, 8878-8886 (1989).

128. Kim, M.Y., Mauro, S., Gevry, N., Lis, J.T. & Kraus, W.L. NAD+-dependent modulation of chromatin structure and transcription by nucleosome binding properties of PARP-1. *Cell* **119**, 803-814 (2004).

129. Annunziato, A. DNA Packaging: Nucleosomes and Chromatin. (Nature Education, 2008).

130. Ju, B.G*., et al.* A topoisomerase IIbeta-mediated dsDNA break required for regulated transcription. *Science* **312**, 1798-1802 (2006).

131. Ding, R., Pommier, Y., Kang, V.H. & Smulson, M. Depletion of poly(ADP-ribose) polymerase by antisense RNA expression results in a delay in DNA strand break rejoining. *J Biol Chem* **267**, 12804-12812 (1992).

132. d'Adda di Fagagna, F*., et al.* Functions of poly(ADP-ribose) polymerase in controlling telomere length and chromosomal stability. *Nat Genet* **23**, 76-80 (1999).

133. Pion, E*., et al.* Poly(ADP-ribose) polymerase-1 dimerizes at a 5' recessed DNA end in vitro: a fluorescence study. *Biochemistry* **42**, 12409-12417 (2003).

134. Moroni, F*., et al.* Poly(ADP-ribose) polymerase inhibitors attenuate necrotic but not apoptotic neuronal death in experimental models of cerebral ischemia. *Cell Death Differ* **8**, 921-932 (2001).

135. Nicholson, D.W*., et al.* Identification and inhibition of the ICE/CED-3 protease necessary for mammalian apoptosis. *Nature* **376**, 37-43 (1995).

136. Virag, L. Structure and function of poly(ADP-ribose) polymerase-1: role in oxidative stress-related pathologies. *Curr Vasc Pharmacol* **3**, 209-214 (2005).

137. Yu, S.W*., et al.* Mediation of poly(ADP-ribose) polymerase-1-dependent cell death by apoptosis-inducing factor. *Science* **297**, 259-263 (2002).

138. Berger, S.J., Sudar, D.C. & Berger, N.A. Metabolic consequences of DNA damage: DNA damage induces alterations in glucose metabolism by activation of poly (ADP-ribose) polymerase. *Biochem Biophys Res Commun* **134**, 227-232 (1986).

139. Zong, W.X., Ditsworth, D., Bauer, D.E., Wang, Z.Q. & Thompson, C.B. Alkylating DNA damage stimulates a regulated form of necrotic cell death. *Genes Dev* **18**, 1272-1282 (2004).

140. Affar el, B., Shah, R.G., Dallaire, A.K., Castonguay, V. & Shah, G.M. Role of poly(ADP-ribose) polymerase in rapid intracellular acidification induced by alkylating DNA damage. *Proc Natl Acad Sci U S A* **99**, 245-250 (2002).

141. Huang, Q., Wu, Y.T., Tan, H.L., Ong, C.N. & Shen, H.M. A novel function of poly(ADP-ribose) polymerase-1 in modulation of autophagy and necrosis under oxidative stress. *Cell Death Differ* **16**, 264-277 (2009).

142. Sodhi, R.K., Singh, N. & Jaggi, A.S. Poly(ADP-ribose) polymerase-1 (PARP-1) and its therapeutic implications. *Vascul Pharmacol* **53**, 77-87 (2010).

143. Soldatenkov, V.A*., et al.* Transcriptional repression by binding of poly(ADP-ribose) polymerase to promoter sequences. *J Biol Chem* **277**, 665-670 (2002).

144. Amiri, K.I., Ha, H.C., Smulson, M.E. & Richmond, A. Differential regulation of CXC ligand 1 transcription in melanoma cell lines by poly(ADP-ribose) polymerase-1. *Oncogene* **25**, 7714-7722 (2006).

145. Cervellera, M.N. & Sala, A. Poly(ADP-ribose) polymerase is a B-MYB coactivator. *J Biol Chem* **275**, 10692-10696 (2000).

146. Pavri, R*., et al.* PARP-1 determines specificity in a retinoid signaling pathway via direct modulation of mediator. *Mol Cell* **18**, 83-96 (2005).

147. Anderson, M.G., Scoggin, K.E., Simbulan-Rosenthal, C.M. & Steadman, J.A. Identification of poly(ADP-ribose) polymerase as a transcriptional coactivator of the human T-cell leukemia virus type 1 Tax protein. *J Virol* **74**, 2169-2177 (2000).

148. Ju, B.G*., et al.* Activating the PARP-1 sensor component of the groucho/TLE1 corepressor complex mediates a CaMKinase IIdelta-dependent neurogenic gene activation pathway. *Cell* **119**, 815-829 (2004).

149. Zaniolo, K., Desnoyers, S., Leclerc, S. & Guerin, S.L. Regulation of poly(ADP-ribose) polymerase-1 (PARP-1) gene expression through the post-translational modification of Sp1: a nuclear target protein of PARP-1. *BMC Mol Biol* **8**, 96 (2007).

150. Valdor, R*., et al.* Regulation of NFAT by poly(ADP-ribose) polymerase activity in T cells. *Mol Immunol* **45**, 1863-1871 (2008).

151. Olabisi, O.A*., et al.* Regulation of transcription factor NFAT by ADP-ribosylation. *Mol Cell Biol* **28**, 2860-2871 (2008).

152. Cohen-Armon, M*., et al.* DNA-independent PARP-1 activation by phosphorylated ERK2 increases Elk1 activity: a link to histone acetylation. *Mol Cell* **25**, 297-308 (2007).

153. Oei, S.L. & Shi, Y. Poly(ADP-ribosyl)ation of transcription factor Yin Yang 1 under conditions of DNA damage. *Biochem Biophys Res Commun* **285**, 27-31 (2001).

154. Wallace, J.A. & Felsenfeld, G. We gather together: insulators and genome organization. *Curr Opin Genet Dev* **17**, 400-407 (2007).

155. Yu, W*., et al.* Poly(ADP-ribosyl)ation regulates CTCF-dependent chromatin insulation. *Nat Genet* **36**, 1105-1110 (2004).

156. Hassa, P.O*., et al.* Acetylation of poly(ADP-ribose) polymerase-1 by p300/CREB-binding protein regulates coactivation of NF-kappaB-dependent transcription. *J Biol Chem* **280**, 40450-40464 (2005).

157. Kauppinen, T.M*., et al.* Direct phosphorylation and regulation of poly(ADP-ribose) polymerase-1 by extracellular signal-regulated kinases 1/2. *Proc Natl Acad Sci U S A* **103**, 7136-7141 (2006).

158. Kitamura, T., Sekimata, M., Kikuchi, S. & Homma, Y. Involvement of poly(ADP-ribose) polymerase 1 in ERBB2 expression in rheumatoid synovial cells. *Am J Physiol Cell Physiol* **289**, C82-88 (2005).

159. Quiles-Perez, R*., et al.* Inhibition of poly adenosine diphosphate-ribose polymerase decreases hepatocellular carcinoma growth by modulation of tumor-related gene expression. *Hepatology* **51**, 255-266 (2010).

160. Hasko, G*., et al.* Poly(ADP-ribose) polymerase is a regulator of chemokine production: relevance for the pathogenesis of shock and inflammation. *Mol Med* **8**, 283-289 (2002).

161. Zingarelli, B*., et al.* Differential regulation of activator protein-1 and heat shock factor-1 in myocardial ischemia and reperfusion injury: role of poly(ADP-ribose) polymerase-1. *Am J Physiol Heart Circ Physiol* **286**, H1408-1415 (2004).

162. Oliver, F.J*., et al.* Resistance to endotoxic shock as a consequence of defective NF-kappaB activation in poly (ADP-ribose) polymerase-1 deficient mice. *EMBO J* **18**, 4446-4454 (1999).

163. Rajesh, M*., et al.* Poly(ADP-ribose)polymerase inhibition decreases angiogenesis. *Biochem Biophys Res Commun* **350**, 1056-1062 (2006).

164. Obrosova, I.G*., et al.* Poly(ADP-ribose) polymerase inhibitors counteract diabetes- and hypoxia-induced retinal vascular endothelial growth factor overexpression. *Int J Mol Med* **14**, 55-64 (2004).

165. Tentori, L*., et al.* Poly(ADP-ribose) polymerase (PARP) inhibition or PARP-1 gene deletion reduces angiogenesis. *Eur J Cancer* **43**, 2124-2133 (2007).

166. Tentori, L*., et al.* Stable depletion of poly (ADP-ribose) polymerase-1 reduces in vivo melanoma growth and increases chemosensitivity. *Eur J Cancer* **44**, 1302-1314 (2008).

167. Takahashi, S*., et al.* Enhancement of DEN initiation of liver carcinogenesis by inhibitors of NAD+ ADP ribosyl transferase in rats. *Carcinogenesis* **5**, 901-906 (1984).

168. Tsujiuchi, T*., et al.* Possible involvement of poly ADP-ribosylation in phenobarbital promotion of rat hepatocarcinogenesis. *Carcinogenesis* **11**, 1783-1787 (1990).

169. Epstein, J.H. & Cleaver, J.E. 3-Aminobenzamide can act as a cocarcinogen for ultraviolet light-induced carcinogenesis in mouse skin. *Cancer Res* **52**, 4053-4054 (1992).

170. Yamagami, T., Miwa, A., Takasawa, S., Yamamoto, H. & Okamoto, H. Induction of rat pancreatic B-cell tumors by the combined administration of streptozotocin or alloxan and poly(adenosine diphosphate ribose) synthetase inhibitors. *Cancer Res* **45**, 1845-1849 (1985).

171. Tsutsumi, M*., et al.* Increased susceptibility of poly(ADP-ribose) polymerase-1 knockout mice to nitrosamine carcinogenicity. *Carcinogenesis* **22**, 1-3 (2001).

172. Wang, Z.Q*., et al.* Mice lacking ADPRT and poly(ADP-ribosyl)ation develop normally but are susceptible to skin disease. *Genes Dev* **9**, 509-520 (1995).

173. Tong, W.M*., et al.* Poly(ADP-ribose) polymerase-1 plays a role in suppressing mammary tumourigenesis in mice. *Oncogene* **26**, 3857-3867 (2007).

174. Tong, W.M*., et al.* Synergistic role of Ku80 and poly(ADP-ribose) polymerase in suppressing chromosomal aberrations and liver cancer formation. *Cancer Res* **62**, 6990-6996 (2002).

175. Tong, W.M., Hande, M.P., Lansdorp, P.M. & Wang, Z.Q. DNA strand break-sensing molecule poly(ADP-Ribose) polymerase cooperates with p53 in telomere function, chromosome stability, and tumor suppression. *Mol Cell Biol* **21**, 4046-4054 (2001).

176. Beneke, R. & Moroy, T. Inhibition of poly(ADP-ribose) polymerase activity accelerates T-cell lymphomagenesis in p53 deficient mice. *Oncogene* **20**, 8136-8141 (2001).

177. Tong, W.M*., et al.* Null mutation of DNA strand break-binding molecule poly(ADP-ribose) polymerase causes medulloblastomas in p53(-/-) mice. *Am J Pathol* **162**, 343-352 (2003).

178. Morrison, C*., et al.* Genetic interaction between PARP and DNA-PK in V(D)J recombination and tumorigenesis. *Nat Genet* **17**, 479-482 (1997).

179. Cherney, B.W*., et al.* cDNA sequence, protein structure, and chromosomal location of the human gene for poly(ADP-ribose) polymerase. *Proc Natl Acad Sci U S A* **84**, 8370-8374 (1987).

180. Nosho, K*., et al.* Overexpression of poly(ADP-ribose) polymerase-1 (PARP-1) in the early stage of colorectal carcinogenesis. *Eur J Cancer* **42**, 2374-2381 (2006).

181. Kovacs, G. Preferential involvement of chromosome 1q in a primary breast carcinoma. *Cancer Genet Cytogenet* **3**, 125-129 (1981).

182. Larramendy, M.L*., et al.* Comparative genomic hybridization reveals complex genetic changes in primary breast cancer tumors and their cell lines. *Cancer Genet Cytogenet* **119**, 132-138 (2000).

183. Bieche, I., Champeme, M.H. & Lidereau, R. Loss and gain of distinct regions of chromosome 1q in primary breast cancer. *Clin Cancer Res* **1**, 123-127 (1995).

184. Sanger, I. Catalogue Of Somatic Mutations In Cancer. Vol. 2012 (Sanger Institute, 2012).

185. Twyman, R.M. & Primrose, S.B. Techniques patents for SNP genotyping. *Pharmacogenomics* **4**, 67-79 (2003).

186. Cottet, F*., et al.* New polymorphisms in the human poly(ADP-ribose) polymerase-1 coding sequence: lack of association with longevity or with increased cellular poly(ADP-ribosyl)ation capacity. *J Mol Med (Berl)* **78**, 431-440 (2000).

187. Lockett, K.L*., et al.* The ADPRT V762A genetic variant contributes to prostate cancer susceptibility and deficient enzyme function. *Cancer Res* **64**, 6344-6348 (2004).

188. Wang, X.G., Wang, Z.Q., Tong, W.M. & Shen, Y. PARP1 Val762Ala polymorphism reduces enzymatic activity. *Biochem Biophys Res Commun* **354**, 122-126 (2007).

189. Cao, W.H*., et al.* Analysis of genetic variants of the poly(ADP-ribose) polymerase-1 gene in breast cancer in French patients. *Mutat Res* **632**, 20-28 (2007).

190. Zhai, X*., et al.* Polymorphisms of ADPRT Val762Ala and XRCC1 Arg399Glu and risk of breast cancer in Chinese women: a case control analysis. *Oncol Rep* **15**, 247-252 (2006).

191. Hao, B*., et al.* Identification of genetic variants in base excision repair pathway and their associations with risk of esophageal squamous cell carcinoma. *Cancer Res* **64**, 4378-4384 (2004).

192. Zhang, X*., et al.* Polymorphisms in DNA base excision repair genes ADPRT and XRCC1 and risk of lung cancer. *Cancer Res* **65**, 722-726 (2005).

193. Fougerousse, F., Meloni, R., Roudaut, C. & Beckmann, J.S. Dinucleotide repeat polymorphism at the human poly (ADP-ribose) polymerase gene (PPOL). *Nucleic Acids Res* **20**, 1166 (1992).

194. Oei, S.L. & Shi, Y. Transcription factor Yin Yang 1 stimulates poly(ADP-ribosyl)ation and DNA repair. *Biochem Biophys Res Commun* **284**, 450-454 (2001).

195. Ossovskaya, V., Koo, I.C., Kaldjian, E.P., Alvares, C. & Sherman, B.M. Upregulation of Poly (ADP-Ribose) Polymerase-1 (PARP1) in Triple-Negative Breast Cancer and Other Primary Human Tumor Types. *Genes Cancer* **1**, 812-821 (2010).

196. de Murcia, G., Menissier-de Murcia, J. & Schreiber, V. Poly(ADP-ribose) polymerase: molecular biological aspects. *Bioessays* **13**, 455-462 (1991).

197. Bieche, I., de Murcia, G. & Lidereau, R. Poly(ADP-ribose) polymerase gene expression status and genomic instability in human breast cancer. *Clin Cancer Res* **2**, 1163-1167 (1996).

198. Crawley, J.J. & Furge, K.A. Identification of frequent cytogenetic aberrations in hepatocellular carcinoma using gene-expression microarray data. *Genome Biol* **3**, RESEARCH0075 (2002).

199. Tomoda, T*., et al.* Enhanced expression of poly(ADP-ribose) synthetase gene in malignant lymphoma. *Am J Hematol* **37**, 223-227 (1991).

200. Goncalves, A*., et al.* Poly(ADP-ribose) polymerase-1 mRNA expression in human breast cancer: a meta-analysis. *Breast Cancer Res Treat* **127**, 273-281 (2011).

201. Brustmann, H. Poly(adenosine diphosphate-ribose) polymerase expression in serous ovarian carcinoma: correlation with p53, MIB-1, and outcome. *Int J Gynecol Pathol* **26**, 147-153 (2007).

202. Csete, B., Lengyel, Z., Kadar, Z. & Battyani, Z. Poly(adenosine diphosphate-ribose) polymerase-1 expression in cutaneous malignant

melanomas as a new molecular marker of aggressive tumor. *Pathol Oncol Res* **15**, 47-53 (2009).

203. Chang, D.T.*, et al.* Expression of p16(INK4A) but not hypoxia markers or poly adenosine diphosphate-ribose polymerase is associated with improved survival in patients with pancreatic adenocarcinoma. *Cancer* **116**, 5179-5187 (2010).

204. Prasad, S.C., Thraves, P.J., Bhatia, K.G., Smulson, M.E. & Dritschilo, A. Enhanced poly(adenosine diphosphate ribose) polymerase activity and gene expression in Ewing's sarcoma cells. *Cancer Res* **50**, 38-43 (1990).

205. Soldatenkov, V.A.*, et al.* Regulation of the human poly(ADP-ribose) polymerase promoter by the ETS transcription factor. *Oncogene* **18**, 3954-3962 (1999).

206. Shiobara, M.*, et al.* Enhanced polyadenosine diphosphate-ribosylation in cirrhotic liver and carcinoma tissues in patients with hepatocellular carcinoma. *J Gastroenterol Hepatol* **16**, 338-344 (2001).

207. Hirai, K., Ueda, K. & Hayaishi, O. Aberration of poly(adenosine diphosphate-ribose) metabolism in human colon adenomatous polyps and cancers. *Cancer Res* **43**, 3441-3446 (1983).

208. Fukushima, M., Kuzuya, K., Ota, K. & Ikai, K. Poly(ADP-ribose) synthesis in human cervical cancer cell-diagnostic cytological usefulness. *Cancer Lett* **14**, 227-236 (1981).

209. Wielckens, K., Garbrecht, M., Kittler, M. & Hilz, H. ADP-ribosylation of nuclear proteins in normal lymphocytes and in low-grade malignant non-Hodgkin lymphoma cells. *Eur J Biochem* **104**, 279-287 (1980).

210. Pero, R.W., Roush, G.C., Markowitz, M.M. & Miller, D.G. Oxidative stress, DNA repair, and cancer susceptibility. *Cancer Detect Prev* **14**, 555-561 (1990).

211. Rajaee-Behbahani, N.*, et al.* Reduced poly(ADP-ribosyl)ation in lymphocytes of laryngeal cancer patients: results of a case-control study. *Int J Cancer* **98**, 780-784 (2002).

212. Shimizu, S.*, et al.* Expression of poly(ADP-ribose) polymerase in human hepatocellular carcinoma and analysis of biopsy specimens obtained under sonographic guidance. *Oncol Rep* **12**, 821-825 (2004).

213. Idogawa, M.*, et al.* Poly(ADP-ribose) polymerase-1 is a component of the oncogenic T-cell factor-4/beta-catenin complex. *Gastroenterology* **128**, 1919-1936 (2005).

214. Southan, G.J. & Szabo, C. Poly(ADP-ribose) polymerase inhibitors. *Curr Med Chem* **10**, 321-340 (2003).

215. Fujimura, S., Hasegawa, S., Shimizu, Y. & Sugimura, T. Polymerization of the adenosine 5'-diphosphate-ribose moiety of nicotinamide-adenine dinucleotide by nuclear enzyme. I. Enzymatic reactions. *Biochim Biophys Acta* **145**, 247-259 (1967).

216. Clark, J.B., Ferris, G.M. & Pinder, S. Inhibition of nuclear NAD nucleosidase and poly ADP-ribose polymerase activity from rat liver by nicotinamide and 5'-methyl nicotinamide. *Biochim Biophys Acta* **238**, 82-85 (1971).

217. Purnell, M.R. & Whish, W.J. Novel inhibitors of poly(ADP-ribose) synthetase. *Biochem J* **185**, 775-777 (1980).

218. Rankin, P.W., Jacobson, E.L., Benjamin, R.C., Moss, J. & Jacobson, M.K. Quantitative studies of inhibitors of ADP-ribosylation in vitro and in vivo. *J Biol Chem* **264**, 4312-4317 (1989).

219. Sestili, P., *et al.* Structural requirements for inhibitors of poly(ADP-ribose) polymerase. *J Cancer Res Clin Oncol* **116**, 615-622 (1990).

220. Banasik, M., Komura, H., Shimoyama, M. & Ueda, K. Specific inhibitors of poly(ADP-ribose) synthetase and mono(ADP-ribosyl)transferase. *J Biol Chem* **267**, 1569-1575 (1992).

221. Rodon, J., Iniesta, M.D. & Papadopoulos, K. Development of PARP inhibitors in oncology. *Expert Opin Investig Drugs* **18**, 31-43 (2009).

222. Donawho, C.K., *et al.* ABT-888, an orally active poly(ADP-ribose) polymerase inhibitor that potentiates DNA-damaging agents in preclinical tumor models. *Clin Cancer Res* **13**, 2728-2737 (2007).

223. Calabrese, C.R., *et al.* Identification of potent nontoxic poly(ADP-Ribose) polymerase-1 inhibitors: chemopotentiation and pharmacological studies. *Clin Cancer Res* **9**, 2711-2718 (2003).

224. Cockcroft, X.L., *et al.* Phthalazinones 2: Optimisation and synthesis of novel potent inhibitors of poly(ADP-ribose)polymerase. *Bioorg Med Chem Lett* **16**, 1040-1044 (2006).

225. Thomas, H.D., *et al.* Preclinical selection of a novel poly(ADP-ribose) polymerase inhibitor for clinical trial. *Mol Cancer Ther* **6**, 945-956 (2007).

226. Guha, M. PARP inhibitors stumble in breast cancer. *Nat Biotechnol* **29**, 373-374 (2011).

227. Dobzhansky, T. Genetics of Natural Populations. Xiii. Recombination and Variability in Populations of Drosophila Pseudoobscura. *Genetics* **31**, 269-290 (1946).

228. Kaelin, W.G., Jr. The concept of synthetic lethality in the context of anticancer therapy. *Nat Rev Cancer* **5**, 689-698 (2005).

229. Ashworth, A. A synthetic lethal therapeutic approach: poly(ADP) ribose polymerase inhibitors for the treatment of cancers deficient in DNA double-strand break repair. *J Clin Oncol* **26**, 3785-3790 (2008).

230. Yoshida, K. & Miki, Y. Role of BRCA1 and BRCA2 as regulators of DNA repair, transcription, and cell cycle in response to DNA damage. *Cancer Sci* **95**, 866-871 (2004).

231. Bryant, H.E., *et al.* PARP is activated at stalled forks to mediate Mre11-dependent replication restart and recombination. *EMBO J* **28**, 2601-2615 (2009).

232. Farmer, H., *et al.* Targeting the DNA repair defect in BRCA mutant cells as a therapeutic strategy. *Nature* **434**, 917-921 (2005).

233. Bryant, H.E., *et al.* Specific killing of BRCA2-deficient tumours with inhibitors of poly(ADP-ribose) polymerase. *Nature* **434**, 913-917 (2005).

234. Evers, B., *et al.* Selective inhibition of BRCA2-deficient mammary tumor cell growth by AZD2281 and cisplatin. *Clin Cancer Res* **14**, 3916-3925 (2008).

235. Rottenberg, S., *et al.* High sensitivity of BRCA1-deficient mammary tumors to the PARP inhibitor AZD2281 alone and in combination with platinum drugs. *Proc Natl Acad Sci U S A* **105**, 17079-17084 (2008).

236. McCabe, N., *et al.* BRCA2-deficient CAPAN-1 cells are extremely sensitive to the inhibition of Poly (ADP-Ribose) polymerase: an issue of potency. *Cancer Biol Ther* **4**, 934-936 (2005).

237. Gallmeier, E. & Kern, S.E. Absence of specific cell killing of the BRCA2-deficient human cancer cell line CAPAN1 by poly(ADP-ribose) polymerase inhibition. *Cancer Biol Ther* **4**, 703-706 (2005).

238. Wang, W. & Figg, W.D. Secondary BRCA1 and BRCA2 alterations and acquired chemoresistance. *Cancer Biol Ther* **7**, 1004-1005 (2008).

239. Turner, N., Tutt, A. & Ashworth, A. Hallmarks of 'BRCAness' in sporadic cancers. *Nat Rev Cancer* **4**, 814-819 (2004).

240. Rice, J.C., Ozcelik, H., Maxeiner, P., Andrulis, I. & Futscher, B.W. Methylation of the BRCA1 promoter is associated with decreased BRCA1 mRNA levels in clinical breast cancer specimens. *Carcinogenesis* **21**, 1761-1765 (2000).

241. Esteller, M*., et al.* Promoter hypermethylation and BRCA1 inactivation in sporadic breast and ovarian tumors. *J Natl Cancer Inst* **92**, 564-569 (2000).

242. Baldassarre, G*., et al.* Negative regulation of BRCA1 gene expression by HMGA1 proteins accounts for the reduced BRCA1 protein levels in sporadic breast carcinoma. *Mol Cell Biol* **23**, 2225-2238 (2003).

243. Turner, N.C*., et al.* BRCA1 dysfunction in sporadic basal-like breast cancer. *Oncogene* **26**, 2126-2132 (2007).

244. Pongsavee, M*., et al.* The BRCA1 3'-UTR: 5711+421T/T_5711+1286T/T genotype is a possible breast and ovarian cancer risk factor. *Genet Test Mol Biomarkers* **13**, 307-317 (2009).

245. Garcia, A.I*., et al.* Down-regulation of BRCA1 expression by miR-146a and miR-146b-5p in triple negative sporadic breast cancers. *EMBO Mol Med* **3**, 279-290 (2011).

246. Moskwa, P*., et al.* miR-182-mediated downregulation of BRCA1 impacts DNA repair and sensitivity to PARP inhibitors. *Mol Cell* **41**, 210-220 (2011).

247. Collins, N., Wooster, R. & Stratton, M.R. Absence of methylation of CpG dinucleotides within the promoter of the breast cancer susceptibility gene BRCA2 in normal tissues and in breast and ovarian cancers. *Br J Cancer* **76**, 1150-1156 (1997).

248. Hughes-Davies, L*., et al.* EMSY links the BRCA2 pathway to sporadic breast and ovarian cancer. *Cell* **115**, 523-535 (2003).

249. Foulkes, W.D*., et al.* Germline BRCA1 mutations and a basal epithelial phenotype in breast cancer. *J Natl Cancer Inst* **95**, 1482-1485 (2003).

250. Anders, C.K*., et al.* Poly(ADP-Ribose) polymerase inhibition: "targeted" therapy for triple-negative breast cancer. *Clin Cancer Res* **16**, 4702-4710 (2010).

251. Alli, E., Sharma, V.B., Sunderesakumar, P. & Ford, J.M. Defective repair of oxidative dna damage in triple-negative breast cancer confers sensitivity to inhibition of poly(ADP-ribose) polymerase. *Cancer Res* **69**, 3589-3596 (2009).

252. Hastak, K., Alli, E. & Ford, J.M. Synergistic chemosensivity of triple-negative breast cancer cell lines to poly(ADP-Ribose) polymerase inhibition, gemcitabine, and cisplatin. *Cancer Res* **70**, 7970-7980 (2010).

253. McCabe, N*., et al.* Deficiency in the repair of DNA damage by homologous recombination and sensitivity to poly(ADP-ribose) polymerase inhibition. *Cancer Res* **66**, 8109-8115 (2006).

254. Weston, V.J*., et al.* The PARP inhibitor olaparib induces significant killing of ATM-deficient lymphoid tumor cells in vitro and in vivo. *Blood* **116**, 4578-4587 (2010).

255. Sourisseau, T*., et al.* Aurora-A expressing tumour cells are deficient for homology-directed DNA double strand-break repair and sensitive to PARP inhibition. *EMBO Mol Med* **2**, 130-142 (2010).

256. Tentori, L. & Graziani, G. Chemopotentiation by PARP inhibitors in cancer therapy. *Pharmacol Res* **52**, 25-33 (2005).

257. Beidler, D.R., Chang, J.Y., Zhou, B.S. & Cheng, Y.C. Camptothecin resistance involving steps subsequent to the formation of protein-linked DNA breaks in human camptothecin-resistant KB cell lines. *Cancer Res* **56**, 345-353 (1996).

258. Delaney, C.A*., et al.* Potentiation of temozolomide and topotecan growth inhibition and cytotoxicity by novel poly(adenosine diphosphoribose) polymerase inhibitors in a panel of human tumor cell lines. *Clin Cancer Res* **6**, 2860-2867 (2000).

259. Munoz-Gamez, J.A*., et al.* PARP inhibition sensitizes p53-deficient breast cancer cells to doxorubicin-induced apoptosis. *Biochem J* **386**, 119-125 (2005).

260. Chen, G. & Zeller, W.J. Reversal of acquired cisplatin resistance by nicotinamide in vitro and in vivo. *Cancer Chemother Pharmacol* **33**, 157-162 (1993).

261. Miknyoczki, S.J*., et al.* Chemopotentiation of temozolomide, irinotecan, and cisplatin activity by CEP-6800, a poly(ADP-ribose) polymerase inhibitor. *Mol Cancer Ther* **2**, 371-382 (2003).

262. Calabrese, C.R*., et al.* Anticancer chemosensitization and radiosensitization by the novel poly(ADP-ribose) polymerase-1 inhibitor AG14361. *J Natl Cancer Inst* **96**, 56-67 (2004).

263. Mason, K.A., Valdecanas, D., Hunter, N.R. & Milas, L. INO-1001, a novel inhibitor of poly(ADP-ribose) polymerase, enhances tumor response to doxorubicin. *Invest New Drugs* **26**, 1-5 (2008).

264. Williamson, C.T*., et al.* Enhanced cytotoxicity of PARP inhibition in mantle cell lymphoma harbouring mutations in both ATM and p53. *EMBO Mol Med* (2012).

265. Zander, S.A*., et al.* Sensitivity and acquired resistance of BRCA1;p53-deficient mouse mammary tumors to the topoisomerase I inhibitor topotecan. *Cancer Res* **70**, 1700-1710 (2010).

266. van Vuurden, D.G*., et al.* PARP inhibition sensitizes childhood high grade glioma, medulloblastoma and ependymoma to radiation. *Oncotarget* **2**, 984-996 (2011).

267. Vance, S*., et al.* Selective radiosensitization of p53 mutant pancreatic cancer cells by combined inhibition of Chk1 and PARP1. *Cell Cycle* **10**, 4321-4329 (2011).

268. Senra, J.M*., et al.* Inhibition of PARP-1 by olaparib (AZD2281) increases the radiosensitivity of a lung tumor xenograft. *Mol Cancer Ther* **10**, 1949-1958 (2011).

269. Huehls, A.M*., et al.* Poly(ADP-Ribose) polymerase inhibition synergizes with 5-fluorodeoxyuridine but not 5-fluorouracil in ovarian cancer cells. *Cancer Res* **71**, 4944-4954 (2011).

270. Johnson, N*., et al.* Compromised CDK1 activity sensitizes BRCA-proficient cancers to PARP inhibition. *Nat Med* **17**, 875-882 (2011).

271. Nowsheen, S*., et al.* Cetuximab augments cytotoxicity with poly (adp-ribose) polymerase inhibition in head and neck cancer. *PLoS One* **6**, e24148 (2011).

272. Fong, P.C*., et al.* Inhibition of poly(ADP-ribose) polymerase in tumors from BRCA mutation carriers. *N Engl J Med* **361**, 123-134 (2009).

273. Therasse, P*., et al.* New guidelines to evaluate the response to treatment in solid tumors. European Organization for Research and Treatment of Cancer, National Cancer Institute of the United States, National Cancer Institute of Canada. *J Natl Cancer Inst* **92**, 205-216 (2000).

274. Tutt, A*., et al.* Oral poly(ADP-ribose) polymerase inhibitor olaparib in patients with BRCA1 or BRCA2 mutations and advanced breast cancer: a proof-of-concept trial. *Lancet* **376**, 235-244 (2010).

275. Liu, X*., et al.* Iniparib Nonselectively Modifies Cysteine-Containing Proteins in Tumor Cells and Is Not a Bona Fide PARP Inhibitor. *Clin Cancer Res* **18**, 510-523 (2012).

276. Patel, A.G., De Lorenzo, S.B., Flatten, K.S., Poirier, G.G. & Kaufmann, S.H. Failure of Iniparib to Inhibit Poly(ADP-Ribose) Polymerase In Vitro. *Clin Cancer Res* **18**, 1655-1662 (2012).

277. Moulder, S. A Phase 1b study to assess the safety and tolerability of iniparib (BSI-201) in combination with irinotecan for the treatment of metastatic breast cancer. Vol. P6-15-01 (ed. SABCS) (2010).

278. O'Shaughnessy, J*., et al.* Iniparib plus chemotherapy in metastatic triple-negative breast cancer. *N Engl J Med* **364**, 205-214 (2011).

279. O'Shaughnessy, J. A randomized phase III study of iniparib (BSI-201) in combination with gemcitabine/carboplatin (G/C) in metastatic triple-negative breast cancer (TNBC). *J Clin Oncol* **29**(2011).

280. Dent, R.A. Safety and efficacy of the oral PARP inhibitor olaparib (AZD2281) in combination with paclitaxel for the first- or second-line treatment of patients with metastatic triple-negative breast cancer: Results from the safety cohort of a phase I/II multicenter trial. *J Clin Oncol* **28:15s (suppl; abstr 1018)** (2010).

281. Wood, R.D., Mitchell, M. & Lindahl, T. Human DNA repair genes, 2005. *Mutat Res* **577**, 275-283 (2005).

282. Lord, C.J., McDonald, S., Swift, S., Turner, N.C. & Ashworth, A. A high-throughput RNA interference screen for DNA repair determinants of PARP inhibitor sensitivity. *DNA Repair (Amst)* **7**, 2010-2019 (2008).

283. Lau, A. Identification of gene expression biomarkers that predict sensitivity to the PARP inhibitor olaparib in *AACR-NCI-EORTC International Conference*, Vol. 8 (ed. AACR) (Molecular Cancer Therapeutics, Boston, 2009).

284. Banuelos, C.A., Banath, J.P., Kim, J.Y., Aquino-Parsons, C. & Olive, P.L. gammaH2AX expression in tumors exposed to cisplatin and fractionated irradiation. *Clin Cancer Res* **15**, 3344-3353 (2009).

285. Asakawa, H*., et al.* Prediction of breast cancer sensitivity to neoadjuvant chemotherapy based on status of DNA damage repair proteins. *Breast Cancer Res* **12**, R17 (2010).

286. Elston, C.W. & Ellis, I.O. Pathological prognostic factors in breast cancer. I. The value of histological grade in breast cancer: experience from a large study with long-term follow-up. *Histopathology* **19**, 403-410 (1991).

287.   Urruticoechea, A., Smith, I.E. & Dowsett, M. Proliferation marker Ki-67 in early breast cancer. *J Clin Oncol* **23**, 7212-7220 (2005).

288.   Rojo, F.*, et al.* Mitogen-activated protein kinase phosphatase-1 in human breast cancer independently predicts prognosis and is repressed by doxorubicin. *Clin Cancer Res* **15**, 3530-3539 (2009).

289.   Generali, D.*, et al.* Phosphorylated ERalpha, HIF-1alpha, and MAPK signaling as predictors of primary endocrine treatment response and resistance in patients with breast cancer. *J Clin Oncol* **27**, 227-234 (2009).

290.   Smid, M.*, et al.* Patterns and incidence of chromosomal instability and their prognostic relevance in breast cancer subtypes. *Breast Cancer Res Treat* **128**, 23-30 (2011).

291.   Vollebergh, M.A., Jonkers, J. & Linn, S.C. Genomic instability in breast and ovarian cancers: translation into clinical predictive biomarkers. *Cell Mol Life Sci* **69**, 223-245 (2012).

292.   Kao, J.*, et al.* Molecular profiling of breast cancer cell lines defines relevant tumor models and provides a resource for cancer gene discovery. *PLoS One* **4**, e6146 (2009).

293.   Plummer, R.*, et al.* Phase I study of the poly(ADP-ribose) polymerase inhibitor, AG014699, in combination with temozolomide in patients with advanced solid tumors. *Clin Cancer Res* **14**, 7917-7923 (2008).

294.   Inbar-Rozensal, D.*, et al.* A selective eradication of human nonhereditary breast cancer cells by phenanthridine-derived polyADP-ribose polymerase inhibitors. *Breast Cancer Res* **11**, R78 (2009).

295.   Elstrodt, F.*, et al.* BRCA1 mutation analysis of 41 human breast cancer cell lines reveals three new deleterious mutants. *Cancer Res* **66**, 41-45 (2006).

296.   Goggins, M.*, et al.* Germline BRCA2 gene mutations in patients with apparently sporadic pancreatic carcinomas. *Cancer Res* **56**, 5360-5364 (1996).

297.   Shimo, T.*, et al.* Antitumor and anticancer stem cell activity of a poly ADP-ribose polymerase inhibitor olaparib in breast cancer cells. *Breast Cancer* (2012).

298.   Boone, J.J., Bhosle, J., Tilby, M.J., Hartley, J.A. & Hochhauser, D. Involvement of the HER2 pathway in repair of DNA damage produced by chemotherapeutic agents. *Mol Cancer Ther* **8**, 3015-3023 (2009).

299.   Mayfield, S., Vaughn, J.P. & Kute, T.E. DNA strand breaks and cell cycle perturbation in herceptin treated breast cancer cell lines. *Breast Cancer Res Treat* **70**, 123-129 (2001).

300.   Pietras, R.J.*, et al.* Antibody to HER-2/neu receptor blocks DNA repair after cisplatin in human breast and ovarian cancer cells. *Oncogene* **9**, 1829-1838 (1994).

301.   Johnson, E.*, et al.* HER2/ErbB2-induced breast cancer cell migration and invasion require p120 catenin activation of Rac1 and Cdc42. *J Biol Chem* **285**, 29491-29501 (2010).

302.   Gakhar, G., Wight-Carter, M., Andrews, G., Olson, S. & Nguyen, T.A. Hydronephrosis and urine retention in estrogen-implanted athymic nude mice. *Vet Pathol* **46**, 505-508 (2009).

303.   Newman, R.E., Soldatenkov, V.A., Dritschilo, A. & Notario, V. Poly(ADP-ribose) polymerase turnover alterations do not contribute to PARP overexpression in Ewing's sarcoma cells. *Oncol Rep* **9**, 529-532 (2002).

304. Menegazzi, M*., et al.* Increase of poly(ADP-ribose) polymerase mRNA levels during TPA-induced differentiation of human lymphocytes. *FEBS Lett* **297**, 59-62 (1992).

305. Zaremba, T*., et al.* Poly(ADP-ribose) polymerase-1 polymorphisms, expression and activity in selected human tumour cell lines. *Br J Cancer* **101**, 256-262 (2009).

306. Tempera, I*., et al.* Poly(ADP-ribose)polymerase activity is reduced in circulating mononuclear cells from type 2 diabetic patients. *J Cell Physiol* **205**, 387-392 (2005).

307. Germain, M*., et al.* Cleavage of automodified poly(ADP-ribose) polymerase during apoptosis. Evidence for involvement of caspase-7. *J Biol Chem* **274**, 28379-28384 (1999).

308. Barretina, J*., et al.* The Cancer Cell Line Encyclopedia enables predictive modelling of anticancer drug sensitivity. *Nature* **483**, 603-607 (2012).

309. Zaremba, T. Poly(ADP-ribose)polymerase-1 (PARP-1) genomics in relation to activity in healthy volunteers and cancer patients. . in *99th Annual Meeting of the American fo Cancer Research*, Vol. Abstract nr 540 (2008).

310. Ghabreau, L*., et al.* Poly(ADP-ribose) polymerase-1, a novel partner of progesterone receptors in endometrial cancer and its precursors. *Int J Cancer* **109**, 317-321 (2004).

311. Domagala, P., Huzarski, T., Lubinski, J., Gugala, K. & Domagala, W. PARP-1 expression in breast cancer including BRCA1-associated, triple negative and basal-like tumors: possible implications for PARP-1 inhibitor therapy. *Breast Cancer Res Treat* **127**, 861-869 (2011).

312. Graeser, M*., et al.* A marker of homologous recombination predicts pathologic complete response to neoadjuvant chemotherapy in primary breast cancer. *Clin Cancer Res* **16**, 6159-6168 (2010).

313. Klauschen, F*., et al.* High nuclear poly-(ADP-ribose)-polymerase expression is prognostic of improved survival in pancreatic cancer. *Histopathology* (2012).

314. Shin, M.S*., et al.* Mutations of tumor necrosis factor-related apoptosis-inducing ligand receptor 1 (TRAIL-R1) and receptor 2 (TRAIL-R2) genes in metastatic breast cancers. *Cancer Res* **61**, 4942-4946 (2001).

315. Staibano, S*., et al.* Poly(adenosine diphosphate-ribose) polymerase 1 expression in malignant melanomas from photoexposed areas of the head and neck region. *Hum Pathol* **36**, 724-731 (2005).

316. Wallace-Brodeur, R.R. & Lowe, S.W. Clinical implications of p53 mutations. *Cell Mol Life Sci* **55**, 64-75 (1999).

317. Tang, L*., et al.* Expression of apoptosis regulators in cutaneous malignant melanoma. *Clin Cancer Res* **4**, 1865-1871 (1998).

318. Helmbach, H*., et al.* Drug resistance towards etoposide and cisplatin in human melanoma cells is associated with drug-dependent apoptosis deficiency. *J Invest Dermatol* **118**, 923-932 (2002).

319. Pyriochou, A., Olah, G., Deitch, E.A., Szabo, C. & Papapetropoulos, A. Inhibition of angiogenesis by the poly(ADP-ribose) polymerase inhibitor PJ-34. *Int J Mol Med* **22**, 113-118 (2008).

320. Lacal, P.M*., et al.* Pharmacological inhibition of poly(ADP-ribose) polymerase activity down-regulates the expression of syndecan-4 and Id-1 in endothelial cells. *Int J Oncol* **34**, 861-872 (2009).

321. Yeo, E.J., Chun, Y.S. & Park, J.W. New anticancer strategies targeting HIF-1. *Biochem Pharmacol* **68**, 1061-1069 (2004).

322. Martin-Oliva, D*., et al.* Inhibition of poly(ADP-ribose) polymerase modulates tumor-related gene expression, including hypoxia-inducible factor-1 activation, during skin carcinogenesis. *Cancer Res* **66**, 5744-5756 (2006).

323. Wu, J.T. & Kral, J.G. The NF-kappaB/IkappaB signaling system: a molecular target in breast cancer therapy. *J Surg Res* **123**, 158-169 (2005).

324. Rayet, B. & Gelinas, C. Aberrant rel/nfkb genes and activity in human cancer. *Oncogene* **18**, 6938-6947 (1999).

325. Montagut, C*., et al.* Activation of nuclear factor-kappa B is linked to resistance to neoadjuvant chemotherapy in breast cancer patients. *Endocr Relat Cancer* **13**, 607-616 (2006).

326. Hassa, P.O. & Hottiger, M.O. A role of poly (ADP-ribose) polymerase in NF-kappaB transcriptional activation. *Biol Chem* **380**, 953-959 (1999).

327. Cai, L., Threadgill, M.D., Wang, Y. & Li, M. Effect of poly (ADP-ribose) polymerase-1 inhibition on the proliferation of murine colon carcinoma CT26 cells. *Pathol Oncol Res* **15**, 323-328 (2009).

328. von Minckwitz G, M.l.B., Loibl S, Blohmer JU, duBois A,Huober J, Kandolf R, Budczies J, Denkert C. PARP is expressed in all subtypes of early breast cancer and is a predictive factor for response to neoadjuvant chemotherapy. *Eur J Cancer* **Suppl 8**(2010).

329. Rodriguez, A.A*., et al.* DNA repair signature is associated with anthracycline response in triple negative breast cancer patients. *Breast Cancer Res Treat* **123**, 189-196 (2010).

330. Fridlyand, J*., et al.* Breast tumor copy number aberration phenotypes and genomic instability. *BMC Cancer* **6**, 96 (2006).

331. Weigman, V.J*., et al.* Basal-like Breast cancer DNA copy number losses identify genes involved in genomic instability, response to therapy, and patient survival. *Breast Cancer Res Treat* (2011).

332. Mao, X., Fan, C., Wei, J., Yao, F. & Jin, F. Genetic mutations and expression of p53 in non-invasive breast lesions. *Mol Med Report* **3**, 929-934 (2010).

333. Tentori, L*., et al.* Inhibition of poly(ADP-ribose) polymerase prevents irinotecan-induced intestinal damage and enhances irinotecan/temozolomide efficacy against colon carcinoma. *FASEB J* **20**, 1709-1711 (2006).

334. Gottipati, P*., et al.* Poly(ADP-ribose) polymerase is hyperactivated in homologous recombination-defective cells. *Cancer Res* **70**, 5389-5398 (2010).

335. Daniel, V.C*., et al.* A primary xenograft model of small-cell lung cancer reveals irreversible changes in gene expression imposed by culture in vitro. *Cancer Res* **69**, 3364-3373 (2009).

336. Pandita, A., Aldape, K.D., Zadeh, G., Guha, A. & James, C.D. Contrasting in vivo and in vitro fates of glioblastoma cell subpopulations with amplified EGFR. *Genes Chromosomes Cancer* **39**, 29-36 (2004).

337. Arnaudeau, C., Lundin, C. & Helleday, T. DNA double-strand breaks associated with replication forks are predominantly repaired by homologous recombination involving an exchange mechanism in mammalian cells. *J Mol Biol* **307**, 1235-1245 (2001).

338. Madison, D.L., Stauffer, D. & Lundblad, J.R. The PARP inhibitor PJ34 causes a PARP1-independent, p21 dependent mitotic arrest. *DNA Repair (Amst)* **10**, 1003-1013 (2011).

339. Chalmers, A.J. The potential role and application of PARP inhibitors in cancer treatment. *Br Med Bull* **89**, 23-40 (2009).

340. Thompson, C., MacDonald, G. & Mueller, C.R. Decreased expression of BRCA1 in SK-BR-3 cells is the result of aberrant activation of the GABP Beta promoter by an NRF-1-containing complex. *Mol Cancer* **10**, 62 (2011).

341. Szanto, A*., et al.* PARP-1 inhibition-induced activation of PI-3-kinase-Akt pathway promotes resistance to taxol. *Biochem Pharmacol* **77**, 1348-1357 (2009).

342. Mah, L.J., El-Osta, A. & Karagiannis, T.C. gammaH2AX: a sensitive molecular marker of DNA damage and repair. *Leukemia* **24**, 679-686 (2010).

343. Collins, A.R., Dobson, V.L., Dusinska, M., Kennedy, G. & Stetina, R. The comet assay: what can it really tell us? *Mutat Res* **375**, 183-193 (1997).

344. Pietras, R.J*., et al.* Monoclonal antibody to HER-2/neureceptor modulates repair of radiation-induced DNA damage and enhances radiosensitivity of human breast cancer cells overexpressing this oncogene. *Cancer Res* **59**, 1347-1355 (1999).

345. Le, X.F*., et al.* Genes affecting the cell cycle, growth, maintenance, and drug sensitivity are preferentially regulated by anti-HER2 antibody through phosphatidylinositol 3-kinase-AKT signaling. *J Biol Chem* **280**, 2092-2104 (2005).

346. You, X.L., Yen, L., Zeng-Rong, N., Al Moustafa, A.E. & Alaoui-Jamali, M.A. Dual effect of erbB-2 depletion on the regulation of DNA repair and cell cycle mechanisms in non-small cell lung cancer cells. *Oncogene* **17**, 3177-3186 (1998).

347. Nitta, M*., et al.* Targeting EGFR induced oxidative stress by PARP1 inhibition in glioblastoma therapy. *PLoS One* **5**, e10767 (2010).

348. Nahta, R. & Esteva, F.J. Herceptin: mechanisms of action and resistance. *Cancer Lett* **232**, 123-138 (2006).

349. Ali, M*., et al.* Vasoactivity of AG014699, a clinically active small molecule inhibitor of poly(ADP-ribose) polymerase: a contributory factor to chemopotentiation in vivo? *Clin Cancer Res* **15**, 6106-6112 (2009).

350. Wang, C.X*., et al.* In vitro and in vivo effects of combination of Trastuzumab (Herceptin) and Tamoxifen in breast cancer. *Breast Cancer Res Treat* **92**, 251-263 (2005).

351. Zhang, J.X*., et al.* Synergistic inhibition of hepatocellular carcinoma growth by cotargeting chromatin modifying enzymes and poly (ADP-ribose) polymerases. *Hepatology* (2011).

352. Frizzell, K.M*., et al.* Global analysis of transcriptional regulation by poly(ADP-ribose) polymerase-1 and poly(ADP-ribose) glycohydrolase in MCF-7 human breast cancer cells. *J Biol Chem* **284**, 33926-33938 (2009).

353. Godon, C*., et al.* PARP inhibition versus PARP-1 silencing: different outcomes in terms of single-strand break repair and radiation susceptibility. *Nucleic Acids Res* **36**, 4454-4464 (2008).

354. Virag, L*., et al.* Effects of poly(ADP-ribose) polymerase inhibition on inflammatory cell migration in a murine model of asthma. *Med Sci Monit* **10**, BR77-83 (2004).

355.   Zingarelli, B., Salzman, A.L. & Szabo, C. Genetic disruption of poly (ADP-ribose) synthetase inhibits the expression of P-selectin and intercellular adhesion molecule-1 in myocardial ischemia/reperfusion injury. *Circ Res* **83**, 85-94 (1998).

356.   Badache, A. & Hynes, N.E. Interleukin 6 inhibits proliferation and, in cooperation with an epidermal growth factor receptor autocrine loop, increases migration of T47D breast cancer cells. *Cancer Res* **61**, 383-391 (2001).

357.   Akekawatchai, C., Holland, J.D., Kochetkova, M., Wallace, J.C. & McColl, S.R. Transactivation of CXCR4 by the insulin-like growth factor-1 receptor (IGF-1R) in human MDA-MB-231 breast cancer epithelial cells. *J Biol Chem* **280**, 39701-39708 (2005).

358.   Turner, D.P., Findlay, V.J., Kirven, A.D., Moussa, O. & Watson, D.K. Global gene expression analysis identifies PDEF transcriptional networks regulating cell migration during cancer progression. *Mol Biol Cell* **19**, 3745-3757 (2008).

359.   Conde, C.*, et al.* Loss of poly(ADP-ribose) polymerase-1 causes increased tumour latency in p53-deficient mice. *EMBO J* **20**, 3535-3543 (2001).

360.   Melnikova, V.O., Bolshakov, S.V., Walker, C. & Ananthaswamy, H.N. Genomic alterations in spontaneous and carcinogen-induced murine melanoma cell lines. *Oncogene* **23**, 2347-2356 (2004).

361.   Sigma. Features of lentiviral vector for shRNA expression from Sigma website:http://www.sigmaaldrich.com/life-science/functional-genomics-and-rnai/shrna/library-information/vector-map.html. (2011).

362.   Sturn, A., Quackenbush, J. & Trajanoski, Z. Genesis: cluster analysis of microarray data. *Bioinformatics* **18**, 207-208 (2002).

363.   Roche. Universal ProbeLibrary Assay Design Center; http://www.roche-applied-science.com/sis/rtpcr/upl/index.jsp?id=UP030000. (2011).

364.   McShane, L.M.*, et al.* REporting recommendations for tumor MARKer prognostic studies (REMARK). *Nat Clin Pract Urol* **2**, 416-422 (2005).

PUBLICATIONS

PUBLICATIONS PRESENTED IN THIS THESIS

Some of the results of this PhD thesis have been compiled in the following publication:

Authors:

F. Rojo, J. Garcia-Parra, S. Zazo, I. Tusquets, J. Ferrer-Lozano, S. Menéndez, P. Eroles, C. Chamizo, S. Servitja, N. Ramírez-Merino, F. Lobo, B. Bellosillo, J.M. Corominas, J. Yélamos, S. Serrano, A. Lluch & A. Rovira & J. Albanell

Title: Nuclear PARP-1 protein overexpression is associated with poor overall survival in early breast cancer

Journal: Annals of Oncology. doi:10.1093/annonc/mdr361

Some of the results of the preclinical models included in this PhD thesis are being compiled in the following publication under preparation:

Authors:

J. Garcia-Parra, O. Arpí, S. Zazo, S. Menéndez, C. Chamizo, S. Servitja, J.M. Corominas, I. Tusquets, J. Yélamos, F. Rojo, A. Rovira, J. Albanell

Title: Poly(ADP-ribose)polymerase inhibition enhances trastuzumab antitumor effects in HER2 overexpressing breast cancer

Journal: Not determined

Rojo F, Garcia-Parra J, Zazo S, Tusquets I, Ferrer-Lozano J, Menendez S, et al. **Nuclear PARP-1 protein overexpression is associated with poor overall survival in early breast cancer.** Ann Oncol. 2012 May; 23(5):1156-1164.